

Mikhail Kravchenko ECE 444 Microwave Circuits. Dr. Aly Farhat

Microwave Engineering David M. Pozar. The University of Tennessee  
EECS Minkao

kravchenko.mij@gmail.com  
mkravche@vols.utk.edu

352-281-1960

## Chapter 1 Electromagnetic Theory

We begin our study of microwave engineering with a brief overview of the history and major applications of microwave technology, followed by a brief review of some of the fundamentals in electromagnetic theory that we will need throughout the book. Further discussion of these topics may be found in references [1-8].

**1.1 Microwave Engineering :** The field of Radio frequency (RF) and microwave engineering generally covers the behaviour of alternating current signals with frequencies in the range of  $100\text{ MHz}$  ( $1\text{MHz} = 10^6\text{ Hz}$ ) to  $1000\text{ GHz}$  ( $1\text{GHz} = 10^9\text{ Hz}$ ). RF frequencies range from very high frequency (VHF) ( $30\text{-}300\text{ MHz}$ ) to the ultra high frequency (UHF) ( $300\text{-}3000\text{ MHz}$ ), while the term microwave is typically used for frequencies between 3 and  $300\text{ GHz}$ , with a corresponding electrical wavelength between  $\lambda = c/f = 10\text{cm}$  and  $\lambda = 1\text{mm}$ , respectively. Signals with wavelength on the order of millimeters are often referred as mm-waves. Figure 1.1 shows the location of the RF and  $\mu$ -wave frequency bands in the electromagnetic spectrum. Because of the high frequencies (and short wavelength), standard circuit theory often cannot be used directly to solve microwave network problems. In a sense, standard circuit theory often cannot be used directly to solve microwave network problems is an approximation, or special case, of the broader theory of electromagnetics as described by Maxwell's equations.

This is due to the fact that, in general, the lumped circuit element approximation of circuit theory may not be valid at high RF and  $\mu$ -wave frequencies.  $\mu$ -wave components act as distributed elements, where the phase of the voltage or current changes significantly over the physical extent of the device because the device dimensions are on the order of the electrical wavelength. At much lower frequencies the wavelength is large enough that there is insignificant phase variation across the dimensions of a component. The other extreme of frequency can be identified as optical engineering, in which the wavelength is much shorter than the dimensions of a component. The other extreme of frequency can be identified. In this case Maxwell's equations can be simplified to the geometrical optics regime, and optical systems can be designed with the theory of geometrical optics. Such techniques are sometimes applicable to mm-wave systems, where they are referred to as quasi-optical.

In RF and  $\mu$ -wave engineering, then one must work with Maxwell's equations and their solutions. It is in the nature of these equations that mathematical complexity arises since Maxwell's equations involve vector differential or integral operations on vector field quantities, and these fields are functions of spatial coordinates.

One of the goals of this book is to reduce the complexity of the field theory solution to a result that can be expressed in terms of simpler circuit theory, perhaps extended to include distributed elements (such as transmission lines) and concepts (such as reflection coefficients and scattering parameters). A field theory solution generally provides a complete description of the electromagnetic field at every point in space, which is typically is usually much more information than we need for most practical purposes.

Designed by Margaret Rubiano

Copyright © 2017

Peter Pauper Press, Inc.  
202 Mamaroneck Avenue  
White Plains, NY 10601 USA

All rights reserved

ISBN 978-1-4413-2371-2

Printed in China

14

We are typically more interested in terminal quantities such as power, impedances, voltage and current, which can often be expressed in terms of these extended circuit theory concepts. It is this complexity that adds to the challenge, as well as rewards, of  $\mu$ -wave engineering.

### Typical Frequencies

AM broadcast band	535-1605 MHz
Short wave Radio band	3-30 MHz
FM broadcast band	88-108 MHz
VHF TV (2-4)	54-72 MHz
VHF TV (5-6)	76-88 MHz
UHF TV (7-13)	174-216 MHz
UHF TV (14-83)	470-890 MHz
2G cellular phone	824-849 MHz 869-884 MHz
European GSM cellular	880-915 MHz 925-960 MHz
GPS	1575.42 MHz 1227.60 MHz
Microwave ovens	2.45 GHz
US DBS	11.7-12.5 GHz
US ISM bands	902-928 MHz 2.400-2.484 GHz 5.725-5.850 GHz
US QWB	3.1-10.6 GHz

<u>Approximate Band Designations</u>	
medium frequency	300 kHz-3 MHz
High frequency	3 MHz-30 MHz
very high frequency (VHF)	30 MHz-300 MHz
ultra high frequency (UHF)	300 MHz-3 GHz
L band	1-2 GHz
S band	2-4 GHz
C band	4-8 GHz
X band	8-12 GHz
Ku band	12-18 GHz
K band	18-26 GHz
Ka band	26-40 GHz
Q band	40-60 GHz
V band	50-75 GHz
E band	80-90 GHz
W band	75-110 GHz
F band	90-140 GHz

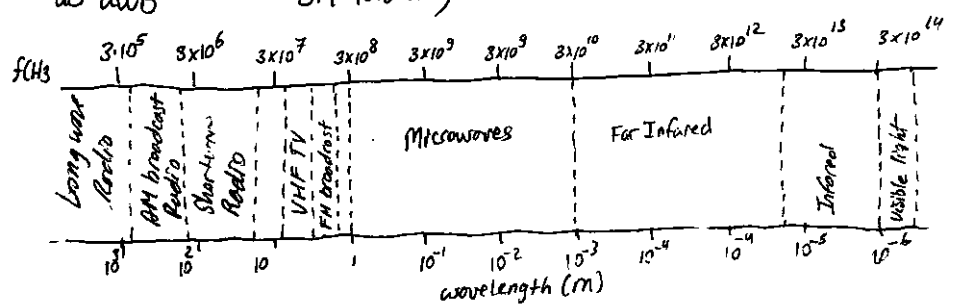


Figure 1.1 The electro magnetic Spectrum.

Applications of Microwave Engineering / Just as the high frequencies and short wavelength of  $\mu$ -wave energy make for difficulties in the analysis and design of microwave devices and systems, these same aspects provide unique opportunities for the application of microwave systems.

The following considerations can be useful in practice :

- Antenna gain is proportional to the electrical size of the antenna. At higher frequencies, more antenna gain can be obtained for a given physical antenna size, and this has important consequences when implementing  $\mu$ -wave systems.
- More bandwidth (directly related to data rate) can be realized at higher frequencies. A 1% bandwidth at 600 MHz is 6 MHz, which (with binary shift keying modulation) can provide a data rate of about 6 Mbps, while at 60 GHz a 1% bandwidth is 600 MHz, allowing a 600 Mbps data rate.
- Microwave signals travel by line of sight and are not bent by the ionosphere as are lower frequency signals. Satellite and terrestrial communication links with very high capacities are therefore possible, with frequency reuse at minimally distant locations.
- The effective reflection area (Radar cross section) of the radar target is usually proportional to the target's electrical size. This fact, coupled with the frequency characteristics of antenna gain, generally makes microwave frequencies preferred over Radar Systems.
- ~~The effective reflection area (Radar cross section)~~ Various molecular, atomic, and nuclear resonances occur at  $\mu$ -wave frequencies, creating a variety of unique applications in areas of science, remote sensing, medical diagnostics, and heating methods.

The majority of today's applications of today's applications of RF and  $\mu$ -wave technology are to wireless networking and communications systems, wireless security systems, radar systems, environmental remote sensing and medical systems. As the frequencies allocations listed in Fig 1.1 show, RF and  $\mu$ -wave communication systems are pervasive, especially ~~as they offer~~ offer ~~wireless communication~~ connectivity promises to provide voice and data access to "anyone, anywhere, anytime."

Modern wireless telephony is based on the concept of cellular frequency reuse, a technology first proposed by Bell Labs in 1947 but not practically implemented until the 1970s. By this time advances in miniaturization, as well as an increasing demand for wireless communications, drove the introduction of several early cellular telephone systems in Europe, U.S., and Japan. The Nordic Mobile Telephone (NMT) System was deployed in 1981 in the Nordic countries, the Advanced Mobile Telephone System (AMPS) was introduced in 1983 by AT&T, and NTT in Japan introduced its first mobile phone service in 1988. All of these early systems used analog FM mode, with their allocated frequency bands divided into thousands of narrow band channels. These early systems referred to now as first generation cellular systems or 1G.

Second-generation (2G) cellular systems achieved improved performance by using various digital modulation schemes, with systems such as GSM, CDMA, DAMPS, PCS and PHS being some of the major standards introduced in the U.S. during the 1990s and in Europe and Japan. These systems can handle digitized voice, as well as some limited data, with data rates typically in the 8-14 kbps range. In recent years there has been a wide variety of new and modified standards to transition to third field services that include voice, text messaging, data networking, positioning, and Internet access.

These standards are variously known as 2.5, 3G, 2.5G, 3G, 3.5G, 3.75G, 4G, with current options to provide data rates up to at least 100 Mbps. The number of subscribers to wireless services seems to be keeping pace with the growing power and access provided by modern handheld wireless devices; as of 2010 there are more than five billion cell phone users worldwide.

Satellite systems also depend on RF and microwave technology, and satellites have been developed to provide cellular (voice), video, and data connections worldwide. Two large satellite constellations, Iridium and Globalstar, were deployed in the late 1990s to provide worldwide telephony service. Unfortunately these systems suffered from technical difficulties and weak business models and have had to withstand billion dollar financial failures. However, smaller satellite systems, such as the Global Positioning System (GPS) and the Direct Broadcast Satellite System (DBS), have been extremely successful.

Wireless local area networks (WLAN) provide high-speed networking between computers over short distances, and demand for this capability is expected to remain strong. One of the newer examples of wireless communication technology is ultra wide band (UWB) radio, where the broadcast signal occupies a very wide frequency band but with a very low power level (typically below radio noise level) to avoid interference with other systems.

Radar systems find application in military, commercial, and scientific fields. Radar is used for detecting and locating air, ground, and sea-going targets, as well as for missile guidance and fire control. In the commercial sector, radar technology is used for air traffic control, motion detectors (door openers and security alarms), vehicle collision avoidance, and distance measurement. Scientific applications of radar include weather prediction, remote sensing of the atmosphere, the oceans and the ground, as well as medical diagnostics and therapy. Microwave radiometry, which is the passive sensing of microwave energy emitted by an object, is used for remote sensing of the atmosphere and the earth, as well as in medical diagnostics and imaging for security.

A Short

## A Short History on Microwave Engineering

Microwave engineering is often considered a fairly mature discipline because the fundamental concepts were developed more than 50 years ago, and probably because radar, the first major application of microwave technology, was developed as far back as WWII. However, recent years have brought substantial and continuing developments in high frequency and solid state devices, microwave integrated circuits, and computer aided design techniques, and the ever-expanding applications of RF and microwave technology to wireless communications, networking, sensing, and security have kept the field active and vibrant.

The foundations of modern electromagnetic theory were stimulated in 1873 by James Clark Maxwell, who hypothesized, solely from mathematical considerations, electromagnetic wave propagation and the idea light was a form of electromagnetic energy. Maxwell's formulations were cast in its modern form by Oliver Heaviside during the period from 1885-1887. Heaviside was a reclusive genius whose efforts removed many of the mathematical complexities of Maxwell's theory, introduced vector notation, and provided a foundation for practical applications of guided waves and transmission lines. Heinrich Hertz, a German professor of physics and a gifted experimentalist who understood the theory published by Maxwell, carried out a set of experiments during the period 1887-1891 that validated Maxwell's theory of electromagnetic waves. Figure 1.2 is a photograph of Hertz' original experiments. It is interesting to observe that this is an instance of a discovery occurring after a prediction has been made through theoretical grounds - a characteristic of many major discoveries throughout history of science. All of the practical applications of electromagnetic theory — radio, TV, radar, cell phones, and wireless networking — owe their existence to the theoretical work of Maxwell.

Because of the lack of reliable microwave sources and other components, the rapid growth of radio technology in the early 1900s occurred primarily in the HF to VHF range. It was not until the 1940s and the advent of radar developed during WWII that microwave theory and technology received substantial interest. In the United States, the Radiation Laboratory was established at the Massachusetts Institute of Technology to develop Radar Theory and Practice. A number of scientists: N. Marcuvitz, I.I. Rabi, J.S. Schwinger, H.A. Bethe, E.M. Purcell, C.G. Montgomery, and R.H. Dicke, among others, gathered for a very intensive period of development in the microwave field. Their work included the theoretical and experimental treatment of waveguide components, flat-top antennas, small-aperture coupling theory, and the beginnings of microwave network theory. Many of these researchers were physicists who returned to physics research after the war.

Their H-wave work is summarized in the classic 28-Volume *Kodichtung Laboratory Series of Books That Still Find Application Today*.

Figure 1.2 Original apparatus used by Hertz for his electromagnetics experiments. (1) 50 MHz Transmitter spark gap and loaded dipole antenna. (2) Testee grid for spot polarization experiments. (3) Vacuum apparatus for cathode ray experiments. (4) Hot-wire galvanometer. (5) Pliss or Kirschner-Hoerner spirals. (6) Slotted-paper galvanometer. (7) Metal sphere probe. (8) Hertz spark micrometer. (9) Coaxial line (10-12) Equipment to demonstrate dielectric polarization effects. (13) Mercury induction coil interrupter. (14) Middinger cell. (15) Bell jar. (16) Induction coil. (17) Bauden cells. (18) Torge-area conductor for charge storage. (19) Circular-loop Receiving antenna. (20) Eight-Sided Receiver detector. (21) Rotating mirror and mercury interrupter. (22) 80-square Loop Receiving antenna. (23) Equipment for refraction and dielectric constant measurement. (24) Two square Loop Receiving antennas. (25) Square Loop Receiving antenna. (26) Transmitter dipole. (27) Induction coil. (28) Coaxial line (29) High-voltage discharger. (30) Cylindrical parabolic reflector/receiver. (31) Cylindrical parabolic reflector/transmitter. (32) Circular loop receiving antenna. (33) Mirror Reflector. (34,35) Battery accumulators. Photographed on October 1, 1913, at the Bavarian Academy of Science, Munich, Germany, with Hertz's assistant, Julius Ammon.

Photograph and identification courtesy of T.H. Bryant.

Communications systems using microwave technology began to be developed soon after the birth of Radar, benefiting from much of the work that was originally done for Radar systems. The advantages offered by microwave systems, including wide bandwidth, line-of-sight propagation, have been critical for both terrestrial and satellite communications systems and have provided an impetus for the continuing development of low-cost miniaturized microwave components. We refer the reader to [1,7] and [2] for further historical perspectives of the fields of wireless communication and microwave engineering.

## 1.2 Maxwell's Equations

Electric and magnetic phenomena at a macroscopic level are described by Maxwell's equations, as published by Maxwell in 1873. This work summarized the state of electromagnetic science at the time and hypothesized from theoretical considerations the existence of electrical displacement current, which led to the experimental discovery by Hertz of electromagnetic wave propagation. Maxwell's work was based on a large body of empirical and theoretical knowledge developed by Gauss, Ampere, Faraday and others, of which basic law of electromagnetics usually follows the historical (or deductive) approach, and it assumes that the reader has had such a prerequisite to the present material. Several references are available [3-7] that provide a good treatment of electromagnetic theory at the undergraduate or graduate level.

This chapter will outline the fundamental concepts of electromagnetic theory that are will require later in the book. Maxwell's equations will be presented, and boundary conditions and the effect of dielectric and magnetic materials will be discussed. Wave phenomena are of essential importance in microwave engineering, and thus much of the chapter is spent on topics related to plane waves. Plane waves are the simplest form of electromagnetic waves and so serve to illustrate a basic number of basic properties associated with wave propagation. Although it is assumed that the reader has studied plane waves before, the present material should help to reinforce the basic principles in the reader's mind and perhaps to introduce some concepts that the reader has not seen previously. This material will also serve as reference to later chapters.

With an awareness of the historical perspective, it is usually advantageous from a pedagogical point of view to present electromagnetic theory from the "inductive," or axiomatic, approach by beginning with Maxwell's equations. The general form of time-varying Maxwell's equations, then, can be written in "Point", or differential, form as:

$$\nabla \times \vec{E} = -\frac{\partial \vec{B}}{\partial t} - \vec{M}, \quad (1.1a)$$

$$\nabla \times \vec{H} = \frac{\partial \vec{D}}{\partial t} + \vec{J}, \quad (1.1b)$$

$$\nabla \cdot \vec{D} = \rho, \quad (1.1c)$$

$$\nabla \cdot \vec{B} = 0. \quad (1.1d)$$

The MKS system of units is used throughout this book. The script quantities represent time-varying vector fields and are real functions of spatial coordinates  $x, y, z$ , and the time variable  $t$ . These quantities are defined as follows:

$\vec{E}$  is the electric field, in volts per meter ( $V/m$ ).

$\vec{H}$  is the magnetic field, in amperes per meter ( $A/m$ ).

$\vec{D}$  is the electric flux density, in coulombs per meter squared ( $Coul/m^2$ ).

$\vec{B}$  is the magnetic flux density, in webers per meter squared ( $Wb/m^2$ ).

$\vec{M}$  is the (fictitious) magnetic current density, in volts per meter ( $V/m^2$ ).

$\vec{J}$  is the electric current density, in amperes per meter squared ( $A/m^2$ ).

$\rho$  is the electric charge density, in coulombs per meter cubed ( $Coul/m^3$ ).

The sources of the electromagnetic field are the currents  $\vec{M}$  and  $\vec{J}$  and the electric charge density  $\rho$ . The magnetic current  $\vec{M}$  is a fictitious source in the sense that it is only a mathematical convenience. The real source of a magnetic current is always a loop of electric current or some similar type of magnetic dipole, as opposed to the flow of an actual magnetic charge (magnetic monopoles are not known to exist). The magnetic current is included here for completeness, as we will have occasion to use it in chapter 4 when dealing with apertures. Since electric current is really the flow of charge, it can be said that the electric charge density  $\rho$  is the ultimate source of the electromagnetic field.

In free-space, the following simple relations hold between the electric and magnetic field intensities and flux densities:

$$\bar{B} = \mu_0 \bar{H} \quad (1.2a)$$

$$\bar{D} = \epsilon_0 \bar{E} \quad (1.2b)$$

where  $\mu_0 = 4\pi \times 10^{-7}$  Henry/m is the permeability of free space, and  $\epsilon_0 = 8.854 \times 10^{-12}$  Farad/m is the permittivity of free space. We will see in the next section how media other than free-space affect these constitutive relations.

Equations (1.1a)-(1.1d) are linear but not independent of each other. For instance, consider the divergence of (1.1a). Since the divergence of the curl of any vector is zero [vector identity (B.12), from Appendix B], we have

$$\nabla \cdot \nabla \times \bar{E} = 0 = -\frac{\partial}{\partial t} (\nabla \cdot \bar{B}) - \nabla \cdot \bar{M}.$$

Since there is no free magnetic charge,  $\nabla \cdot \bar{M} = 0$ , which leads to  $\nabla \cdot \bar{B} = 0$ , or (1.1d).

The continuity equation can be similarly derived by taking the divergence of (1.1b) giving

$$\nabla \cdot \nabla \times \bar{H} = 0 = \frac{\partial \bar{B}}{\partial t} (\nabla \cdot \bar{D}) + \nabla \cdot \bar{J} \Rightarrow \frac{\partial \bar{B}}{\partial t} \cdot \bar{D} + \nabla \cdot \bar{J} = 0 \quad (1.3)$$

where (1.1c) was used. The equation states that charge is conserved, or that current is continuous. Since  $\nabla \cdot \bar{J}$  represents the outflow of the current at a point, and  $\partial \bar{B} / \partial t$  represents the change (flux) with time at the same point. It is this result that led Maxwell to the conclusion that the displacement current density  $\partial \bar{D} / \partial t$  was necessary in (1.1b), which can be seen by taking the divergence of this equation.

The three differential equations can be converted to integral form through the use of various vector integral theorems. Thus applying the divergence theorem (B.15) to (1.1c) and (1.1d) yields:

$$\oint_S \bar{D} \cdot d\bar{s} = \int_V \rho dV = Q \quad (1.4)$$

$$\oint_S \bar{B} \cdot d\bar{s} = 0 \quad (1.5)$$

where  $Q$  in (eq 1.4) represents the total charge contained in a volume  $V$  enclosed by a surface  $S$ . Applying Stokes' theorem (B.16) to (1.1a) gives:

$$\oint_C \bar{E} \cdot d\bar{l} = -\frac{\partial}{\partial t} \int_S \bar{B} \cdot d\bar{s} - \int_S \bar{M} \cdot d\bar{s} \quad (1.6)$$

which, without the  $\bar{M}$  term, is usually the form of Faraday's law and forms the basis for Kirchhoff's voltage law. In (1.6),  $C$  represents the closed contour about a surface  $S$ , as shown in Figure 1.3. Ampere's law can be derived by applying Stokes' theorem to (1.1b):

$$\oint_C \bar{H} \cdot d\bar{l} = \frac{\partial}{\partial t} \int_S \bar{D} \cdot d\bar{s} + \int_S \bar{J} \cdot d\bar{s} = \frac{\partial}{\partial t} \int_S \bar{D} \cdot d\bar{s} + I \quad (1.7)$$

where  $I = \int_S \bar{J} \cdot d\bar{s}$  is the total electric current flow through the surface  $S$ . Equations (1.4)-(1.7) constitute the integral forms of Maxwell's equations.

The above equations are valid for arbitrary time dependence, but most of our work will start the involved with fields having a sinusoidal, or harmonic, time dependence, with steady state conditions assumed. In this case phasor notation is very convenient, and so all field quantities will be assumed to be complex vectors with an implied  $e^{j\omega t}$  time dependence and written with Roman rather than script letters. Thus a sinusoidal electric field polarized in the  $\hat{x}$  direction of the form:

$$\bar{E}(x, y, z, t) = \hat{x} A(x, y, z) \cos(\omega t + \phi) \quad (1.8)$$

where  $A$  is the (real) amplitude,  $\omega$  is the radian frequency, and  $\phi$  is the phase reference of the wave at  $t=0$ , has the phasor for:

$$\bar{E}(x, y, z) = \hat{x} A(x, y, z) e^{j\phi} \quad (1.9)$$

We will assume cosign-based phasors in this book, so the conversion from phasor quantities to the real time-varying quantities is accomplished by multiplying the phasor by  $e^{j\omega t}$  and taking the real part:

$$\bar{E}(x, y, z, t) = \text{Re}\{\bar{E}(x, y, z) e^{j\omega t}\} \quad (1.10)$$

as substituting (1.9) into (1.10) to obtain (1.8) demonstrates. When working with phasor notation, it is customary to suppress the factor  $e^{j\omega t}$  that is common to all terms.

When dealing with power and energy, we will often be interested in the time average of the quadratic quantity, this can be found easily for time harmonic fields. For example, the average of the square of the magnitude of an electric field is given as:

$$\bar{E} = \hat{x} E_1 \cos(\omega t + \phi_1) + \hat{y} E_2 \cos(\omega t + \phi_2) + \hat{z} E_3 \cos(\omega t + \phi_3) \quad (1.11)$$

has the phasor form

$$\bar{E} = \hat{x} E_1 e^{j\phi_1} + \hat{y} E_2 e^{j\phi_2} + \hat{z} E_3 e^{j\phi_3} \quad (1.11)$$

Can be calculated as:

$$|\bar{E}|_{\text{avg}}^2 = \frac{1}{T} \int_0^T \bar{E} \cdot \bar{E} dt = \frac{1}{T} \int_0^T [E_1^2 \cos^2(\omega t + \phi_1) + E_2^2 \cos^2(\omega t + \phi_2) + E_3^2 \cos^2(\omega t + \phi_3)] dt$$

$$|\bar{E}|_{\text{avg}}^2 = \frac{1}{2} (E_1^2 + E_2^2 + E_3^2) = \frac{1}{2} |\bar{E}|^2 = \frac{1}{2} \bar{E} \cdot \bar{E}^* \quad (1.13)$$

Then the Root-mean-square (rms) value is  $|\bar{E}_{\text{rms}}| = |\bar{E}| / \sqrt{2}$

Assuming an  $e^{j\omega t}$  time dependence, we can replace the time derivatives in (1.1a)-(1.1d) with  $j\omega$ . Maxwell's equations in phasor form become:

$$\nabla \times \bar{E} = -j\omega \bar{B} - \bar{J} \quad (1.14a)$$

$$\nabla \times \bar{H} = j\omega \bar{D} + \bar{J} \quad (1.14b)$$

$$\nabla \cdot \bar{D} = \rho \quad (1.14c)$$

$$\nabla \cdot \bar{B} = 0 \quad (1.14d)$$

The Fourier transform can be used to convert a solution to Maxwell's equations for an arbitrary frequency  $\omega$  into a solution for arbitrary time dependence.

The electric and magnetic current sources,  $J$  and  $M$ , in (1.14) are volume current densities with units  $A/m^2$  and  $V/m^2$ . In many cases, however, the actual currents will be in the form of a current sheet, a line current, or an infinitesimal dipole current. These special types of current distributions can always be written as volume current densities through the use of delta functions. Figure 1.4 shows examples of this procedure for electric and magnetic field currents.

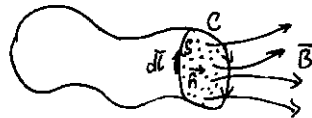


Figure 1.3 The closed contour  $C$  and surface  $S$  associated with Faraday's law.

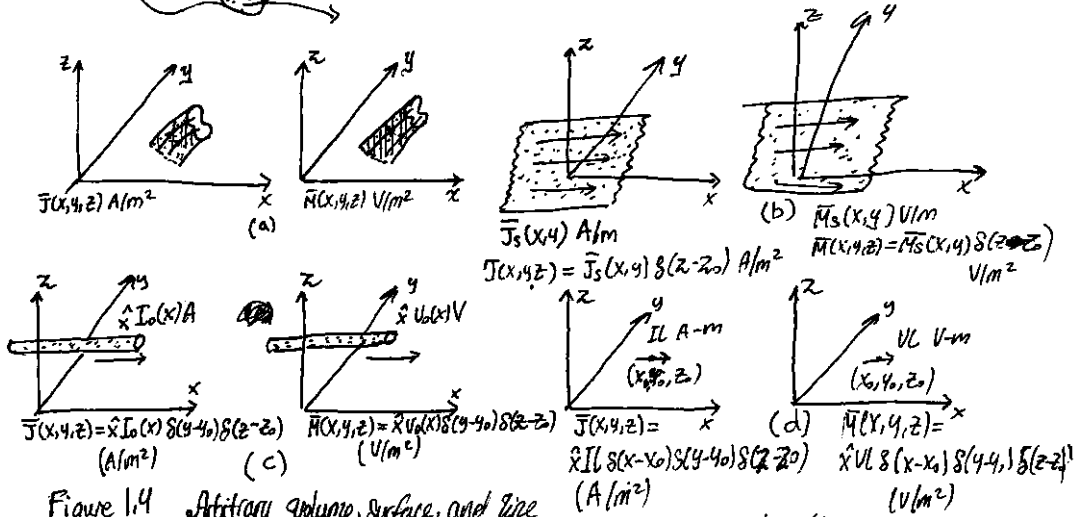


Figure 1.4 Arbitrary volume, surface, and line currents.  
 (a) Arbitrary electric and magnetic volume current densities.  
 (b) Arbitrary electric and magnetic surface current densities in the  $z = Z_0$  plane.  
 (c) Arbitrary electric and magnetic line currents.  
 (d) Infinitesimal electric and magnetic dipoles parallel to the  $x$ -axis.

### 1.3 Fields in media and Boundary Conditions

In the preceding section it was assumed that the electric and magnetic fields were in free space, with no material bodies present. In practice material bodies are often present; this complicates the analysis but allows the useful application of material properties to microwave components. When electromagnetic fields exist in material media, the field vectors ~~are by the~~ are related to each other by the constitutive relations,

For a dielectric material, an applied electric field  $\bar{E}$  causes the polarization of the atoms or molecules of the material to create electric dipole moments that augment the total displacement flux,  $\bar{D}$ . This additional polarization vector is called  $\bar{P}_e$ , the electric polarization, where

$$\bar{D} = \epsilon_0 \bar{E} + \bar{P}_e \quad (1.15)$$

In a linear medium the electric polarization is linearly related to the applied electric field as:

$$\bar{P}_e = \chi_e \epsilon_0 \bar{E} \quad (1.16)$$

where  $\chi_e$ , which may be complex, is the electric susceptibility.

$$\Rightarrow \bar{D} = \epsilon_0 \bar{E} + \bar{P}_e = \epsilon_0 (1 + \chi_e) \bar{E} = \epsilon \bar{E} \quad (1.17)$$

$$\text{where } \epsilon = \epsilon' - j\epsilon'' = \epsilon_0 (1 + \chi_e) \quad (1.18)$$

is the complex permittivity of the medium. The imaginary part of  $\epsilon$  accounts for the loss in the medium (heat) due to the damping of the dipole moments. (Free space having a real  $\epsilon$  is lossless). Due to energy conservation, as we see in Section 1.6, the imaginary part of  $\epsilon$  must be negative ( $\epsilon''$  positive). The loss in the dielectric material may also be considered as an equivalent conductor loss. In a material with conductivity  $\sigma$ , a conduction current density will exist:

$$\bar{J} = \sigma \bar{E} \quad (1.19)$$

which is Ohm's law from an electromagnetic field point of view. Maxwell's curl equation for  $\bar{H}$  in (1.14)b then becomes:

$$\begin{aligned} \nabla \times \bar{H} &= j\omega \bar{D} + \bar{J} \\ &= j\omega \epsilon \bar{E} + \sigma \bar{E} \\ &= j\omega \epsilon'' \bar{E} + (\omega \epsilon'' + \sigma) \bar{E} = j\omega (\epsilon' - j\epsilon'') \bar{E} \end{aligned} \quad (1.20)$$

where it is seen that the loss due to dielectric damping ( $\omega \epsilon''$ ) is indistinguishable from conductivity loss,  $(\sigma)$ . The term  $\omega \epsilon'' + \sigma$  can be considered the loss tangent, defined as:

$$\tan \delta = \frac{\omega \epsilon'' + \sigma}{\omega \epsilon'} \quad (1.21)$$

which is seen to be the ratio of the real to imaginary part of the total displacement current.

Microwave materials are usually characterized by specifying the Real Relative Permittivity (the dielectric constant),  $\epsilon_r$ , with  $\epsilon = \epsilon_r \epsilon_0$ , and the Loss Tangent at a certain frequency. These properties are listed in Appendix G for several types of materials.

It is useful to note now, after a problem has been solved assuming a lossless dielectric, loss can easily be introduced by replacing the real  $\epsilon$  with a complex  $\epsilon = \epsilon' - j\epsilon'' = \epsilon' (1 - j\tan \delta) = \epsilon_0 \epsilon_r (1 - j\tan \delta)$ .

In the preceding discussion it was assumed that  $\bar{P}_e$  was a vector in the same direction as  $\bar{E}$ . Such materials are called isotropic materials, but not all materials have this property.

Some materials are anisotropic and are characterized by a more complicated relation between  $\bar{E}$  and  $\bar{E}$ , or  $\bar{D}$  and  $\bar{E}$ . The most general linear relation between these vectors takes the form of a tensor of Rank Two (a dyad), which can be written in matrix form as

$$\begin{bmatrix} D_x \\ D_y \\ D_z \end{bmatrix} = \begin{bmatrix} E_{xx} & E_{xy} & E_{xz} \\ E_{yx} & E_{yy} & E_{yz} \\ E_{zx} & E_{zy} & E_{zz} \end{bmatrix} \begin{bmatrix} E_x \\ E_y \\ E_z \end{bmatrix} = [E] \begin{bmatrix} E_x \\ E_y \\ E_z \end{bmatrix} \quad (1.22)$$

It is thus seen that a vector component of  $\bar{E}$  gives rise, in general, to three components of  $\bar{D}$ . Crystal structures and ionized ~~gases~~ gases are examples of anisotropic dielectrics. For a linear isotropic material, the matrix of (1.22) reduces to a diagonal matrix with elements  $E$ .

An analogous situation occurs for magnetic materials. An applied magnetic field may align magnetic dipole moments in a magnetic material to produce a magnetic polarization (or magnetization)  $\bar{P}_m$ . Then,

$$\bar{B} = \mu_0 (\bar{H} + \bar{P}_m). \quad (1.23)$$

For a linear magnetic material,  $\bar{P}_m$  is linearly related to  $\bar{H}$  as

$$\bar{P}_m = \chi_m \bar{H} \quad (1.24)$$

where  $\chi_m$  is a complex magnetic susceptibility. From (1.23) and (1.24),

$$\bar{B} = \mu_0 (1 + \chi_m) \bar{H} = \mu \bar{H} \quad (1.25)$$

where  $\mu = \mu_0 (1 + \chi_m) = \mu' - j\mu''$  is the complex permeability of the medium. Again, the imaginary part of  $\chi_m$  or  $\mu$  accounts for the loss due to damping. There is no magnetic conductivity because there is no real magnetic current. As in the electric case, magnetic materials may be anisotropic, in which the dyad tensor can be written as:

$$\begin{bmatrix} B_x \\ B_y \\ B_z \end{bmatrix} = \begin{bmatrix} \mu_{xx} & \mu_{xy} & \mu_{xz} \\ \mu_{yx} & \mu_{yy} & \mu_{yz} \\ \mu_{zx} & \mu_{zy} & \mu_{zz} \end{bmatrix} \begin{bmatrix} H_x \\ H_y \\ H_z \end{bmatrix} = [M] \begin{bmatrix} H_x \\ H_y \\ H_z \end{bmatrix} \quad (1.26)$$

An important example of anisotropic magnetic materials in microwave engineering is the class of ferrimagnetic materials known as ferrites; these materials and their applications will be discussed further in chapter 9.

If a linear medium is assumed ( $\epsilon, M$  not dependent on  $\bar{E}$  or  $\bar{H}$ ), then Maxwell's equations can be written in phasor form as

$$\nabla \times \bar{E} = -j\omega \mu \bar{H} - \bar{M}, \quad (1.27a)$$

$$\nabla \times \bar{H} = j\omega \epsilon \bar{E} - \bar{J}, \quad (1.27b)$$

$$\nabla \cdot \bar{D} = \rho \quad (1.27c)$$

$$\nabla \cdot \bar{B} = 0 \quad (1.27d)$$

The constitutive relations are

$$\bar{D} = \epsilon \bar{E} \quad (1.28a)$$

$$\bar{B} = \mu \bar{H} \quad (1.28b)$$

Note that relations like (1.28a) and (1.28b) generally cannot be written in time domain form, even for linear media, because of the possible phase shift between  $\bar{D}$  and  $\bar{E}$ , or  $\bar{B}$  and  $\bar{H}$ . The phasor representation accounts for this phase shift by the complex form of  $\epsilon$  and  $\mu$ .

Maxwell's equations (1.27a)-(1.27d) in differential form require known boundary conditions for a complete and unique solution. A general method used throughout this book is to solve the source-free Maxwell equations in a certain region to solve for these coefficients. A number of specific cases of boundary conditions to solve for these coefficients of boundary conditions arise, as discussed in what follows.

#### Fields at a General Material Interface

Consider a planar interface between two media, as shown in Figure 1.5. Maxwell's equations in integral form can be used to deduce conditions involving the normal and tangential fields at this interface.

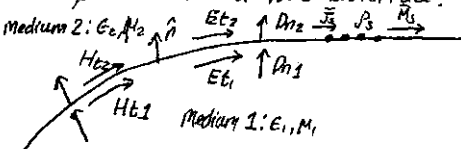


Figure 1.5 Fields, currents, and surface charge at a general interface between two media.

The time-harmonic version of (1.4), where  $S$  is the closed "pillbox"-shaped surface shown in Figure 1.6, can be written as  $\oint \bar{D} \cdot d\bar{s} = \int_V \rho dv$

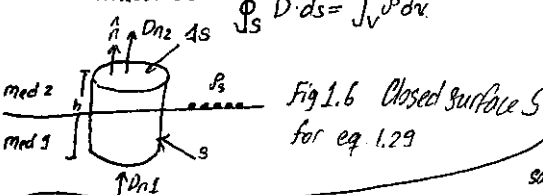


Fig 1.6 Closed surface  $S$  for eq 1.29

In the limit as  $h \rightarrow 0$ , the contribution of  $D_{tan}$  through the sidewalls goes to zero so (eq. 1.29) reduces to:

$$\Delta S D_{en} - \Delta S D_{in} = \Delta S \rho_s \quad \text{or} \quad D_{en} - D_{in} = \rho_s \quad (1.30)$$

where  $\rho_s$  is the surface charge density on the interface. In vector form, we can write  $\hat{n} \cdot (\bar{D}_2 - \bar{D}_1) = \rho_s$

A similar argument for  $\bar{B}$  leads to the result that

$$\hat{n} \cdot \bar{B}_2 - \hat{n} \cdot \bar{B}_1 = 0 \quad (1.32)$$

because there is no free magnetic charge.

For the tangential components of the electric field we use the phasor form of (1.6),

$$\oint_C \bar{E} \cdot d\bar{l} = -j\omega \int_S \bar{B} \cdot d\bar{s} - \int \bar{M} \cdot d\bar{s} \quad (1.33)$$

in connection with the closed contour  $C$  shown in Figure 1.7.

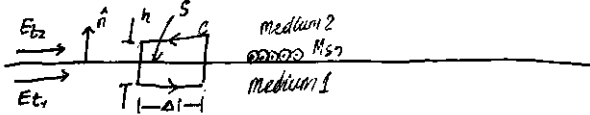


Figure 1.7 Closed contour  $C$  for equation (1.33).

where  $\epsilon$  and  $\mu$  may be complex and may be tensors.

In the limit as  $h \rightarrow 0$ , the surface integral of  $\bar{B}$  vanishes (because  $S=h\hat{n}$  vanishes). The contribution from the surface integral of  $\bar{M}$ , however, may be nonzero if a magnetic surface current density  $\bar{M}_S$  exists on the surface. The dirac delta function can then be used to write:

$$\bar{M} = \bar{M}_S \delta(h) \quad (1.34)$$

where  $h$  is a coordinate measured normal from the interface. Eq (1.33) then gives:

$$\Delta E_{E_2} - \Delta E_{E_1} = -\Delta M_{M_S} \text{ or } E_1 - E_2 = -M_S \quad (1.35)$$

which can be generalized in the vector form as:

$$(\bar{E}_2 - \bar{E}_1) \times \hat{n} = \bar{M}_S \quad (1.36)$$

A similar argument for the magnetic field leads to:

$$\hat{n} \times (\bar{H}_2 - \bar{H}_1) = \bar{J}_S \quad (1.37)$$

where  $\bar{J}_S$  is an electric surface current density that may exist at the interface. Eq (1.31), (1.32), (1.35), (1.36), and (1.37) are the most general expressions for the boundary conditions at an arbitrary interface of materials and/or surface currents.

#### - Fields at a Dielectric Interface.

At an interface between two lossless dielectric materials, no charge or surface current densities will ordinarily exist. Equations (1.31), (1.32), (1.36), and (1.37) then reduce to:

$$\hat{n} \cdot \bar{D}_1 = \hat{n} \cdot \bar{D}_2 \quad (1.38a)$$

$$\hat{n} \cdot \bar{B}_1 = \hat{n} \cdot \bar{B}_2 \quad (1.38b)$$

$$\hat{n} \times \bar{E}_1 = \hat{n} \times \bar{E}_2 \quad (1.38c)$$

$$\hat{n} \times \bar{H}_1 = \hat{n} \times \bar{H}_2 \quad (1.38d)$$

In other words, these equations state that the normal components of  $\bar{D}$  and  $\bar{B}$  are continuous across the interface, and the tangential components are continuous across the interface for  $\bar{E}$  and  $\bar{H}$ . Because Maxwell's equations are not linearly independent, the six boundary conditions contained in the above equations are not all linearly independent. Thus the enforcement of (1.38c) and (1.38d) for the four tangential field components, for example, will automatically force the satisfaction of the equations for the continuity of the normal components.

#### - Fields at the Interface with a Perfect Conductor (Electric Wall).

Many problems in microwave engineering involve boundaries with good conductors, which can often be assumed as lossless ( $\sigma \rightarrow \infty$ ). In this case of a perfect conductor, all field components must be zero inside the conducting region. This result can be seen by considering a conductor with finite conductivity ( $\sigma < \infty$ ) and noting that the skin depth (the depth at which most the microwave power penetrates) goes to zero as  $\sigma \rightarrow \infty$ . (Such analysis will be performed in Section 1.7.) If we also assume here that  $\bar{J}_S = 0$ , which would be the case if the perfect conductor filled all the space on one side of the boundary, then (1.31), (1.32), (1.36), (1.37) reduce to the following:

$$\hat{n} \cdot \bar{D} = \bar{J}_S \quad (1.39a)$$

$$\hat{n} \cdot \bar{B} = 0 \quad (1.39b)$$

$$\hat{n} \times \bar{E} = 0 \quad (1.39c)$$

$$\hat{n} \times \bar{H} = \bar{J}_S \quad (1.39d)$$

where  $\bar{J}_S$  and  $\bar{J}_S$  are the electric surface charge density and current density, respectively, on the interface, and  $\hat{n}$  is the normal unit vector pointing out of the perfect conductor. Such a boundary is also known as an electric wall since the tangential components of  $\bar{E}$  are "shorted out", as seen from (1.39c), and must vanish at the surface of the conductor.

#### The Magnetic Wall Boundary Condition

Dual to the preceding boundary condition is the magnetic wall boundary condition, where the tangential components of  $\bar{H}$  must vanish. Such a boundary does not really exist in practice but may be approximated by a corrugated surface or in certain planar transmission line problems. In addition, the idealization that  $\hat{n} \times \bar{H} = 0$  at an interface is often a convenient simplification, as we will see in later chapters.

We will also see that the magnetic wall boundary condition is analogous to the relations between the voltage and current at the end of an open-circuited transmission line, while the electric wall boundary condition is analogous to the voltage and current at the end of a short-circuited transmission line. The magnetic wall condition, then, provides a completeness in our formulation of boundary conditions and is a useful approximation in several cases of practical interest.

The fields at a magnetic wall satisfy the following conditions:

$$\hat{n} \cdot \bar{D} = 0 \quad (1.40a)$$

$$\hat{n} \cdot \bar{B} = 0 \quad (1.40b)$$

$$\hat{n} \times \bar{E} = -\bar{M}_S \quad (1.40c)$$

$$\hat{n} \times \bar{H} = 0 \quad (1.40d)$$

where  $\hat{n}$  is the normal unit vector pointing out of the magnetic wall region.

**- The Radiation Condition** / When dealing with problems that have one or more infinite boundaries, such as plane waves in an infinite medium, or infinitely long transmission lines, a condition on the fields at infinity must be enforced. This boundary condition is known as the radiation condition and is essentially a statement of energy conservation. It states that, at an infinite distance from a source, the fields must be vanishingly small (zero) or propagate in an outward direction. This result can be seen by allowing the infinite medium to contain a small loss factor (as any physical medium would have). Incoming waves (from infinity) of finite amplitude would then require an infinite source at infinity and so are disallowed.

#### 1.4 The Wave Equation and Basic Plane Wave Solutions

**The Helmholtz Equation** / In a source-free, linear, isotropic, homogeneous region, Maxwell's curl equations in phasor form are:  $\nabla \times \bar{E} = -j\omega \mu \bar{H} \quad (1.41a)$

$$\nabla \times \bar{H} = j\omega \epsilon \bar{E} \quad (1.41b)$$

and constitute two equations for the two unknowns,  $\bar{E}$  and  $\bar{H}$ . As such they can be solved for either  $\bar{E}$  or  $\bar{H}$ . Taking the curl of (1.41a) and using (1.41b) gives

$$\nabla \times \nabla \times \bar{E} = -j\omega \mu \nabla \times \bar{H} = \omega^2 \mu \epsilon \bar{E}$$

which is an equation for  $\bar{E}$ . This result can be simplified through the use of vector identity (B.14),  $\nabla \times \nabla \times \bar{A} = \nabla(\nabla \cdot \bar{A}) - \nabla^2 \bar{A}$ , which is valid for the rectangular components of an arbitrary vector  $\bar{A}$ . Then,

$$\left\{ \begin{array}{l} \nabla \times \nabla \times E = -j\omega \mu \nabla \times H = \omega^2 \mu E \bar{E} \\ \nabla \times \nabla \times A = \nabla(\nabla \cdot \bar{A}) - \nabla^2 \bar{A} \end{array} \right. \Rightarrow \nabla \times \nabla \times E = \nabla(\nabla \cdot \bar{E}) - \nabla^2 \bar{E} = \omega^2 \mu E \bar{E}$$

$$\nabla \cdot \bar{E} = 0 \text{ in a source free region } \Rightarrow \nabla^2 \bar{E} + \omega^2 \mu E \bar{E} = 0 \quad (1.42)$$

Equation 1.42 is the wave equation, or Helmholtz equation, for  $\bar{E}$ . An identical equation for  $\bar{H}$  can be derived in the same manner:  $\nabla^2 \bar{H} + \omega^2 \mu E \bar{E} \bar{H} = 0$  (1.43)

$$\text{Helmholtz wave: } \left\{ \begin{array}{l} \nabla^2 \bar{E} + \omega^2 \mu E \bar{E} = 0 \\ \nabla^2 \bar{H} + \omega^2 \mu E \bar{E} \bar{H} = 0 \end{array} \right. \quad (1.42)$$

$$\text{equations: } \left\{ \begin{array}{l} \nabla^2 \bar{H} + \omega^2 \mu E \bar{E} \bar{H} = 0 \end{array} \right. \quad (1.43)$$

A constant  $k = \omega/c$  is defined as the propagation constant (also known as the phase constant or wave number), of the medium; its units are 'm.

As a way of introducing wave behaviour, we will next study the solutions to the above wave equations in their simplest forms, first for a lossless medium and next, for a lossy (conducting) medium.

-Plane Waves in a Lossless Medium / In a lossless medium,  $\epsilon$  and  $\mu$  are real numbers, and so  $k$  is real. A basic plane wave solution to the above wave equations can be found by considering an electric field with only an  $x$  component and uniform in the  $x$  and  $y$  directions. Then  $\partial E_x / \partial y = 0$ , and the Helmholtz equation of (1.42) reduces to

$$\frac{\partial^2 E_x}{\partial z^2} + k^2 E_x = 0 \quad (1.44)$$

The two independent solutions of this equation are easily seen, by substitution, to be of the form

$$E_x(z) = E^+ e^{-jkz} + E^- e^{jkz} \quad (1.45)$$

where  $E^+$  and  $E^-$  are arbitrary amplitude constants.

The above solution is for the time harmonic case at frequency  $\omega$ . In the time domain, this result is written as

$$E_x(z,t) = E^+ \cos(\omega t - kz) + E^- \cos(\omega t + kz) \quad (1.46)$$

where we have assumed that  $E^+$  and  $E^-$  are real constants. Consider the first term in (1.46), this term represents a wave traveling in the  $+z$  direction because, to maintain a fixed point on the wave ( $\omega t - kz = \text{constant}$ ), one must move in the  $+z$  direction as time increases. Similarly, the second term in (1.46) represents a wave traveling in the negative  $z$  direction - hence a notation  $E^+$  and  $E^-$  for these wave amplitudes. The velocity of the wave in this sense is called a phase velocity because it is a velocity at which a fixed phase point on the wave travels, and is given by

$$v_p = \frac{dz}{dt} = \frac{d}{dt} \left( \frac{\omega t - \text{constant}}{k} \right) = \frac{\omega}{k} = \frac{1}{\sqrt{\mu\epsilon}} \quad (1.47)$$

In free space we have the phase velocity  $v_p = 1/\sqrt{\mu_0\epsilon_0} = c = 2.998 \cdot 10^8 \text{ m/sec}$ , which is the speed of light.

The wavelength,  $\lambda$ , is defined as the distance between two successive maxima (or minima, or any other reference points) on the wave at a fixed instant in time. Thus,

$$(\omega t - kz_1) - (\omega t - kz_2) = 2\pi \quad (1.48)$$

so

$$\lambda = \frac{2\pi}{k} = \frac{2\pi v_p}{\omega} = \frac{v_p}{f} \quad (1.48)$$

A complete specification of the plane wave electromagnetic field should include the magnetic field. In general, whenever  $\bar{E}$  or  $\bar{H}$  is known, the other field vector can be readily found by using one of Maxwell's curl equations. Thus, applying (1.41a) to the electric field of (1.45) gives  $H_x = H_z = 0$ , and

$$H_y = \frac{j}{\omega \mu} \frac{\partial E_x}{\partial z} = \frac{1}{\eta} (E^+ e^{-jkz} - E^- e^{jkz}) \quad (1.49)$$

where  $\eta = \omega \mu / k = \sqrt{\mu/\epsilon}$  is known as the intrinsic impedance of the medium. The ratio of the  $\bar{E}$  or  $\bar{H}$  field components is seen to have units of impedance, known as wave impedance; for planes waves the wave impedance is equal to the intrinsic impedance of the medium. In free-space the intrinsic impedance is  $\eta = \sqrt{\mu_0/\epsilon_0} = 377 \Omega$ . Note that the  $\bar{E}$  and  $\bar{H}$  vectors are orthogonal to each other and orthogonal to the direction of propagation ( $\pm z$ ); this is a characteristic of transverse electromagnetic (TEM) waves.

### - Example 1.1 Basic Wave Parameters

A plane wave propagating in a lossless dielectric medium has an electric field given as  $E_x = E_0 \cos(\omega t - kz)$  with a frequency of 5.0 GHz and a wavelength in the material of 3.0 cm. Determine the propagation constant, the phase velocity, the relative permittivity of the medium, and the wave impedance.

Solution

From (1.48) the propagation constant is  $k = \frac{2\pi}{\lambda} = \frac{2\pi}{0.03} = 209.4 \text{ m}^{-1}$ , and from (1.47) the phase velocity is  $v_p = \frac{\omega}{k} = \frac{2\pi f}{k} = \lambda f = (0.03)(5 \times 10^9) = 1.5 \cdot 10^8 \text{ m/s}$ .

This is slower than the speed of light by a factor of 2.0. The relative permittivity of the medium can be found in (1.47) as

$$\epsilon_r = \left( \frac{c}{v_p} \right)^2 = \left( \frac{3.0 \times 10^8}{1.5 \times 10^8} \right)^2 = 4.0$$

The wave impedance is

$$\eta = \eta_0 = \frac{377}{\sqrt{\epsilon_r}} = 188.5 \Omega$$

## Plane Waves in a General Lossy Medium

Now consider the effect on a lossy medium. If the medium is conductive, with a conductivity  $\sigma$ , Maxwell's curl equations can be written, from (1.4)(a) and (1.20) as

$$\left\{ \begin{array}{l} \nabla \times \bar{E} = -j\omega \mu \bar{H} \\ \nabla \times \bar{H} = j\omega \epsilon \bar{E} + \sigma \bar{E} \end{array} \right. \Rightarrow \nabla \times \bar{E} = -j\omega \mu \bar{H} \quad (1.50a)$$

$$\nabla \times \bar{H} = j\omega \epsilon \bar{E} + \sigma \bar{E} \quad (1.50b)$$

The resulting wave equation for  $\bar{E}$  then becomes

$$\boxed{\nabla^2 \bar{E} + \omega^2 \mu \epsilon \left(1 - \frac{j\sigma}{\omega \epsilon}\right) \bar{E} = 0}. \quad \text{I am going to try deriving this for my own practice.}$$

$$\nabla \times \nabla \times \bar{A} = \nabla (\nabla \cdot \bar{A}) - \nabla^2 \bar{A}$$

$$\text{So taking the curl of } \nabla \times \bar{E} \Rightarrow \nabla \times \nabla \times \bar{E} \Rightarrow \nabla \times \nabla \times \bar{E} = \nabla \cdot (\nabla \cdot \bar{E}) - \nabla^2 \bar{E}$$

$$\text{We also can take the curl of the statement } ' \nabla \times \bar{E} = -j\omega \mu \bar{H}'$$

$$\Rightarrow \nabla \times \nabla \times \bar{E} = -j\omega \mu \nabla \times \bar{H}, \quad \nabla \times \bar{H} = +j\omega \epsilon \bar{E} + \sigma \bar{E} \Rightarrow \nabla \times \nabla \times \bar{E} = -j\omega \mu [ +j\omega \epsilon \bar{E} + \sigma \bar{E} ]$$

$$\Rightarrow \nabla \times \nabla \times \bar{E} = -j^2 \omega^2 \mu \epsilon \bar{E} - j\omega \mu \sigma \bar{E} = +\omega^2 \mu \epsilon \bar{E} - j\omega \mu \sigma \bar{E}$$

$$\Rightarrow \nabla \times \nabla \times \bar{E} = -\omega^2 \mu \epsilon \left(1 + j \frac{\sigma}{\omega \epsilon}\right) \bar{E}$$

$$\nabla \times \nabla \times \bar{E} = \nabla (\nabla \cdot \bar{E}) - \nabla^2 \bar{E} \Rightarrow \nabla (\nabla \cdot \bar{E}) - \nabla^2 \bar{E} = +\omega^2 \mu \epsilon j^2 \bar{E} - j\omega \mu \sigma \bar{E}$$

$$\text{assuming no sources so } (\nabla \cdot \bar{E} = 0) \Rightarrow \nabla (\nabla \cdot \bar{E}) = -j^2 \omega^2 \mu \epsilon \bar{E} - j\omega \mu \sigma \bar{E} + \nabla^2 \bar{E}$$

$$\Rightarrow \nabla^2 \bar{E} + \omega^2 \mu \epsilon \bar{E} - j\omega \mu \sigma \bar{E} = 0$$

$$\boxed{\nabla^2 \bar{E} + \omega^2 \mu \epsilon \left(1 - j \frac{\sigma}{\omega \epsilon}\right) \bar{E} = 0} \quad (1.51)$$

where we see a similarity with (1.42). The wave equation for  $\bar{E}$  in the lossless case,

The difference is that the quantity  $K^2 = \omega^2 \mu \epsilon$  of (1.42) is replaced by  $\omega^2 \mu \epsilon \left[1 - j(\sigma/\omega \epsilon)\right]$  in (1.51). We then define a complex propagation constant for the medium as

$$\gamma = \alpha + j\beta = j\omega \sqrt{\mu \epsilon} \sqrt{1 - j\frac{\sigma}{\omega \epsilon}} \quad (1.52)$$

where  $\alpha$  is the attenuation constant and  $\beta$  is the phase constant. If we again assume an electric field with only an  $\hat{x}$  component and uniform in  $x$  and  $y$ , the wave equation of (1.51) reduces to

$$\frac{j^2 E_x}{z^2} - \gamma^2 E_x = 0 \quad (1.53)$$

$$\text{which has solutions } E_x(z) = E^+ e^{-\gamma z} + E^- e^{\gamma z} \quad (1.54)$$

The positive traveling wave then has a propagation factor of the form

$$e^{-\gamma z} = e^{-\alpha z} e^{-j\beta z}$$

which in the time domain is of the form

$$e^{-\alpha z} \cos(\omega t - j\beta z)$$

We see that this represents a wave traveling in the  $+z$  direction with a phase velocity  $v_p = \omega/\beta$ , a wavelength  $\lambda = 2\pi/\beta$ , and an exponential dampening factor. The rate of decay which distance is given by the attenuation constant,  $\alpha$ . The negative traveling wave term of (1.54) is similarly damped along the  $-z$  axis. If the loss is removed,  $\sigma=0$ , and we have  $\gamma=jk$  and  $\alpha=0$ ,  $\beta=k$ .

As discussed in Section 1.3, loss can also be treated through the use of a complex permittivity. From (1.52) and (1.20) with  $\sigma=0$  but  $\epsilon = \epsilon' - j\epsilon''$  complex, we have that

$$\gamma = -j\omega \sqrt{\mu \epsilon} = jk = j\omega \sqrt{\mu \epsilon' (1 - j\alpha/\omega)} \quad (1.55)$$

where  $\tan \delta = \epsilon''/\epsilon'$  is the loss tangent of the material.

The associated magnetic field can be calculated as

$$H_y = -j \frac{\partial E_x}{\partial z} = \frac{-j\gamma}{\omega \mu} (E^+ e^{-\gamma z} - E^- e^{\gamma z}) \quad (1.56)$$

The intrinsic impedance of the conducting medium is now complex,

$$\eta = \frac{j\omega \mu}{\gamma} \quad (1.57)$$

but is still identified as the wave impedance, which expresses the ratio of electric to magnetic field components. This allows (1.56) to be written as

$$H_y = \frac{1}{\eta} (E^+ e^{-\gamma z} - E^- e^{\gamma z}) \quad (1.58)$$

Note that although  $\eta$  of (1.57) is, in general, complex, it reduces to the lossless case of  $\eta = \sqrt{\mu/\epsilon}$  when  $\gamma = jk = j\omega \sqrt{\mu \epsilon}$

## Plane Waves in a Good Conductor

Many problems of practical interest involve loss or attenuation due to good (but not perfect) conductors. A good conductor is a special case in the preceding analysis, where the conductive current is much greater than the displacement current, which means that  $\sigma \gg \omega \epsilon$ . Most metals can be categorized as good conductors. In terms of a complex  $\epsilon$ , rather than conductivity, this condition is equivalent to  $\epsilon'' > \epsilon'$ . The propagation constant of (1.52) can then be adequately approximated by ignoring the displacement current term, to give:

$$\gamma = \alpha + j\beta \approx j\omega \sqrt{\mu \epsilon} \sqrt{\frac{\sigma}{\omega \epsilon}} = (1 + j) \sqrt{\frac{\omega \mu \sigma}{2}} \quad (1.59)$$

The skin depth, or characteristic depth of penetration, is defined as

$$\delta_s = \frac{1}{\alpha} = \sqrt{\frac{2}{\omega \mu \sigma}} \quad (1.60)$$

Thus the amplitude of the  $\bar{E}$  fields in the conductor will decay by the amount  $1/e$ , or 36.8%, after traveling a distance of one skin depth, because  $e^{-\gamma z} = e^{-\alpha z} e^{-j\beta z} = e^{-\alpha z}$ . At microwave frequencies, for a good conductor, this distance is very small. The practical importance of this result is that only a thin plating of a good conductor (e.g. Silver or gold) is necessary for low-loss microwave components.

### Example 1.2 Skin Depth at Microwave Frequencies

Compute the skin depth of aluminum, copper, gold, and silver at a frequency of 10 GHz.

**Solution /** The conductivities for these metals are listed in Appendix F. Equation (1.60) gives the

$$\text{Skin depth as } \delta_s = \sqrt{\frac{2}{\omega \mu \sigma}} = \sqrt{\frac{1}{\pi \epsilon_0 \mu_0 \sigma}} = \sqrt{\frac{1}{\pi (10^{10})/(4\pi \times 10^{-7})}} \sqrt{\frac{1}{\sigma}} = 5.03 \cdot 10^{-3} \sqrt{\frac{1}{\sigma}}$$

$$\text{For aluminum: } \delta_s = 5.03 \cdot 10^{-3} \sqrt{\frac{1}{3.816 \cdot 10^7}} = 8.14 \cdot 10^{-7} \text{ m}$$

$$\text{for copper: } \delta_s = 5.03 \cdot 10^{-3} \sqrt{\frac{1}{5.818 \cdot 10^7}} = 6.60 \cdot 10^{-7} \text{ m}$$

$$\text{for gold: } \delta_s = 5.03 \cdot 10^{-3} \sqrt{\frac{1}{4.093 \cdot 10^7}} = 7.86 \cdot 10^{-7} \text{ m}$$

$$\text{For silver: } \delta_s = 5.03 \cdot 10^{-3} \sqrt{\frac{1}{6.173 \cdot 10^7}} = 6.40 \cdot 10^{-7} \text{ m}$$

These results show that most of the current flow in a good conductor occurs in an extremely thin region near the surface of the conductor.

Quantity	Type of Medium	
Complex propagation constant	$\gamma = j\omega \sqrt{\mu \epsilon}$	General Lossy
Phase constant (wave number)	$\beta = k = \omega \sqrt{\mu \epsilon}$	Good Conductor ( $\epsilon'' \gg \epsilon'$ or $\sigma \gg \omega \epsilon'$ )
Affection Constant	$a = 0$	$a = \operatorname{Re}\{\gamma\} = \sqrt{\omega \mu / 2}$
Impedance	$\eta = \sqrt{\mu/\epsilon} = \omega \mu/k$	$\eta = j\omega \mu / \beta$
Skin depth	$\delta_s = \infty$	$\delta_s = 1/a$
Wavelength	$\lambda = 2\pi/\beta$	$\lambda = 2\pi/\beta$
Phase velocity	$v_p = \omega/\beta$	$v_p = \omega/\beta$

The intrinsic impedance inside a good conductor can be obtained from (1.57) and (1.59). The result is:

$$\eta = \frac{j\omega \mu}{\gamma} \approx (1+j) \sqrt{\frac{\omega \mu}{2\sigma}} = (1+j) \frac{1}{\sigma \delta_s} \quad (1.61)$$

Notice that the phase angle of this impedance is  $45^\circ$ , a characteristic of good conductors. The phase angle of this impedance for a lossless material is  $0^\circ$ , and the phase angle of the impedance of an arbitrary lossy medium is somewhere between  $0^\circ$  and  $45^\circ$ .

Table 1.1 summarizes the results for plane wave propagation in lossless and lossy homogeneous media.

**1.5 General Plane Wave Solutions /** Some specific features of plane waves were discussed in Section 1.4, but we will now look at plane waves from a more general point of view and solve the wave equation by the method of separation of variables. This technique will find application in succeeding chapters. We will also discuss circularly polarized waves, which will be important for the discussion of satellites in chapter 9.

In free-space, the Helmholtz equation for  $E$  can be written as

$$\nabla^2 E + k_0^2 E = \frac{\partial^2 E}{\partial x^2} + \frac{\partial^2 E}{\partial y^2} + \frac{\partial^2 E}{\partial z^2} + k_0^2 E = 0 \quad (1.62)$$

and this vector wave equation holds for each rectangular component  $\hat{e}^i E$ :

$$\frac{\partial^2 E_i}{\partial x^2} + \frac{\partial^2 E_i}{\partial y^2} + \frac{\partial^2 E_i}{\partial z^2} + k_0^2 E_i = 0 \quad (1.63)$$

where the index  $i = x, y, \text{ or } z$ . This equation can be solved with a method known as separation of variables, a standard technique for treating such partial differential equations. The method begins by assuming that the solution to (1.63) for, say,  $E_x$ , can be written as a product of three functions for each of the three coordinates,

$$E_x(x, y, z) = f(x)g(y)h(z) \quad (1.64)$$

Substituting this form into (1.63) and dividing by  $fgh$  gives

$$\frac{f''}{f} + \frac{g''}{g} + \frac{h''}{h} + k_0^2 = 0 \quad (1.65)$$

where the double primes denote the second derivative. The key step in the argument is to recognize that each of the terms in (1.65) must be equal to a constant because they are independent of each other. That is,  $f''/f$  is only a function of  $x$ , and the remaining terms in (1.65) do not depend on  $x$ , so  $f''/f$  must be a constant, and similarly for the other terms in (1.65). Thus we define three separate constants,  $k_x$ ,  $k_y$ , and  $k_z$ , such that

$$f''/f = -k_x^2; \quad g''/g = -k_y^2; \quad h''/h = -k_z^2.$$

or

$$\frac{d^2 f}{dx^2} + k_x^2 f = 0; \quad \frac{d^2 g}{dy^2} + k_y^2 g = 0; \quad \frac{d^2 h}{dz^2} + k_z^2 h = 0 \quad (1.66)$$

Combining (1.65) and (1.66) shows that

$$k_x^2 + k_y^2 + k_z^2 = k_0^2 \quad (1.67)$$

These partial differential equations of (1.63) has been reduced to three separate ordinary differential equations in (1.66). Solutions to these equations have the forms  $e^{\pm jk_x x}$ ,  $e^{\pm jk_y y}$ , and  $e^{\pm jk_z z}$ , respectively. As we saw in the previous section, the terms with  $+$  signs result in waves traveling in the  $x$ ,  $y$ , or  $z$  direction, while the terms with  $-$  signs result in waves traveling in the positive direction. Both solutions are possible and are valid. The amount to which these various terms are excited is dependent on the source of the fields and the boundary conditions. For our present discussion we will select a plane wave traveling in the  $+z$  direction for each coordinate and

- write the complete solution for  $E_x$  as:

$$E_x(x, y, z) = A e^{-j(k_x x + k_y y + k_z z)} \quad (1.68)$$

where  $A$  is an arbitrary amplitude constant. Now define a wave number vector  $\vec{k}$  as

$$\vec{k} = k_x \hat{x} + k_y \hat{y} + k_z \hat{z} = k_0 \hat{n} \quad (1.69)$$

Then from (1.67),  $|k| = k_0$ , and so  $\hat{n}$  is a unit vector in the direction of propagation. Also define a position vector as

$$\vec{r} = x \hat{x} + y \hat{y} + z \hat{z} \quad (1.70)$$

then (1.68) can be written as

$$E_x(x, y, z) = A e^{-j\vec{k} \cdot \vec{r}} \quad (1.71)$$

Solutions to (1.63) for  $E_y$  and  $E_z$  are, of course, similar to the  $E_x$  of (1.71), but with different amplitude constants:  $E_y(x, y, z) = B e^{-j\vec{k} \cdot \vec{r}}$   $(1.72)$

$$E_z(x, y, z) = C e^{-j\vec{k} \cdot \vec{r}} \quad (1.73)$$

The  $x, y, z$  dependencies of the three components of  $E$  in (1.71)-(1.73) must be the same (same  $k_x, k_y, k_z$ ). Because the divergence condition that

$$\nabla \cdot \vec{E} = \frac{\partial E_x}{\partial x} + \frac{\partial E_y}{\partial y} + \frac{\partial E_z}{\partial z} = 0$$

must also be applied in order to satisfy Maxwell's equations, and this implies that  $E_x, E_y$ , and  $E_z$  must have the same variation in  $x, y, z$ . (Note that the solutions in the preceding section automatically satisfied the divergence condition because  $E_x$  was the only component of  $E$ , and  $E_x$  did not vary with  $x$ .) This condition also imposes a constraint on the amplitude  $A, B$ , and  $C$  because if

$$\vec{E}_0 = A \hat{x} + B \hat{y} + C \hat{z}$$

we have

$$\vec{E} = \vec{E}_0 e^{-j\vec{k} \cdot \vec{r}}$$

and

$$\nabla \cdot \vec{E} = \nabla \cdot (\vec{E}_0 e^{-j\vec{k} \cdot \vec{r}}) = \vec{E}_0 \cdot \nabla e^{-j\vec{k} \cdot \vec{r}} = -j\vec{k} \cdot \vec{E}_0 e^{-j\vec{k} \cdot \vec{r}} = 0$$

where vector identity (B.7) was used.  $[\nabla \cdot (\vec{r} \vec{A}) = \vec{A} \cdot \nabla \vec{r} + \vec{r} \cdot \nabla \vec{A}]$

$$\text{Thus we must have } \vec{k} \cdot \vec{E}_0 = 0 \quad (1.74)$$

which means that the electric field amplitude vector  $\vec{E}_0$  must be perpendicular to the direction of propagation,  $\vec{k}$ . This condition is a general result for which plane waves and implies that only two of the three amplitude constants,  $A, B, C$ , can be chosen independently. The magnetic field can be found from Maxwell's equation,

$$\nabla \times \vec{E} = -j\omega_0 \mu_0 \vec{H} \quad (1.75)$$

$$\text{to give: } \vec{H} = \frac{j}{\omega_0 \mu_0} \nabla \times \vec{E} = \frac{j}{\omega_0 \mu_0} \nabla \times (\vec{E}_0 e^{-j\vec{k} \cdot \vec{r}}) = \frac{-j}{\omega_0 \mu_0} \vec{E}_0 \times \nabla e^{-j\vec{k} \cdot \vec{r}}$$

$$\Rightarrow \vec{H} = \frac{-j}{\omega_0 \mu_0} \vec{E}_0 \times (-j\vec{k}) e^{-j\vec{k} \cdot \vec{r}} = \frac{k_0}{\omega_0 \mu_0} \hat{n} \times \vec{E}_0 e^{-j\vec{k} \cdot \vec{r}}$$

$$\Rightarrow \frac{1}{\eta_0} \hat{n} \times \vec{E}_0 e^{-j\vec{k} \cdot \vec{r}} = \frac{1}{\eta_0} \hat{n} \times \vec{E} \quad (1.76)$$

where vector identity (B.9) was used in obtaining the second line. This result shows that the magnetic field vector  $\vec{H}$  lies in a plane normal to  $\vec{k}$ , the direction of propagation, and that  $\vec{H}$  lies in a plane normal to  $\vec{E}$ , the direction of propagation, and that  $\vec{H}$  is perpendicular to  $\vec{E}$ . See figure 1.8 for an illustration of these vector relations. The quantity  $\eta_0 = \sqrt{\mu_0/\epsilon_0} = 877.0$  in (1.76) is the intrinsic impedance of free-space. The time domain expression for the electric field can be found as

$$\begin{aligned} \vec{E}(x, y, z, t) &= \operatorname{Re}\{\vec{E}(x, y, z)e^{j\omega t}\} = \operatorname{Re}\{\vec{E}_0 e^{-j\vec{k} \cdot \vec{r}} e^{j\omega t}\} \\ &= \vec{E}_0 \cos(\vec{k} \cdot \vec{r} - \omega t) \end{aligned} \quad (1.77)$$

assuming that the amplitude constants  $A, B, C$  contained in  $\vec{E}_0$  are real. If these constants are not real, their phases should be included inside the cosine form of (1.77). It is easy to show that the wavelength and phase velocity for this solution are the same as obtained in section 1.4. B9:  $[\nabla \times (\vec{F} \vec{A}) = (\vec{F} \vec{A}) \times \vec{A} + \vec{A} \times \nabla \vec{A}]$

### - Example 1.3 Current Sheets as Sources of Plane Waves

An infinite sheet of surface current can be considered as a source for plane waves. If an electric surface current density  $\vec{J}_s = J_0 \hat{x}$  exists on the  $z=0$  plane in free space, finding the resulting fields by assuming plane waves on either side of the current sheet and enforcing boundary conditions.

Solution / Since the source does not vary with  $x$  or  $y$ , the fields will not vary with  $x$  or  $y$  but will propagate away from the source in the  $\pm z$  direction. The boundary conditions to be satisfied at  $z=0$  are:  $\{\hat{x} \times (\vec{E}_+ - \vec{E}_-) = \hat{z} \times (\vec{E}_+ - \vec{E}_-) = 0,$

$$\hat{x} \times (\vec{H}_+ - \vec{H}_-) = \hat{z} \times (\vec{H}_+ - \vec{H}_-) = J_s \hat{x}$$

where  $\vec{E}_+$ ,  $\vec{H}_+$  are the fields for  $z < 0$ , and  $\vec{E}_-$ ,  $\vec{H}_-$  are the fields for  $z > 0$ . To satisfy the second condition,  $\vec{H}$  must have a  $\hat{y}$  component. Then for  $\vec{E}$  to be orthogonal to  $\vec{H}$  and  $\vec{z}$ ,  $\vec{E}$  must have an  $\hat{x}$  component. Thus the fields will have the following form:

$$\text{for } z < 0, \quad \vec{E}_+ = \hat{x} A \eta_0 e^{jk_0 z}, \quad \vec{H}_+ = -\hat{y} A e^{jk_0 z}$$

$$\text{for } z > 0, \quad \vec{E}_- = \hat{x} B \eta_0 e^{-jk_0 z}, \quad \vec{H}_- = \hat{y} B e^{-jk_0 z}$$

where  $A$  and  $B$  are arbitrary amplitude constants. The first boundary condition, that  $E_x$  is continuous at  $z=0$ , yields  $A=B$ , while the boundary condition for  $H$  yields the equation

$$-B + A = J_s$$

Solving for  $A, B$  gives

$$A = B = -J_s/2$$

which completes the solution.

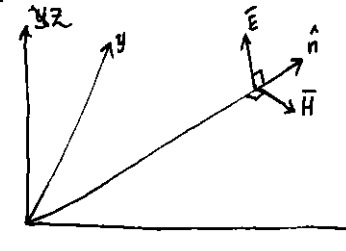


Figure 1.8 Orientation of the  $\vec{E}$ ,  $\vec{H}$ , and  $\vec{k} = k_0 \hat{n}$  vectors for a general plane wave.

**Circularly Polarized Waves** / The plane waves discussed previously all had their electric vector pointing in a fixed direction and so are called linearly polarized waves. In general, the polarization of a plane wave refers to the orientation of the electric field vector, which may be in a fixed direction or may change in time.

Consider the superposition of an  $\hat{x}$  linearly polarized wave with an amplitude  $E_1$  and a  $\hat{y}$  linearly polarized wave with amplitude  $E_2$ , both traveling in the positive  $\hat{z}$  direction, or say the total electric field can be written as:

$$\bar{E} = (E_1 \hat{x} + E_2 \hat{y}) e^{-jk_0 z} \quad (1.78)$$

A number of possibilities now arise. If  $E_1 \neq 0$  and  $E_2 = 0$ , we have a plane that is linearly polarized in the  $\hat{x}$  direction. Similarly, if  $E_1 = 0$  and  $E_2 \neq 0$ , we have a plane that is linearly polarized in the  $\hat{y}$  direction. If  $E_1$  and  $E_2$  are both real and non-zero, we have a plane wave linearly polarized at the angle  $\phi$  where:

$$\phi = \tan^{-1} \left( \frac{E_2}{E_1} \right)$$

For example if  $E_1 = E_2 = E_0$ , we have

$$\bar{E} = E_0 (\hat{x} + \hat{y}) e^{-jk_0 z}$$

which represents the electric field vector at  $45^\circ$  angle from the  $x$ -axis.

Now consider the case in which  $E_1 = jE_2 = E_0$ , where  $E_0$  is real. So that

$$\bar{E} = E_0 (\hat{x} - j\hat{y}) e^{-jk_0 z} \quad (1.79)$$

The time domain form of this field is

$$\bar{E}(z, t) = E_0 [\hat{x} \cos(\omega t - k_0 z) + \hat{y} \cos(\omega t - k_0 z - \pi/2)] \quad (1.80)$$

This expression shows that the electric field vector changes with time or equivalently, with distance along the  $z$ -axis. To see this, pick a fixed position, say  $z=0$ . Equation (1.80) then reduces to:

$$\bar{E}(0, t) = E_0 [\hat{x} \cos \omega t + \hat{y} \sin \omega t] \quad (1.81)$$

So as  $\omega t$  increases from zero, the electric field vector rotates counter-clockwise from the  $x$ -axis. The resulting angle from the  $x$ -axis of the electric field vector at time  $t$ , at  $z=0$ , is then:

$$\phi = \tan^{-1} \left( \frac{\sin \omega t}{\cos \omega t} \right) = \omega t$$

which shows that the polarization rotates at a uniform angular velocity  $\omega$ . Since the fingers of the right hand point in the direction of the rotation of the electric field vector when the thumb points in the direction of the rotation of the electric field vector when the thumb points in the direction of the propagation, this type of wave is referred to as right-hand circularly polarized (RHCP) wave. Similarly, a field of the form:

$$\bar{E} = E_0 (\hat{x} + j\hat{y}) e^{-jk_0 z} \quad (1.82)$$

constitutes a left-hand circularly polarized (LHCP) wave, where the electric field vector rotates in the opposite direction. See figure 1.9 for a sketch of the polarization vectors for RHCP and LHCP waves.

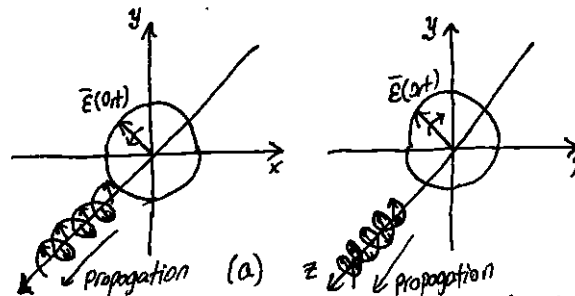


Figure 1.9 Electric field polarization for (a) RHCP (b) LHCP plane waves.

The magnetic field associated with the circularly polarized wave may be found from Maxwell's equations or by using the wave impedance applied to each component of the electric field. For example, applying (1.76) to the electric field of a RHCP wave as given in (1.79) yields:

$$\bar{H} = \frac{E_0}{\eta_0} \hat{z} \times (\hat{x} - j\hat{y}) e^{-jk_0 z} = \frac{E_0}{\eta_0} (\hat{y} + j\hat{x}) e^{-jk_0 z} = j \frac{E_0}{\eta_0} (\hat{x} - j\hat{y}) e^{-jk_0 z}$$

which is also seen to represent a vector rotating in the RHCP sense.

$$(1.76) \quad \bar{H} = \frac{1}{\eta_0} \hat{n} \times E_0 \hat{e}^{jkr} \quad (1.79) \quad \bar{E} = E_0 (\hat{x} - j\hat{y}) e^{-jk_0 z}$$

$$\left\{ \bar{H} = \frac{1}{\eta_0} \hat{n} \times \bar{E}, \langle 1.79 \rangle \Rightarrow \bar{H} = \frac{1}{\eta_0} \hat{n} \times [E_0 (\hat{x} - j\hat{y}) e^{-jk_0 z}] \right\}$$

but the direction of propagation is in the  $\hat{z}$  direction so:

$$\bar{H} = \frac{E_0}{\eta_0} \hat{z} \times (\hat{x} - j\hat{y}) e^{-jk_0 z} = \frac{E_0}{\eta_0} (\hat{y} + j\hat{x}) e^{-jk_0 z} = j \frac{E_0}{\eta_0} (\hat{x} + j\hat{y}) e^{-jk_0 z}$$

**1.6 Energy and Power** / In general, a source of electromagnetic energy sets up fields that store electric and magnetic energy and carry power that may be transmitted or dissipated as loss.

In the sinusoidal steady state case, the time-average stored electric energy in a volume  $V$  is given by

$$We = \frac{1}{4} \operatorname{Re} \int_V \bar{E} \cdot \bar{D}^* dV \quad (1.83)$$

which in the case of simple lossless isotropic, homogeneous, linear media, where  $\epsilon$  is a real scalar constant, reduces to:

$$We = \frac{\epsilon}{4} \int_V \bar{E} \cdot \bar{E}^* dV \quad (1.84)$$

Similarly, the time-averaged magnetic energy stored in the volume  $V$  is

$$Wm = \frac{1}{4} \operatorname{Re} \int_V \bar{H} \cdot \bar{B}^* dV \quad (1.85)$$

which becomes

$$Wm = \mu \int_V \bar{H} \cdot \bar{H}^* dV \quad (1.86)$$

for a real, constant, scalar,  $\mu$

We can now derive Poynting's theorem, which leads to energy conservation for electromagnetic fields and sources. If we have an electric current source  $\bar{J}_S$  and a conduction current  $\sigma\bar{E}$  as defined in (1.19), then the total electric current density is  $\bar{J} = \bar{J}_S + \sigma\bar{E}$ .

Multiplying (1.27a) by  $H^*$  and multiplying the conjugate of (1.27b) by  $E$  yields:

$$\bar{H}^* \cdot (\nabla \times \bar{E}) = -j\omega\mu |H|^2 - H^* \cdot \bar{M}_S,$$

$$\bar{E} \cdot (\nabla \times \bar{H}^*) = \bar{E} \cdot \bar{J}^* - j\omega\epsilon^* |E|^2 = \bar{E} \cdot \bar{J}_S^* + \sigma |E|^2 - j\omega\epsilon^* |\bar{E}|^2$$

with (1.27a):  $\nabla \times E = -j\omega\mu H - \bar{J}$  and (1.27b):  $\nabla \times H = j\omega\epsilon E + \bar{J}$

where  $\bar{M}_S$  is the magnetic source current. Using these two results in the vector identity (B.8)  $\langle B.8 \rangle: [\nabla \cdot (\bar{A} \times \bar{B}) = (\nabla \times \bar{A}) \cdot \bar{B} - (\nabla \times \bar{B}) \cdot \bar{A}]$  gives:

$$\nabla \cdot (\bar{E} \times \bar{H}^*) = \bar{H}^* \cdot (\nabla \times \bar{E}) - \bar{E} \cdot (\nabla \times \bar{H}^*) = -\sigma |\bar{E}|^2 + j\omega(\epsilon^* |E|^2 - \mu |H|^2) + \dots$$

$$\dots - (\bar{E} \cdot \bar{J}_S^* + \bar{H}^* \cdot \bar{M}_S)$$

Now integrate over a volume  $V$  and use the divergence theorem:

$$\int_V \nabla \cdot (\bar{E} \times \bar{H}^*) dV = \oint_S \bar{E} \times \bar{H}^* \cdot d\bar{s}$$

$$\Rightarrow -\sigma \int_V |\bar{E}|^2 dV + j\omega \int_V (\epsilon^* |E|^2 - \mu |H|^2) dV - \int_V (\bar{E} \cdot \bar{J}_S^* + \bar{H}^* \cdot \bar{M}_S) dV \quad (1.87)$$

where  $S$  is a closed surface enclosing the volume  $V$ , as shown in Figure 1.10. Allowing  $\epsilon = \epsilon' - j\epsilon''$  and  $\mu = \mu' - j\mu''$  to complete the complex To allow for loss, and Recomitting (1.87) gives:  $-\frac{1}{2} \int_V (\bar{E} \cdot \bar{J}_S^* + \bar{H}^* \cdot \bar{M}_S) dV = \frac{1}{2} \oint_S \bar{E} \times \bar{H}^* \cdot d\bar{s} + \frac{\sigma}{2} \int_V |\bar{E}|^2 dV$

$$+ \frac{\omega}{2} \int_V (\epsilon'' |E|^2 + \mu'' |H|^2) dV + j\frac{\omega}{2} \int_V (\mu |H|^2 - \epsilon' |E|^2) dV \quad (1.88)$$

This result is known as Poynting's theorem, after the physicist J.H. Poynting (1852-1914), and basically is a power-balance equation. Thus the integral on the left-hand side represents the complex power  $P_S$  delivered by the sources  $\bar{J}_S$  and  $\bar{M}_S$  inside  $S$ :

$$P_S = -\frac{1}{2} \int_V (\bar{E} \cdot \bar{J}_S^* + \bar{H}^* \cdot \bar{M}_S) dV \quad (1.89)$$

The first integral on the RHS of (1.88) represents complex power flow out of the closed surface  $S$ . If we define the quantity  $\bar{S}$ , called the Poynting vector, as

$$\bar{S} = \bar{E} \times \bar{H}^* \quad (1.90)$$

then this power can be expressed as

$$P_S = \frac{1}{2} \oint_S \bar{E} \times \bar{H}^* \cdot d\bar{s} = \frac{1}{2} \oint_S \bar{S} \cdot d\bar{s} \quad (1.91)$$



Figure 1.10 A Volume  $V$ , enclosed by the closed surface  $S$ , containing fields  $\bar{E}, \bar{H}$ , and current sources  $\bar{J}_S, \bar{M}_S$ .

The surface  $S$  in (1.91) must be a closed surface for this representation to be valid. The real parts  $P_S$  and  $P_E$  in (1.89) and (1.91) represent time-average powers.

The second and third integrals (1.88) are real quantities representing the time avg power dissipated in the volume  $V$  due to conductivity, dielectric, and magnetic losses. If we define this power  $P_E$  we have

$$P_E = \frac{\sigma}{2} \int_V |\bar{E}|^2 dV + \frac{\omega}{2} \int_V (\epsilon'' |E|^2 + \mu'' |H|^2) dV \quad (1.92)$$

which is sometimes referred to as Joule's law. The last integral in (1.88) can be seen to be related to the stored electric and magnetic energies, as defined in (1.84) and (1.86).

$$W_E = \frac{\epsilon}{4} \int_V \bar{E} \cdot \bar{E}^* dV, \quad W_M = \frac{\mu}{4} \int_V \bar{H} \cdot \bar{H}^* dV$$

With the above definitions, Poynting's theorem can be rewritten as

$$P_S = P_E + P_E + 2j\omega(W_M - W_E) \quad (1.93)$$

In words this complex power balance equation states that the power delivered by the sources ( $P_S$ ) is equal to the sum of the power transmitted through the surface ( $P_E$ ), the power lost to heat in the ~~the~~ Volume ( $P_E$ ) and  $2\omega$  the net reactive energy stored in the volume.

Power Absorbed by a Good Conductor / practical transmission lines involve imperfect conductors, leading to attenuation and power losses, as well as the generation of noise. To calculate loss and attenuation due to an imperfect conductor we must find the power dissipated in the conductor. We will show that this can be accomplished using only the fields at the surface of the conductor, which is a very helpful simplification when calculating attenuation.

Consider the geometry of Figure 1.11, which shows the interface between a lossless medium and a conductor. A field is incident from  $Z < 0$ , and the field penetrates into a conducting region,  $Z > 0$ . The real average power entering the conductor volume defined by the cross-sectional area  $S_0$  at the interface and the surface  $S$  is given from (1.81) as:

$$P_{avg} = \frac{1}{2} P_E \int_{S_0 + S} \bar{E} \times \bar{H}^* \cdot \hat{n} d\bar{s} \quad (1.94)$$

where  $\hat{n}$  is a unit normal vector pointing into the closed surface  $S_0 + S$ , and  $\bar{E}, \bar{H}$  are the fields over this surface.

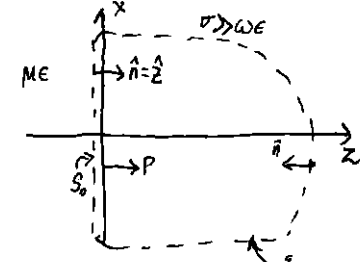


Figure 1.11 An Interface between a lossless medium and a good conductor with a closed Surface  $S_0 + S$  for computing the power dissipated in the Surface.

The contribution to the integral in (1.94) from the surface  $S$  can be made zero by proper selection of this surface. For example, if the field is a normally incident plane wave, the Poynting vector  $\vec{S} = \vec{E} \times \vec{H}^*$  will be in the  $\hat{z}$  direction, and so tangential to the top, bottom, front, and back of  $S$ , if these walls are made parallel to the  $z$ -axis. If the wave is obliquely incident, these walls can be slanted to obtain the result. If the conductor is good, the decay of the fields away from the interface at  $z=0$  will be very rapid, so the right-hand end of  $S$  can be made far enough away from  $z=0$  such that there is negligible contribution to the integral from this part of the surface  $S$ .

The time-average power entering through  $S$  to the conductor can be written as

$$P_{\text{avg}} = \frac{1}{2} \operatorname{Re} \int_{S_0} \vec{E} \times \vec{H}^* \cdot \hat{z} ds \quad (1.95)$$

From vector identity B3:

$$[\vec{A} \cdot \vec{B} \times \vec{C} = \vec{A} \times \vec{B} \cdot \vec{C} = \vec{C} \times \vec{A} \cdot \vec{B}] \text{ we have } \hat{z} \cdot (\vec{E} \times \vec{H}^*) = (\hat{z} \times \vec{E}) \cdot \vec{H}^* = \eta \vec{H} \cdot \vec{H}^* \quad (1.96)$$

Since  $\vec{H} = \hat{n} \times \vec{E}$ , as generalized form from (1.76) for conductive media, where  $\eta$  is the intrinsic impedance of the conductor. Equation 1.95 can be written as

$$P_{\text{avg}} = \frac{\eta_s}{2} \int_{S_0} |\vec{H}|^2 ds \quad (1.97)$$

$$\text{where } \eta_s = \operatorname{Re}\{\eta_s\} = \operatorname{Re} \left\{ (1+j) \sqrt{\frac{\omega \mu}{2\sigma}} \right\} = \sqrt{\frac{\omega \mu}{2\sigma}} = \frac{1}{\sigma \delta s} \quad (1.98)$$

is defined as the surface resistance of the conductor. The magnetic field  $\vec{H}$  in (1.97) is tangential to the conductor and needs to only be evaluated at the surface of the conductor. Since  $H_t$  is continuous at  $z=0$ , it does not matter whether this field is evaluated just outside the conductor or just inside the conductor. In the next section we will show how (1.97) can be evaluated in terms of a surface current density flowing on the surface of the conductor, where the conductor can be approximated as perfect.

### - 1.7 Plane wave reflection from a media interface.

A number of problems to be considered in later chapters involve the behaviour of electromagnetic fields at the interface of various types of media, including lossless media, lossy media, a good conductor, or a perfect conductor, and so it is beneficial at this time to study the reflection of a plane wave normally incident from free-space onto a half-space of an arbitrary material. The geometry is shown in Figure 1.12, where the material half-space  $z > 0$  is characterized by the parameters  $\epsilon_M$ ,  $\mu_M$ , and  $\sigma$ .

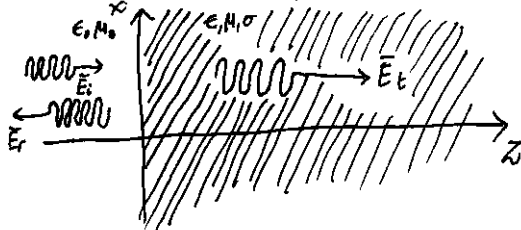


Figure 1.12 Plane wave reflection from an arbitrary medium; normal incidence.

**General Medium** / With no loss of generality we can assume that the incident plane wave has an electric field vector oriented along the  $x$ -axis and is propagating along the positive  $z$ -axis. The incident fields can be written, for  $z < 0$ , as:

$$\vec{E}_i = \hat{x} E_0 e^{-jk_0 z} \quad (1.99a)$$

$$\vec{H}_i = \hat{y} \frac{1}{\eta_0} E_0 e^{-jk_0 z} \quad (1.99b)$$

where  $\eta_0$  is the impedance of free-space and  $E_0$  is an arbitrary amplitude. Also in the region  $z < 0$ , a reflected wave may exist with the form:

$$\vec{E}_r = \hat{x} \Gamma E_0 e^{+jk_0 z} \quad (1.100a)$$

$$\vec{H}_r = -\hat{y} \Gamma E_0 e^{+jk_0 z} \quad (1.100b)$$

where  $\Gamma$  is the unknown reflection coefficient of the reflected electric field. Note that in (1.100), the sign of the exponential terms has been chosen to be positive, to represent waves traveling in the  $-\hat{z}$  direction of propagation, as clarified in Eq (1.46). This is also consistent with the Poynting vector  $S_r = \vec{E}_r \times \vec{H}_r^* = -|\Gamma|^2 E_0^2 \hat{z} / \eta_0$ , which shows power to be traveling in the  $-\hat{z}$  direction for the reflected wave.

As shown in Section 1.4, from equations (1.54) and (1.58), the transmitted fields for  $z > 0$  in a lossy medium can be written as

$$\vec{E}_t = \hat{x} T E_0 e^{-\gamma z} \quad (1.101a)$$

$$\vec{H}_t = \hat{y} T E_0 e^{-\gamma z} \quad (1.101b)$$

where  $T$  is the transmission coefficient of the transmitted electric field and  $\gamma$  is the intrinsic impedance (complex) of the lossy medium in the region  $z > 0$ . From (1.57) and (1.52) the intrinsic impedance is

$$\gamma = j\omega \mu \quad (1.102)$$

and the propagation constant is:  $\gamma = \alpha + j\beta = j\omega \sqrt{\mu \epsilon} \sqrt{1 - \sigma/\omega_0}$  (1.103)

We now have a boundary value problem where the form of the fields are given via (1.99)-(1.101) on either side of the material discontinuity at  $z=0$ . The two unknowns are constants  $\Gamma$  and  $T$  are found by applying boundary conditions for  $E_x$  and  $H_y$  at  $z=0$ . Since these tangential field components must be continuous at  $z=0$ , we arrive at the following two equations.

$$1 + \Gamma = T \quad (1.104a)$$

$$\frac{1 - \Gamma}{\eta_0} = \frac{T}{\eta} \quad (1.104b)$$

Solving these equations for the reflection and transmission coefficient gives

$$T = \frac{\eta - \eta_0}{\eta + \eta_0} \quad (1.105a)$$

$$\Gamma = 1 + T = \frac{2\eta}{\eta + \eta_0} \quad (1.105b)$$

This is a general solution for reflection and transmission of a normally incident wave at the interface of an arbitrary material, where  $\eta$  is the intrinsic impedance of the material. We now consider three special cases of this result.

### Lossless Medium

If the region for  $z > 0$  is a lossless dielectric, then  $\sigma = 0$ , and  $\mu$  and  $\epsilon$  are real quantities. The propagation constant in this case is purely imaginary and can be written as

$$\gamma = j\beta = j\omega\sqrt{\mu\epsilon} = jk_0\sqrt{\mu_r\epsilon_r} \quad (1.106)$$

where  $k_0 = \omega/c$  is the propagation constant (wavenumber) of a plane wave in free-space. The wavelength in the dielectric is

$$\lambda = \frac{2\pi}{\beta} = \frac{2\pi}{\omega\sqrt{\mu\epsilon}} = \frac{\lambda_0}{\sqrt{\mu_r\epsilon_r}} \quad (1.107)$$

The phase velocity is

$$v_p = \frac{\omega}{\beta} = \frac{1}{\sqrt{\mu\epsilon}} = \frac{c}{\sqrt{\mu_r\epsilon_r}} \quad (1.108)$$

(slower than the speed of light in free-space) and the intrinsic impedance of the dielectric is

$$\eta = \frac{\omega\mu}{\gamma} = \sqrt{\mu} = \eta_0\sqrt{\mu_r/\epsilon_r} \quad (1.109)$$

For this lossless case,  $\eta$  is real, so both  $\Gamma$  and  $T$  from (1.105) are real, and  $\bar{E}$  and  $\bar{H}$  are in phase with each other in both regions.

Power conservation for the incident, reflected, and transmitted waves can be demonstrated by computing the Poynting vectors in the two regions. Thus for  $z < 0$ , the complex Poynting vector is found from the total fields in the region as:

$$\begin{aligned} \bar{S}^+ &= \bar{E} \times \bar{H}^* = (\bar{E}_i + \bar{E}_r) \times (\bar{H}_i + \bar{H}_r)^* = \hat{z} |E_0|^2 \frac{1}{\eta_0} (e^{ik_0 z} + \Gamma e^{ik_0 z})(e^{-ik_0 z} - \Gamma^* e^{-ik_0 z})^* \\ &= \hat{z} |E_0|^2 \frac{1}{\eta_0} (1 - |\Gamma|^2 + \Gamma e^{2ik_0 z} - \Gamma^* e^{-2ik_0 z}) \end{aligned}$$

$$S^+ = \hat{z} |E_0|^2 \frac{1}{\eta_0} (1 - |\Gamma|^2 + 2i\Gamma \sin 2k_0 z) \quad (1.110a)$$

Since  $\Gamma$  is real, for  $z > 0$  the complex Poynting vector is

$$\bar{S}^+ = \bar{E}_t \times \bar{H}_t^* = \hat{z} |E_0|^2 \frac{1}{\eta} |\Gamma|^2 \quad (1.110b)$$

which can be rewritten, using (1.105) as:

$$S^+ = \hat{z} |E_0|^2 \frac{4\eta}{(\eta + \eta_0)^2} = \hat{z} |E_0|^2 \frac{1}{\eta_0} (1 - |\Gamma|^2) \quad (1.110b)$$

Now observe that at  $z=0$ ,  $\bar{S}^- = \bar{S}^+$ , so the complex power flow is conserved across the interface. Next consider the time-average power-flux in the two regions. For  $z < 0$  the time average power-flow through a  $1m^2$  cross section is

$$P^- = \frac{1}{2} \operatorname{Re} \{ \bar{S}^- \cdot \hat{z} \} = \frac{1}{2} |E_0|^2 \frac{1}{\eta_0} (1 - |\Gamma|^2) \quad (1.111a)$$

and for  $z > 0$ , the time average power flow through a  $1m^2$  cross section is

$$P^+ = \frac{1}{2} \operatorname{Re} \{ \bar{S}^+ \cdot \hat{z} \} = \frac{1}{2} |E_0|^2 \frac{1}{\eta_0} (1 - |\Gamma|^2) = P^- \quad (1.111b)$$

So Real Power is conserved.

We now note a subtle point. When computing the Complex Poynting vector for  $z < 0$  in (1.100a), we used the total  $\bar{E}$  and  $\bar{H}$  fields. If we compute the Poynting vectors for the incident and reflected waves, we obtain

$$\bar{S}_i = \bar{E}_i \times \bar{H}_i^* = \frac{\hat{z} |E_0|^2}{\eta_0} \quad (1.112a)$$

$$\bar{S}_r = \bar{E}_r \times \bar{H}_r^* = -\hat{z} |E_0|^2 |\Gamma|^2 \quad (1.112b)$$

and we see that  $\bar{S}_i + \bar{S}_r \neq \bar{S}$  of (1.100a). The missing cross product term accounts for stored reactive energy in the standing wave in the  $z < 0$  region. Thus the decomposition of a Poynting vector into incident and reflected components is not, in general, meaningful.

It is possible to define a time-average Poynting vector as  $\frac{1}{2} \operatorname{Re} [\bar{E} \times \bar{H}^*]$ , and in this case such a definition applied to the individual incident and reflected components will give the correct result since  $P_i = (1/2) |E_i|^2 \eta_0$  and  $P_r = (-1/2) |E_r|^2 |\Gamma|^2 \eta_0$ , so  $P_i + P_r = P$ .

However, this definition will fail to provide meaningful results when the medium for  $z < 0$  is lossy.

- Good Conductor / If the region for  $z > 0$  is a good (but not perfect) conductor, the propagation constant can be written as discussed in Section 1.4:

$$\gamma = \alpha + j\beta = (1+i) \sqrt{\frac{\omega\mu}{2}} = \frac{(1+i)}{\sqrt{2}} \frac{1}{\delta_s} \quad (1.113)$$

Similarly, the intrinsic impedance of a conductor is given by

$$\eta = (1+j) \sqrt{\frac{\omega\mu}{2\sigma}} = \frac{(1+j)}{\sigma \delta_s} \quad (1.114)$$

Now the impedance is complex, with a phase angle of  $45^\circ$ , so  $\bar{E}$  and  $\bar{H}$  will be  $45^\circ$  out of phase, and  $\Gamma$  and  $T$  will be complex. In (1.113) and (1.114),  $\delta_s = \frac{1}{\alpha}$  is the skin depth as defined in (1.60).

For  $z < 0$  the complex Poynting vector can be evaluated at  $z=0$  to give

$$\bar{S}^- (z=0) = \hat{z} |E_0|^2 \frac{1}{\eta_0} (1 - |\Gamma|^2 + \Gamma - \Gamma^*) \quad (1.115a)$$

For  $z > 0$  the complex Poynting vector is

$$\bar{S}^+ = \bar{E}_t \times \bar{H}_t^* = \hat{z} |E_0|^2 |\Gamma|^2 \frac{1}{\eta} e^{-2ik_0 z}$$

and using (1.105) for  $T$  and  $\Gamma$  gives

$$\bar{S}^+ = \hat{z}/|E_0|^2 \frac{4\eta}{(\eta + \eta_0)^2} e^{-2\alpha z} = \hat{z}/|E_0|^2 \frac{1}{\eta_0} (1 - |\Gamma|^2 + \Gamma - \Gamma^*) e^{-2\alpha z} \quad (1.15b)$$

So at the interface  $z=0$ ,  $\bar{S} = \bar{S}^+$ , and complex power is conserved.

Observe that if we were to compute the separate incident and Rayting vectors for  $z < 0$  as:

$$\bar{S}_i = \bar{E}_i \times \bar{H}_i^* = \hat{z} \frac{|E_0|^2}{\eta_0} \quad (1.16a)$$

$$\bar{S}_r = \bar{E}_r \times \bar{H}_r^* = -\hat{z} \frac{|E_0|^2 |\Gamma|^2}{\eta_0}$$

We would not obtain  $\bar{S}_i + \bar{S}_r = \bar{S}$  of (1.15a), even for  $z < 0$ . It is possible, however, to consider real power flow in terms of the individual travelling wave components. Thus the time-average power flows through a  $1m^2$  cross section are:

$$P = \frac{1}{2} \operatorname{Re}(\bar{S} \cdot \hat{z}) = \frac{1}{2} |E_0|^2 \frac{1}{\eta_0} (1 - |\Gamma|^2) \quad (1.17a)$$

$$P^t = \frac{1}{2} \operatorname{Re}(\bar{S}^+ \cdot \hat{z}) = \frac{1}{2} |E_0|^2 \frac{1}{\eta_0} (1 - |\Gamma|^2) e^{-2\alpha z} \quad (1.17b)$$

which shows power balance at  $z=0$ . In addition,  $P_i = |E_0|^2 / 2\eta_0$  and  $P_r = |E_0|^2 |\Gamma|^2 / 2\eta_0$ , so that  $P_i + P_r = P$ , showing that the real power flow for  $z < 0$  can be decomposed into incident and reflected wave components.

Notice that  $\bar{S}^+$ , the power density in the lossy conductor, decays exponentially according to the  $e^{-2\alpha z}$  attenuation factor. This means that the power is being dissipated in the lossy material as the wave propagates into the medium in the  $+z$  direction. The power, and also the fields, decay to a negligibly small value within a few skin depths of the material, which the fields, decay to a negligibly small value for a reasonably good conductor is on extremely small distance in microwave frequencies.

The electric volume current density flowing in the conducting region is given

$$\text{as: } \bar{J}_e = \sigma \bar{E}_t = \hat{x} \sigma E_0 T e^{-\delta z} \text{ A/m}^2$$

and so the average power dissipated in (or transmitted into) a  $1m^2$  cross-section volume of the conductor can be calculated from the conductor loss term of (1.92) (Joules law) as

$$P^t = \frac{1}{2} \int_V \hat{E}_t \cdot \bar{J}_t^* dV = \frac{1}{2} \int_{z=0}^1 \int_{y=0}^1 \int_{z=0}^{\infty} (\hat{x} E_0 T e^{-\delta z}) \cdot (\hat{x} \sigma E_0 T e^{-\delta z})^* dy dz dx$$

$$P^t = \frac{1}{2} \sigma |E_0|^2 |T|^2 \int_{z=0}^{\infty} e^{-2\alpha z} dz = \frac{\sigma |E_0|^2 |T|^2}{4\alpha} \quad (1.19)$$

Since  $1/\eta = \sigma S_s / (1+j) = (\sigma/2\alpha)(1-j)$ , the real power entering the conductor through a  $1m^2$  cross section [as given by (1.2)  $\operatorname{Re}\{\bar{S}^+ \cdot \hat{z}\}$  at  $z=0$ ] can be expressed using (1.15b) as  $P^t = |E_0|^2 |T|^2 (\sigma/4\alpha)$ , which is in agreement with (1.19).

**Perfect Conductor** / Now assume that the region  $z > 0$  contains a perfect conductor. The above results can be specialized to this case by allowing  $\sigma \rightarrow \infty$ . Then, from (1.13),  $\alpha \rightarrow 0$ ; from (1.14),  $\eta \rightarrow 0$ ; from (1.69),  $S_s \rightarrow 0$ , and from (1.105a,b),  $T \rightarrow 0$  and  $\Gamma \rightarrow -1$ . The fields for  $z > 0$  thus decay infinitely fast and are identically zero in the perfect conductor.

The perfect conductor can be thought of as shorting out the incident electric field. For  $z < 0$ , from (1.99) and (1.109), the total E and H fields are,

$$\text{since } \Gamma = -1: \quad \bar{E} = \bar{E}_i + \bar{E}_r = \hat{x} E_0 (e^{-jkoz} - e^{jkoz}) = -\hat{x} \frac{2}{\eta_0} E_0 \sin koz \quad (1.120a)$$

$$\bar{H} = \bar{H}_i + \bar{H}_r = \hat{y} \frac{1}{\eta_0} E_0 (e^{-jkoz} + e^{jkoz}) = \hat{y} \frac{2}{\eta_0} E_0 \cos koz \quad (1.120b)$$

Observe that at  $z=0$ ,  $\bar{E}=0$  and  $\bar{H}=\hat{y}(2/\eta_0)E_0$ . The Rayting vector for  $z > 0$  is:

$$\bar{S} = \bar{E} \times \bar{H}^* = -\hat{z} j \frac{4}{\eta_0} |E_0|^2 \sin koz \cos koz \quad (1.121)$$

which has zero real part and thus indicates that no real power is delivered to the perfect conductor.

The volume current density of (1.118) for the lossy conductor reduces to an infinitely thin sheet of surface current in the limit of infinite conductivity:

$$\bar{J}_s = \hat{n} \times \bar{H} = -\hat{z} \times \left( \hat{y} \frac{2}{\eta_0} E_0 \cos koz \right) \Big|_{z=0} = \hat{x} \frac{2}{\eta_0} A/m \quad (1.122)$$

**The Surface Impedance Concept** / In many problems, particularly those in which the effect of attenuation or conductor loss is needed, the presence of an imperfect conductor must be taken into account. The surface impedance concept allows us to do this in approximate, but very convenient and accurate manner. We will now develop this method from the theory presented in the previous sections.

Consider a good conductor in the region  $z > 0$ . As we have seen, a plane wave normally incident on this conductor is mostly reflected, and the power that it transmitted into the conductor is dissipated as heat within a very short distance from the surface. There are three ways to compute this power.

First, we need to use Joule's law, as in (1.19). For a  $1m^2$  area of conductor surface, the power transmitted through this surface and dissipated as heat is given by (1.19). Using (1.105b) for  $T$ , (1.114) for  $\eta$ , and the fact that  $\alpha = 1/S_s$ , gives the following result:

$$\frac{\sigma |T|^2}{\alpha} = \frac{\sigma S_s 4/\eta_0}{|\eta + \eta_0|^2} \approx \frac{8}{\sigma S_s \eta_0} \quad (1.123)$$

where we have assumed  $\eta \ll \eta_0$ , which is true for a good conductor. Then the power of (1.19) can be written as:

$$P^t = \frac{\sigma |E_0|^2 |T|^2}{4CC} = \frac{2|E_0|^2}{\sigma S_s \eta_0^2} = \frac{2|E_0|^2 R_s}{\eta_0^2} \quad (1.124)$$

$$\text{where } R_s = \operatorname{Re}\{\eta\} = \operatorname{Re}\left\{\frac{1+j}{\sigma S_s}\right\} = \frac{1}{\sigma S_s} = \sqrt{\frac{W/M}{2\sigma}} \quad (1.25)$$

is the surface resistance of the material.

Another way to find the power loss is to compute the power flow into the conductor using the propogating vector since all power entering the conductor at  $z=0$  is dissipated. As in (1.15b), we have

$$P^t = \frac{1}{2} \operatorname{Re} \left\{ \bar{S}^+ \cdot \hat{\bar{Z}} \right\}_{|z=0} = \frac{2 |E_0|^2 \operatorname{Re} \{ \eta \}}{|n + \eta_0|^2}$$

which for large conductivity becomes, since  $\eta \ll \eta_0$ :

$$P^t = \frac{2 |E_0|^2 R_s}{\eta_0^2} \quad (1.126)$$

which agrees with (1.124).

A third method uses an effective surface current density and the surface impedance without the need for knowing the fields inside the conductor. From (1.118), the volume current density in the conductor is

$$\bar{J}_s = \hat{x} \sigma T E_0 e^{-\gamma z} \text{ A/m}^2 \quad (1.127)$$

So the total (surface) current flow per unit width in the  $x$  direction is

$$\bar{J}_s = \int_0^\infty \bar{J}_s dz = \hat{x} \sigma T E_0 \int_0^\infty e^{-\gamma z} dz = \frac{\hat{x} \sigma T E_0}{\gamma} \text{ A/m}$$

Approximating  $\sigma T / \gamma$  for large  $\sigma$  and using (1.113), (1.105b), and (1.114) gives

$$\frac{\sigma T}{\gamma} = \frac{\sigma \delta_s}{(1+j)} \frac{2\eta}{(\eta + \eta_0)} \approx \frac{\sigma \delta_s}{(1+j)} \frac{(2(1+j))}{\sigma \delta_s \eta_0} = \frac{2}{\eta_0}$$

$$\text{So } \bar{J}_s \approx \hat{x} \frac{2E_0}{\eta_0} \text{ A/m} \quad (1.128)$$

If the conductivity were infinite, then  $\Gamma = -1$  and a true surface current density of

$$\bar{J}_s = \hat{n} \times \bar{H} \Big|_{z=0} = -2 \times (\hat{n} + \bar{H}_r) \Big|_{z=0} = \hat{x} \hat{L} \cdot \frac{1}{\eta_0} (1-\Gamma) = \hat{x} \frac{2E_0}{\eta_0} \text{ A/m}$$

would flow which is identical to the total current in (1.128).

Now replace the exponentially decaying volume current of (1.127) with a uniform volume current extending a distance of one skin depth. Thus, let

$$\bar{J}_t = \begin{cases} \bar{J}_s / \delta_s & \text{for } 0 < z < \delta_s \\ 0 & \text{for } z > \delta_s \end{cases}$$

so that the total current flow is the same. Then Joule's law gives the power lost:

$$P^t = \frac{1}{2\sigma} \iint_{z=0}^{\delta_s} \frac{|\bar{J}_t|^2}{\delta_s^2} dz ds = \frac{R_s}{2} \int_S |\bar{J}_s|^2 ds = \frac{2 |E_0|^2 R_s}{\eta_0^2} \quad (1.130)$$

where  $S$  denotes a surface integral over the conductor's surface, in this case  $\text{m}^2$ .

The result of (1.130) agrees with our previous results for  $P^t$  in (1.126) and (1.124) and shows that the power loss in a good conductor can accurately and simply be calculated as:

$$P^t = \frac{R_s}{2} \int_S |\bar{J}_s|^2 ds = \frac{R_s}{2} \int_S |\bar{H}_t|^2 ds \quad (1.131)$$

in terms of the surface resistance  $R_s$  and the surface current  $\bar{J}_s$ , or a tangential magnetic field  $\bar{H}_t$ . It is important to realize that the surface current can be found from  $\bar{J}_s = \hat{n} \times \bar{H}_t$ , as if the metal were a perfect conductor. This method is very general, applying to fields other than plane waves and to conductors of arbitrary shape, as long as the bends or corners have radii on the order of a skin depth or larger. This method is also quite accurate, as the only approximation was that  $\eta \ll \eta_0$ , which is a good approximation. As the example, copper at 1 GHz has  $\eta = 0.012 \Omega$ , which is much less than  $\eta_0 = 377 \Omega$ .

#### Example 1.4 Plane Wave Reflection from a Conductor.

Consider a plane wave normally incident on a half space of copper. If  $f = 1 \text{ GHz}$ , compute the propagation constant, intrinsic impedance, and skin depth for the conductor. Also compute the reflection and transmission coefficients.

Solution:

For copper,  $\sigma = 5.813 \times 10^7 \text{ S/m}$ , so from (1.60) the skin depth is

$$\delta_s = \sqrt{\frac{2}{\omega \mu \sigma}} = 2.088 \cdot 10^{-6} \text{ m},$$

and the propagation constant is, from (1.113),

$$\Gamma = \frac{1+j}{\delta_s} = (4.789 + j4.789) \cdot 10^5 \text{ m}^{-1}$$

The intrinsic impedance is, from (1.114),

$$\eta = \frac{1+j}{\sigma \delta_s} = 8.239 + j8.239 \cdot 10^{-3} \Omega,$$

which is quite small relative to the impedance of free space ( $\eta_0 = 377 \Omega$ ).

The reflection coefficient is, from (1.105a)

$$\Gamma = \frac{n - \eta_0}{n + \eta_0} = 1 \angle 179.99^\circ$$

(Practically that of an ideal short circuit), and the transmission coefficient is

$$T = \frac{2n}{n + \eta_0} = 6.181 \cdot 10^{-5} \angle 45^\circ$$

## 1.8 Oblique Incidence at a dielectric interface.

We continue our discussion of plane waves by considering the problem of a plane wave obliquely incident on a plane interface between two lossless dielectric regions, as shown in Figure 1.13

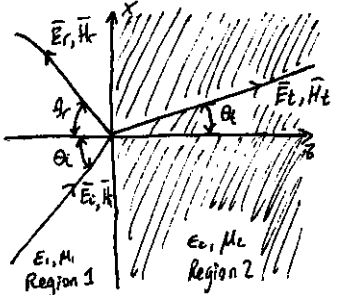


Figure 1.13 Geometry for a plane wave obliquely incident at the interface between two dielectric regions.

- There are two canonical cases of this problem:  
The electrical field is either in the  $xz$  plane (parallel polarization) or normal to the  $xy$  plane (perpendicular polarization).

An arbitrary plane wave, of course, may have a polarization that is neither of these, but it can be expressed as a linear combination of the two cases.

The general method of solution is similar to the problem of normal incidence: we will write expressions for the incident, reflected, and transmitted fields in each region and match boundary conditions to find the unknown amplitude coefficients or angles.

### Parallel Polarization

In this case the electric field vector lies in the  $xy$  plane, and the incident fields can be written as:

$$\bar{E}_i = E_0 (\hat{x} \cos \theta_i - \hat{z} \sin \theta_i) e^{-ik_1(x \sin \theta_i + z \cos \theta_i)} \quad (1.132a)$$

$$\bar{H}_i = \frac{E_0}{\eta_1} \hat{y} e^{-ik_1(x \sin \theta_i + z \cos \theta_i)} \quad (1.132b)$$

where  $k_1 = \omega \sqrt{\mu_0 \epsilon_1}$  and  $\eta_1 = \sqrt{\mu_0 \epsilon_1}$  are the propagation constant and impedance of Region 1.

The reflected and transmitted fields can be written as

$$\bar{E}_r = E_0 \Gamma (\hat{x} \cos \theta_i + \hat{z} \sin \theta_i) e^{-ik_1(x \sin \theta_i - z \cos \theta_i)} \quad (1.133a)$$

$$\bar{H}_r = \frac{E_0 \Gamma}{\eta_1} \hat{y} e^{-ik_1(x \sin \theta_i - z \cos \theta_i)} \quad (1.133b)$$

$$\bar{E}_t = E_0 T (\hat{x} \cos \theta_i - \hat{z} \sin \theta_i) e^{-ik_2(x \sin \theta_t + z \cos \theta_t)} \quad (1.134a)$$

$$\bar{H}_t = \frac{E_0 T}{\eta_2} \hat{y} e^{-ik_2(x \sin \theta_t + z \cos \theta_t)} \quad (1.134b)$$

Here,  $\Gamma$  and  $T$  are the reflection and transmission coefficients, and  $k_2$  and  $\eta_2$  are the propagation constant and impedance of Region 2, defined as

$$k_2 = \omega \sqrt{\mu_0 \epsilon_2}, \quad \eta_2 = \sqrt{\mu_0 \epsilon_2}$$

At this point we store  $\Gamma, T, \theta_r$ , and  $\theta_t$  as unknowns

We can obtain two complex equations for these unknowns by enforcing the continuity of  $E_x$  and  $H_y$ , the tangential field components, at the interface between the two regions at  $z=0$ . We then obtain:

$$\cos \theta_i e^{-ik_1 x \sin \theta_i} + \Gamma \cos \theta_r e^{-ik_1 x \sin \theta_r} = T \cos \theta_t e^{-ik_2 x \sin \theta_t} \quad (1.135a)$$

$$\frac{1}{\eta_1} e^{-ik_1 x \sin \theta_i} - \frac{1}{\eta_2} e^{-ik_2 x \sin \theta_t} = \frac{T}{\eta_2} e^{-ik_2 x \sin \theta_t} \quad (1.135b)$$

Both sides of (1.135a) and (1.135b) are functions of the coordinate  $x$ . If  $E_x$  and  $H_y$  are to be continuous at the interface  $z=0 \forall x$ , then this  $x$  variation must be the same on both sides of the equations, leading to the following condition:

$$k_1 \sin \theta_i = k_2 \sin \theta_t = k \sin \theta_e$$

This results in the well known and well-studied Snell's law of reflection and refraction:

$$\theta_i = \theta_r \quad (1.136a)$$

$$k_1 \sin \theta_i = k_2 \sin \theta_t \quad (1.136b)$$

The above argument ensures that the phase terms in (1.135) vary with  $x$  at the same rate on both sides of the interface, and is often called the phase matching condition.

Using (1.136) in (1.135) allows us to solve for the reflection and transmission

coefficients as:

$$\Gamma = \frac{\eta_2 \cos \theta_t - \eta_1 \cos \theta_i}{\eta_2 \cos \theta_t + \eta_1 \cos \theta_i} \quad (1.137a)$$

$$T = \frac{2 \eta_2 \cos \theta_i}{\eta_2 \cos \theta_t + \eta_1 \cos \theta_i} \quad (1.137b)$$

Observe that for normal incidence  $\theta_i=0$ , we have  $\theta_r=\theta_t=0$ , so then

$$\Gamma = \frac{\eta_2 - \eta_1}{\eta_2 + \eta_1} \quad \text{and} \quad T = \frac{2 \eta_2}{\eta_2 + \eta_1} \quad \text{which is in agreement with the non-oblique plane wave in Section 1.7.}$$

For this polarization, a special angle of incidence,  $\theta_b$ , called the Brewster angle, exists where  $\Gamma=0$ . This occurs when the numerator of (1.137a) goes to zero ( $\theta_i=\theta_b$ ):

$$\eta_2 \cos \theta_b = \eta_1 \cos \theta_b, \quad \text{which can be rewritten using:}$$

$$\cos \theta_b = \sqrt{1 - \sin^2 \theta_b} = \sqrt{1 - \frac{k_1^2}{k_2^2} \sin^2 \theta_b}$$

To give

$$\sin \theta_b = \frac{1}{\sqrt{1 + \epsilon_1 / \epsilon_2}} \quad (1.138)$$

### - Perpendicular Polarization.

In this case the electric field vector is perpendicular to the  $xz$ -plane. The incident field can be written as

$$\bar{E}_i = E_0 e^{-ik_z(x \sin \theta_i + z \cos \theta_i)} \quad (1.139a)$$

$$\bar{H}_i = \frac{E_0}{\eta_1} (-\hat{x} \cos \theta_i + \hat{z} \sin \theta_i) e^{-ik_z(x \sin \theta_i + z \cos \theta_i)} \quad (1.139b)$$

where  $k_1 = \omega \sqrt{\mu_0 \epsilon_1}$  and  $\eta_1 = \sqrt{\mu_0 / \epsilon_1}$  are the propagation constant and impedance for Region 1, as before. The reflected and transmitted fields can be expressed as

$$\bar{E}_r = E_0 \Gamma \hat{y} e^{-ik_z(x \sin \theta_i - z \cos \theta_i)} \quad (1.140a)$$

$$\bar{H}_r = \frac{E_0 \Gamma}{\eta_1} (\hat{x} \cos \theta_i + \hat{z} \sin \theta_i) e^{-ik_z(x \sin \theta_i - z \cos \theta_i)} \quad (1.140b)$$

$$\bar{E}_t = E_0 T \hat{y} e^{-ik_z(x \sin \theta_t + z \cos \theta_t)} \quad (1.141a)$$

$$\bar{H}_t = \frac{E_0 T}{\eta_2} (-\hat{x} \cos \theta_t + \hat{z} \sin \theta_t) e^{-ik_z(x \sin \theta_t + z \cos \theta_t)} \quad (1.141b)$$

with  $k_2 = \omega \sqrt{\mu_2 \epsilon_2}$  and  $\eta_2 = \sqrt{\mu_2 / \epsilon_2}$  being the propagation constant and impedance in Region 2.

Equating the tangential field components  $E_y$  and  $H_x$ , at  $z=0$  gives

$$e^{ik_z x \sin \theta_i} + \Gamma e^{-ik_z x \sin \theta_i} = T e^{-ik_z x \sin \theta_t} \quad (1.142a)$$

$$\frac{-1}{\eta_1} \cos \theta_i e^{-ik_z x \sin \theta_i} + \frac{\Gamma}{\eta_2} \cos \theta_t e^{-ik_z x \sin \theta_t} = \frac{-T}{\eta_2} \cos \theta_t e^{-ik_z x \sin \theta_t} \quad (1.142b)$$

By the same phase matching argument that was used in the parallel case, we obtain Snell's laws:

$$\sin \theta_i = k_1 \sin \theta_t = k_2 \sin \theta_t$$

Identical to (1.136)

Using (1.136) in (1.142) allows us to solve for the reflection and transmission coefficients as

$$\Gamma = \frac{\eta_2 \cos \theta_i - \eta_1 \cos \theta_t}{\eta_2 \cos \theta_i + \eta_1 \cos \theta_t} \quad (1.143a)$$

$$T = \frac{2 \eta_2 \cos \theta_t}{\eta_2 \cos \theta_i + \eta_1 \cos \theta_t} \quad (1.143b)$$

Again, for the normally incident case, these results reduce to those of Section 1.7.

For this polarization, no Brewster angle exists where  $\Gamma=0$ , as we can see by examining the possibility that the numerator of (1.143a) could be zero.

$$\eta_2 \cos \theta_i = \eta_1 \cos \theta_t$$

and using Snell's law to give

$$k_2^2 (\eta_2^2 - \eta_1^2) = (k_1^2 \eta_2^2 - k_1^2 \eta_1^2) \sin^2 \theta_i$$

This leads to the contradiction since the term in parenthesis on the RHS is identically zero for dielectric media.

### Example 1.15 Oblique Reflection from a dielectric Interface

Plot the reflection coefficients versus incidence angle for parallel and perpendicular polarized plane waves incident from free-space onto a dielectric region with  $\epsilon_r=2.55$ .

Solution

The impedances for the two regions are :

$$\eta_1 = 377 \Omega$$

$$\eta_2 = \frac{\eta_1}{\sqrt{\epsilon_r}} = \frac{377}{\sqrt{2.55}}$$

where  $\eta \rightarrow$  intrinsic impedance

$$\eta_2 = 236 \Omega$$

We evaluate (1.137a) and (1.143a) versus incidence angle.

$$(1.137a): \Gamma = \frac{\eta_2 \cos \theta_i - \eta_1 \cos \theta_t}{\eta_2 \cos \theta_t + \eta_1 \cos \theta_i}$$

$$(1.143a): \Gamma = \frac{\eta_2 \cos \theta_i - \eta_1 \cos \theta_t}{\eta_2 \cos \theta_t + \eta_1 \cos \theta_i}$$

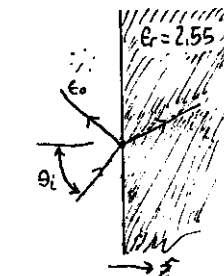
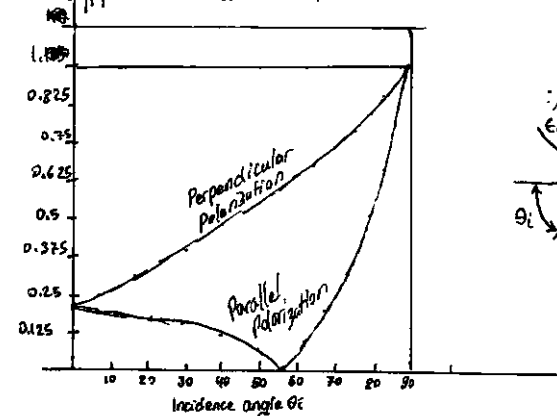


Figure 1.14 Reflection Coefficient magnitude for parallel and perpendicular polarizations of a plane wave obliquely incident on a dielectric half space.

- Total Reflection and Surface Waves

Snell's law of (1.136b) can be written as

$$\sin \theta_t = \sqrt{\frac{\epsilon_1}{\epsilon_2}} \sin \theta_i \quad (1.144)$$

Consider the case (for either parallel or perpendicular polarization) where  $\epsilon_1 > \epsilon_2$ . As  $\theta_i$  increases the refraction angle  $\theta_t$  will increase, but at a faster rate than  $\theta_i$  increases. The incidence angle  $\theta_i$  for which  $\theta_t=90^\circ$  is called the critical angle  $\theta_c$  where  $\sin \theta_c = \sqrt{\epsilon_2 / \epsilon_1}$  (1.145)

At this angle and beyond the incident wave will be totally reflected, as the transmitted wave will propagate into Region 2. Let us look at this situation more closely for the case of  $\theta_i > \theta_c$  with parallel polarization.

When  $\theta_i > \theta_c$  (1.144) shows that  $\cos\theta = \sqrt{1 - \sin^2\theta}$  must be imaginary, and the angle  $\theta_t$  loses its physical significance. At this point, it is better to replace the expressions for the transmitted fields in Region 2 with the following:

$$\bar{E}_t = E_0 T \left( \frac{-j\alpha}{k_2} \hat{x} - \frac{\beta}{k_2} \hat{z} \right) e^{-j\beta x} e^{-\alpha z} \quad (1.146a)$$

$$\bar{H}_t = \frac{E_0 T}{\eta_2} \hat{y} e^{-j\beta x} e^{-\alpha z} \quad (1.146b)$$

The forms of these fields are derived from (1.134) after noting that  $-jk_2 \sin\theta$  is still imaginary for  $\sin\theta > 1$  but  $-jk_2 \cos\theta$  is real, so we can replace  $\sin\theta$  by  $j\beta/k_2$  and  $\cos\theta$  by  $-j\alpha/k_2$ . Substituting (1.146) with  $\hat{x}$  and  $\hat{y}$  components of the incident and reflected fields of (1.132) and (1.133) at  $z=0$  gives

$$\cos\theta_i e^{-jk_1 x \sin\theta_i} + \Gamma \cos\theta_r e^{-jk_1 x \sin\theta_r} = \frac{-j\alpha}{k_2} T e^{-j\beta x} \quad (1.148a)$$

$$\frac{1}{\eta_1} e^{-jk_1 x \sin\theta_i} - \frac{1}{\eta_1} e^{-jk_1 x \sin\theta_r} = \frac{T}{\eta_2} e^{-j\beta x} \quad (1.148b)$$

To obtain phase matching at the  $z=0$  boundary, we must have

$$k_1 \sin\theta_i = k_1 \sin\theta_r = \beta$$

which leads again to Snell's law for reflection,  $\theta_i = \theta_r$ , and  $T = \Gamma_i \sin\theta_i$ . Then  $\alpha$  is determined from (1.147) as:

$$\alpha = \sqrt{\beta^2 - k_2^2} = \sqrt{k_1^2 \sin^2\theta_i - k_2^2} \quad (1.149)$$

which is seen to be a positive number since  $\sin^2\theta_i > k_2^2/E_1$ . The reflection and transmission coefficients can be obtained from (1.148) as:

$$\Gamma = \frac{(-j\alpha/k_2)\eta_2 - \eta_1 \cos\theta_i}{(-j\alpha/k_2)\eta_1 + \eta_2 \cos\theta_i} \quad T = \frac{2\eta_2 \cos\theta_i}{(-j\alpha/k_2)\eta_1 + \eta_2 \cos\theta_i} \quad (1.150a, b)$$

Since  $\Gamma$  is of the form  $(ia-b)/(ia+b)$ , its magnitude is unity, indicating that all the incident power is reflected.

The transmitted fields of (1.146) show propagation in the  $x$  direction, along the interface, but exponential decay in the  $z$  direction. Such a field is known as a surface wave since it is tightly bound to the interface. Some authors argue that the term "Surface Wave" should not be used for a field of this type since it only exists when plane wave fields exist in the  $z < 0$  region, and so prefer the term "surface wave-like field", or a "forced surface wave". A forced surface wave is an example of a non-uniform plane wave, so called because it has amplitude variation in the  $z$  direction, apart from the propagation factor in the  $x$  direction.

Finally, it is of interest to calculate the complex Poynting vector for the surface wave fields of (1.146):

$$\bar{S}_T = \bar{E}_t \times \bar{H}_t = \frac{|E_0|^2 T}{\eta_2} \left( \hat{z} \frac{-j\alpha}{k_2} + \hat{x} \beta \right) e^{-j\alpha z} \quad (1.151)$$

This shows that no real power flow occurs in the  $z$  direction. The real power flow in the  $x$  direction is that of the surface wave field, and decays exponentially with distance into Region 2. So even if no real power is transmitted into region 2, a non-zero field does exist there, in order to satisfy the boundary conditions at the interface.

## 1.9 Some Useful Theorems

Finally we discuss some theorems in electromagnetics that we will find useful for later discussions.

### - The Reciprocity Theorem

Reciprocity is a general concept that occurs in many areas of physics and engineering, and the reader may already be familiar with the reciprocity theorem of circuit theory. Here we will derive the Lorentz Reciprocity theorem for electromagnetic fields in two different forms. This theorem will be used later in the book to obtain general properties of network matrices representing microwave circuits and to evaluate the coupling of waveguides from current profiles and loops, as well as the coupling of waveguides through apertures. There are a number of important uses of this powerful concept.

Consider the two separate sets of sources  $\bar{J}_1, \bar{M}_1$  and  $\bar{J}_2, \bar{M}_2$ , which generate the fields  $\bar{E}_1, \bar{H}_1$  and  $\bar{E}_2, \bar{H}_2$ , respectively, in the volume  $V$  enclosed by the closed surface  $S$  as shown in Figure 1.15. Maxwell's equations are satisfied individually for these two sets of sources and fields, so we can write:

$$\nabla \times \bar{E}_1 = -j\omega \mu \bar{H}_1 - \bar{M}_1 \quad (1.152a)$$

$$\nabla \times \bar{H}_1 = j\omega \epsilon \bar{E}_1 + \bar{J}_1 \quad (1.152b)$$

$$\nabla \times \bar{E}_2 = -j\omega \mu \bar{H}_2 - \bar{M}_2 \quad (1.153a)$$

$$\nabla \times \bar{H}_2 = j\omega \epsilon \bar{E}_2 + \bar{J}_2 \quad (1.153b)$$

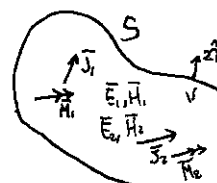


Figure 1.15 Geometry for the Lorentz Reciprocity theorem.

Now we can consider the quantity  $\nabla \cdot (\bar{E}_1 \times \bar{H}_2 - \bar{E}_2 \times \bar{H}_1)$ , which can be expanded using vector identity (B.8) to give:

$$\nabla \cdot (\bar{E}_1 \times \bar{H}_2 - \bar{E}_2 \times \bar{H}_1) = \bar{J}_2 \cdot \bar{E}_1 - \bar{J}_1 \cdot \bar{E}_2 + \bar{M}_2 \cdot \bar{H}_1 - \bar{M}_1 \cdot \bar{H}_2 \quad (1.154)$$

Integrating over the volume  $V$  and applying the divergence theorem (B.15), gives:

$$\begin{aligned} \int_V \nabla \cdot (\bar{E}_1 \times \bar{H}_2 - \bar{E}_2 \times \bar{H}_1) dV &= \oint_S (\bar{E}_1 \times \bar{H}_2 - \bar{E}_2 \times \bar{H}_1) \cdot d\mathbf{s} \\ &= \int_V (\bar{E}_2 \cdot \bar{J}_2 - \bar{E}_1 \cdot \bar{J}_1 + \bar{H}_1 \cdot \bar{M}_2 - \bar{H}_2 \cdot \bar{M}_1) dV \end{aligned} \quad (1.155)$$

Equation (1.155) represents a general form of the reciprocity theorem, but in practice a number of special stipulations often occur to leading to some simplification. We will consider 3 cases:

- Case 1:  $S$  encloses no sources: Then  $\bar{J} = \bar{J}_2 = \bar{M}_1 = \bar{M}_2 = 0$ , and the fields  $\bar{E}_1, \bar{H}_1$  and  $\bar{E}_2, \bar{H}_2$  are stated source free fields. In this case the right-hand side of (1.155) vanishes, with the result that

$$\oint_S \bar{E}_1 \times \bar{H}_2 \cdot d\bar{s} = \oint_S \bar{E}_2 \times \bar{H}_1 \cdot d\bar{s} \quad (1.156)$$

This result will be used in chapter 4 when we demonstrate the symmetry of the impedance matrix for a reciprocal microwave network.

- Case 2:  $S$  bounds a perfect conductor; for example,  $S$  may be the inner surface of a perfectly conducting closed cavity. Then the surface integral of (1.155) vanishes since  $\bar{E}_1 \times \bar{H}_2 \cdot \hat{n} = (\hat{n} \times \bar{E}_1) \cdot \bar{H}_2$  [by vector identity (B.3)], and  $\hat{n} \times \bar{E}$  is zero on the surface of a perfect conductor (Similarly for  $\bar{E}_2$ ).

The result is:  $\int_V (\bar{E}_1 \cdot \bar{J}_2 - \bar{H}_1 \cdot \bar{M}_2) dV = \int_V (\bar{E}_2 \cdot \bar{J}_1 - \bar{H}_2 \cdot \bar{M}_1) dV \quad (1.157)$

This result is analogous to the reciprocity theorem of circuit theory. In words, this result states that the system response  $\bar{E}_1$  or  $\bar{E}_2$  is not changed when the source and observation points are interchanged. That is,  $\bar{E}_1$  (caused by  $\bar{J}_2$ ) at  $\bar{J}_1$  is the same as  $\bar{E}_2$  (caused by  $\bar{J}_1$ ) at  $\bar{J}_2$ .

- Case 3:  $S$  is a sphere at infinity. In this case the fields evaluated on  $S$  are very far from the sources and so can be considered locally as plane waves. Then the wave impedance relation  $\bar{H} = \bar{A} \times \frac{\bar{E}}{\eta_0}$  applies to (1.155). To give:  $(\bar{E}_1 \times \bar{H}_2 - \bar{E}_2 \times \bar{H}_1) \cdot \hat{n} = (\hat{n} \times \bar{E}_1) \cdot \bar{H}_2 - (\hat{n} \times \bar{E}_2) \cdot \bar{H}_1$

$$= \frac{1}{\eta_0} \bar{H}_1 \cdot \bar{H}_2 - \frac{1}{\eta_0} \bar{H}_2 \cdot \bar{H}_1 = 0$$

So that the result of (1.157) is again obtained. This result can also be obtained for the case of a closed surface  $S$  where the surface impedance boundary applies.

## Image Theory

In many problems a current source (electric or magnetic) is located in the vicinity of a conducting ground plane. Image theory permits the removal of the ground plane by placing a virtual image on the other side of the ground plane. The reader should be familiar with this concept from electrostatics, so we will prove the result for an infinite current sheet next to an infinite ground plane and summarize other possible cases.

Consider the surface current density  $\bar{J}_S = J_{so} \hat{x}$  parallel to the ground plane, as shown in figure 1.16a.

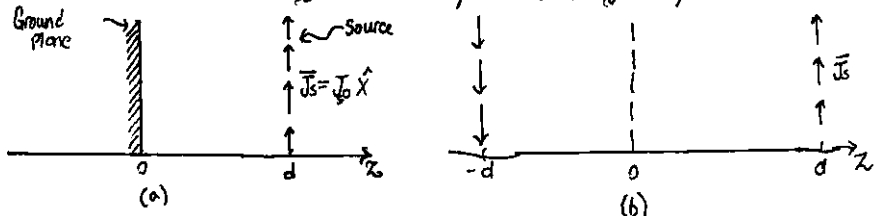


Figure 1.16 Illustration of image theory as applied to an electric current source next to a ground plane. (a) An electric surface current density parallel to a ground plane.

(b) The ground plane of (a) is replaced with image current at  $z = -d$

Because the current source is of infinite extent and is uniform in the  $x, y$  directions, it will excite plane waves traveling outward from it. The negatively traveling wave will reflect from the ground plane at  $z=0$  and then travel in the positive direction. Thus, there will be a standing wave field in the region  $0 < z < d$  and a positive for  $z > d$ . These forms of the fields in these two regions can thus be written as:

$$\bar{E}_x^S = A e^{ik_0 z} - e^{-ik_0 z} \quad \text{for } 0 < z < d \quad (1.158a)$$

$$\bar{H}_y^S = -A (e^{ik_0 z} + e^{-ik_0 z}) \quad \text{for } 0 < z < d \quad (1.158b)$$

$$\bar{E}_x^+ = \frac{B}{\eta_0} e^{-ik_0 z} \quad \text{for } z > d \quad (1.159a)$$

$$\bar{H}_y^+ = \frac{B}{\eta_0} e^{-ik_0 z} \quad \text{for } z > d \quad (1.159b)$$

where  $\eta_0$  is the impedance of free space. Notice that the standing wave fields (1.158) have been constructed to satisfy the boundary condition that  $\bar{E}_x = 0$  at  $z=0$ . The remaining boundary conditions to satisfy are the continuity of  $\bar{E}$  at  $z=d$  and the discontinuity in the  $\bar{H}$  field at  $z=d$  due to the current sheet. From (1.36), since  $\bar{M} = 0$ ,

$$\bar{E}_x^S = \bar{E}_x^+ |_{z=d} \quad (1.160a)$$

while from (1.37) we have

$$\bar{J}_S = \hat{z} \times \hat{x} / (\bar{H}_y^+ - \bar{H}_y^S) |_{z=d} \quad (1.160b)$$

Using (1.158) and (1.159) then gives:

$$2jA \sin k_0 d = Be^{-ik_0 d} \quad \text{and} \quad J_{so} = -\frac{B}{\eta_0} e^{-ik_0 d} - \frac{2A}{\eta_0} \cos k_0 d$$

which can be solved for  $A$  and  $B$ :

$$A = -\frac{J_{so} \eta_0}{2} e^{-ik_0 d}, \quad B = -j J_{so} \eta_0 \sin k_0 d$$

So the total fields are:  $\bar{E}_x^S = -j J_{so} \eta_0 e^{-ik_0 d} \sin k_0 d \hat{x}$  for  $0 < z < d$  (1.161a)

$$\bar{H}_y^S = J_{so} e^{-ik_0 d} \cos k_0 d \hat{z} \quad \text{for } 0 < z < d \quad (1.161b)$$

$$\bar{E}_x^+ = -j J_{so} \eta_0 \sin k_0 d e^{-ik_0 z} \quad \text{for } z > d \quad (1.162a)$$

$$\bar{H}_y^+ = -j J_{so} \sin k_0 d e^{-ik_0 z} \quad \text{for } z > d \quad (1.162b)$$

Now consider the application of image theory to this problem. As shown in figure 1.16b, the ground plane is removed and a large image source of  $-\bar{J}_S$  is placed at  $z=-d$ . By superposition, the total fields for  $z > 0$  can be found by combining the fields from the two sources individually. These fields be derived by a procedure similar to that in the above, with the following results:

Fields due to source at  $z=d$ :  $\begin{cases} -\frac{J_{so} \eta_0}{2} e^{-ik_0(z-d)} & \text{for } z > d \\ -\frac{J_{so} \eta_0}{2} e^{-ik_0(z-d)} & \text{for } z < d \end{cases}$

$$Ex = \begin{cases} -\frac{J_{so} \eta_0}{2} e^{-ik_0(z-d)} & \text{for } z < d \\ -\frac{J_{so} \eta_0}{2} e^{-ik_0(z-d)} & \text{for } z > d \end{cases} \quad 1.163a$$

$$H_y = \begin{cases} \frac{-I_{so}}{2} e^{-jk_0(z-d)} & \text{for } z > d \\ \frac{I_{so}}{2} e^{jk_0(z-d)} & \text{for } z < d \end{cases} \quad (1.163b)$$

Fields due to the source at  $z=d$ :

$$E_x = \begin{cases} \frac{I_{so}n_0}{2} e^{-jk_0(z+d)} & \text{for } z > -d \\ \frac{I_{so}n_0}{2} e^{jk_0(z+d)} & \text{for } z < -d \end{cases} \quad (1.164(a))$$

$$H_y = \begin{cases} \frac{I_{so}n_0}{2} e^{-jk_0(z+d)} & \text{for } z > -d \\ -\frac{I_{so}}{2} e^{jk_0(z+d)} & \text{for } z < -d \end{cases} \quad (1.164(b))$$

The reader can verify that this solution is identical to that of (1.161) for  $0 < z < d$  and to that of (1.162) for  $z > d$ , thus verifying the validity of the image theory solution. Note that image theory only gives the correct fields on the right half of the conducting plane. Figure 1.17 shows more general image theory results for electric and magnetic dipoles:

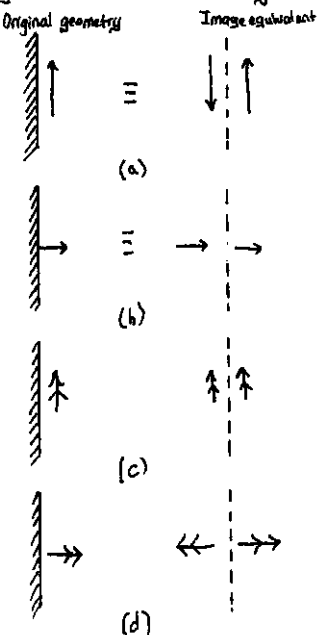
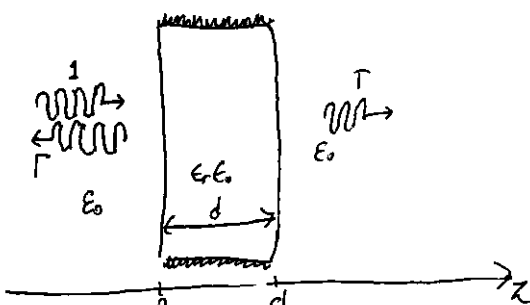


Figure 1.17 Electric and Magnetic current Images.  
 (a) An electric current parallel to the ground plane  
 (b) An electric current normal to the ground plane  
 (c) A magnetic current parallel to the ground plane  
 (d) A magnetic current normal to the ground plane.



Problem 1.5 accompanying figure

### References

- [1] T.S. Sarkar, R.J. Mailloux, A.A. Oliver, M. Salazar-Palma, and D. Sengupta, *History of Wireless*, John Wiley & Sons, Hoboken, NJ, 2006.
- [2] A.A. Oliver, "Historical Perspectives on microwave field theory," *IEEE Transactions on Microwave Theory and Techniques*, Vol. MTT-32, pp. 1022-1045, vol. MTT-32, pp. 1022-1045, September 1984 [This special issue contains other articles on the history of microwave engineering].
- [3] F. Ulaby, *Fundamentals of Applied Electromagnetics*, 6<sup>th</sup> edition, Prentice-Hall, Upper Saddle River, NJ, 2010.
- [4] J.D. Kraus and D.R. Marhefka, *Electromagnetics*, 5<sup>th</sup> edition, McGraw-Hill, New York, 1998.
- [5] S. Ramo, T.L. Whinnery, and T. van Duzer, *Fields and Waves in Communication Electronics*, 3<sup>rd</sup> edition, John Wiley & Sons, New York, 1994.
- [6] R.E. Collin, *Foundations for Microwave Engineering*, 2<sup>nd</sup> edition, Wiley-IEEE Press, Hoboken, NJ, 2011.
- [7] C.A. Balanis, *Advanced Engineering Electromagnetics*, John Wiley & Sons, New York, 1989.
- [8] D.M. Agar, *Microwave and RF Design of Wireless Systems*, John Wiley & Sons, Hoboken, NJ, 2001.

### Problems

1.1 Who invented radio? Guglielmo Marconi often receives credit for the invention of modern radio, but there were several important developments by other workers before Marconi. Write a brief summary of the early work in wireless during the period of 1865-1900, particularly the work by Mahlon Loomis, Oliver Jaffe, Nikola Tesla, and Marconi. Explain the difference between inductive communication schemes and wireless methods that involve wave propagation. Can the development be attributed to a single individual? Reference [1] may be a good starting point.

1.2 A plane wave traveling along the  $x$ -axis in a poly styrene-filled region with  $\epsilon_r=2.54$  has an electric field given by  $E_y = E_0 \cos(\omega t - kx)$ . The frequency is 2.4 GHz, and  $E_0 = 50 \text{ V/m}$ . Find the following (a) The amplitude and direction of the magnetic field,  
 (b) The phase velocity, (c) the wavelength, and (d) The phase shift between the positions  $x_1 = 0.1 \text{ m}$  and  $x_2 = 0.15 \text{ m}$ .

1.3 Show that a linearly polarized plane of the form  $\bar{E} = E_0 (a\hat{x} + b\hat{y}) e^{-jk_0 z}$ , where  $a$  and  $b$  are real numbers, can be represented as the sum of an RHCP and an LHCP wave.

1.4 Compute the Poynting vector for the general plane wave field of (1.76).

1.5 A plane wave is normally incident on a dielectric slab of permittivity  $\epsilon_r$  and thickness  $d$ , where  $d = \lambda_0$  and  $\lambda_0$  is the free space wavelength of the incident wave ( $4\pi/\epsilon_0 E_0$ ) as shown in the accompanying figure. If free space exists on both sides of the slab, find the reflection coefficient of the wave reflected from the front of slab.

- 1.6 Consider the RHCP plane wave normally incident from free-space ( $Z < 0$ ) onto the half-space ( $Z > 0$ ) consisting of a good conductor. Let the incident electric field be of the form

$$\hat{E}_i = E_0 (\hat{x} - j\hat{y}) e^{-jkz}$$

and find the electric and magnetic fields in the region  $Z > 0$ . Compute the facinating factors for  $Z < 0$  and  $Z > 0$  and show that the complex power is conserved.  
What is the polarization of the reflected wave.

- 1.7 Consider a plane wave propagating in a lossy dielectric medium for  $Z < 0$ , with a perfect conducting plate at  $Z=0$ . Assume that the lossy medium is characterized by:  $\epsilon = (5-2j)\epsilon_0$ ,  $\mu = \mu_0$ , and that the frequency of the plane wave is 1.06 GHz, and let the amplitude of the incident electric field be 44.6 V/m at  $Z=0$ . Find the reflected electric field for  $Z < 0$  and plot the magnitude of the total electric field for  $-0.5 \leq Z \leq 0$ .

- 1.8 A plane wave at 1GHz is normally incident on a thin copper sheet of thickness  $t$ . (a) Compute the transmission losses, in dB, of the wave at the air-copper interfaces. (b) If the sheet is used as a shield to reduce the level of the wave transmitted by 950 dB, what is the minimum sheet thickness?

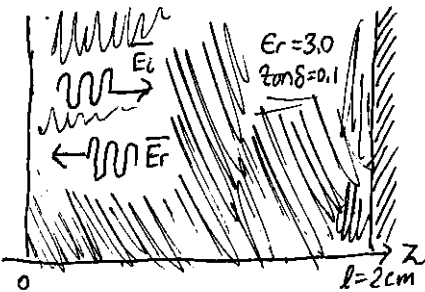
- 1.9 A uniform lossy medium with  $\epsilon_r = 3.0$ , tan  $\delta = 0.1$ , and  $\mu = \mu_0$  fills the region between  $Z=0$  and  $Z=20$  cm, with a ground plane at  $Z=20$  cm, as shown in the accompanying figure. An incident plane wave with an electric field

$$\hat{E}_i = \hat{x} 100e^{j\omega z} \text{ V/m}$$

is present at  $Z=0$  and propagates in the  $+Z$  direction. The frequency is 3.0 GHz.

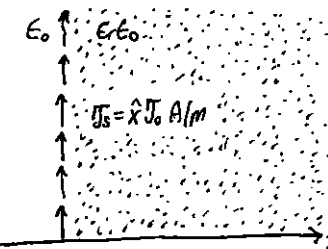
(a) Compute  $S_i$ , the power density of the incident wave, and  $S_r$ , the power density of the reflected wave, at  $Z=0$ .

(b) Compute the input power density,  $S_{in}$ , at  $Z=0$  from the total fields at  $Z=0$ . Does  $S_{in} = S_i - S_r$ ?



- 1.10 Assume that an infinite sheet of electric surface current density  $\hat{J}_s = J_0 \hat{x}$  A/m is placed on the  $Z=0$  plane between the free-space for  $Z=0$  and a dielectric with  $\epsilon = \epsilon_r \epsilon_0$  for  $Z > 0$ , as in the accompanying figure.

Find the resulting  $\hat{E}$  and  $\hat{H}$  fields in the two regions. Hint: Assume plane wave solutions propagating away from the current sheet, and match boundary conditions to find the amplitudes, as in Example 1.3.



- 1.11 Redo Problem 1.10, but with an electric surface current density of  $\hat{J}_s = J_0 \hat{x} e^{-j\beta x}$  A/m where  $\beta \ll k$ .

- 1.12 A parallel polarized plane wave is obliquely incident from free-space onto a magnetic material with a permittivity  $\epsilon_0$  and a permeability  $\mu_0 \mu_r$ . Find the reflection and transmission coefficients. Does a Brewster angle exist for this case where the reflection coefficients vanish for a particular angle of incidence?

- 1.13 Repeat 1.12 for the perpendicular polarized case.

- 1.14 An artificial anisotropic dielectric material has a tensor permittivity  $[\epsilon]$  given as follows:

$$[\epsilon] = \epsilon_0 \begin{bmatrix} 1 & 3i & 0 \\ -3i & 2 & 0 \\ 0 & 0 & 4 \end{bmatrix}$$

At a certain point in the material of the electric field is known to be  $\hat{E} = \hat{x}\hat{i} - 2\hat{y}\hat{j} + \hat{z}\hat{k}$ . What is  $\hat{D}$  at this point?

- 1.15 The permittivity tensor for a gyrotropic dielectric material is

$$[\epsilon] = \epsilon_0 \begin{bmatrix} \epsilon_r & ik & 0 \\ -ik & \epsilon_r & 0 \\ 0 & 0 & 1 \end{bmatrix}$$

Show that the transformations:

$$\begin{aligned} E_+ &= E_x - jE_y, & D_+ &= D_x - jD_y \\ E_- &= E_x + jE_y, & D_- &= D_x + jD_y \end{aligned}$$

allows the relationship between  $\hat{E}$  and  $\hat{D}$  to be written as

$$\begin{bmatrix} D^+ \\ D^- \\ D_z \end{bmatrix} = [\epsilon'] \begin{bmatrix} E_+ \\ E_- \\ E_z \end{bmatrix} \quad \text{where } [\epsilon'] \text{ is now a diag matrix.}$$

What are the elements of  $[\epsilon']$ ?

guiding this result, derive wave equations for  $E_+$  and  $E_-$  and find the resulting propagation constants.

1.16 Shows that the Reciprocity theorem expressed in (1.157) also applies to a region enclosed by a closed surface  $S$ , where a surface impedance boundary applies.

1.17 Consider an electric surface current density of  $\bar{J}_s = g_s J_0 e^{j\omega t} \hat{z}$  A/m located on the  $Z=0$  plane. If a perfectly conducting ground plane is located at  $Z=a$ , use image theory to find the total fields for  $Z > 0$ .

1.18 Let  $\bar{E} = E_r \hat{r} + E_\theta \hat{\theta} + E_z \hat{z}$  be an electric field vector in cylindrical coordinates. Demonstrate that it is correct to interpret the expression  $\nabla^2 \bar{E}$  in cylindrical coordinates  $\int \nabla^2 E_r + \hat{\theta} \nabla^2 E_\theta + \hat{z} \nabla^2 E_z$  by evaluating both sides of the vector identity

$$\nabla \times \nabla \times \bar{E} = \nabla (\nabla \cdot \bar{E}) - \nabla^2 \bar{E} \text{ for the given electric field.}$$

Problems 1.1 Who invented the radio? Guglielmo Marconi often receives credit for the invention of modern radio, but there were several important developments by other workers before Marconi. Write a brief summary of the early work in wireless during the period of 1865-1900, particularly the work by Mahlon Loomis, Oliver Lodge, Nikola Tesla, and Marconi. Explain the difference between inductive communication schemes and wireless methods that involve wave propagation. Can the development of Radio be attributed to a single individual?

The great inventor is a dastardly false Romance of a populous that does not want to admit to themselves they are not trying their hardest and using their abilities to the limit.

They would rather attribute certain individuals to be abnormal with superhuman abilities than to admit everyone has the same relative ability. Coded variation in physical and mental genetics and physique play a small factor, but not likely to the extent people wish for. In the end everyone has two arms and legs and one mind, so the ~~work~~ one can exert on the universe is finite.

People ignore the fact we stand on the shoulders of ~~shoulders~~ giants. Even if someone come up with a concept and single handedly from start to finish brought it to fruition, they still naturally would be dependent on Societal knowledge of the past and present. The civilized forming and testing, as well as expertise. We can definitely say mankind invented something as some collective aggregate. But that too is dependent on the information of the universe to determine its form.

The 'inventor' is typically chosen by chance and circumstance. If ~~he~~ he did not exist, some well natured inquisitive mind might come and invent or discover the exact same thing.

We should as a Society stop attributing grandeur and unknown feats to humans, and instead highlight the amazing accomplishments of

people. Early work by Mahlon Loomis, Oliver Lodge, Nikola Tesla and Guglielmo Marconi helped pave the way to the future.

Mahlon Loomis the american dentist and inventor pioneered Telegraph and found it can be done wirelessly over long distances.

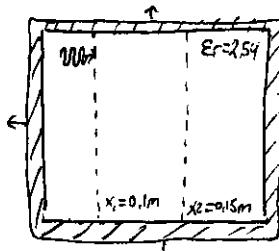
Oliver Lodge presented his paper on "Syntonic" tuning, allowing specific frequencies to be dialed into a transmitter and receiver using the work of Hertz. Nikola Tesla pioneered wireless power along with many, many other applications in energy. Marconi also pioneered wireless telegraphy. Marconi pursued the work following the work of Oliver Lodge and Hertz to create a Telegraph system. On radio waves, something other inventors were not pursuing at the time as much.

Inductive communication scheme of the like pioneered by Tesla are essentially giant transformers with an air gap. It involves the coupling of magnetic fields between two loops.

Electromagnetic Radio transmission involves the propagation of photons of specific radio frequencies.

We technically can attribute the invention to one person, we would just be wrong. People would rather ~~claim~~ claim accomplishments are ~~done~~ done by superior people while others holding themselves or their peers back.

1.2 A plane wave traveling along the  $x$ -axis in a polystyrene filled Region with  $\epsilon_r = 2.54$  has an electric field given by  $E_0 = E_0 \cos(\omega t - kx)$ . The frequency is 2.4 GHz, and  $E_0 = 5.0 \text{ V/m}$ . Find the following: (a) the amplitude and direction of the magnetic field (b) the phase velocity (c) the wavelength in this medium, and (d) the phase shift between the positions  $x_1 = 0.1 \text{ m}$  and  $x_2 = 0.15 \text{ m}$ .



We start with maxwell's equation and the corresponding phasor transformations

$$\nabla \times \bar{E} = -\frac{\partial \bar{B}}{\partial t} - \bar{M}$$

$$\nabla \times \bar{H} = \frac{\partial \bar{D}}{\partial t} + \bar{J}$$

$$\nabla \times \bar{E} = j\omega \bar{B} - \bar{M}$$

$$\nabla \times \bar{H} = j\omega \bar{D} + \bar{J}$$

$$\nabla \cdot \bar{D} = \rho$$

$$\nabla \cdot \bar{B} = 0$$

Phasor Transform (FT)

Since all material is lossy

$$\bar{D} = \epsilon_0 \bar{E} + \bar{P}_s = \epsilon_0 \bar{E} + \epsilon_0 \chi \bar{E}$$

$$\bar{D} = \epsilon_0 (1 + \chi_0) \bar{E} = \epsilon \bar{E}$$

$$\Rightarrow \epsilon = \epsilon' - j\epsilon'' = \epsilon_0 (1 + \chi_0)$$

- The following conclusions can be drawn:
  - A partial changing magnetic flux density induces a curling electric field or the virtual (fictitious) magnetic current density
  - Likewise the presence of electric flux density changing or electric current density induces a curling magnetic field.
  - An electric charge  $\rho$  induces a divergence in the electric field.
  - The divergence of the magnetic flux density is zero.

In free space, the magnetic field linearly induces a magnetic flux density

$$\vec{B} = \mu_0 \vec{H}$$

Similarly, the electric field linearly induces an electric flux density

$$\vec{P} = \epsilon_0 \vec{E}$$

$$\begin{aligned} e^{ix} &= \cos x + i \sin x \\ \cos x &= \operatorname{Re}(e^{ix}) = \frac{e^{ix} + e^{-ix}}{2} \\ \sin x &= \operatorname{Im}(e^{ix}) = \frac{e^{ix} - e^{-ix}}{2i} \end{aligned}$$

$$\begin{aligned} \bar{E}(x, y, z, t) &= \operatorname{Re}\{\hat{x}A(x, y, z)e^{i\phi} e^{i\omega t}\} \\ \bar{E}(x, y, z, t) &= \operatorname{Re}\{\hat{x}A(x, y, z)e^{i(\omega t + \phi)}\} \\ \bar{E}(x, y, z, t) &= \operatorname{Re}\{\hat{x}A(x, y, z)[\cos(\omega t + \phi) + i \sin(\omega t + \phi)]\} \\ \bar{E}(x, y, z, t) &= \hat{x}A(x, y, z) \cos(\omega t + \phi) \end{aligned}$$

↓ Phasor form

$$\bar{E} = \hat{x}E_1 \cos(\omega t + \phi_1) + \hat{y}E_2 \cos(\omega t + \phi_2) + \hat{z}E_3 \cos(\omega t + \phi_3)$$

$$\bar{E} = (\hat{x}E_1 e^{i\phi_1} + \hat{y}E_2 e^{i\phi_2} + \hat{z}E_3 e^{i\phi_3}) e^{i\omega t + \phi_0}$$

$$\bar{E} = \hat{x}E_1 e^{j\phi_1} + \hat{y}E_2 e^{j\phi_2} + \hat{z}E_3 e^{j\phi_3} \leftarrow e^{\theta \rightarrow 1}$$

$$\bar{E}_y = E_0 \cos(\omega t - kx) \hat{y} \longleftrightarrow \bar{E}_y = E_0 \hat{y} e^{j(\omega t - kx)} \Rightarrow \bar{E}_y = E_0 \hat{y} e^{-jkx} \leftarrow \bar{E}_y = \begin{pmatrix} 0 \\ E_0 e^{-jkx} \\ 0 \end{pmatrix}$$

Let us first consider (b), (c), and (d). The phase velocity, wavelength and phase shift between  $x_i = 0.1m$  and  $x_o = 0.15m$ . These more concern the properties of the material than the electric field inducing them.

The wavelength  $\lambda$  is the distance between two maxima so  $(\omega t - kx) - (\omega t - k(z+\lambda)) = 2\pi$

The wavelength  $\lambda = \frac{v_p}{f} = \frac{2\pi}{k} = \frac{c\pi v_p}{\omega}$  where  $k$  is the propagation constant.

The propagation of a wave through a medium is slower than free space because of the intrinsic impedance of the medium.

The relative permittivity  $\epsilon_r$  for polystyrene is 2.54

$$\epsilon_r = \left( \frac{C}{v_p} \right) = \left( \frac{3e8}{v_p} \right)^2 \Rightarrow v_p = \frac{C}{\sqrt{\epsilon_r}} = \frac{C}{\sqrt{2.54}} = \frac{3e8}{\sqrt{2.54}}$$

$$(b) (b) The phase velocity  $v_p$  is \frac{C}{\sqrt{\epsilon_r}} = \frac{3e8}{\sqrt{2.54}} = \frac{3e8}{1.5937} = 188,236,741 \frac{m}{s}$$

$$v_p = 1.88e8 \text{ m/s}$$

$$\text{The wave impedance } \eta = \frac{\eta_0}{\sqrt{\epsilon_r}} = \frac{377}{\sqrt{2.54}} = 236.65 \Omega$$

The wavelength of the wave in freespace would simply be

$$\lambda = \frac{C}{f} \frac{(\text{m/s})}{(\text{1/s})} = \frac{3e8 \text{ m/s}}{2.4e9 \text{ Hz}} = 12.491 \text{ cm}$$

(c) going through a medium compresses it resulting in a shorter wavelength.

$$\lambda = \frac{v_p}{f} = \frac{C}{f\sqrt{\epsilon_r}} = \frac{3e8}{2.4e9 \sqrt{2.54}} = 0.07848 \text{ m}$$

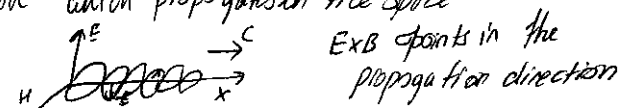
$$\text{The propagation constant } k \text{ is } \frac{2\pi}{\lambda} = \frac{2\pi}{0.07843 \text{ m}} = 80,109 \text{ m}^{-1}$$

Now we return to (a) deriving the amplitude and direction of the magnetic field  $\vec{H}$ . where  $E$  is a plane wave consisting of one or electric field vector in the  $\hat{y}$  direction. So  $\bar{E}_y$  takes the form

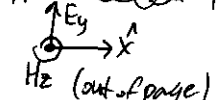
$$\bar{E}_y = \begin{pmatrix} 0 \\ E_0 e^{-jkx} \\ 0 \end{pmatrix} \text{ where } E_0 = 5.0 \text{ V/m}$$

Consider the following em wave which propagates in free space

$$\begin{aligned} E &= E_0 \cos(kx - \omega t) \\ B &= B_0 \cos(kx - \omega t) \end{aligned}$$



So we know the  $H$  field is in the  $\hat{z}$  direction for a corresponding  $E$  field polarized in the  $\hat{y}$  direction traveling in the  $\hat{x}$  direction.



$$\text{The curl } \nabla \times F = \begin{vmatrix} \hat{x} & \hat{y} & \hat{z} \\ \frac{\partial}{\partial x} & \frac{\partial}{\partial y} & \frac{\partial}{\partial z} \\ F_x & F_y & F_z \end{vmatrix} \Rightarrow \begin{pmatrix} \frac{\partial F_z}{\partial y} - \frac{\partial F_y}{\partial z} \\ \frac{\partial F_x}{\partial z} - \frac{\partial F_z}{\partial x} \\ \frac{\partial F_y}{\partial x} - \frac{\partial F_x}{\partial y} \end{pmatrix} = \underbrace{\left( j\omega E + \sigma E \right)}_{j\omega E + \sigma E}$$

Since we are solving for  $\bar{H}$  the moving  $\bar{E}$  field induces a curling  $H$  field such that

$$\nabla \times H = \begin{pmatrix} \frac{\partial H_z}{\partial y} - \frac{\partial H_y}{\partial z} \\ \frac{\partial H_x}{\partial z} - \frac{\partial H_z}{\partial x} \\ \frac{\partial H_y}{\partial x} - \frac{\partial H_x}{\partial y} \end{pmatrix} = j\omega \bar{D} + \bar{J} = j\omega \epsilon \bar{E} + \sigma \bar{E} = (j\omega \epsilon + \sigma) \begin{pmatrix} 0 \\ E_0 e^{-jkx} \\ 0 \end{pmatrix}$$

~~Since~~ This leaves us with three equations and three unknowns

$$\frac{\partial H_z}{\partial y} - \frac{\partial H_y}{\partial z} = \frac{\partial H_x}{\partial y} - \frac{\partial H_x}{\partial z} = 0$$

$$\frac{\partial H_x}{\partial z} - \frac{\partial H_z}{\partial x} = (j\omega \epsilon + \sigma) E_0 e^{-jkx}$$

~~or~~  $\frac{\partial H_y}{\partial x} - \frac{\partial H_x}{\partial y} = 0$  we assume there is negligible current in the  $y$  plane

$$\frac{\partial H_x}{\partial z} - \frac{\partial H_z}{\partial x} = j\omega \epsilon E_0 e^{-jkx}$$

We also know of the form that the  $H$  field takes being in the  $+z$  direction.

$$\bar{H} = \bar{H}_z = \begin{pmatrix} 0 \\ 0 \\ H_3 \end{pmatrix} \text{ so } H_x \text{ and } H_y \text{ are } 0.$$

so the equation is modified to  $\frac{\partial H_3}{\partial x} = j\omega \epsilon E_0 e^{-jkx}$ .

$$\text{or } \frac{\partial H_3}{\partial x} + j\omega \epsilon E_0 e^{-jkx} = 0$$

for a general lossy medium  $\nabla \times \bar{E} = j\omega \mu \bar{H}$ ,  $\nabla \times \bar{H} = j\omega \epsilon \bar{E} + \sigma \bar{E}$   
So going by the first equation:

$$\left( \frac{\partial E_z}{\partial y} - \frac{\partial E_y}{\partial z} \right) \hat{x} + \left( \frac{\partial E_x}{\partial z} - \frac{\partial E_z}{\partial x} \right) \hat{y} + \left( \frac{\partial E_y}{\partial x} - \frac{\partial E_x}{\partial y} \right) \hat{z} = -j\omega \mu (F_x \hat{x} + H_y \hat{y} + H_z \hat{z})$$

$$E_x = E_z = 0 \Rightarrow -\cancel{\frac{\partial E_y}{\partial z}} \hat{x} + \frac{\partial E_y}{\partial x} \hat{z} = -j\omega \mu H_z \hat{z}$$

We can consider the electric field uniform along the  $z$  axis

so  $E_y$  does not change with respect to  $z$

$$\Rightarrow \frac{\partial E_y}{\partial x} = 0$$

leaving us with:

$$-\cancel{\frac{\partial E_y}{\partial z}} \hat{z} = -j\omega \mu H_z \hat{z}$$

or

$$\Rightarrow \frac{\partial E_y}{\partial z} = -j\omega \mu H_z$$

$$\Rightarrow H_z = -\frac{\partial E_y}{\partial z} \cdot \frac{1}{j\omega \mu}$$

We know  $E_y = E_0 e^{-jkx}$  so  $\frac{\partial E_y}{\partial z} = -jK E_0 e^{-jkx}$

$$\Rightarrow H_z = jKE_0 e^{-jkx} \cdot \frac{1}{j\omega \mu} = \frac{K}{\omega \mu} E_0 e^{-jkx}$$

(a) So the amplitude for the magnetic field in this case is  $\frac{E_0 K}{\omega \mu}$  in the  $+z$  direction.  
Assuming there is no conductive losses.

$$\eta_0 = \sqrt{\mu_0 \epsilon_0} = 377 \Omega \quad \text{so the amplitude for this idealized plane wave}$$

$$\eta_0 = \frac{\omega \mu}{K} = \frac{\eta_0}{\sqrt{\epsilon_0}} \Rightarrow \frac{E_0}{\eta_0} = \frac{E_0 \cdot \eta_0}{\sqrt{\epsilon_0}}$$

$\frac{E_0 \cdot 377}{\sqrt{2.54}} = \frac{5V/m \cdot 377 \Omega}{\sqrt{2.54} m} = 1182.75$

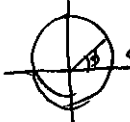
This also ignores the mutual self coupling of the planar  $z$  sense? Check units!

(d) finally we need to calculate the changing phase from point:  $x_1=0.1m$ ,  $x_2=0.15m$

The phase velocity  $v_p = 188,236,741 \text{ m/s}$   
is how far the phase travels in 1 second.

or electric field in phasor form is

$E_0 e^{-jkr}$  or  $E_0 L - kx$   
; but we care about the phase angle.



→ The frequency cycles at 2.4 GHz per along the +X direction  
so one rotation corresponds to one wavelength in the medium along the X axis.

our propagation constant  $k = \frac{89.109}{m}$

with a difference of 0.05m we get  $k \cdot \Delta x = 4 \text{ radians}$   
so  $\Delta\phi = k \Delta x = 229.49538^\circ$  or  $229.5^\circ$

I prefer the nomenclature of phase difference.

1.3. Show that a ~~randomly~~ polarized plane of the form  $\bar{E} = E_0(\hat{x}f + \hat{y}g)$

1.1. check and validate the solution to (a)

having  $\bar{H}_z = \frac{E_0 \cdot \eta_0}{\epsilon_0 \sqrt{\epsilon_r}}$  in the  $\hat{z}$  direction being the valid

solution to an induced  $\bar{E}$  vector in the  $\hat{y}$  direction traveling in the  $\hat{x}$  direction.

one possible validation is  $\bar{E} \times \bar{H}$  will point in the direction of the propagation.

taking the electromagnetic field of the form  $E_0 \sin(kx - wt)$

the magnetic field of the form  $B_0 \sin(kx - wt)$

the solutions of these magnitudes must be the

$$\frac{E_m}{B_m} = c$$

$$\Rightarrow B_m = \frac{E_m}{c} = \frac{5 \text{ V/m}}{c} = 1.668 \cdot 10^8 \text{ kg/(s}^2\text{A}) = 1.668 \cdot 10^8 \text{ T}$$

A setting is that we need to hold  $\nabla \cdot \bar{E} = 0$  for all the positions

So we need to prove whether  $|\bar{E}| = c$  regardless of the medium

and whether or not being in a medium slows down this constant or not, and what it may be.

So the magnitude of the  $|\bar{E}|$  vector is  $\sqrt{E_x^2 + E_y^2 + E_z^2}$   
and the magnitude of the  $|\bar{H}|$  vector is  $\sqrt{H_x^2 + H_y^2 + H_z^2}$

for free space we know for sure the ratio is  $c$ , but how do we prove it.

$$\nabla \times \bar{E} = j2\pi f \mu_0 \bar{H} = -j\omega \mu_0 \bar{H}$$

the magnetic field can be found from maxwell's equation  
to give  $\bar{H} = \frac{j}{\omega \mu_0} \nabla \times \bar{E} = \frac{j}{\omega \mu_0} (\bar{E}_0 e^{-jk\bar{r}}) = \frac{-j}{\omega \mu_0} \bar{E}_0 \times (-\hat{k}) e^{-jk\bar{r}}$

$$\Rightarrow \bar{H} = \frac{k_0}{\omega \mu_0} \hat{n} \times \bar{E}_0 e^{-jk\bar{r}} = \frac{1}{\eta_0} \hat{n} \times \bar{E}_0 e^{-jk\bar{r}}$$

$$\bar{H} = \frac{1}{\eta_0} \hat{n} \times \bar{E}$$

in our case  $\hat{n} = \langle 1, 0, 0 \rangle = \hat{x} + 0 \cdot \hat{y} + 0 \cdot \hat{z}$   
and  $\bar{E} = \langle 0, E_0, 0 \rangle = 0 \cdot \hat{x} + E_0 \cdot \hat{y} + 0 \cdot \hat{z}$

$$\hat{n} \times \bar{E} = \begin{vmatrix} \hat{x} & \hat{y} & \hat{z} \\ 1 & 0 & 0 \\ 0 & E_0 & 0 \end{vmatrix} = -0 - 0 + E_0 \cdot \hat{z} \Rightarrow H = \frac{\hat{z} E_0}{\eta_0}$$

for freespace,

$$|\bar{H}| = \frac{5 \text{ V/m}}{377 \Omega} \rightarrow \text{a virtual magnetic current?}$$

$$\eta_0 = \sqrt{\mu_0 \epsilon_0} = \frac{\omega \mu_0}{k_0} = \sqrt{\frac{\mu_0}{\epsilon_0}} \quad v_p = \frac{\omega}{k} = \lambda f \Rightarrow \frac{dx}{dt} = \frac{1}{\sqrt{\mu_0 \epsilon_0}} = \text{constant}$$

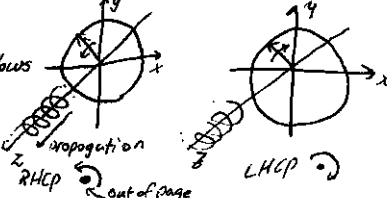
$$\text{Note! } \eta_0 = \sqrt{\mu_0 \epsilon_0} \quad v_{p0} = \frac{1}{\eta_0} = \frac{1}{\sqrt{\mu_0 \epsilon_0}} = c$$

The explanation is

$$Z_0 = \frac{F}{H} = \mu_0 c_0 = \frac{\mu_0}{\sqrt{\epsilon_0 \epsilon_0}} = \frac{1}{\epsilon_0 G}$$

1.3 Show that a linearly polarized plane of the form  $\bar{E} = E_0(a\hat{x} + b\hat{y})e^{-jk_0z}$  where  $a$  and  $b$  are real numbers, can be represented as a RHP and a LHP plane wave.

The notation going to be used is as follows:  
Just having  $(a \neq 0)$  will only result in  
a polarized propagation.



In the case of  $a=b=1$ , we have the even combination of the two orthogonal vectors.

$$\Rightarrow \bar{E} = E_0(\hat{x} + \hat{y})e^{-jk_0z} \rightarrow$$

$$\begin{aligned}\bar{E} &= (a\hat{x} + b\hat{y})E_0e^{-jk_0z} \\ \bar{E}(x,y,z=0) &= E_0(a\hat{x} + b\hat{y})\end{aligned}$$

$$\begin{aligned}\text{(i)} \rightarrow \bar{E} &= E_0 \cos \alpha \hat{x} + E_0 \cos \beta \hat{y} \\ &\begin{array}{c} \text{---} \\ \text{---} \end{array} \\ &\begin{array}{c} (a=0, b=1) \\ (a=b=\sqrt{2}/2) \\ (a=1, b=0) \end{array} \\ &\begin{array}{c} \text{---} \\ \text{---} \end{array} \\ &\begin{array}{c} (a=0, b=-1) \\ (a=-b=\sqrt{2}/2) \\ (a=-1, b=0) \end{array} \\ &\begin{array}{c} \text{---} \\ \text{---} \end{array}\end{aligned}$$

If we have a function that results in a Real number such as sin or cos  $\rightarrow [-1, 1]$

which results in the ranges

$$\begin{cases} -1 \leq a \leq 1 \\ -1 \leq b \leq 1 \end{cases}$$

$$\text{So } a = \cos \alpha \text{ and } b = \frac{\sin \beta}{\cos \alpha} \rightarrow \text{(i)}$$

Since we can generate any point on the circle as a Real number pair of  $a, b$  we can indeed use the a parametric function to cycle between this circle for a circularly polarizing wave.

This CP wave takes the form

$$\bar{E}(0, t) = E_0 \left[ \hat{x} \cos(wt - k_0 z) + \hat{y} \cos(wt - k_0 z - \frac{\pi}{2}) \right]$$

for a RHP wave.

Similarly for a LHP?

$$\bar{E}(0, t) = E_0 \left[ \hat{x} \cos(wt - k_0 z) + \hat{y} \left( e^{\frac{i(wt - k_0 z - \frac{\pi}{2})}{2}} \right) \left( \frac{e^{i(wt - k_0 z)}}{2} - \frac{e^{i(wt - k_0 z)}}{2} \right) \right]$$

Here even though cosine and sine include complex numbers in their derivation with Euler's identity, the resulting value is Real.

1.4 Compute the Poynting vector for the general plane wave field of (1.76).

$$\nabla \times \bar{E} = -j\omega \mu_0 \bar{H}^{(1.76)}, \quad \bar{H} = \frac{1}{\mu_0} \hat{n} \times \bar{E} \quad (1.76)$$

The Poynting vector  $\bar{S}$  is the cross product of  $E \times H^*$   
 $\bar{S} = \bar{E} \times \bar{H}^*$

We are tasked of computing this vector given only with  $\bar{H} = \frac{1}{\mu_0} \hat{n} \times \bar{E}$  (1.76), or at least that is how

I interpret this problem.

$$\Rightarrow \bar{S} = \bar{E} \times \left( \frac{1}{\mu_0} \hat{n} \times \bar{E} \right)^* = E \times \left( \frac{j}{\omega \mu_0} \nabla \times E \right)^* = E \times \left( \frac{j}{\omega \mu_0} \nabla \times E e^{-jk_0 z} \right)^*$$

$$\bar{S} = \bar{E} \times \left( \frac{1}{\mu_0} \hat{n} \times \bar{E} e^{-jk_0 z} \right)^*$$

Conjugation brings phasors of the form  $e^{j\theta} \rightarrow e^{j\theta}$  which is a negation?

The cross product of two vectors  $\bar{a}$  and  $\bar{b}$  where  $\bar{a} = a_1 \hat{x} + a_2 \hat{y} + a_3 \hat{z}$  and  $\bar{b} = b_1 \hat{x} + b_2 \hat{y} + b_3 \hat{z}$

$$\Rightarrow \bar{a} \times \bar{b} = (a_2 b_3 - a_3 b_2) \hat{x} + (a_3 b_1 - a_1 b_3) \hat{y} + (a_1 b_2 - a_2 b_1) \hat{z}$$

We also know the cross product between two phasors is  $\|\bar{a} \times \bar{b}\| = \|a\| \|b\| \sin \theta$

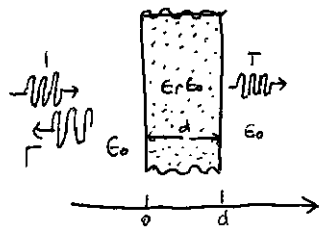
$$\text{Assuming } \hat{n} \text{ is } \perp \text{ to } \bar{E} : \left\| \frac{1}{\mu_0} \hat{n} \times \bar{E} e^{-jk_0 z} \right\| = \frac{E_0}{\mu_0}$$

Unsure how to work this problem, it seems already solved.

Is it asking to simplify the expression?

I also don't know how to take the conjugate of an  $\mathbb{R}^3$  vector

1.5 A plane wave normally incident on a dielectric slab of permittivity  $\epsilon_r$ , and a thickness  $d$ , where  $d = \frac{\lambda_0}{4\pi f}$  and  $\lambda_0$  is the free space wavelength of the incident wave, as shown in the accompanying figure. If free-space exists on both sides of the slab, find the reflection coefficient of the wave reflected from the front of the slab.



There is a reflection whenever a medium is changed.

The initial reflection as well as the subsequent internal reflections that correspondingly bleed out and lose power on each successive hit.

The first interface

The problems of ch 1 are to be considered at a later date as I am in poor health.  
Consider the motivation of solving and rederiving these problems.

To be continued. I want to continue translating the book.  
The problems will be redone in a problem book.

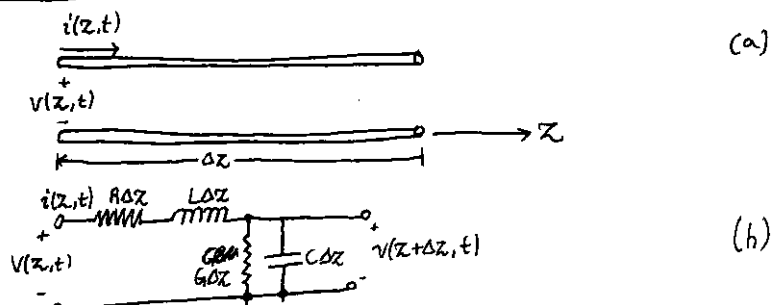


Figure 2.1 Voltage and Current definitions and equivalent circuit for an infinitesimal length of transmission line. (a) Voltage and current definitions  
(b) Lumped element equivalent circuit.

## Chapter Two : Transmission Line Theory

Transmission line theory bridges the gap between field analysis and basic circuit theory and therefore is of significant importance in the analysis of microwave circuits and devices. As we will see, the phenomenon of wave propagation on transmission lines can be approached from an extension of circuit theory or from a specialization of Maxwell's equations; we shall present both viewpoints and show how this wave propagation is described by equations very similar to those used in Chapter 1 for plane wave propagation.

### 2.1 The Lumped-element circuit model for a transmission line.

The key difference between circuit theory and transmission line theory is electrical size. Circuit analysis assumes that the physical dimensions of the network are much smaller than the electrical wavelength, while transmission lines may be a considerable fraction of a wavelength, or many wavelengths, in size. Thus a transmission line is a distributed parameter network, where voltages and currents can vary and magnitude and phase over its length, while ordinary circuit analysis deals with lumped elements, where voltage and current do not vary appreciably over the physical dimension of the element.

As shown in Figure 2.1a, a transmission line is often schematically represented as a two-wire line. Since transmission lines (for transverse electromagnetic [TEM] wave propagation) always have at least two conductors. The piece of line of infinitesimal length  $\Delta z$  of Figure 2.1a can be modeled as a lumped element circuit, as shown in Figure 2.1b, where  $R, L, G, C$  are per-unit-length quantities defined as follows :

$R$  = Series resistance per unit length, for both conductors in  $\Omega/m$ .

$L$  = Series inductance per unit length, for both conductors, in  $H/m$ .

$G$  = Shunt conductance per unit length, in  $S/m$ .

$C$  = Shunt capacitance per unit length

The Series inductance  $L$  represents the total self-inductance of the two conductors, and the shunt capacitance  $C$  is due to the close proximity of the two conductors. The series resistance  $R$  represents the resistance due to the finite conductivity of the individual conductors, and the shunt conductance  $G$  is due to dielectric loss in the material between the conductors.  $R$  and  $G$ , therefore, represent loss. A finite length of transmission line can be viewed from a cascade of sections of the form shown in Figure 2.1b.

from the circuit of Figure 2.1b Kirchhoff's voltage law can be applied to give

$$v(z,t) - R \Delta z i(z,t) - L \Delta z \frac{dv(z,t)}{\Delta z} - v(z+\Delta z,t) = 0 \quad (2.1a)$$

and Kirchhoff's current law leads to

$$i(z,t) - G \Delta z v(z+\Delta z,t) - C \Delta z \frac{dv(z+\Delta z,t)}{\Delta z} - i(z,t) = 0 \quad (2.1b)$$

Dividing (2.1a) and (2.1b) by  $\Delta z$  and taking the limit as  $\Delta z \rightarrow 0$  gives the following differential equations:

$$\frac{\partial v(z,t)}{\partial z} = -Ri(z,t) - L \frac{\partial i(z,t)}{\partial t} \quad (2.2a)$$

$$\frac{\partial i(z,t)}{\partial z} = -Gi(z,t) - C \frac{\partial v(z,t)}{\partial t} \quad (2.2b)$$

$$\begin{aligned} & v(z,t) - R\Delta z i(z,t) - L \Delta z \frac{\partial i(z,t)}{\partial t} - v(z+\Delta z,t) = 0 \\ \Rightarrow & \frac{v(z,t)}{\Delta z} - R \cdot i(z,t) - L \frac{\partial i(z,t)}{\partial t} - \frac{v(z+\Delta z,t)}{\Delta z} = 0 \\ \Rightarrow & \lim_{z \rightarrow 0} \frac{v(z+\Delta z,t) - v(z,t)}{\Delta z} = -Ri(z,t) - L \frac{\partial i(z,t)}{\partial t} \\ \Rightarrow & \frac{\partial v(z,t)}{\partial z} = -Ri(z,t) - L \frac{\partial i(z,t)}{\partial t} \\ & i(z,t) - G\Delta z v(z+\Delta z,t) - C\Delta z \frac{\partial v(z+\Delta z,t)}{\partial z} - i(z+\Delta z,t) = 0 \\ \Rightarrow & \frac{i(z,t)}{\Delta z} - G \frac{v(z+\Delta z,t)}{\Delta z} - C \frac{\partial v(z+\Delta z,t)}{\partial z} - \frac{i(z+\Delta z,t)}{\Delta z} = 0 \\ \Rightarrow & \frac{i(z+\Delta z,t)}{\Delta z} - \frac{i(z+\Delta z,t)}{\Delta z} = -G(v(z+\Delta z,t)) - C \frac{\partial v(z+\Delta z,t)}{\partial z} \\ \Rightarrow & \lim_{z \rightarrow 0} \frac{i(z+\Delta z,t) - i(z,t)}{\Delta z} = -G \cdot v(z+\Delta z,t) - C \frac{\partial v(z+\Delta z,t)}{\partial z} \\ \Rightarrow & \frac{\partial i(z,t)}{\partial z} = -G \cdot v(z,t) - C \frac{\partial v(z,t)}{\partial z} \end{aligned}$$

These are the time domain forms of the transmission line equations, also known as the Telegrapher equations for the sinusoidal steady-state conditions, with casion-based phasors, (2.2a) and (2.2b)

simplify to  $\frac{dV(z)}{dz} = -(R+j\omega L)I(z)$  (2.3a)

$$\frac{dI(z)}{dz} = -(G+j\omega C)V(z) \quad (2.3b)$$

Notice the similarity in the form of (2.3a) and (2.3b) and Maxwell's curl equations of (1.41a) and (1.41b).

$$\nabla \times \vec{E} = -ic\mu_0 \vec{H} \quad (1.41a)$$

$$\nabla \times \vec{H} = i\omega \epsilon_0 \vec{E} \quad (1.41b)$$

### - Wave Propagation on a Transmission Line.

The two equations (2.3a) and (2.3b) can be solved simultaneously to give wave equations for  $V(z)$  and  $I(z)$ :

$$\frac{d^2 V(z)}{dz^2} - \gamma^2 V(z) = 0, \quad \frac{d^2 I(z)}{dz^2} - \gamma^2 I(z) = 0 \quad (2.4 a, b)$$

$$\text{where } \gamma = \alpha + j\beta = \sqrt{(R+j\omega L)(G+j\omega C)}$$

$$\gamma = \alpha + j\beta = \sqrt{(R+j\omega L)(G+j\omega C)} \Rightarrow \gamma^2 = (\alpha + j\beta)^2 = (R+j\omega L)(G+j\omega C)$$

$$\frac{dV(z)}{dz} = -(R+j\omega L)I(z), \quad \frac{dI(z)}{dt} = -(G+j\omega C)V(z)$$

$$\gamma^2 = (\alpha + j\beta)^2 = (R+j\omega L)(G+j\omega C) = RG + j\omega LG + Rj\omega C + j\omega^2 LC = -\omega^2 LC + j\omega(LG + RC) + RG$$

$$dV(z) = \frac{dI(z)}{dz} \cdot \frac{-1}{(G+j\omega C)} \rightarrow \frac{dV(z)}{dt} = \frac{dV(z)}{dz} \cdot \frac{d}{dz} \frac{dI(z)}{dz} \cdot \frac{-1}{(G+j\omega C)} = -(R+j\omega L)I(z)$$

$$\Rightarrow \frac{d^2 I(z)}{dz^2} = -(G+j\omega C) \cdot -(R+j\omega L)I(z) = \gamma^2 I(z)$$

$$\Rightarrow \boxed{\frac{d^2 I(z)}{dz^2} = \gamma^2 I(z) = 0}$$

$$I(z) = \frac{dV(z)}{dt} \cdot \frac{-1}{(R+j\omega L)} \rightarrow \frac{dV(z)}{dt} = \frac{d}{dt} \frac{dV(z)}{dz} \cdot \frac{-1}{(R+j\omega L)} = -(G+j\omega C)V(z)$$

$$\Rightarrow \frac{d^2 V(z)}{dz^2} = -(R+j\omega L) \cdot -(G+j\omega C)V(z) = \gamma^2 V(z)$$

$$\Rightarrow \boxed{\frac{d^2 V(z)}{dz^2} = \gamma^2 V(z)}$$

$\gamma$  is the complex propagation constant, which is a function of frequency. Traveling wave solutions to (2.4) can be found as the homogeneous and particular solution using:

$$V(z) = V_0 e^{-\gamma z} + V_0' e^{\gamma z} \quad 2.6(a)$$

$$I(z) = I_0 e^{-\gamma z} + I_0' e^{\gamma z} \quad 2.6(b)$$

where the  $e^{\gamma z}$  term represents the wave propagation in the  $+z$  direction, and the  $e^{-\gamma z}$  represents the wave propagation in the  $-z$  direction. Applying (2.3) to the voltage of (2.6a) gives the current on the line:

$$I(z) = \frac{\gamma}{R+j\omega L} (V_0 e^{-\gamma z} - V_0' e^{\gamma z})$$

$$\frac{dI(z)}{dz} = \frac{\gamma(R+j\omega L)I(z)}{dz} \quad \text{equation 2.3a} \quad \left( \frac{dV(z)}{dz} \right) = -(R+j\omega L)I(z)$$

$$\text{so } V(z) = V_0 e^{-\gamma z} + V_0' e^{\gamma z}$$

$$\frac{dV(z)}{dz} = -(R+j\omega L) I(z) \quad \text{where } V(z) = (V_0^+ e^{-j\beta z} + V_0^- e^{j\beta z})$$

$$\Rightarrow \frac{d}{dz} (V_0^+ e^{-j\beta z} + V_0^- e^{j\beta z}) = -(R+j\omega L) I(z)$$

$$\Rightarrow V_0^+ \frac{de^{-j\beta z}}{dz} + V_0^- \frac{de^{j\beta z}}{dz} = -(R+j\omega L) I(z)$$

$$\Rightarrow -j\beta e^{-j\beta z} + j\beta e^{j\beta z} V_0^- = -(R+j\omega L) I(z)$$

$$\Rightarrow I(z) = \frac{\gamma (-V_0^+ e^{-j\beta z} + V_0^- e^{j\beta z})}{(R+j\omega L)} \Rightarrow I(z) = \frac{\gamma}{(R+j\omega L)} (V_0^+ e^{-j\beta z} - V_0^- e^{j\beta z})$$

Comparing with (2.6b) where  $I(z) = I_0^+ e^{-j\beta z} + I_0^- e^{j\beta z}$

$$I_0^+ e^{-j\beta z} + I_0^- e^{j\beta z} = \frac{\gamma}{(R+j\omega L)} (V_0^+ e^{-j\beta z} - V_0^- e^{j\beta z})$$

$$\Rightarrow \frac{(V_0^+ e^{-j\beta z} - V_0^- e^{j\beta z})}{(I_0^+ e^{-j\beta z} + I_0^- e^{j\beta z})} = Z_0 = \frac{(R+j\omega L)}{\gamma}$$

$$\text{Since } \gamma = \sqrt{(R+j\omega L)(G+j\omega C)} \Rightarrow Z_0 = \frac{(R+j\omega L)}{\sqrt{(R+j\omega L)(G+j\omega C)}} = \frac{\sqrt{R+j\omega L} \cdot \sqrt{R+j\omega L}}{\sqrt{R+j\omega L} \cdot \sqrt{G+j\omega C}}$$

$$\Rightarrow Z_0 = \frac{\sqrt{R+j\omega L}}{\sqrt{G+j\omega C}}$$

this shows that the characteristic impedance,  $Z_0$ , is:

$$Z_0 = \frac{R+j\omega L}{\gamma} = \frac{\sqrt{R+j\omega L}}{\sqrt{G+j\omega C}} \quad (2.7)$$

$$\text{To relate the voltage and current: } \frac{V_0^+}{I_0^+} = Z_0 = \frac{-V_0^-}{I_0^-}$$

Then (2.6b) can be rewritten in the following form:

$$I(z) = \frac{V_0^+}{Z_0} e^{-j\beta z} - \frac{V_0^-}{Z_0} e^{j\beta z} \quad (2.8)$$

Converting back to the time domain, we can express the voltage waveform as

$$V(z, t) = [V_0^+ \cos(\omega t - \beta z + \phi) e^{-j\beta z} + V_0^- \cos(\omega t + \beta z + \phi) e^{j\beta z}] \quad (2.9)$$

where  $\phi$  is the phase angle of the complex voltage  $V_0^+$ . Using arguments similar to those in Section 1.4, we find that the wavelength on the line is

$$\lambda = \frac{2\pi}{\beta} \quad (2.10)$$

$$\text{and the phase velocity } v_p = \frac{\omega}{\beta} = \lambda f \quad (2.11)$$

### The Lossless Line

The above solution is for a general transmission line, including loss effects, and it was seen that the propagation constant and characteristic impedance were complex. In many practical cases, however, the loss of the line is small and so can be neglected, resulting in a simplification of the results. Setting  $R=G=0$  in (2.5), gives the propagation constant as:  $\gamma = \alpha + j\beta = j\omega\sqrt{LC}$ ,

$$\Rightarrow \beta = \omega\sqrt{LC} \text{ and } \alpha = 0. \quad (2.12) \quad a, b$$

As expected for a lossless line, the attenuation constant  $\alpha$  is zero. The characteristic impedance of (2.7) reduces to

$$Z_0 = \sqrt{\frac{L}{C}} \quad (2.13)$$

which is now a real number. The general solutions for voltage and current on a lossless transmission line can then be written as:

$$V(z) = V_0^+ e^{-j\beta z} + V_0^- e^{j\beta z} \quad (2.14a)$$

$$I(z) = \frac{V_0^+}{Z_0} e^{-j\beta z} - \frac{V_0^-}{Z_0} e^{j\beta z} \quad (2.14b)$$

The wavelength is

$$\lambda = \frac{2\pi}{\beta} = \frac{2\pi}{\omega\sqrt{LC}} \quad (2.15)$$

and the phase velocity is

$$v_p = \frac{\omega}{\beta} = \frac{1}{\sqrt{LC}} \quad (2.16)$$

### 2.2 Field Analysis of Transmission Lines

In this section we will derive the time-harmonic form of the telegrapher's equations starting from Maxwell's equations. We will begin by deriving the transmission line parameters ( $R, L, G, C$ ) in terms of the electric and magnetic fields of the transmission line and then derive the telegrapher's equations using these parameters for the specific case of a coaxial line.

#### Transmission Line Parameters

Consider a 1m length of a uniform transmission line with fields  $\vec{E}$  and  $\vec{H}$ , as shown in Figure 2.2, where  $S$  is the cross-sectional surface area of the line. Let the voltage between the conductors between the conductors be  $V_0 e^{\pm j\beta z}$  and the current be  $I_0 e^{\pm j\beta z}$ . The line averaged stored magnetic energy for this 1m length of line can be written, from (1.86) as:

$$W_m = \frac{\mu}{4\pi} \int_S \vec{H} \cdot \vec{H}^* ds$$

while circuit theory gives  $W_m = L|I_0|^2/4$  in terms of the current on the line. We can thus identify the self-inductance per unit length as

$$L = \frac{\mu}{4\pi} \int_S \vec{H} \cdot \vec{H}^* ds \frac{1}{1m} \quad (2.17)$$

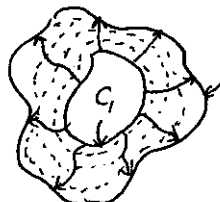


Figure 2.2 fields lines on some arbitrary TEM transmission line

Similarly, the time-average stored electrical energy per unit length can be found from (1.84) as

$$We = \frac{\epsilon}{4} \int_S \bar{E} \cdot \bar{E}^* ds$$

while circuit theory gives  $We = C(U_0)^2 / 4$ . Resulting in the following expression for the capacitance per unit length.

$$C = \frac{\epsilon}{(U_0)^2} \int_S \bar{E} \cdot \bar{E}^* ds \text{ F/m} \quad (2.18)$$

From (1.131), the power loss per unit length due to the metallic conductor is:

$$P_c = \frac{R_s}{2} \int_{C_1 + C_2} \bar{H} \cdot \bar{H}^* dl$$

(assuming  $\bar{H}$  is tangential to  $S$ ), while circuit theory gives  $P_c = R/I^2 I^2/2$ , so the series resistance  $R$  per unit length of line is

$$R = \frac{R_s}{(I_0)^2} \int_{C_1 + C_2} \bar{H} \cdot \bar{H}^* dl \Omega/m \quad (2.19)$$

In (2.19),  $R_s = 1/\sigma S_0$  is the surface resistance of the conductors, and  $C_1 + C_2$  represents integration paths over the conductor boundaries. From (1.92), the time-average power dissipation per unit length in a lossy dielectric is

$$P_d = \frac{\omega \epsilon''}{2} \int_S \bar{E} \cdot \bar{E}^* ds$$

where  $\epsilon''$  is the imaginary part of the complex permittivity  $\epsilon = \epsilon' - \epsilon'' = \epsilon'(1 - j\omega \delta)$ .

Circuit theory gives  $P_d = G(U_0)^2/2$ , so the shunt conductance per unit length can be written as:  $G = \frac{\omega \epsilon''}{(U_0)^2} \int_S \bar{E} \cdot \bar{E}^* ds \text{ S/m} \quad (2.20)$

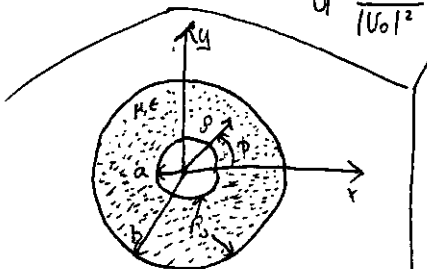


Figure 2.3 Geometry of a coaxial line with surface resistance  $R_s$  on the inner and outer conductors.

**Example 2.1** Transmission Line Parameters of a Coaxial Line. The fields of a traveling TEM wave inside the coaxial line of Figure 2.3 can be expressed as:

$$\bar{E} = \frac{V_0 \hat{r}}{j \ln(b/a)} e^{-j\gamma z}, \quad \bar{H} = \frac{I_0 \hat{\phi}}{2\pi r_0} e^{-j\gamma z}$$

where  $\gamma$  is the propagation constant of the line.

The conductors are assumed to have a surface resistivity  $R_s$ , and the material filling the space between the conductors is assumed to have a complex permittivity  $\epsilon = \epsilon' - j\epsilon''$  and a permeability  $\mu_0 \mu_r$ .

Determine the transmission line parameters.

**Solution:** From (2.17)-(2.20) and the given fields the parameters of the coaxial line can be calculated as:

$$Z = \frac{M}{(2\pi)^2} \int_{\phi=0}^{2\pi} \int_{p=a}^b \frac{1}{\rho^2} \rho d\rho d\phi = \frac{M}{2\pi} \ln(b/a) \text{ N/m},$$

$$C = \frac{\epsilon'}{(\ln(b/a))^2} \int_{\phi=0}^{2\pi} \int_{p=a}^b \frac{1}{\rho^2} \rho d\rho d\phi = \frac{2\pi \epsilon'}{\ln(b/a)} \text{ F/m},$$

$$R = \frac{R_s}{(2\pi)^2} \left\{ \int_{\phi=0}^{2\pi} \frac{1}{a^2} a d\phi + \int_{\phi=0}^{2\pi} \frac{1}{b^2} b d\phi \right\} = \frac{R_s}{2\pi} \left( \frac{1}{a} + \frac{1}{b} \right) \Omega/m,$$

$$G = \frac{\omega \epsilon''}{(\ln(b/a))^2} \int_{\phi=0}^{2\pi} \int_{p=a}^b \frac{1}{\rho^2} \rho d\rho d\phi = \frac{2\pi \omega \epsilon''}{\ln(b/a)} \text{ S/m}.$$

Table 2.1 summarizes the parameters for coaxial, two-wire, and parallel plate lines.

As we will see in the next chapter, the propagation constant, characteristic impedance, and attenuation of most transmission lines are usually derived directly from a field theory solution; the approach here of first finding the equivalent circuit parameters ( $L, C, R, G$ ) is useful only for very simple lines. Nevertheless it provides a helpful intuition structure for understanding the properties of a transmission line to its equivalent circuit model.

Table 2.1 Transmission Line Parameters for Some Common Lines

	Coax	Two-Wire	Parallel Plate
$L$	$\frac{M}{2\pi} \ln \frac{b}{a}$	$\frac{M}{\pi} \cosh^{-1} \left( \frac{D}{2a} \right)$	$\frac{\mu_0}{\omega}$
$C$	$\frac{2\pi \epsilon'}{\ln(b/a)}$	$\frac{\pi \epsilon'}{\cosh^{-1}(D/2a)}$	$\frac{\epsilon' \omega}{d}$
$R$	$\frac{R_s}{2\pi} \left( \frac{1}{a} + \frac{1}{b} \right)$	$\frac{R_s}{\pi a}$	$\frac{2R_s}{\omega}$
$G$	$\frac{2\pi \omega \epsilon''}{\ln(b/a)}$	$\frac{\pi \omega \epsilon''}{\cosh^{-1}(D/2a)}$	$\frac{\omega \epsilon'' w}{d}$



## Propagation Constant, Impedance, and Power flow for the lossless Coaxial Line

Equations (2.24a) and (2.24b) for  $E_p$  and  $H_\phi$  can be simultaneously solved to yield a wave equation for  $E_p$  (or  $H_\phi$ ):

$$\frac{\partial^2 E_p}{\partial z^2} + \omega^2 \mu \epsilon E_p = 0 \quad (2.29)$$

$$\left\{ \begin{array}{l} \frac{\partial E_p}{\partial z} = -j\omega \mu H_\phi \\ \frac{\partial H_\phi}{\partial z} = -j\omega \epsilon E_p \end{array} \right. \Rightarrow \frac{H_\phi}{E_p} = \frac{2\mu}{2\epsilon} = \frac{2\mu}{\omega^2 \mu \epsilon} = \frac{2}{\omega^2 \epsilon} = \frac{2}{\omega^2 Z_0^2} = \frac{2}{\omega^2 Z_0^2} e^{j\beta z} \quad (2.29)$$

$$\Rightarrow \frac{\partial^2 H_\phi}{\partial z^2} = -\omega^2 \mu \epsilon E_p \Rightarrow \frac{\partial^2 H_\phi}{\partial z^2} + \omega^2 \mu \epsilon H_\phi = 0$$

Similarly

$$\frac{\partial^2 E_p}{\partial z^2} + \omega^2 \mu \epsilon E_p = 0$$

from which it is seen that the propagation constant is  $\beta = \sqrt{\omega^2 \mu \epsilon}$ , which, for lossless media reduces to

$$\beta = \sqrt{\mu \epsilon} = \omega / Z_0$$

where the last result is from (2.12). Observe that the propagation constant is of the same form as that for plane waves in a lossless dielectric medium. This is a general result for TEM transmission lines.

The wave impedance for the coaxial line is defined as  $Z_0 = E_p / H_\phi$ , which can be calculated from (2.24a), assuming an  $e^{-j\beta z}$  dependence, to give:

$$Z_0 = \frac{E_p}{H_\phi} = \frac{\omega \mu}{\beta} = \sqrt{\mu \epsilon} = \eta \quad (2.31)$$

This wave impedance is seen to be identical to the intrinsic impedance of the medium,  $\eta$ , and is a general result for TEM transmission lines.

The characteristic impedance of the coax line is defined as:

$$Z_0 = \frac{V_o}{I_o} = \frac{E_p \ln b/a}{2\pi H_\phi} = \frac{\eta \ln b/a}{2\pi} = \sqrt{\epsilon} \frac{\ln b/a}{2\pi} \quad (2.32)$$

where the forms for  $E_p$  and  $H_\phi$  from example 2.1 have been used. The characteristic impedance is geometry dependent and will be different for other transmission line configurations.

Finally, the power flow (in the  $z$  direction) on the coax line may be computed from the Poynting vector as:

$$P = \frac{1}{2} \int_S \bar{E} \times \bar{H}^* dS = \frac{1}{2} \int_0^{2\pi} \int_{r=a}^b \frac{V_o I_o}{2\pi \mu^2 \ln b/a} P_d r d\phi = \frac{1}{2} V_o I_o^*$$

A result with clear agreement with circuit theory. This shows that the flow of power in a transmission line takes place entirely via the electric and magnetic fields of the conductors; power is not transmitted through the conductors themselves. As we will see later, for the case of finite conductivity, power may enter the conductors, but this power is lost as heat and not delivered to load.

## 2.3 The Terminated Lossless Transmission Line

Figure 2.4 shows a lossless transmission line terminated in an arbitrary load impedance  $Z_L$ . This problem will illustrate the wave reflection of transmission lines, a fundamental property of distributed systems.

Assume that an incident wave of the form  $V_o^+ e^{-j\beta z}$  is generated from the source at  $z < 0$ . We have seen that the ratio of voltage to current for such a traveling wave is  $Z_0$ , the characteristic impedance of the line. However, when the line is terminated in an arbitrary load  $Z_L \neq Z_0$ , the ratio of voltage to current at the load must be  $Z_L$ . Thus a reflected wave must be excited with the appropriate amplitude to satisfy this condition. The total voltage on the line can be written as in (2.14a), as the sum of incident and reflected waves:

$$V(z) = V_o^+ e^{-j\beta z} + V_o^- e^{j\beta z} \quad (2.34a)$$

Similarly, the total current on the line is described by (2.14b):

$$I(z) = \frac{V_o^+}{Z_0} e^{-j\beta z} - \frac{V_o^-}{Z_0} e^{j\beta z} \quad (2.34b)$$

The total voltage and current at the load are related by the load impedance. So at  $z = 0$  we must have:  $Z_L = \frac{V(0)}{I(0)} = \frac{V_o^+ + V_o^-}{V_o^+ - V_o^-} Z_0$

$$\text{Solving for } V_o^- \text{ gives } V_o^- = \frac{Z_L - Z_0}{Z_L + Z_0} V_o^+$$

The amplitude of the reflected voltage wave normalized to the amplitude of the incident voltage wave is defined as the voltage reflection coefficient,  $\Gamma$ :

$$\Gamma = \frac{V_o^-}{V_o^+} = \frac{Z_L - Z_0}{Z_L + Z_0} \quad (2.35)$$

The total voltage and current waves on the line can then be written as:

$$V(z) = V_o^+ (e^{-j\beta z} + \Gamma e^{j\beta z}) \quad , \quad I(z) = \frac{V_o^+}{Z_0} (e^{-j\beta z} - \Gamma e^{j\beta z}) \quad (2.36a, b)$$

From these equations it is seen that the voltage and current on the line consists of a superposition of an incident and reflected wave; such waves are called standing waves. Only when  $\Gamma = 0$  is there no reflected wave. To obtain  $\Gamma = 0$ , the load impedance  $Z_L$  must be equal to the characteristic impedance  $Z_0$  of the transmission line, as seen from (2.35). Such a load is said to be matched in the line since there is no reflection of the incident wave.

Now consider the time-average power flow along the line at the point  $z$ :

$$P_{avg} = \frac{1}{2} \operatorname{Re} \{ V(z) I(z)^* \} = \frac{1}{2} \frac{|V_o|^2}{Z_0} \operatorname{Re} \{ 1 - \Gamma^* e^{-2j\beta z} + \Gamma e^{2j\beta z} - |\Gamma|^2 \}$$

where (2.36) has been used.

The middle two terms in the brackets are of the form  $A \cdot \beta^k = 2j \operatorname{Im} \{A\}$ , and so are purely imaginary. This result simplifies to:  $P_{avg} = \frac{1}{2} \frac{|V_0|^2}{Z_0} (1 - |\Gamma|^2)^2$  (2.37)

which shows that the average power flow is constant at any point on the line and that the total power delivered to the load ( $P_{avg}$ ) is equal to the incident power ( $|V_0|^2/2Z_0$ ) minus the reflected power ( $|V_0|^2|\Gamma|^2/2Z_0$ ). If  $\Gamma=0$ , maximum power is delivered to the load, while no power is delivered for  $\Gamma=1$ . The above discussion assumes that the generator is matched, so that there is no re-reflection of the reflected waves from  $Z_G$ .

When the load is mismatched, not all the available power from the generator is delivered to the load. This 'loss' is called the return loss ( $RL$ ), and is defined (in dB) as

$$RL = -20 \log |\Gamma| \text{ dB}$$
 (2.38)

So that a matched load ( $\Gamma=0$ ) has a return loss of  $\infty$  dB (no reflected power), while a total reflection ( $|\Gamma|=1$ ) has a return loss of 0dB (all incident power is reflected). Note the return loss is a non-negative quantity for reflection from a passive network.

If the load is matched to the line,  $\Gamma=0$  and the magnitude of the voltage on the line is  $|V(Z)| = |V_0|/l$ , which is constant. Such a line is sometimes said to be flat. When the load is mismatched, however, the presence of the reflected waves leads to standing waves, and the magnitude of the voltage on the line is not constant.

$|V(Z)| = |V_0|/(1 + \Gamma e^{j\beta Z}) = |V_0|/(1 + |\Gamma| e^{j(\theta - \beta Z)})$  (2.39)

where  $l=z$  is the positive distance measured from the load at  $z=0$ , and  $\theta$  is the phase of the reflection coefficient ( $\Gamma = |V| e^{j\theta}$ ). This result shows that the voltage magnitude oscillates with position  $z$  along the line. The maximum value occurs when the phase term  $e^{j(\theta - \beta z)} = 1$  and is given by:

$$V_{max} = |V_0|/(1 + |\Gamma|)$$
 (2.40a)

The minimum value occurs when the phase term  $e^{j(\theta - \beta z)} = -1$  and is given by

$$V_{min} = |V_0|/(1 - |\Gamma|)$$
 (2.40b)

As  $|\Gamma|$  increases, the ratio of  $V_{max}$  to  $V_{min}$  increases. So a measure of the mismatch of a line is called the SWR, it can be defined as:

$$\text{SWR} = \frac{V_{max}}{V_{min}} = \frac{1 + |\Gamma|}{1 - |\Gamma|}$$
 (2.41)

This quantity is also known as the voltage standing wave ratio and is sometimes identified as VSWR. From (2.41) it is seen that SWR is a real number such that  $1 \leq \text{SWR} \leq \infty$ , where  $\text{SWR}=1$  implies a matched load.

From (2.33), it is best seen by the distance between two successive voltage maxima (or minima) is  $l = 2\pi/2\beta = \pi\lambda/2\pi = \lambda/2$ , while the successive distance between the maximum and minimum is  $l = \pi/2\beta = \lambda/4$ , where  $\lambda$  is the wavelength on the transmission line.

The reflection coefficient of (2.35) was defined as the ratio of the reflected to the incident voltage wave amplitudes at the load ( $l=0$ ), but this quantity can be generalized to any point  $l$  along the line as follows. From (2.34a), with  $z=-l$ , the ratio of the reflected

component to the incident component is:  $\Gamma(l) = \frac{V_0 e^{-j\beta l}}{V_0 e^{j\beta l}} = \Gamma(0) e^{-2j\beta l}$  (2.42)

where  $\Gamma(0) = \Gamma(0)$  is the reflection coefficient at  $z=0$ , as given by (2.35). This result is useful when transforming the effect of a load mismatch down the line.

We have seen that the real power flow on the line is a constant (for a lossless line) but the voltage amplitude, at least for a mismatched line, is oscillatory with position on the line. The perceptive reader may therefore have concluded that the impedance seen looking into the line must vary with position, and this is indeed the case. At a distance  $l=2$  from the load, the input impedance seen looking toward the load is

$$Z_{in} = \frac{V(l-l)}{I(l-l)} = \frac{V_0^+ (e^{j\beta l} + \Gamma e^{-j\beta l})}{V_0^+ (e^{j\beta l} + (-\Gamma) e^{-j\beta l})} Z_0 = \frac{1 + \Gamma e^{-2j\beta l}}{1 - \Gamma e^{-2j\beta l}} Z_0$$
 (2.43)

where (2.36a,b) have been used for  $V(z)$  and  $I(z)$ . A more usable form may be obtained by using (2.35) for  $\Gamma$  in (2.43):

$$Z_{in} = Z_0 \frac{(Z_L + Z_0) e^{j\beta l} + (Z_L - Z_0) e^{-j\beta l}}{(Z_L + Z_0) e^{j\beta l} + (Z_L - Z_0) e^{-j\beta l}} = Z_0 \frac{Z_L \cos \beta l + j Z_0 \sin \beta l}{Z_0 \cos \beta l + j Z_L \sin \beta l}$$

$$Z_{in} = Z_0 \frac{Z_L \cos \beta l + j Z_0 \sin \beta l}{Z_0 \cos \beta l + j Z_L \sin \beta l}$$
 (2.44)

This is an important result giving an input impedance of a length of transmission line with an arbitrary load impedance. We will refer to this result as the transmission line impedance equation; some special cases will be considered next.

### Special Cases of Lossless Terminated Lines.

A number of special cases of lossless terminated transmission lines will frequently appear in our line of work, so it is appropriate to consider the properties of these special cases.

Consider first the transmission line circuit shown in Figure 2.5, where a line is terminated in a short circuit,  $Z_L = 0$ ,

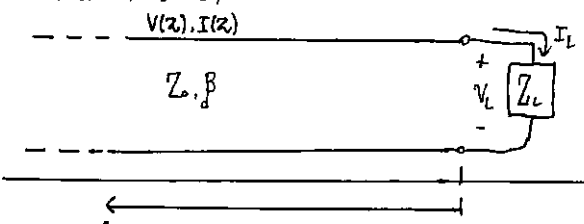


Figure 2.4 A transmission line terminated in a load impedance  $Z_L$

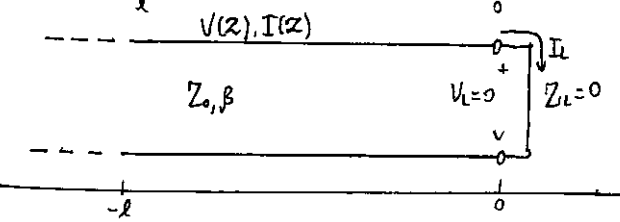


Figure 2.5 A transmission line terminated in a short circuit.

From (2.35) it is seen that the reflection coefficient for a short circuit load is  $\Gamma = -1$ ; it then follows from (2.41) that the standing wave ratio is infinite. From (2.36) the voltage and current on the line are

$$V(z) = V_0^+ (e^{-jBz} - e^{jBz}) = 2jV_0^+ \sin\beta z \quad (2.45a)$$

$$I(z) = \frac{V_0^+}{Z_0} (e^{-jBz} + e^{jBz}) = \frac{2V_0^+}{Z_0} \cos\beta z \quad (2.45b)$$

which shows that  $V=0$  at the load (as expected for a short circuit), while the current is a maximum there. From (2.44), or the ratio  $V(z=0)/I(z=0)$ , the input impedance is

$$Z_{in} = jZ_0 \tan\beta l \quad (2.45c)$$

which is seen to be purely imaginary for any length  $l$  and to take on all values between  $+j\infty$  and  $-j\infty$ . For example, when  $l=0$  we have  $Z_{in}=0$ , but for  $l=\lambda/4$  we have  $Z_{in}=\infty$  (open circuit). Equation (2.45c) also shows that the impedance is periodic in  $l$ , repeating for multiples of  $\lambda/2$ . The voltage, current, and short-circuited input reactance for the short-circuited line are plotted in Figure 2.6.

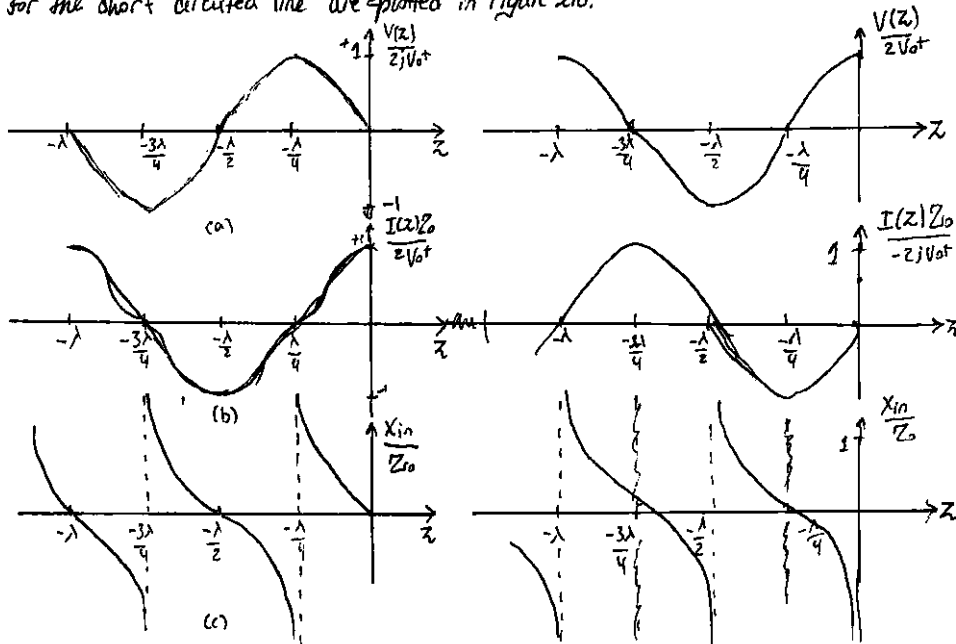


Figure 2.6: (a) Voltage, (b) current, (c) impedance ( $R_{in}=0$  or  $\infty$ ) variation along a short-circuited transmission line.

Figure 2.6 (a) Voltage, (b) current, and (c) impedance ( $R_{in}=0$  or  $\infty$ ) variation along an open-circuited transmission line.

Next consider the open-circuited line shown in Figure 2.7, where  $Z_L=\infty$ . Dividing the numerator and denominator of (2.35) by  $Z_L$  and allowing  $Z_L \rightarrow \infty$  shows that the reflection coefficient for this case is  $\Gamma=1$ , and the standing wave ratio is again infinite.

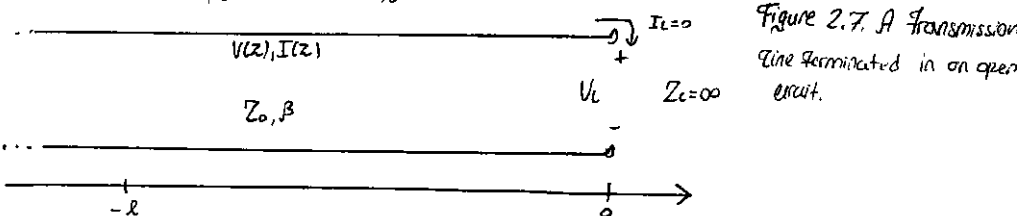


Figure 2.7. A transmission line terminated in an open circuit.

From (2.36) the voltages and currents on the line are:

$$V(z) = V_0^+ (e^{-jBz} + e^{jBz}) = 2V_0^+ \cos\beta z, \quad I(z) = \frac{V_0^+}{Z_0} (e^{-jBz} - e^{jBz}) = -\frac{2V_0^+}{Z_0} \sin\beta z \quad (2.46a, b)$$

which shows that now  $I=0$  at the load, as expected for an open circuit, while the voltage is a maximum. The input impedance is:  $Z_{in} = -jZ_0 \cot\beta l$  (2.46c) which is also purely imaginary for any length  $l$ . The voltage, current, and input reactance of the open-circuited line are plotted in Figure 2.8.

Now consider terminated transmission lines with some special length. If  $l=\lambda/2$ , (2.47) shows that

$$Z_{in} = Z_L \quad (2.47)$$

meaning that a half-wavelength line (or any multiple of  $\lambda/2$ ) does not alter or transform the load impedance, regardless of its characteristic impedance.

If the line is a quarter wavelength long or, more generally,  $l=\lambda/4 + n\lambda/2$ , for  $n=1, 2, 3, \dots$ , (2.44) shows that the input impedance is given by:

$$Z_{in} = \frac{Z_0^2}{Z_L} \quad (2.48)$$

Such a line is known as a quarter-wave transformer because it has the effect of transforming the load impedance in an inverse manner, depending on the characteristic impedance of the line. We will study this case more thoroughly in Section 2.5.

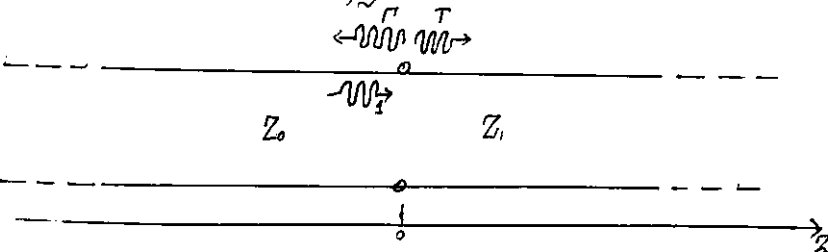


Figure 2.9. Reflection and transmission at the junction of two transmission lines with different characteristic impedances.

Next consider a transmission line of characteristic impedance  $Z_0$  feeding a line of a different characteristic impedance,  $Z_1$ , as shown in figure 2.9. If the load line is infinitely long, or if it is terminated in its own characteristic impedance, so that there are no reflections from its far end, then the input impedance seen by the feed line is  $Z_1$ , so that the reflection coefficient  $\Gamma$  is :

$$\Gamma = \frac{Z_1 - Z_0}{Z_1 + Z_0} \quad (2.49)$$

Not all of the incident wave is reflected; some is transmitted onto the second line with a voltage amplitude given by a transmission coefficient.

From (2.36a) the voltage for  $Z=0$  is:

$$V(Z) = V_0 + (e^{j\beta Z} + \Gamma e^{-j\beta Z}), \quad Z=0 \quad (2.50a)$$

where  $V_0$  is the amplitude of the incident voltage wave on the feedline. The voltage wave for  $Z>0$ , in the absence of reflections, is outgoing only and can be written as:

$$V(Z) = V_0 e^{j\beta Z} \quad \text{for } Z>0 \quad (2.50b)$$

Equating these voltages at  $Z=0$  gives the transmission coefficient,  $T$  as

$$T = 1 + \Gamma = 1 + \frac{Z_1 - Z_0}{Z_1 + Z_0} = \frac{2Z_1}{Z_1 + Z_0} \quad (2.51)$$

The transmission coefficient between two points in a circuit is often expressed in dB as the insertion loss,  $IL$

$$IL = -20 \log |T| \text{ dB} \quad (2.52)$$

#### + Point of Interest: Decibels and nepers.

Often the ratio of two power levels ~~is~~  $P_1$  and  $P_2$  in a microwave system can be expressed in decibels as

$$10 \log \frac{P_1}{P_2} \text{ dB}$$

Thus the power ratio of 2 is equivalent to 3dB, while a power ratio of 0.1 is equivalent to -10dB. Using power ratios in dB makes it easy to calculate the power loss or gain through a series of components since multiplicative loss or gain factors can be accounted for by adding the loss or gain in dB for each stage. For example, a signal passing through a 6dB attenuator followed by a 23dB amplifier will have an overall gain of  $23-6=17$ dB.

Decibels are used only to represent power ratios, but if  $P_1 = V_1^2/R_1$  and  $P_2 = V_2^2/R_2$ , then the resulting power ratio in terms of voltage is:

$$10 \log \frac{V_1^2 R_2}{V_2^2 R_1} = 20 \log \frac{V_1}{V_2} \sqrt{\frac{R_2}{R_1}} \text{ dB}$$

where  $R_1, R_2$  are the load resistances and  $V_1, V_2$  are the voltages appearing across the loads.

If the load resistances are equal, then this formula simplifies to

$$20 \log \frac{V_1}{V_2} \text{ dB}$$

The ratio of voltages across equal load resistances can also be expressed in terms of Nepers (Np.) as

$$\ln \frac{V_1}{V_2} \text{ Np.}$$

The corresponding expression in terms of powers is :

$$\frac{1}{2} \ln \frac{P_1}{P_2} \text{ Np}$$

Since voltage is proportional to the square root of power, transmission line attenuation is sometimes expressed as nepers. Since  $1\text{Np}$  corresponds to a power ratio of  $e^2$ , the conversion between nepers and decibels is

$$1\text{Np} = 10 \log e^2 = 8.686 \text{dB}$$

Absolute power can also be expressed in decibel notation if a reference power level is assumed. If we let  $P_0 = 1\text{mW}$ , then the power  $P$  can be expressed in dBm as

$$10 \log \frac{P}{1\text{mW}} \text{ dBm}$$

Thus a power of  $1\text{mW}$  is equivalent to 0 dBm, while a power of  $1\text{W}$  is equivalent to 30dBm, and so on.

**2.4 The Smith chart** / The Smith chart is a graphical aid that can be very useful for solving transmission line problems. Although there are a number of other impedance and reflection coefficient charts that could be used for such problems [5-7], the Smith chart is the best well known and widely used. It was developed by P. Smith in 1939 at the Bell Telephone Laboratories [9]. The reader might feel that in this day of personal computers and computer aided design tools (CAD), graphical solutions have no place in modern engineering. The Smith chart, however, is more than a graphical technique. Besides being an integral part of the current CAD software and testing equipment for microwave design, the Smith chart provides a useful way of visualizing transmission line phenomena without the need for detailed numerical calculations. A microwave engineer can develop a good intuition about transmission lines and impedance-matching problems by learning to think in terms of a Smith chart.

At first glance the Smith chart may seem intimidating, but the key to understanding is to realize that it is an a polar plot of the voltage reflection coefficient,  $\Gamma$ . Let the reflection coefficient be expressed in magnitude and phase (polar) form as  $\Gamma = |\Gamma| e^{j\theta}$ . Then the magnitude  $|\Gamma|$  is plotted as a radius (~~phase~~) from the center of the chart, and the angle  $\theta$  ( $-180^\circ \leq \theta \leq 180^\circ$ ) is measured counter clockwise from the right hand side of the horizontal diameter. Any passively realizable ( $|\Gamma| \leq 1$ ) reflection coefficient can then be plotted as a unique point on the Smith chart.

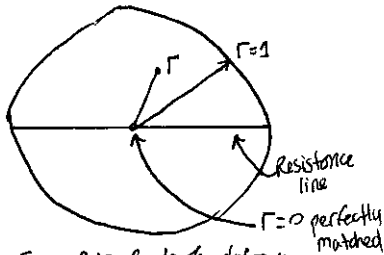


Figure 2.10 Crude hand drawn

The real utility of the Smith chart, however lies in the fact it can convert from reflection coefficients to normalized impedances (or admittances) and vice versa by using the impedance (or admittance) circles printed on the chart.

When dealing with impedances on a Smith chart, normalized quantities are generally used, which we will denote by lowercase letters. The normalization

depiction of a Smith chart, normalized quantities are generally used, which we will denote by lowercase letters. The normalization constant is usually the characteristic impedance of the transmission line. Thus  $z = Z/Z_0$  represents the normalized version of the impedance  $Z$ .

If a lossless line of characteristic impedance  $Z_0$  is terminated with a load impedance  $Z_L$ , the reflection coefficient at the load can be written from (2.35) as

$$\Gamma = \frac{V_L}{V_0} = \frac{Z_L - Z_0}{Z_L + Z_0} \rightarrow \Gamma = \frac{Z_L - 1}{Z_L + 1} = |\Gamma| e^{j\theta} \quad (2.53)$$

where  $z_L = Z_L/Z_0$  is the normalized impedance. This relation can be solved for  $Z_L$  in terms of  $\Gamma$  to give [or, from (2.43) with  $\ell=0$ ]

$$z_L = \frac{1 + |\Gamma| e^{j\theta}}{1 - |\Gamma| e^{j\theta}} \quad (2.54)$$

This complex equation can be reduced to two real equations by writing  $\Gamma$  and  $z_L$  in terms of their real and imaginary components,  $\Gamma = \Gamma_R + j\Gamma_I$ , and  $z_L = z_R + jz_I$ , giving

$$z_L = \frac{(1 + \Gamma_R) + j\Gamma_I}{(1 - \Gamma_R) - j\Gamma_I}$$

The real and imaginary parts of this equation can be separated by multiplying the numerator and denominator by the complex conjugate of the denominator to give,

$$z_L = \frac{1 - \Gamma_R^2 - \Gamma_I^2}{(1 - \Gamma_R)^2 + \Gamma_I^2} \quad (2.55a)$$

$$z_I = \frac{2\Gamma_I}{(1 - \Gamma_R)^2 + \Gamma_I^2} \quad (2.55b)$$

Rearranging (2.55) gives

$$\left(\Gamma_R - \frac{z_L}{1 + z_L}\right)^2 + \Gamma_I^2 = \left(\frac{1}{1 + z_L}\right)^2 \quad (2.56a),$$

$$(\Gamma_R - 1)^2 + \left(\Gamma_I - \frac{1}{z_L}\right)^2 = \left(\frac{1}{z_L}\right)^2 \quad (2.56b)$$

which are seen as two families of circles in the  $\Gamma_R, \Gamma_I$  plane. Resistance circles are defined by (2.56a) and reactance circles are defined by (2.56b). For example, the  $z_L = 1$  circle has a center at  $\Gamma_R = 0.5$ ,  $\Gamma_I = 0$ , and has a radius of 0.5, and so it passes through the center of the Smith chart. All the resistance circles of (2.56a) have centers on the horizontal  $\Gamma_I = 0$  axis and pass through the  $\Gamma = 1$  point on the right-hand side of the chart.

The centers of all the reactance circles of (2.56b) lie on the vertical  $\Gamma_R = 1$  line (off the chart), and these circles also pass through the  $\Gamma = 1$  point.

The resistance and reactance circles are orthogonal.

The Smith chart can also be used to graphically solve the transmission line impedance equation of (2.41) since this can be written in terms of the generalized reflection coefficient as:

$$Z_{in} = Z_0 \frac{1 + \Gamma e^{-j\beta l}}{1 - \Gamma e^{-j\beta l}} \quad (2.57)$$

where  $\Gamma$  is the reflection coefficient at the load and  $l$  is the (positive) length of transmission line. We then see that (2.57) is of the same form as (2.54), differing only by the phase angles of the  $\Gamma$  terms. Thus, if we have plotted the reflection coefficient  $|\Gamma| e^{j\theta}$  at the load, the normalized input impedance seen looking into a length of  $l$  transmission line terminated with  $Z_L$  can be found by rotating the point counter-clockwise by an amount  $2\beta l$  (subtracting  $2\beta l$  from  $\theta$ ) around the center of the chart. The radius stays the same since the magnitude of  $\Gamma$  does not change with position along the line. (assuming a lossless line).

To facilitate such rotations, the Smith chart has scales around its periphery calibrated in electrical wavelength, toward and away from the "generator" (which simply means away from the load). These scales are relative, so only the difference in wavelength between two points on the Smith chart is meaningful. The scales cover a range of 0 to 2.5 wavelengths, which reflects the fact that the Smith chart automatically includes the periodicity of transmission line phenomena. Thus, a line length  $\lambda/2$  (or any multiple) requires the rotation of  $2\beta l = 2\pi$  around the center of the chart, carrying a point back to its original position, showing that the input impedance of a load seen through a  $\lambda/2$  line is unchanged. We will now illustrate the use of the Smith chart for a variety of typical transmission line problems through examples.

### Example 2.2 Basic Smith Chart Operations

A load impedance of  $40 + 70j \Omega$  terminates a  $1M\Omega$  transmission line that is  $0.3\lambda$  long. Find the reflection coefficient at the load, the reflection coefficient at the input to the line, the input impedance, the standing wave ratio on the line, and the return loss.

Solution: The normalized load impedance is:

$$z_L = \frac{Z_L}{Z_0} = 0.4 + j0.7$$

which can be plotted on the Smith chart as shown in Figure 2.11. By using a drawing compass and the voltage coefficient scale printed below the chart, one can read off the reflection coefficient magnitude at the load as  $|\Gamma| = 0.59$ . This same compass setting can then be applied to the standing wave ratio (SWR) scale to read SWR = 3.87 and the return loss (RL) (in dB) scale to read  $RL = 4.6\text{dB}$ . Now draw a radial line through the load impedance point and read the angle of the reflection coefficient at the load from the outer scale of the chart as  $104^\circ$ .

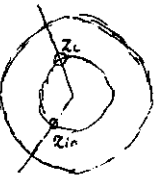


Figure 2.11  
Smith chart for Example 2.2.

depiction... I should  
probably speak in  
an actual one.

Now draw an SWR circle through the load impedance point.

Reading the reference position of the load on the wavelength-toward-generator (WTG) scale gives a value of  $0.06\lambda$ . Moving down the line  $0.3\lambda$  toward the generator brings us to  $0.406\lambda$  on the WTG scale. Drawing a radial line at this position gives the normalized input impedance at the intersection with SWR circle of  $Z_{in} = 0.365 - j0.611$ . Then the input impedance of the line is

$$Z_{in} = Z_0 Z_{in} = 36.5 - j61.1 \Omega$$

The reflection coefficient at the input still has a magnitude of  $|V| = 0.59$ , the phase is read from the radial line at the phase scale as  $248^\circ$ .

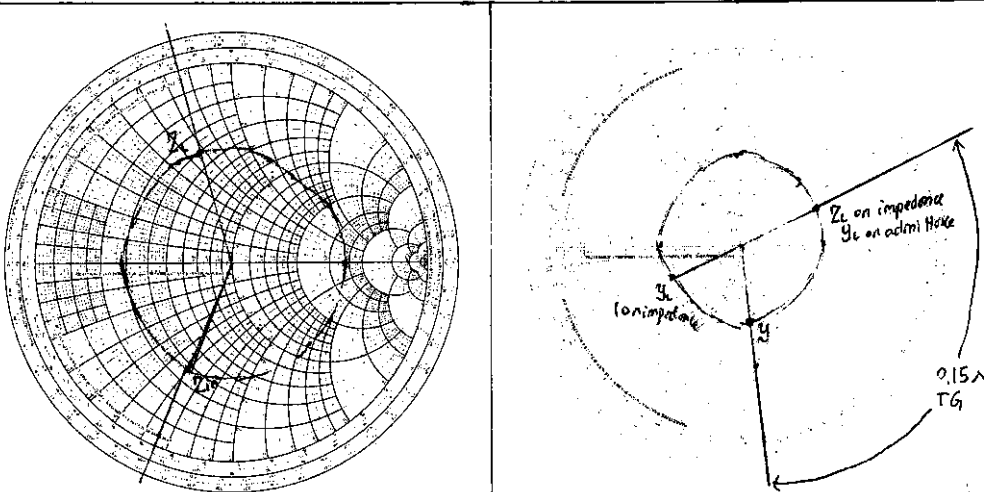


Figure 2.11 Smith chart for Example 2.2

Figure 2.12 ZY Smith chart with solution for example 2.3.

### The Combined Impedance-Admittance Smith Chart.

The Smith chart can be used for normalized admittance in the same way that it is used for normalized impedances, and it can be used to convert impedance and admittance. The latter technique is based on the fact that, in normalized form, the short impedance of a load  $Z_L$  connected to a  $\lambda/4$  line is, from (2.44),

$$Z_{in} = 1/Z_L$$

which has the effect of converting a normalized impedance to normalized admittance.

Since a complete revolution around the Smith chart corresponds to a line length of  $\lambda/2$ , a  $\lambda/4$  transformation is equivalent to a  $180^\circ$  rotation. This is also equivalent to imaging a given impedance (or admittance) point across the center of the chart to obtain the corresponding admittance (or impedance point).

Thus, a Smith chart can be used for both impedance and admittance calculations during the solution of a given problem. At different stages of a solution, then, the chart may be either an impedance Smith chart or an admittance Smith chart. This procedure can be made less confusing by using a Smith chart that has been rotated  $180^\circ$ , as shown in Fig 2.12. Such a chart is referred to as an impedance & admittance Smith chart, and usually has different colors for the  $Y$  and  $Z$ .

### Example 2.3 Smith Chart Operations Using Admittance.

A load of  $Z_L = 100 + j50 \Omega$  terminates a  $50\Omega$  line. What are the load admittance and input admittance if the line is  $0.15\lambda$  long?

Solution

The normalized load impedance is  $Z_L = 2 + j1$ . A standard Smith chart can be used for this problem by initially considering it as an impedance chart and plotting  $Z_L$  and the SWR circle. Conversion to admittance can be accomplished with a  $\lambda/4$  rotation of  $Z_L$  (easily obtained by drawing a straight line through  $Z_L$  and the center of the chart to intersect the other side of the SWR circle). The chart can now be considered as an admittance chart, and the input admittance can be found by rotating  $0.15\lambda$  from  $Y_L$ .

Alternatively, we can use the combined Z-Y chart of Figure 2.12, where the conversion between impedance and admittance is accomplished merely by reading the appropriate scales. Plotting  $Z_L$  on the impedance scale and reading the admittance scale at this same point gives  $Y_L = 0.49 - j0.20$ . The actual load admittance is then:

$$Y_L = y_L Y_0 = \frac{y_L}{Y_0} = 0.0080 - j0.0040 S.$$

Then, on the WTG scale, the load admittance is seen to have a reference position of  $0.214\lambda$ . Moving  $0.15\lambda$  past this point brings us to  $0.364\lambda$ . A radial line at this point on the WTG scale intersects the SWR circle at an admittance of  $Y = 0.61 + j0.66$ . The actual input admittance is then  $Y = 0.0122 + j0.0312 S$ .

### The Slotted Line

A slotted line is a transmission line configuration (usually a waveguide or coaxial line) that allows the sampling of the electric field amplitude of a standing wave on a terminated line. With this device the SWR and the distance of the first voltage minimum from the load can be measured, and from this data the load impedance can be determined. Note that because the load impedance is, in general, a complex number — (with two degrees of freedom), two distinct quantities must be measured with the slotted line to uniquely determine this impedance. A typical waveguide slotted line is shown in Fig 2.13. [Figure 2.13 An X-band waveguide slotted line]

Although slotted lines usually used to be the principal way of measuring an unknown impedance at microwave frequencies, they have largely been superseded by a modern vector network analyser in terms of accuracy, versatility, and convenience. The slotted line still has use, however, in certain applications such as high millimeter wave frequencies or where it is desired to avoid connector mismatches by connecting the unknown load directly to the slotted line, thus avoiding the use of imperfect transitions. Another reason for studying the slotted line is that it provides an unexcelled tool for learning the basic concepts of standing waves and mismatched lines. We will derive expressions for finding the unknown load impedance from slotted line measurements and will also show how the Smith chart can be used for the same purpose.

Assume that, for a certain terminated line, we have measured the SWR on the line and  $l_{\min}$ , the distance from the load to the first voltage minimum on the line. The load impedance  $Z_L$  can then be determined as follows. From (2.41) the magnitude of the reflection coefficient on the line is found from the standing wave ratio as:

$$|\Gamma| = \frac{SWR - 1}{SWR + 1} \quad (2.58)$$

From Section 2.3, we know that a voltage minimum occurs when  $e^{i(\theta - \beta l)} = -1$ , where  $\theta$  is the phase angle of the reflection coefficient,  $\Gamma = |\Gamma| e^{j\theta}$ . The phase of the reflection coefficient is then:

$$\theta = \pi + 2\beta l_{\min} \quad (2.59)$$

where  $l_{\min}$  is the distance from the load to the first voltage minimum. Actually, since the voltage minima repeat every  $\lambda/2$ , where  $\lambda$  is the wavelength on the line, any multiple of  $\lambda/2$  can be added to  $l_{\min}$  without changing the result in (2.59) because this just amounts to adding  $2\pi n \lambda/2 = i\pi n$  to  $\theta$ , which will not change  $|\Gamma|$ . Thus the two quantities SWR and  $l_{\min}$  can be used to find the complex reflection coefficient  $\Gamma$  at the load. It is then straightforward to use (2.43) with  $l=0$  to find the load impedance from  $\Gamma$ :

$$Z_L = Z_0 \frac{1 + \Gamma}{1 - \Gamma} \quad (2.60)$$

The use of the Smith chart in solving this problem is best illustrated by an example.

#### Example 2.4 Impedance Measurement with a Slotted Line.

The following two-step procedure has been carried out with a 50-Ω coaxial slotted line to determine the unknown load impedance.

1. A short circuit is placed at the load plane, resulting in a standing wave on the line with infinite SWR and sharply defined voltage minima, as shown in Figure 2.14a. In the arbitrary positioned scale on the slotted line, voltage minima are recorded at:

$$z = 0.2\text{ cm}, 2.2\text{ cm}, 4.2\text{ cm}.$$

2. The short circuit is removed and replaced with the unknown line load. The standing wave ratio is measured as  $SWR = 1.5$ , and voltage minima, which are not as sharply defined as those in step 1, are recorded at

$$z = 0.72\text{ cm}, 2.72\text{ cm}, 4.72\text{ cm}$$

as shown in Figure 2.14b. Find the load impedance.

**Solution**

Knowing that voltage minima repeat every  $\lambda/2$ , we can see from data of step 1 that  $\lambda = 4.2\text{ cm}$ . In addition, because the reflection coefficient and input impedance also repeat every  $\lambda/2$ , we can consider the load terminals to be effectively located at any of the voltage minima locations listed in step 1. Thus, if we say the load is at 4.2 cm, then the data from step 2 show that the next voltage minimum away from the load occurs at 2.72 cm, giving  $l_{\min} = 4.2 - 2.72 = 1.48\text{ cm} = 0.37\lambda$ .

From Section 2.3, we know that a voltage minimum occurs when  $e^{i(\theta - \beta l)} = -1$ , where  $\theta$  is the phase angle of the reflection coefficient,  $\Gamma = |\Gamma| e^{j\theta}$ . The phase of the reflection coefficient is then:

Applying (2.58)-(2.60) to these data gives:

$$|\Gamma| = \frac{1.5 - 1}{1.5 + 1} = 0.2 \quad \theta = \pi + \frac{4\pi}{4.0} (1.48) = 86.4^\circ$$

$$\text{so} \quad \Gamma = 0.2 e^{j86.4^\circ} = 0.0126 + j0.1996.$$

The load impedance is then

$$Z_L = 50 \left( \frac{1 + \Gamma}{1 - \Gamma} \right) = 47.3 + j19.7 \Omega$$

For the Smith chart version of this solution, we begin by drawing the SWR circle for  $SWR = 1.5$ , as shown in Figure 2.15; the unknown normalized load impedance must lie on this circle. The reference that we have is that the load is  $0.37\lambda$  away from the first voltage minimum. On the Smith chart the position of a voltage minimum corresponds to the minimum impedance point (minimum voltage, maximum current), which is the horizontal axis (Zero Reactance) to the left of the origin. Thus, we begin at the voltage minimum point and move  $0.37\lambda$  toward the load (Counterclockwise), to the normalized impedance load point,  $z_L = 0.95 + j0.4$ , as shown in Figure 2.15. The actual load impedance is then  $Z_L = 47.3 + j19.7 \Omega$ , in close agreement with the above result using equations.

Note that, in principle, the voltage maxima locations could be used as well as voltage minima positions, but voltage minima are more sharply defined than voltage maxima and so usually result in greater accuracy.

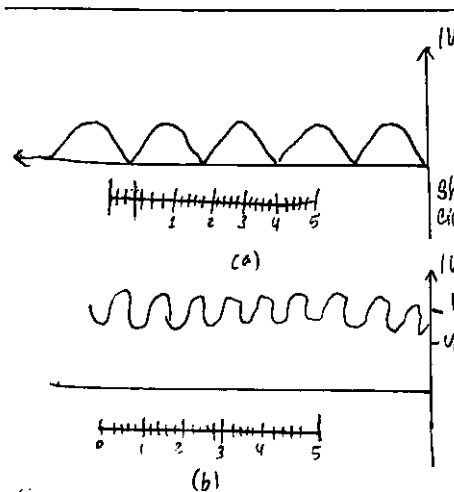


Figure 2.14 Voltage standing wave patterns for example 2.4. (a) Standing wave for a short circuit load. (b) Standing wave for unknown load.

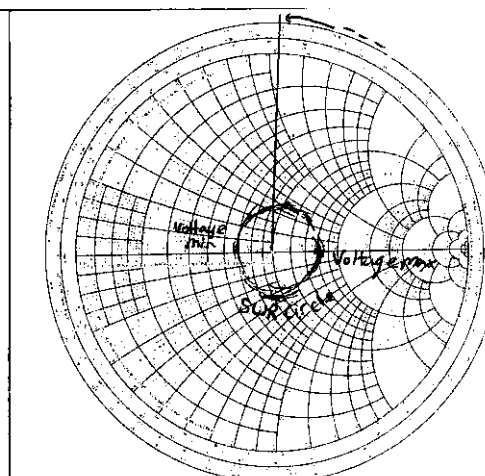


Figure 2.15 Smith chart for Example 2.4

## 2.5 The Quarter-Wave Transformer.

The quarter-wave transformer is useful and practical to build a circuit for impedance matching and also provides a simple transmission line circuit to further illustrate the properties of standing waves on a mismatched line. Although we will study the design and performance of quarter wave transformers more extensively in chapters, the main purpose here is the application of the previously developed transmission line theory to a basic transmission line circuit. We will first approach the problem from the impedance viewpoint and then show how this result can also be interpreted in terms of an infinite set of multiple reflections on the matching section.

### The Impedance Viewpoint

Figure 2.16 shows a circuit employing a quarter-wave transformer. The load resistance  $R_L$  and the feedline characteristics of impedance  $Z_0$  are both real and assumed to be known. These two components are connected with a lossless piece of transmission line of unknown characteristic impedance  $Z_L$  and length  $\lambda/4$ . It is desired to match the load to the  $Z_0$  line by using the  $\lambda/4$  section of line and so make  $\Gamma=0$  looking into the  $\lambda/4$  matching section.

From (2.44) the input impedance  $Z_{in}$  can be found as

$$Z_{in} = Z_L \frac{R_L + jZ_0 \tan \beta L}{Z_L + jR_L \tan \beta L} \quad (2.61)$$

To evaluate this for  $\beta L = (2\pi/\lambda)(\lambda/4) = \pi/2$ , we can divide the numerator and denominator by  $j\pi\beta L$  and take the limit as  $\beta L \rightarrow \pi/2$  to get

$$Z_{in} = \frac{Z_L^2}{R_L} \quad (2.62)$$

In order for  $\Gamma=0$ , we must have  $Z_{in}=Z_0$ , which yields the characteristic impedance  $Z_L$  as

$$\boxed{Z_L = \sqrt{Z_0 R_L}} \quad (2.63)$$

Figure 2.16 The quarter-wave matching Transformer.

which is the geometric mean of the load and source impedance. Then there will be no standing waves on the feedline ( $SWR=1$ ), although there will be standing waves on the  $\lambda/4$  section. In addition, the above condition applies only when the matching section is  $\lambda/4$  or an odd multiple of  $\lambda/4$  long, so a perfect match may be achieved at one frequency, but impedance mismatch will occur at other frequencies.

## Example 2.5 Frequency Response of a Quarter-Wave Transformer

Consider a load resistance  $R_L = 190\Omega$  to be matched to a  $50\Omega$  line with a quarter-wave transformer. Find the characteristic impedance of the matching section and plot the magnitude of the reflection coefficient versus the normalized frequency,  $f/f_0$ , where  $f_0$  is the frequency at which the line is  $\lambda/4$  long.

Solution

From (2.63), the necessary characteristic impedance is

$$Z_L = \sqrt{50 \times 190} = 70.71\Omega$$

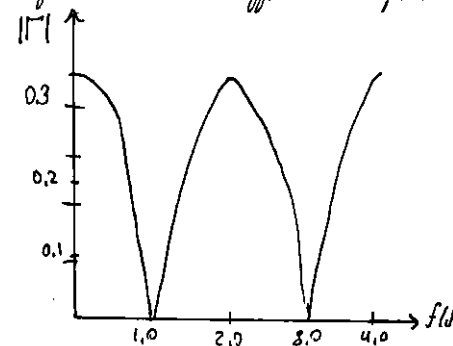
The reflection coefficient magnitude is given as:

$$|\Gamma| = \left| \frac{Z_{in} - Z_0}{Z_{in} + Z_0} \right|,$$

where the input impedance  $Z_{in}$  is a function of frequency as given by (2.44). The frequency dependence in (2.44) comes from the  $\beta L$  term, which can be written in terms of  $f/f_0$  as:

$$\beta L = \left( \frac{2\pi}{\lambda} \right) \left( \frac{\lambda_0}{4} \right) = \left( \frac{2\pi f}{v_p} \right) \left( \frac{v_p}{4f_0} \right) = \frac{\pi f}{2f_0}$$

where it can be seen that  $\beta L = \pi/2$  for  $f=f_0$ , as expected. For higher frequencies the matching section looks electrically longer, and for lower frequencies, it looks shorter. The magnitude of the reflection coefficient is plotted versus  $f/f_0$  in figure 2.17.



This appropriate method of impedance matching is limited to real load impedances, although a complex load impedance can easily be made real, at a single frequency, by transformation through an appropriate length of line.

This above analysis shows how useful the impedance concept can be when solving transmission line problems, and this method is the preferred method in practice. It may aid our understanding of the quarter wave transformer (and other transmission line circuits). However, if we now look at it from the viewpoint of multiple reflections.

### The Multiple-reflection Viewpoint

Figure 2.18 Shows The quarter-wave Transformer circuit with Reflection and Transmission coefficients defined as follows:

$\Gamma$  → overall reflection coefficient of a wave incident on a  $1/4$  transformer

$\Gamma_1$  → partial reflection coefficient of a wave incident on a load  $R_L$ , from the  $Z_0$  line.

$\Gamma_2$  → Partial reflection coefficient of a wave incident on a load  $Z_0$ , from the  $Z_1$  line.

$\Gamma_3$  → Partial reflection coefficient of a wave incident on a load  $R_L$ , from the  $Z_1$  line.

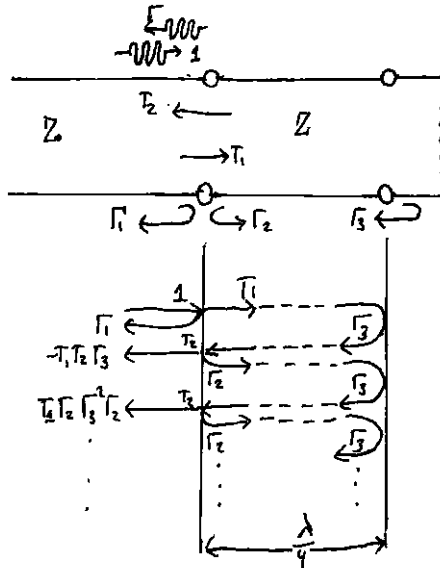


Figure 2.18 Multiple reflection analysis of the quarter wave transformer.

Reflection coefficient  $\Gamma_1$  is the sum of all of these reflection coefficients. Since each Round trip path up and down the  $1/4$  Transformer section results in a  $180^\circ$  phase shift, the Total Reflection coefficient can be expressed as :

$$\Gamma = \Gamma_1 + T_1 T_2 \Gamma_3 + T_1 T_2 T_3 \Gamma_3^2 + T_1 T_2 \Gamma_2 \Gamma_3^3 + \dots \quad (2.65)$$

$$\Gamma = \Gamma_1 - T_1 T_2 \Gamma_3 \sum_{n=0}^{\infty} (-\Gamma_2 \Gamma_3)^n$$

These Coefficients may be expressed as

$$\Gamma_1 = \frac{Z_0 - Z_0}{Z_0 + Z_0}, \quad \Gamma_2 = \frac{Z_0 - Z_1}{Z_0 + Z_1} = -\Gamma_1 \quad (2.64a)$$

$$(2.64b)$$

$$\Gamma_3 = \frac{R_L - Z_1}{R_L + Z_1}, \quad (2.64c)$$

$$T_1 = \frac{2Z_1}{Z_0 + Z_0}, \quad T_2 = \frac{2Z_0}{Z_1 + Z_0} \quad (2.64d, e)$$

Since  $|\Gamma_1| < 1$  and  $|\Gamma_2| < 1$ , the infinite series in (2.65) can be summed up using the geometric series result:

$$\sum_{n=0}^{\infty} x^n = \frac{1}{1-x} \quad \text{for } |x| < 1$$

$$\text{To give: } \Gamma = \Gamma_1 - \frac{T_1 T_2 \Gamma_3}{1 + \Gamma_2 \Gamma_3} = \frac{\Gamma_1 + \Gamma_1 \Gamma_2 \Gamma_3 - T_1 T_2 \Gamma_3}{1 + \Gamma_2 \Gamma_3} \quad (2.66)$$

The numerator of this expression can be simplified using (2.64) To give:

$$\Gamma_1 - \Gamma_3 (\Gamma_1^2 + T_1 T_2) = \Gamma_1 - \Gamma_3 \left[ \frac{(Z_1 - Z_0)^2}{(Z_1 + Z_0)^2} + \frac{4Z_1 Z_0}{(Z_1 + Z_0)^2} \right]$$

$$\text{LHS} = \frac{\Gamma_1 (Z_1 - Z_0)(R_L + Z_1) - (R_L - Z_1)(Z_1 + Z_0)}{(Z_1 + Z_0)(R_L + Z_1)}$$

$$\text{LHS} = \frac{2(Z_1^2 - Z_0 R_L)}{(Z_1 + Z_0)(R_L + Z_1)}$$

which is seen to vanish if we choose  $Z_1 = \sqrt{Z_0 R_L}$  as in (2.63). Then  $\Gamma$  of (2.66) is zero, and the line is perfectly matched. This analysis shows that the matching property of the quarter wave Transformer comes about by properly selecting the characteristic impedance and length of the matching section so the superposition of all the partial reflections adds to zero. Under steady-state conditions, an infinite sum of waves traveling in the same direction with the same phase velocity can be combined into a single traveling wave. Thus, the infinite set of waves traveling in the forward and reverse directions on the matching section can be reduced to two waves traveling in opposite directions. See Problem 2.25.

### 2.6 Generator and Load Mismatches

In Section 2.3 we treated the terminated (mismatched) transmission line assuming that the generator was matched, so that no reflection occurred at the generator. In general, however, both generators and load may present mismatched impedances to the transmission line. We will study this case and also see the condition for maximum power transfer from the generator to the load may, in some situations, involve a standing wave on the line.

Figure 2.19 Shows a transmission line circuit with arbitrary generator and load impedances  $Z_g$  and  $Z_L$ , which may be complex. The transmission line is assumed to be lossless, with a length  $l$  and a characteristic impedance  $Z_0$ . This circuit is general enough to model most passive and active networks that occur in practice.

Because both the generator and the load are mismatched, multiple reflections can occur on the line, as in the problem of the quarter-wave transformer. The present circuit could thus be analysed using an infinite series to represent the multiple bounces, as in Section 2.5,

But we will use the easier and more useful method of impedance Transformation. The input impedance looking into the terminated transmission line from the generator end is, from (2.43) and (2.44),

$$Z_{in} = Z_0 \frac{1 + \Gamma_e e^{-2j\beta l}}{1 - \Gamma_e e^{-2j\beta l}} = Z_0 \frac{Z_e + jZ_0 \tan \beta l}{Z_0 + jZ_e \tan \beta l} \quad (2.67)$$

where  $\Gamma_e$  is the reflection coefficient of the load:

$$\Gamma_e = \frac{Z_e - Z_0}{Z_e + Z_0} \quad (2.68)$$

The voltage on the line can be written as

$$V(z) = V_0^+ (e^{-j\beta z} + \Gamma_e e^{j\beta z}) \quad (2.69)$$

and we can find  $V_0^+$  from the voltage at the generator end of the line, where  $z = -l$

$$V(-l) = V_g \frac{Z_{in}}{Z_{in} + Z_g} = V_0^+ (e^{j\beta l} + \Gamma_e e^{-j\beta l})$$

so that

$$V_0^+ = V_g \frac{Z_{in}}{Z_{in} + Z_g} \frac{1}{(e^{j\beta l} + \Gamma_e e^{-j\beta l})} \quad (2.70)$$

This can be rewritten, using (2.67) as

$$V_0^+ = V_g \frac{Z_0}{Z_0 + Z_g} \cdot \frac{e^{j\beta l}}{(1 - \Gamma_e \Gamma_g e^{-2j\beta l})} \quad (2.71)$$

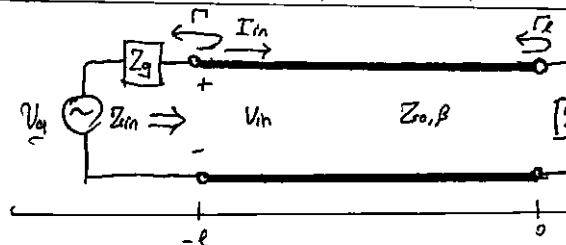


Figure 2.19 Transmission line circuit for mismatched load and generator.

where  $\Gamma_g$  is the reflection coefficient seen looking into the generator.

$$\Gamma_g = \frac{Z_g - Z_0}{Z_g + Z_0} \quad (2.72)$$

The standing wave ratio on the line is then

$$SWR = \frac{1 + |\Gamma_e|}{1 - |\Gamma_e|} \quad (2.73)$$

The power delivered to the load is:

$$P = \frac{1}{2} \operatorname{Re} \left\{ V_{in} I_{in} \right\} = \frac{1}{2} |V_{in}|^2 \operatorname{Re} \left\{ \frac{1}{Z_{in}} \right\} = \frac{1}{2} |V_g|^2 \left| \frac{Z_{in}}{Z_{in} + Z_g} \right|^2 \operatorname{Re} \left\{ \frac{1}{Z_{in}} \right\} \quad (2.74)$$

Now let  $Z_{in} = R_{in} + jX_{in}$  and  $Z_g = R_g + jX_g$ ; then (2.74) can be reduced to:

$$P = \frac{1}{2} |V_g|^2 \frac{R_{in}}{(R_{in} + R_g)^2 + (X_{in} + X_g)^2} \quad (2.75)$$

We now assume that the generator impedance,  $Z_g$ , is fixed, and consider three cases of load impedance.

### Load Matched To Line

In this case we have  $Z_e = Z_0$ , so  $\Gamma_e = 0$ , and  $SWR = 1$ , from (2.68) and (2.73). Then the input impedance is  $Z_{in} = Z_0$ , and the power delivered to the load is, from (2.75),

$$P = \frac{1}{2} |V_g|^2 \frac{Z_0}{(Z_0 + R_g)^2 + X_g^2} \quad (2.76)$$

### Generator matched to loaded line

In this case the load impedance  $Z_e$  and/or the transmission line parameters  $\beta l$ ,  $Z_0$  are chosen to make the input impedance  $Z_{in} = Z_g$ , so that the generator is matched to the load presented by the terminated transmission line.

Then the overall reflection coefficient,  $\Gamma_e$ , is zero:

$$\Gamma_e = \frac{Z_{in} - Z_g}{Z_{in} + Z_g} = 0 \quad (2.77)$$

There may, however, be a standing wave on the line since  $\Gamma_e$  may not be zero. The power delivered to the load is:

$$P = \frac{1}{2} |V_g|^2 \frac{R_g}{4(R_g^2 + X_g^2)} \quad (2.78)$$

Observe that even though the loaded line is matched to the generator, the power delivered to the load may not be less than that of (2.76), where the loaded line was not necessarily matched to the generator. Thus we are led to the question of what is the optimum load impedance, or equivalently the optimum input impedance, to achieve maximum power transfer to a load for a given generator impedance.

## Congugate Matching

Assuming that the generator series impedance  $Z_g$  is fixed, we may vary the input impedance  $Z_{in}$  until we achieve the maximum power delivered to the load. Denoting  $Z_{in}$ , it is then easy to find the corresponding load impedance  $Z_L$  via an impedance transformation along the line. To maximize  $P$ , we differentiate with respect to the real and imaginary part of  $Z_{in}$ . Using (2.75) gives:

$$\frac{\partial P}{\partial R_{in}} = 0 \rightarrow \frac{1}{(R_{in} + R_g)^2 + (X_{in} + X_g)^2} + \frac{-2R_{in}(R_{in} + R_g)}{[(R_{in} + R_g)^2 + (X_{in} + X_g)^2]^2} = 0$$

or

$$R_g^2 - R_{in}^2 + (X_{in} + X_g)^2 = 0 \quad (2.79a)$$

and

$$\frac{\partial P}{\partial X_{in}} = 0 \rightarrow \frac{-2R_{in}(X_{in} + X_g)}{[(R_{in} + R_g)^2 + (X_{in} + X_g)^2]^2}$$

or

$$X_{in}(X_{in} + X_g) = 0 \quad (2.79b)$$

Solving (2.79a) and (2.79b) simultaneously after  $R_{in}$  and  $X_{in}$  gives

$$R_{in} = R_g, \quad X_{in} = -X_g \quad (2.80)$$

or

$$Z_{in} = Z_g^*$$

This condition is known as conjugate matching and it results in maximum power transfer to the load for a fixed generator impedance. The power delivered is, from (2.75) and (2.76) and (2.80),

$$P = \frac{1}{2} \left| \frac{V_g}{Z_g} \right|^2 \frac{1}{4R_g} \quad (2.81)$$

which is seen to be greater than or equal to the powers of (2.76) or (2.78). This is also the maximum available power from the generator. Note that the reflection coefficients  $\Gamma_e$ ,  $\Gamma_g$ , and  $\Gamma$  may be nonpro. Physically, this means

that in some cases the power in the multiple reflections on a mismatched line may add in phase to deliver more power to the load than would be delivered if the line were flat (no reflection). If the generator impedance is real ( $X_g = 0$ ), then the last two terms reduce to the same result, which is that maximum power is delivered to the load when the loaded line is matched to the generator ( $R_{in} = R_g$ , with  $X_{in} = X_g = 0$ ).

Finally, note that neither matching for zero reflection ( $Z_0 = Z_0$ ) nor conjugate matching ( $Z_{in} = Z_g^*$ ) necessarily yields a system with the best efficiency. For example, if  $Z_g = Z_L = Z_0$  then both load and generator is delivered to the load (the other half is lost in  $Z_g$ ), for a transmission efficiency of 50%. The efficiency can be improved —

by making  $Z_g$  as small as possible.

## The Low-Loss Line

In most practical microwave and RF transmission lines the loss is small—if this were not the case, the line would be of little value in practice. When the loss is small, some approximations can be made to simplify the expressions for general transmission line parameters of  $\gamma = \alpha + j\beta$  and  $Z_0$ .

The general expression for the complex propagation constant is from (2.5)

$$\gamma = \sqrt{(R + j\omega L)(G + j\omega C)} \quad (2.82)$$

which can be rearranged as

$$\begin{aligned} \gamma &= \sqrt{(j\omega L)(j\omega C) \left( 1 + \frac{R}{j\omega L} \right) \left( 1 + \frac{G}{j\omega C} \right)} \\ (\text{HS}) &= j\omega\sqrt{LC} \sqrt{1 - j\left(\frac{R}{\omega L} + \frac{G}{\omega C}\right) - \frac{RG}{\omega^2 LC}} \end{aligned} \quad (2.83)$$

for a low-loss line both conductor and dielectric loss will be small, and we can assume that  $R \ll \omega L$  and  $G \ll \omega C$ . Then,  $RG \ll \omega^2 LC$ , and (2.83) reduces to

$$\gamma \approx j\omega\sqrt{LC} \sqrt{1 - j\left(\frac{R}{\omega L} + \frac{G}{\omega C}\right)} \quad (2.84)$$

If we were to ignore the  $\left(\frac{R}{\omega L} + \frac{G}{\omega C}\right)$  term we would obtain the result that  $\gamma$  was purely imaginary (no loss), so we will instead use the first few terms of the Taylor's Series expansion for  $\sqrt{1+x} \approx 1 + \frac{x}{2} + \dots$  to give the first higher order real term for  $\gamma$ :

$$\gamma \approx j\omega\sqrt{LC} \left[ 1 - \frac{j}{2} \left( \frac{R}{\omega L} + \frac{G}{\omega C} \right) \right]$$

so that

$$\alpha \approx \frac{1}{2} \left( R \sqrt{\frac{C}{L}} + G \sqrt{\frac{L}{C}} \right) = \frac{1}{2} \left( \frac{R}{Z_0} + G Z_0 \right) \quad (2.85a)$$

$$\beta \approx \omega\sqrt{LC} \quad (2.85b)$$

where  $Z_0 = \sqrt{LC}$  is the characteristic impedance of the line in the absence of loss. Note from (2.85b) that the propagation constant  $\beta$  is identical to that of the lossless case of (2.12). By the same order of approximation, the characteristic impedance  $Z_0$  can be approximated as a real quantity:

$$Z_0 = \sqrt{\frac{R + j\omega L}{G + j\omega C}} \approx \sqrt{\frac{L}{C}} \quad (2.86)$$

Equations (2.85)-(2.86) are known as the high-frequency, low-loss approximations for transmission lines, and they are important because they show that the propagation constant and characteristic impedance for a low-loss line can be closely approximated by considering the line as lossless.

### Example 2.6 Attenuation Constant of the Coaxial Line.

In Example 2.1 the  $Z$ ,  $C$ ,  $R$ , and  $G$  parameters were derived for a lossy coaxial line. Assuming the loss is small, derive the attenuation constant from (2.85a) with the result from Example 2.1.

Solution / From (2.85a)

$$\alpha = \frac{1}{2} \left( R \sqrt{\frac{C}{L}} + G \sqrt{\frac{L}{C}} \right)$$

Using the results for  $R$  and  $G$  derived in Example 2.1 gives

$$\alpha = \frac{1}{2} \left[ \frac{R_s}{\eta_{\text{intrinsic}}} \left( \frac{1}{a} + \frac{1}{b} \right) + \omega \epsilon' \eta \right]$$

where  $\eta = \sqrt{\mu/\epsilon'}$  is the intrinsic impedance of the dielectric material filling the coaxial line. In addition,  $\beta = \omega \sqrt{LC} = \omega \sqrt{\mu \epsilon'}$  and  $Z_0 = \sqrt{LC} = (\eta/2\pi) \ln(b/a)$ .

*Note:* This method for the calculation of attenuation requires that the line parameters  $Z$ ,  $C$ ,  $R$ , and  $G$  be known. These can sometimes be derived using the formulas (2.17)-(2.20), but a more direct and versatile procedure is to use the perturbation method, to be discussed shortly.

### The Distortionless Line

As seen from the exact equations (2.82 & 2.83) for the propagation constant of a lossy line, the phase term  $\beta$  is generally a complicated function of frequency  $\omega$  when loss is present. In particular, we note that  $\beta$  is generally not exactly a linear function of frequency, as in (2.85b), unless the line is lossless. If  $\beta$  is not a linear function of frequency (of the form  $\beta = \alpha\omega$ ), then the phase velocity will vary with frequency ( $v_p = \omega/\beta$ ). The implication of this is that the various frequency components of a wideband signal will travel with different phase velocities and so arrive at the receiver end of the transmission line at slightly different times. This will lead to dispersion, a distortion of the signal, and is generally an undesirable effect. Granted, as we have argued, the departure of  $\beta$  from a linear function may be quite small, but the effect can be significant if the line is very long. This effect leads to the concept of group velocity, which we will address in detail in Section 3.10.

There is a special case, however, of a lossy line that has a linear phase factor as a function of frequency. Such a line is called a distortionless line, and it is characterized by line parameters that satisfy the relation:

$$\frac{R}{L} = \frac{G}{C}$$

$$(2.87)$$

From (2.83) the exact complex propagation constant, under the condition specified by (2.87), reduces to

$$\begin{aligned} \gamma &= j\omega \sqrt{LC} \sqrt{1 - 2j\frac{R}{\omega L} - \frac{R^2}{\omega^2 C^2}} \\ \text{LHS} &= j\omega \sqrt{LC} \left( 1 - j\frac{R}{\omega L} \right) \\ \gamma &= R \sqrt{\frac{C}{L}} + j\omega \sqrt{LC} = \alpha + j\beta \end{aligned} \quad (2.88)$$

which shows that  $\beta = \omega \sqrt{LC}$  is now a linear function of frequency. Equation (2.88) also shows that the attenuation constant,  $\alpha = R \sqrt{CL}$ , does not depend on frequency, so that all frequency components of a signal will be attenuated by the same amount (actually  $R$  is usually a weak function of frequency). Thus, the distortionless line is not loss free but capable of passing a pulse or modulation envelope without distortion. To obtain a transmission line with parameters that satisfy (2.87) often requires that  $Z$  be increased by adding series loading coils spaced periodically along the line.

The above theory for the distortionless line was first developed by Oliver Heaviside (1850-1925), who solved many problems in transmission line theory and reworked Maxwell's original theory of electromagnetism into the modern version that we are familiar with today. [5]

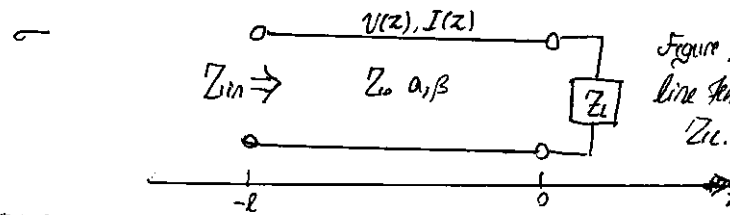


Figure 2.20 A lossy transmission line terminated in the impedance  $Z_L$ .

### The Terminated Lossy Line

Figure 2.20 shows a length  $l$  on a long transmission line terminated at a load impedance  $Z_L$ . Thus  $\gamma = \alpha + j\beta$  is complex, but we assume the loss is small, so that  $Z_0$  is approximately real, as in (2.86).

In (2.36), expressions for the voltage and current wave on a lossless line are given.

The analogous expressions for the lossy case are

$$V(z) = V_0^+ (e^{-\gamma z} + \Gamma e^{\gamma z}) \quad (2.89a)$$

$$I(z) = \frac{V_0^+}{Z_0} (e^{-\gamma z} - \Gamma e^{\gamma z})$$

where  $\Gamma$  is the reflection coefficient of the load, as given in (2.35), and  $V_0^+$  is the incident voltage amplitude referenced by  $z=0$ . From (2.42) the reflection coefficient at a distance  $l$  from a load is:

From (2.42) the reflection coefficient at a distance  $l$  from a load is:

$$\Gamma(l) = \frac{1}{2} e^{-j\beta l} e^{-2al} = \frac{1}{2} e^{-2al} \quad (2.90)$$

The input impedance  $Z_{in}$  at a distance  $l$  from the load is then

$$Z_{in} = \frac{V(l)}{I(l)} = Z_0 \frac{Z_L + Z_0 \tan \alpha l}{Z_0 + Z_L \tan \alpha l} \quad (2.91)$$

We can compute the power delivered to the input of the terminated line at  $z=0$

$$\begin{aligned} P_{in} &= \frac{1}{2} \operatorname{Re} \{ V(l) I^*(l) \} = \frac{|V_0|^2}{2 Z_0} (e^{2al} - |\Gamma(l)|^2 e^{-2al}) \\ P_L &= \frac{|V_0|^2}{2 Z_0} (1 - |\Gamma(l)|^2) e^{-2al} \end{aligned} \quad (2.92)$$

where (2.89) has been used for  $V(l)$  and  $I(l)$ . The power actually delivered to the load is:

$$P_L = \frac{1}{2} \operatorname{Re} \{ V(0) I^*(0) \} = \frac{|V_0|^2}{2 Z_0} (1 - |\Gamma|^2) \quad (2.93)$$

The difference in these powers corresponds to the power lost in the line:

$$P_{loss} = P_{in} - P_L = \frac{|V_0|^2}{2 Z_0} [e^{2al} - 1] + |\Gamma|^2 (1 - e^{-2al}) \quad (2.94)$$

The first term in (2.94) accounts for the power loss of the incident wave, while the second term accounts for the power loss of the reflected wave; note that both terms increase as  $\alpha$  increases.

#### The Perturbation Method for Calculating perturbation

Here we derive a useful and standard technique for finding the attenuation constant of a low-loss line. The method avoids the use of transmission line parameters,  $L, C, R, G$  and instead relies on the fields of the lossless line, with the assumption that the fields of the lossy line are not greatly different from the fields of the lossless line — hence the term, perturbation method.

We have seen that the power flow along the transmission line, in the absence of reflections, is of the form:  $P(z) = P_0 e^{-2az}$  (2.95)

where  $P_0$  is the power at the  $z=0$  plane and  $a$  is the attenuation constant we wish to determine. Now define the power loss per unit length along the line as:  $P_L = \frac{-dP}{dz} = 2aP_0 e^{-2az} = 2aP(z)$

where the negative sign on the derivative was introduced so that  $P_L$  would be a positive quantity. From this the attenuation constant can be determined as

$$\alpha = \frac{P_L(z)}{2P(z)} = \frac{P_L(z=0)}{2P_0}$$

This equation states that  $\alpha$  can be determined from  $P_0$ , the power on the line, and  $P_L$ , the power loss per unit line. It is important to realize that  $P_0$  can be computed from the fields of the lossless line and can account for both conductor loss [using (1.131)] and dielectric loss [using (1.92)].

#### Example 2.7 Using The Perturbation Method To Find The Attenuation Constant

Use the perturbation method to find the attenuation constant of a coaxial line having a lossy dielectric and lossy conductors.

##### Solution

From Example 2.1 and (2.32) the fields of the coaxial line are, for a PCB,

$$\bar{E} = \frac{V_0 \hat{\phi}}{2\pi b/a} e^{-j\beta z} \quad \bar{H} = \frac{V_0 \hat{\phi}}{2\pi P Z_0} e^{-j\beta z}$$

where  $Z_0 = (\eta/2\pi)^{1/b/a}$  is the characteristic impedance of the coaxial line and  $V_0$  is the voltage across the line at  $z=0$ . The first step is to find  $P_0$ , the power flowing on the lossless line:

$$P_0 = \frac{1}{2} \operatorname{Re} \int_S \bar{E} \times \bar{H}^* \cdot d\bar{s} = \frac{|V_0|^2}{2 Z_0} \int_{p=a}^b \int_{\phi=0}^{2\pi} \frac{P_0 p d\phi dz}{2\pi p^2 \ln b/a} = \frac{|V_0|^2}{2 Z_0}$$

as it is expected from the basic circuit theory.

The loss per unit length,  $P_L$ , comes from conductor loss ( $P_{c,c}$ ) and dielectric loss ( $P_{d,d}$ ). From (1.131), the conductor loss in a 1m length of line can be found as

$$P_{c,c} = \frac{R_s}{2} \int_S |H_\phi|^2 ds = \frac{R_s}{2} \int_{z=0}^1 \left\{ \int_{\phi=0}^{2\pi} |H_\phi(p=a)|^2 d\phi + \int_{\phi=0}^{2\pi} |H_\phi(p=b)|^2 b d\phi \right\} dz$$

$$\Rightarrow P_{c,c} = \frac{R_s |V_0|^2}{4\pi Z_0^2} \left( \frac{1}{a} + \frac{1}{b} \right)$$

The dielectric loss in a 1m length of line is from (1.92)

$$P_{d,d} = \frac{\omega E''}{2} \int_V |E|^2 ds = \frac{\omega E''}{2} \int_{p=a}^b \int_{\phi=0}^{2\pi} \int_{z=0}^1 |E_\phi|^2 p dp d\phi dz = \frac{\pi \omega E''}{\ln b/a} |V_0|^2$$

where  $E''$  is the imaginary part of the complex permittivity,  $E = E' - jE''$ . Finally, applying (2.96) gives

$$\begin{aligned} \alpha &= \frac{P_{c,c} + P_{d,d}}{2P_0} = \frac{R_s}{4\pi Z_0} \left( \frac{1}{a} + \frac{1}{b} \right) + \frac{\pi \omega E'' Z_0}{\ln b/a} \\ &= \frac{R_s}{2\pi \ln b/a} \left( \frac{1}{a} + \frac{1}{b} \right) + \frac{\omega E'' \eta}{2} \end{aligned}$$

where  $\eta = \sqrt{\mu \epsilon}$ . This result is seen to agree with that of Example 2.6.

## The Wheeler Incremental Inductance Rule

Another useful technique for the practical evaluation due to conductor loss for TEM or quasi-TEM lines is the Wheeler incremental inductance rule [6]. This method is based on the similarity of the equations for the inductance per unit length and resistance per unit length of a transmission line, as given by (2.17) and (2.19), respectively. In other words, the conductor loss of a line is due to current flow inside of the conductor, which, as was shown in Section 1.7, is directly related to the tangential magnetic field at the surface of the conductor and thus to the inductance of the line.

From (1.31), thus the power loss into a cross section  $S$  of a good (but not perfect) conductor is:

$$P_s = \frac{R_s}{2} \int_S |\bar{J}_s|^2 ds = \frac{R_s}{2} \int |\bar{H}_t|^2 ds \text{ W/m}^2 \quad (2.97)$$

So the power loss per unit length of a uniform transmission line is:

$$P_t = \frac{R_s}{2} \int_C |\bar{H}_t|^2 dl \text{ W/m} \quad (2.98)$$

where the line integral of (2.98) is over the cross-sectional contours of both conductors. From (2.17), the inductance per unit length of the line is

$$\mathcal{L} = \frac{\mu}{|I|^2} \int_S |\bar{H}|^2 ds$$

which is computed assuming conductors are lossless. When the conductors have small loss, the  $\bar{H}$  field in the conductor is no longer zero, and this field contributes a small, additional, "incremental," inductance,  $\Delta L$ , to that of (2.97). As discussed in Chapter 1, the fields inside the conductor decay exponentially. So that the integration into the conductor dimension can be evaluated as

$$\Delta L = \frac{\mu_0 S_s}{2 |I|^2} \int_C |\bar{H}_t|^2 dl$$

since  $\int_0^\infty e^{-2\pi j k_s z} dz = S_s/2$ . (The skin depth is  $S_s = \sqrt{2/\mu_0 \sigma_0}$ .) Then  $P_t$  from (2.97) can be written in terms of  $\Delta L$  as:

$$P_t = \frac{R_s |I|^2 \Delta L}{\mu_0 S_s} = \frac{|I|^2 \Delta L}{2 \mu_0 S_s^2} = \frac{|I|^2 \omega \Delta L}{Z} \text{ W/m} \quad (2.101)$$

Since  $R_s = \sqrt{\omega \mu_0 / 2\sigma} = 1/\sigma S_s$ . Then from (2.96) the attenuation due to conductor loss can be evaluated as

$$\alpha_c = \frac{P_t}{2 P_0} = \frac{\omega \Delta L}{2 Z_0} \quad (2.102)$$

Since  $P_0$ , the total power flow down the line, is  $P_0 = |I|^2 Z_0 / 2$ . In (2.102),  $\Delta L$  is evaluated as the change in inductance when all conductor walls recede by an amount  $S_s/2$ .



Equation (2.102) can also be written as the change in characteristic impedance since

$$Z_0 = \frac{\sqrt{\mu}}{\sqrt{\epsilon} c} = \frac{L}{R_s} \quad (2.103) \text{ so that } \alpha_c = \frac{\beta \Delta Z_0}{2 Z_0} \quad (2.104)$$

where  $\Delta Z_0$  is the change in characteristic impedance when all the conductor walls recede by an amount  $S_s/2$ . Yet another form of the incremental inductance rule can be obtained by using the first two terms of a Taylor series expansion for  $Z_0$ , thus,

$$Z_0 \left( \frac{S_s}{2} \right) \approx Z_0 + \frac{S_s}{2} \frac{dZ_0}{dl} \quad (2.105)$$

so that

$$\Delta Z_0 = Z_0 \left( \frac{S_s}{2} \right) - Z_0 = \frac{S_s}{2} \frac{dZ_0}{dl}$$

where  $Z_0(S_s/2)$  refers to the characteristic impedance of the line when the walls recede by  $S_s/2$ , and  $l$  refers to the distance into the conductors. Then (2.104) can be written as:  $\alpha_c = \frac{\beta S_s}{4 \pi Z_0} \frac{dZ_0}{dt} = \frac{R_s}{2 Z_0 \eta} \frac{dZ_0}{dl}$

where  $\eta = \sqrt{\mu_0 \epsilon_0}$  is the intrinsic impedance of the dielectric and  $R_s$  is the surface resistivity of the conductor. Equation (2.106) is one of the most practical forms of the incremental inductance rule because the characteristic impedance is known for a wide variety of transmission lines.

- Example 2.8 Using The Wheeler Incremental Inductance Rule To Find The Attenuation Constant

Calculate the attenuation due to conductor loss of a coaxial line using the Wheeler inductance rule.

Solution

From (2.32) the characteristic impedance of the coaxial line is

$$Z_0 = \frac{\eta}{2 \pi} \ln \frac{b}{a}$$

From the incremental inductance rule given in (2.106), the attenuation due to conductor loss is

$$\alpha_c = \frac{R_s}{2 Z_0} \frac{dZ_0}{dl} = \frac{R_s}{4 \pi Z_0} \left( \frac{d \ln b/a}{dt} - \frac{d \ln b/a}{da} \right) = \frac{R_s}{4 \pi Z_0} \left( \frac{1}{b} + \frac{1}{a} \right)$$

which is seen in agreement with the result of Example 2.7. The negative sign on the second differentiation in this equation is because the derivative for the inner conductor is in the  $-z$  direction (receding wall).

Regardless of how attenuation is calculated, measured attenuator values for practical transmission lines are higher. One reason for the discrepancy is the fact that realistic transmission lines have metallic surfaces with a certain amount of roughness, which introduces loss, while our theoretical calculations assume perfectly smooth conductors. A quasi-empirical formula that can be used to approximate account for surface roughness for a transmission line is [7]

$$d_c' = d_c \left[ 1 + \frac{2}{\pi} \tan^{-1} 1.4 \left( \frac{\Delta}{S_s} \right)^2 \right] \quad (2.107)$$

where  $d_c$  is the attenuation due to perfectly smooth conductors,  $d_c'$  is the attenuation corrected for surface roughness,  $\Delta$  is the RMS surface roughness, and  $S_s$  is the skin depth of the conductors.

## 2.8 Transients on Transmission Lines

So far, we have concentrated on the behaviour of transmission lines at a single frequency, and in many cases of practical interest the viewpoint is entirely satisfactory. In some situations, however, where short pulses or very wideband signals are propagating on a transmission line, it is useful to consider wave propagation from a transient, or time domain, point of view.

In this section we will discuss the reflection of transient pulses from terminated transmission lines, including special cases of a matched line, a short-circuited line, and an open-circuited line. We will conclude with a description of pulse diagrams, which can be used to describe multiple reflections of pulses on transmission lines.

### Reflection of pulses from a terminated transmission line.

A transient transmission line circuit is shown in Figure 2.21a, where a DC source is switched on at  $t=0$ . We first consider the case in which the line has a characteristic impedance of  $Z_0$ , the source impedance is  $Z_0$ , and the load impedance is  $Z_0$ . It is assumed that the voltage on the line is initially zero:  $v(z,t)=0 \forall z$ , for  $t < 0$ . We want to determine the voltage response on the transmission line as a function of time and position.

Because of the finite transit time on the line, its input impedance will appear to be equal to the characteristic impedance of  $Z_0$ . The source impedance is  $Z_0$ , and the load impedance is  $Z_0$ . It is assumed that the voltage on the line is initially zero:  $v(z,t)=0 \forall z$ , for  $t < 0$ . Line for  $t < l/v_p$ , where  $v_p$  is the phase velocity of the line. In words, the line looks infinitely long until the pulse has time to reach the load and (possibly) reflect back the input. Therefore, when the switch closes at  $t=0$ , the circuit appears as a voltage divider consisting of the source impedance and the input impedance, both being  $Z_0$ . The initial voltage on the line is thus  $V_0/2$ , and the voltage waveform propagates to the load with a velocity  $v_p$ . The leading edge of the pulse will be at position  $z$  on the line at time  $t=z/v_p$ , as shown in Figure 2.21b.

The pulse reaches the load at time  $t=l/v_p$ . Since the load is matched to the line, there is no reflection to the pulse from the load. The circuit is now in a steady-state condition, and voltage on the line is constant:  $v(z,t)=V_0/2 \forall t > l/v_p$ , as shown in Figure 2.21c. This is, of course, the DC value we would get for a voltage divider consisting of equal source and input impedances.

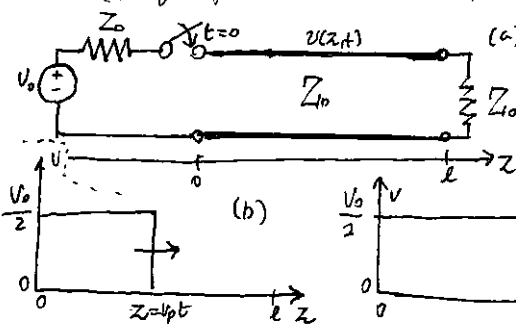


Figure 2.21 Transient response of a transmission line terminated with a matched load.

(a) Transmission line circuit with a step voltage source.

(b) Response for  $0 < t < l/v_p$ .

(c) Response for  $t > l/v_p$  or  $t > 2l/v_p$ . There is no reflection from the load.

Next consider the transmission line circuit of Figure 2.22a, where the line is now terminated with a short circuit. Initially, the impedance input of the line again appears as  $Z_0$ , and the initial incident pulse again has the amplitude of  $V_0/2$ , as shown in Figure 2.22b. The short-circuit load has a reflection coefficient of  $\Gamma=-1$ , which has the effect of inverting the reflected pulse as it travels back towards the source. The superposition of the forward and reverse-travelling pulses leads to cancellation, as shown in Figure 2.22c, for the period where  $l/v_p < t < 2l/v_p$ . When the return pulse reaches the source, at  $t=2l/v_p$ , the superposition it will not be re-reflected because the source is matched to the line. The circuit is then in steady state, with zero voltage everywhere on the line. Again this is consistent with circuit theory, as the shorted DC line appears as a short at its input, leading to a terminal voltage of zero.

The voltage waveform at a fixed point  $z$  on the line will consist of a rectangular pulse of amplitude  $V_0/2$  existing only over the time period  $(z < t < (2l-z)) / v_p$ . This effect can be used to create pulses of a very short duration.

Finally, consider the effect of a transmission line with an open-circuit termination, as shown in Figure 2.23a. As in previous cases, the input impedance on the line initially appears as  $Z_0$ , and the initial incident pulse has an amplitude of  $V_0/2$ , as shown in Figure 2.23b. The open-circuit load has a reflection coefficient of  $\Gamma = 1$ , which reflects the incident waveform with the same polarity as the source. The amplitudes of the forward and reverse pulses add to create a wave with an amplitude  $V_0$ , as shown in Figure 2.23c. At  $t=2l/v_p$  the return pulse reaches the source, but it is not reflected since the source is matched to the line.

By DC Analysis, the open-circuited line presents an open circuit at its terminals, leading the terminal voltage equal to source voltage.

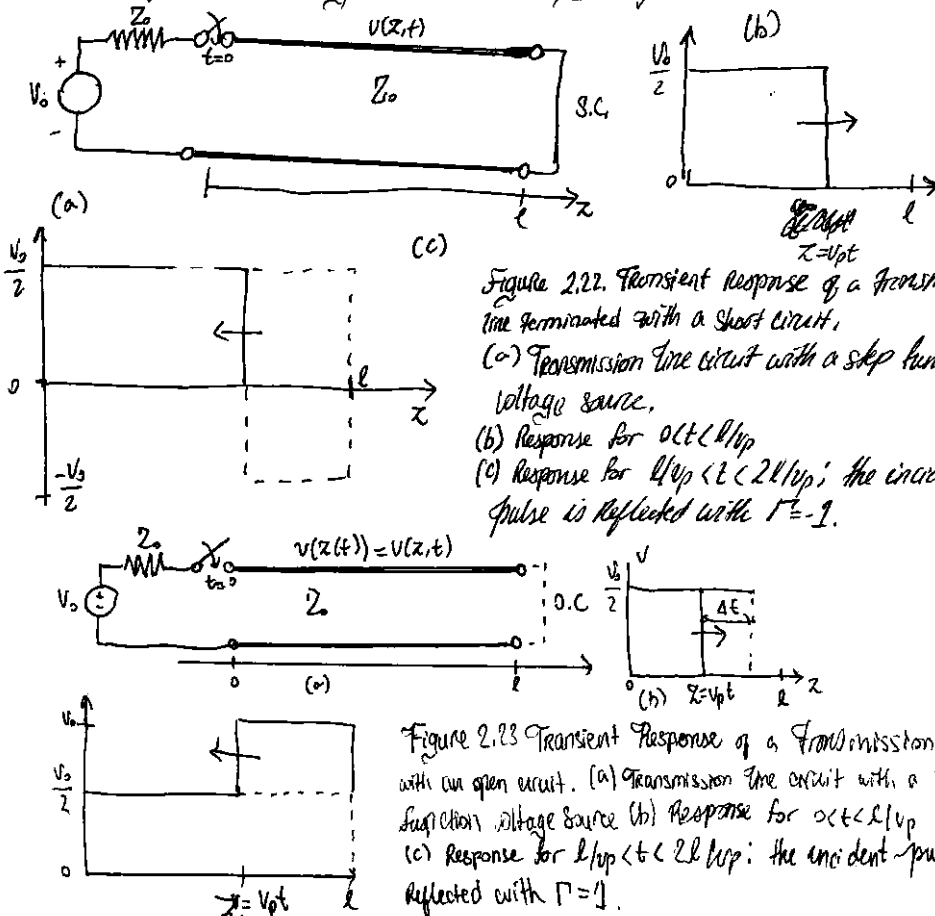


Figure 2.22 Transient response of a transmission line terminated with a short circuit.  
 (a) Transmission line circuit with a step function voltage source.  
 (b) Response for  $0 < t < l/v_p$   
 (c) Response for  $l/v_p < t < 2l/v_p$ ; the incident pulse is reflected with  $\Gamma = -1$ .

### Bounce Diagrams for Transient Propagation

The plots in Figures 2.21-2.23 show the voltage of a propagating pulse versus position along the transmission line but do not directly show the time variable, nor do they show very clearly the contributions of reflections on the waveform (especially when multiple reflections are present). An alternative way of viewing the progress of a propagating wave in time and position along a transmission line is with a bounce diagram.

As an example, Figure 2.24 shows the bounce diagram for the transient circuit of figure 2.23a. The horizontal axis represents position on the line, while the vertical axis represents time. The ray representing the incident wave begins at  $z=0, t=0$  and travels to the right (increasing  $|z|$ ) and up (for increasing  $t$ ). This ray is labeled with the amplitude of the incident wave,  $V_0/2$ . At  $t=l/v_p$ , the incident wave reaches the open-circuit load and is reflected to produce a wave of amplitude  $V_0/2$  traveling back to the source. The ray for this reflected wave thus moves left and up, until it reaches the source at  $z=0$  and  $t=2l/v_p$ , at which point steady state is reached. The total voltage at any position  $z$  and time  $t$  can be easily found by drawing a vertical line through the point  $z$  and extending up from  $t=0$  to  $t$ . The total voltage is found by adding the voltages of each forward or reverse traveling wave component, as represented by the rays that intersect this vertical line.

The next example shows how a bounce diagram can be applied to circuits that have multiple reflections.

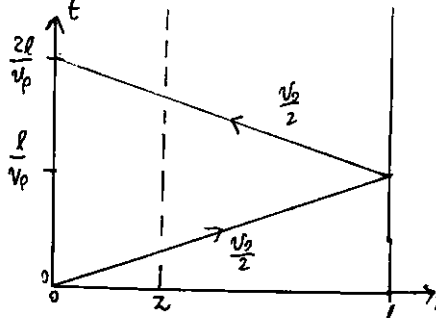


Figure 2.24 Bounce diagram for the transient circuit of Figure 2.23a.

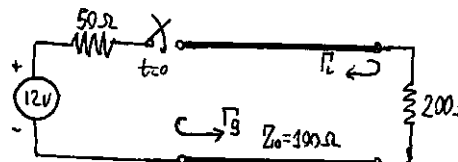


Figure 2.25  
Circuit for Example 2.25

### Example 2.25 Circuit for Example 2.8

### Example 2.9 Bounce Diagram for a Transient circuit with Multiple Reflections

Show the bounce diagram for the transient circuit of Figure 2.25, including the first three reflections.

Solution

The amplitude of the incident wave is given by the voltage divider as

$$V^+ = 12 \cdot \frac{100}{50+100} = 8.0V$$

The incident ray can be plotted as a line from the origin to the point  $Z=0$  and  $t=L/v_p$ . The reflection coefficients at the generator and load are:

$$\Gamma_g = \frac{50-100}{50+100} = -\frac{1}{3} \quad \text{and} \quad \Gamma_L = \frac{200-100}{200+100} = \frac{1}{3}$$

So the amplitude of the wave reflected from the load is  $8/3V$ . When the wave reaches the source, it will be reflected to form a wave of amplitude  $-8/9V$ . The next reflection from the load will have an amplitude of  $-8/27V$ . These four waves are shown in the bounce diagram of Figure 2.26.

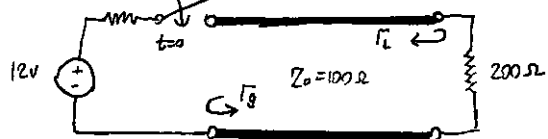


Figure 2.25  
Circuit for Example 2.9

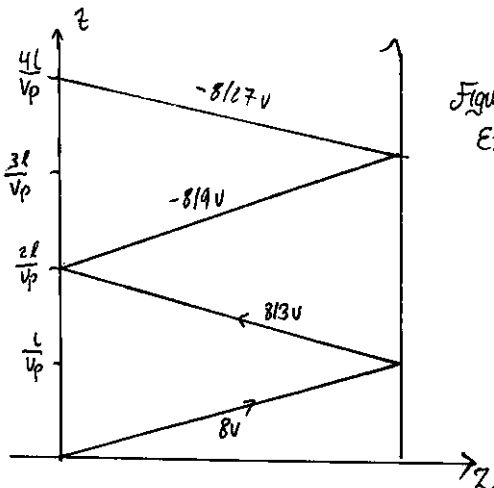


Figure 2.26 Bounce diagram for  
Example 2.9

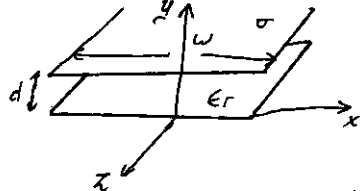
### References

- [1] S. Ramo, J.R. Whinnery, and T. Van Duzer, *Fields and Waves in Communication Electronics*, 3rd edition, John Wiley & Sons, New York, 1994.
- [2] J.A. Stratton, *Electromagnetic Theory*, McGraw-Hill, New York, 1941.
- [3] H.A. Wheeler, "Reflection Charts Relating To Impedance matching," *IEEE Transactions on Microwave Theory and Techniques*, vol. MTT-32, pp 1008-1021, September 1984.
- [4] P.H. Smith, "Transmission Line Calculator," *Electronics*, vol. 12 No., pp. 29-31, January 1939.
- [5] P.J. Nahin, *Oliver Heaviside : Sage in Solitude*, IEEE press, New York, 1988.
- [6] H.A. Wheeler, "Formulas for the Stein effect," *Proceedings of the IRE*, Vol. 30, pp 412-424, September 1942.
- [7] T.C. Edwards, *Foundations for microstrip circuit design*, John Wiley & Sons, New York, 1987.

### Problems

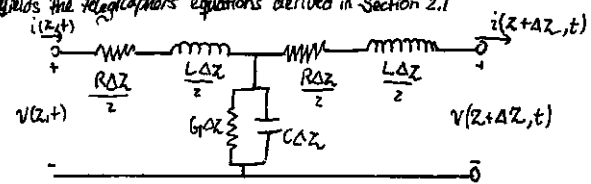
- 2.1 A 75Ω coaxial line has a current  $i(z,t) = 1.8 \cos(3.77 \times 10^8 t - 18.13z) \text{ mA}$ . Determine (a) the frequency, (b) the phase velocity, (c) the wavelength, (d) the relative permittivity of the line, (e) the phasor form of the current, and (f) the time domain voltage on the line.
- 2.2. A transmission line has the following per-unit-length parameters:  $Z = 0.5 \mu\text{H/m}$ ,  $C = 200 \text{ pF/m}$ ,  $R = 4.0 \Omega/\text{m}$ , and  $G = 0.02 \text{ S/m}$ . Calculate the propagation constant and characteristic impedance of this line at 800 MHz. If the line is 30 cm long, what is the attenuation in dB? Recalculate these quantities in the absence of loss ( $R=G=0$ )?
- 2.3 RG-402U Semirigid coaxial standard cable has an inner conductor diameter of 0.91 mm and a dielectric diameter (equal to the inner diameter of the outer conductor) of 3.02 mm. Both conductors are copper, and the dielectric material is Teflon. Compute the  $R$ ,  $L$ ,  $G$ ,  $C$  parameters of this line at 1.6 GHz, and use these results to find the characteristic impedance and attenuation of the line at 1.0 GHz. Compare your results with the manufacturer's specifications of 50Ω and 0.43 dB/m, and discuss the reasoning for the difference.
- 2.4 Compute and plot the attenuation of the coaxial line of Problem 2.3, in dB/m, over a frequency range of 1 MHz to 100 GHz. use log-log graph paper or graph.

- 2.5 For the parallel plate line shown in the accompanying figure, derive the R,L,G,C parameters. Assume  $W \gg d$



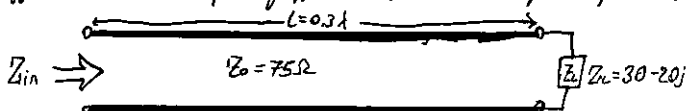
- 2.6 For the parallel plate line of problem 2.5, derive the Telegrapher equations using the field theory approach.

- 2.7 Show that the T-model of a transmission line shown in the accompanying figure also yields the Telegrapher equations derived in Section 2.1



- 2.7 Show that the

- 2.8 A lossless transmission line of electrical length  $\ell = 0.3\lambda$  is terminated with a complex load impedance as shown in the accompanying figure. Find the reflection coefficient at the load, the SWR on the line, and reflection coefficient at the input of the line, and the input impedance of the line.



- 2.9 A  $75\Omega$  coaxial transmission line with  $Z_0 = 60\Omega$  has a reflection coefficient at the load at  $\Gamma = 0.4/60^\circ$ . (a) what is the load impedance, (b) what is the reflection coefficient  $0.3\lambda$  away from the load (c) what is the input impedance at this point?

- 2.10 A terminated transmission line with  $Z_0 = 60\Omega$

- 2.9 A  $75\Omega$  coaxial transmission line has a length of 2.0 cm and is terminated with a load impedance of  $37.5 + j75\Omega$ . If the relative permittivity of the line is 2.56 and the frequency is 3.0 GHz, find the input impedance of the line, the reflection coefficient at the load, the reflection coefficient at the input, and the SWR on the line.

- 2.10 A terminated transmission line with  $Z_0 = 60\Omega$  has a reflection coefficient at the load of  $\Gamma = 0.4/60^\circ$ . (a) what is the load impedance? (b) what is the reflection coefficient  $0.3\lambda$  away from the load? (c) what is the input impedance at this point?

- 2.11 A  $100\Omega$  transmission line is terminated with a  $100\Omega$  load

- 2.11 A  $300\Omega$  transmission line has an effective dielectric constant of 1.65. Find the shortest open-circuit length of this line that appears as its input capacitor of 5pF at 2.5GHz. Repeat for an inductance of  $5nH$

- 2.12 A lossless transmission line is terminated with a  $100\Omega$  line. If the SWR on the line is 1.5, find the two possible values for the characteristic impedance of the line.

- 2.13 Let  $Z_{sc}$  be the input impedance of a length of coaxial line when one end is short-circuited, and let  $Z_{oc}$  be the input impedance of the line when one end is open-circuited. Derive an expression for the characteristic impedance of a cable in terms of  $Z_{sc}$  and  $Z_{oc}$ .

- 2.14 A radio transmitter is connected to an antenna having an impedance  $80 + j40\Omega$  with a  $50\Omega$  coaxial cable. If the  $50\Omega$  transmitter can deliver 80W when connected to a  $50\Omega$  load, how much power is delivered to the antenna?

- 2.15 Calculate Standing Wave Ratio, Reflection coefficient magnitude, and Return Loss values to complete the entries in the following table

SWR	$ \Gamma $	RL (dB)
1.00	0.00	00
1.01	—	—
—	0.01	—
1.05	—	—
—	—	30.0
1.10	—	—
1.20	—	—
—	0.10	—
1.50	—	—
—	—	10.0
2.00	—	—
2.50	—	—

- 2.16 The transmission line circuit in the accompanying figure has  $V_g = 15 \text{ V rms}$ ,  $Z_g = 75 \Omega$ ,  $Z_0 = 75 \Omega$ ,  $Z_L = 60 + j40 \Omega$ , and  $l = 0.7\lambda$ . Compute the power delivered to the load using three different techniques:

$$(a) \text{Find } \Gamma \text{ and compute: } P_L = \left( \frac{|V_g|}{Z_0} \right)^2 \frac{l}{Z_0} / (1 - |\Gamma|^2)$$

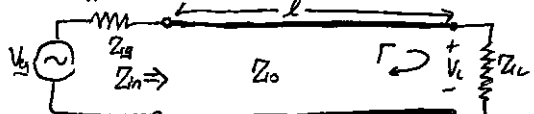
(b) Find  $Z_{in}$  and compute

$$P_L = \left| \frac{V_g}{Z_g + Z_{in}} \right|^2 \operatorname{Re}\{Z_{in}\}$$

(c) Find  $V_L$  and compute

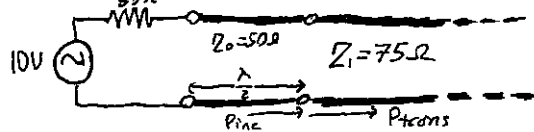
$$P_L = \left| \frac{V_L}{Z_L} \right|^2 \operatorname{Re}\{Z_L\}$$

Discuss the rationale for each of these methods. Which methods can be used if the line is not lossless.

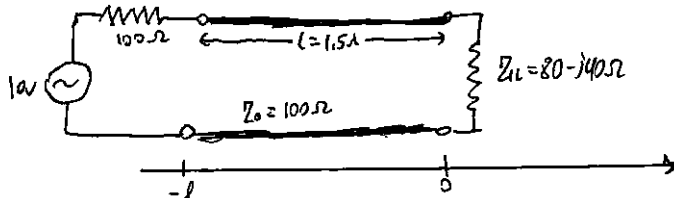


- 2.17 For a purely reactive load impedance of the form  $Z_L = jX$ , Show that the reflection coefficient magnitude  $|\Gamma|$  is always unity. Assume that the characteristic impedance  $Z_0$  is real.

- 2.18 Consider the transmission line circuit shown in the accompanying figure. Compute the incident power, the reflected power, and the power transmitted to an infinite  $75 \Omega$  line. Show that power conservation is satisfied.

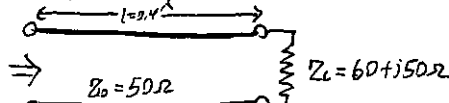


- 2.19 A generator is connected to a transmission line as shown in the accompanying figure. Find the voltage as a function of  $z$  along a transmission line. Plot the magnitude of this voltage for  $-l \leq z \leq 0$ .



- 2.20 Use the Smith chart to find the following quantities for the transmission line circuit shown in the accompanying figure:

- (a) The SWR of the line
- (b) The reflection coefficient at the load.
- (c) The load admittance
- (d) The input impedance
- (e) The distance from the load to the first voltage minimum
- (f) The distance from the load to the first voltage maximum.



- 2.21 Use the Smith chart to find the shortest length of the short-circuited line

• b 75Ω to give the following input impedance.

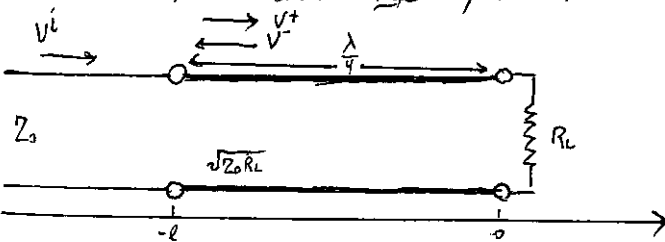
- (a)  $Z_{in}=0$
- (c)  $Z_{in}=j75\Omega$
- (e)  $Z_{in}=j10\Omega$
- (b)  $Z_{in}=\infty$
- (d)  $Z_{in}=-j50\Omega$

- 2.22 Repeat 2.21 for an open-circuited length of line of  $75\Omega$ .

- 2.23 A slotted line experiment is performed with the following results: distance between successive minima =  $2.1\text{cm}$ ; distance of the first voltage minimum from load =  $0.9\text{cm}$ ; SWR to load =  $2.5$ . If  $Z_0=50\Omega$ , find the load impedance.

- 2.24 Design a quarter-wave matching transformer to match a  $40\Omega$  load to a  $75\Omega$  line. Plot the SWR for  $0.5 \leq f/f_0 \leq 2.0$ , where  $f_0$  is the frequency at which the line is  $\lambda/4$  long.

- 2.25 Consider the quarter-wave matching transformer circuit shown in the accompanying figure. Derive expressions for  $V^+$  and  $V^-$ , the respective amplitudes of the forward and reverse traveling waves on the quarter-wave line section, in terms of  $V_i^+$ , the incident voltage amplitude.

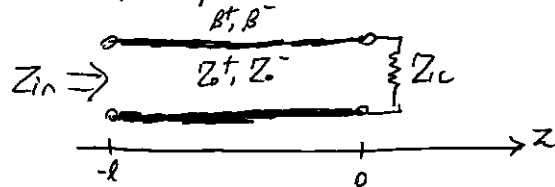


- 2.26. Derive equation (2.71) from (2.70)

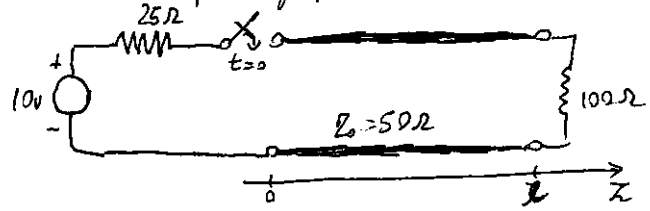
- 2.27 In Example 2.7, the attenuation of a coaxial line due to finite conductivity is
- $$\alpha_c = \frac{R_s}{2\pi b \ln b/a} \left( \frac{1}{a} + \frac{1}{b} \right)$$

Show that  $\alpha_c$  is minimized for a conductor radius such that  $x/\ln x = 1+x$ , where  $x=b/a$ . Solve this equation for  $x$ , and show that the corresponding impedance for  $\epsilon_r=1$  is  $77\Omega$ .

- 2.28 Compute and plot the factor by which attenuation is increased due to surface roughness, for rms roughness ranging from 0 to 0.01 mm. Assume copper conductors at 10 GHz.
- 2.29. A 50Ω transmission line is matched to a 10V source and feeds a load  $Z = 100\Omega$ . If the line is  $2\lambda$  long and has an attenuation constant  $\alpha = 0.5 \text{ dB}/\lambda$ , find the powers that are delivered by the source, lost in the line, and delivered to the load.
- 2.30 Consider a nonreciprocal transmission line having different propagation constants,  $\beta^+$  and  $\beta^-$ , for propagation in the forward and reverse directions, with corresponding characteristic impedances  $Z_0^+$  and  $Z_0^-$ . (An example of such a line could be a microstrip transmission line on a magnetized ferrite substrate.) If the line is terminated as shown in the accompanying figure, derive expressions for the reflection coefficient and impedance seen at the input of the line.



- 2.31 Plot the source diagram for the transient circuit shown in the accompanying figure. Include at least three reflections. What is the total voltage at the midpoint of the line ( $z = l/2$ ), at time  $t = 3\lambda/v_p$ ?



As with the first chapter, this chapter, and all following, the problems and solutions ~~were~~ are written in the accompanying problem book.

### Chapter 3. Transmission Lines and Waveguides

One of the early milestones in microwave engineering was the development of waveguide and other transmission lines for the low-loss transmission of power at high frequencies. Although Heaviside considered the possibility of propagation of electromagnetic waves inside a closed hollow tube in 1893, he rejected the idea because he believed the two conductors were necessary for the transfer of electromagnetic energy [1]. In 1897, Lord Rayleigh (John William Strutt) mathematically proved that wave propagation in waveguides was possible for both circular and rectangular cross-sections [2]. Rayleigh also noted the infinite set of waveguide modes of the TE and TM type that were possible and the existence of a cutoff frequency, but no experimental verification was made at the time. The waveguides were then essentially forgotten until it was rediscovered independently in 1936 by two researchers [3]. After preliminary experiments in 1932, George C Southworth of the AT&T Company in New York presented a paper on the waveguide in 1936. At the same meeting, W.L. Borow of MIT presented a paper on the circular waveguide, with experimental confirmation of propagation.

Early RF and microwave systems relied on waveguides, two-wire lines, and coaxial lines for transmission. Waveguides have the advantage of high power-handling capability and low loss but are bulky and expensive, especially at lower frequencies. Two-wire lines are inexpensive but lack shielding. Coaxial lines are shielded but are a difficult medium in which to fabricate complex microwave components. Planar transmission lines provide an alternative, in the form of stripline, microstrip lines, slotlines, coplanar waveguides, and several other types of related geometries. Such transmission lines are compact, low in cost, and capable of being easily integrated with active circuit devices, such as diodes and transistors, to form microwave integrated circuits. The first planar transmission line may have been a flat strip coaxial line, similar to a stripline, used in the production power divider networks in WWII [4], but planar lines did not see intense development until the 1950s. Microstrip lines used a relatively thick dielectric substrate, which accentuated the non-TEM mode behaviour and frequency dispersion of the line. This characteristic made it less desirable than a strip line until the 1960s, when much thinner substrates began to be used. This reduced the frequency dependence of the line, and now microstrip lines are the preferred medium for microwave integrated circuits.

In this chapter we will study the properties of several types of transmission lines and waveguides that are in common use. As we know from Chapter 2, a transmission line is characterized by a propagation constant, an attenuation constant, and a characteristic impedance. These quantities will be derived by field theory analysis for the various lines and waveguides treated here.

We begin with a discussion of the different types of wave propagation modes that can exist on general transmission lines and waveguides. Transmission lines that consist of two or more conductors may support transverse electromagnetic (TEM) waves, characterized by the lack of longitudinal field components. Such lines have a uniquely defined voltage, current, and characteristic impedance. Waveguides, often consisting of a single conductor, support transverse electric (TE) and/or transverse magnetic (TM) waves, characterized by the presence of longitudinal magnetic or electric field components. As we will see in Chapter 4, a unique definition of characteristic impedance is not possible for such waves, although definitions can be chosen so that the characteristic impedance concept can be extended to waveguides with meaningful results.

### 3.1 General Solutions for TEM, TE, and TM Waves

In this section we will find general solutions to Maxwell's equations for the specific cases of TEM, TE, and TM wave propagation on cylindrical transmission lines or waveguides. The geometry on an arbitrary transmission line or waveguide is shown in Figure 3.1 and is characterized by conductor boundaries that are parallel to the  $z$ -axis. These structures are assumed to be uniform in shape and dimension in the  $z$ -direction and infinitely long.

The conductors will have initially be assumed to be perfectly conducting, but attenuation can be found by the perturbation method discussed in chapter 2.

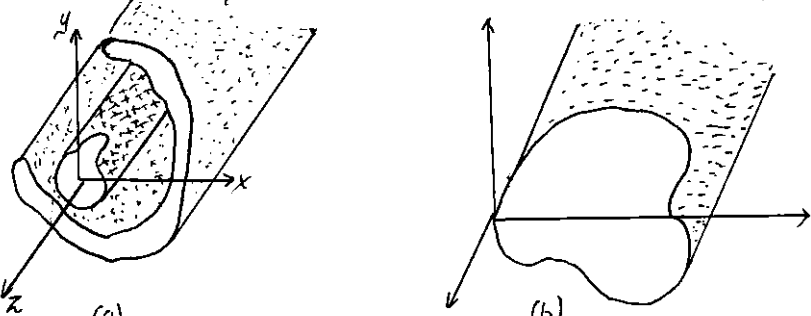


Figure 3.1 (a) General two-conductor transmission line and (b) closed waveguide.

We assume time-harmonic fields with an  $e^{j\omega t}$  dependence and wave propagating along the  $z$ -axis. The electric and magnetic fields can be written as

$$\bar{E}(x,y,z) = [\bar{e}_x(x,y) + \hat{e}_y e_z(x,y)] e^{-jBz} \quad (3.1a)$$

$$\bar{H}(x,y,z) = [h_x(x,y) + \hat{h}_y e_z(x,y)] e^{-jBz} \quad (3.1b)$$

where  $\bar{e}(x,y)$  and  $\hat{e}(x,y)$  representing the transverse  $(x,y)$  electric and magnetic field components, and  $e_z$  and  $h_z$  are the longitudinal electric and magnetic field components. In (3.1) the wave is propagating in the  $+z$  direction;  $-z$  propagation can be obtained by replacing  $B$  with  $-B$ . In addition, if conductor or dielectric loss is present, the propagation constant will be complex;  $j\beta$  should then be replaced with  $\gamma = \alpha + j\beta$ .

Assuming that the transmission line or waveguide region is source free, we can write Maxwell's equations as

$$\nabla \times \bar{E} = -j\omega \mu \bar{H} \quad (3.2a)$$

$$\nabla \times \bar{H} = j\omega \epsilon \bar{E} \quad (3.2b)$$

With an  $e^{jBz}$   $z$  dependence, the three components of each of these vector equations can be reduced to the following:

$$\frac{\partial E_z}{\partial y} + j\beta E_y = -j\omega \mu H_x \quad (3.3a)$$

$$-j\beta E_z - \frac{\partial E_x}{\partial y} = -j\omega \mu H_y \quad (3.3b)$$

$$\frac{\partial E_y}{\partial x} - \frac{\partial E_x}{\partial y} = -j\omega \mu H_z \quad (3.3c)$$

$$\frac{\partial H_z}{\partial y} + j\beta H_y = j\omega E_x \quad (3.3d) \quad (3.4a)$$

$$-j\beta H_z - \frac{\partial H_x}{\partial x} = j\omega E_y \quad (3.4b)$$

$$\frac{\partial H_x}{\partial x} - \frac{\partial H_z}{\partial y} = j\omega E_z \quad (3.4c)$$

These six equations can be solved for the four transverse field components in terms of  $E_z$  [e.g.  $H_x$  can be determined by eliminating  $E_y$  from (3.3a) and (3.3b) as follows:

$$H_x = \frac{j}{K_c^2} \left( \omega \frac{\partial E_z}{\partial y} - \beta \frac{\partial H_z}{\partial x} \right), \quad H_y = \frac{-j}{K_c^2} \left( \frac{\partial E_z}{\partial x} \omega + \beta \frac{\partial H_z}{\partial y} \right) \quad (3.5a,b)$$

$$E_x = \frac{-j}{K_c^2} \left( \beta \frac{\partial E_z}{\partial x} + \omega \mu \frac{\partial H_z}{\partial y} \right), \quad E_y = \frac{j}{K_c^2} \left( -\beta \frac{\partial E_z}{\partial y} + \omega \mu \frac{\partial H_z}{\partial x} \right) \quad (3.5c,d)$$

where

$$k_c^2 = K^2 - \beta^2 \quad (3.6)$$

is defined as the cutoff wave number; the reason for this terminology will become clear later. As in previous chapters

$$k = \omega \sqrt{\mu \epsilon} = 2\pi/\lambda \quad (3.7)$$

is the wave number of the material filling the transmission line or waveguide region. If dielectric loss is present,  $\epsilon$  can be made complex by using  $\epsilon = \epsilon_0 \epsilon_r (1 - j\alpha \tau_s)$ , where  $\alpha \tau_s$  is the loss tangent of the material.

Equations (3.5a)-(3.5d) are general results that can be applied to a variety of waveguiding systems. We will now specialize these results to specific wave types.

### TEM Waves

Transverse electromagnetic (TEM) waves are characterized by  $E_z = H_z = 0$ . Observe from (3.5) that if  $E_z = H_z = 0$ , then the transverse fields are also zero, unless  $k_c^2 = 0 \Rightarrow K^2 = \beta^2$ , in which case we have an indeterminate result. However, we can return to (3.3)-(3.4) and apply the condition that  $E_z = H_z = 0$ . Then from (3.3a) and (3.4b) we can eliminate  $H_x$  to obtain:

$$\beta^2 E_y = \omega^2 \mu \epsilon E_y$$

or

$$\beta = \omega \sqrt{\mu \epsilon} = K \quad (3.8)$$

as noted earlier. [This result can also be obtained from (3.3b) and (3.4a).] The cutoff wave number,  $k_c = \sqrt{K^2 - \beta^2}$ , is thus zero for TEM waves.

The Helmholtz wave equation for  $E_x$  is, from (1.142),

$$\left( \frac{\partial^2}{\partial x^2} + \frac{\partial^2}{\partial y^2} + \frac{\partial^2}{\partial z^2} + k^2 \right) E_x = 0 \quad (3.9)$$

but for  $e^{-j\beta z}$  dependence,  $\left( \frac{\partial^2}{\partial z^2} \right) E_x = -\beta^2 E_x = -K^2 E_x$ , so (3.9) reduces to

$$\left( \frac{\partial^2}{\partial x^2} + \frac{\partial^2}{\partial y^2} \right) E_x = 0 \quad (3.10)$$

A similar result also applies to  $E_y$ , so using the form of  $\vec{E}$  assumed in (3.1a), we can write:

$$\nabla_t^2 \vec{E}(x, y) = 0 \quad (3.11)$$

where  $\nabla_t^2 = \partial^2 / \partial x^2 + \partial^2 / \partial y^2$  is the Laplacian operator in the two transverse directions.

The result of (3.11) shows that the transverse electric fields,  $\vec{e}(x, y)$ , of a TEM wave satisfy Laplace's equation. It is easy to show in the same way that the transverse magnetic fields also satisfy Laplace's equation:

$$\nabla_t^2 \vec{h}(x, y) = 0 \quad (3.12)$$

The transverse fields of a TEM wave are thus the same as the static fields between the conductors. In the electrostatic case, we know the electric field can be expressed as the gradient of scalar potential,  $\Phi(x, y)$ :

$$\vec{e}(x, y) = -\nabla_t \Phi(x, y) \quad (3.13)$$

where  $\nabla_t = \hat{x} \frac{\partial}{\partial x} + \hat{y} \frac{\partial}{\partial y}$  is the transverse gradient operator in two dimensions. For the relation in (3.13) to be valid, the curl of  $\vec{e}$  must vanish, and this is indeed the case here since:

$$\nabla_t \times \vec{e} = -j\omega \mu \epsilon \hat{z} = 0$$

Using the fact that  $\nabla \cdot \vec{D} = \epsilon \cdot \nabla_t \cdot \vec{e} = 0$  with (3.13) shows that  $\Phi(x, y)$  also satisfies Laplace's equation,

$$\nabla_t^2 \Phi(x, y) = 0 \quad (3.14)$$

As to be expected from electrostatics, the voltage between the conductors can be found as

$$V_{12} = \Phi_1 - \Phi_2 = \int_1^2 \vec{E} \cdot d\vec{l} \quad (3.15)$$

where  $\Phi_1$  and  $\Phi_2$  represent the potential of conductors 1 and 2 respectively. The current flow on a given conductor can be found as from Ampere's law as

$$I = \oint_C \vec{H} \cdot d\vec{l} \quad (3.16)$$

where  $C$  is the cross-sectional contour of the conductor.

TEM waves cannot exist when two or more conductors are present. Plane waves are also examples of TEM waves since there are no field component in the direction of propagation; in this case the transmission line conductors may be considered to be two infinitely large plates separated to infinity. The above results show that a closed conductor (such as a rectangular waveguide) cannot support TEM waves since the corresponding static potential in such a region would be zero (or possibly a constant), leading to  $\vec{e} = 0$ .

The wave impedance of a TEM mode can be found as the ratio of the transverse electric and magnetic fields:

$$Z_{\text{TEM}} = \frac{E_x}{H_y} = \frac{\omega M}{\beta} = \sqrt{\frac{\mu}{\epsilon}} = \eta \quad (3.17a)$$

where (3.4a) was used [ $\partial H_z / \partial y + j\beta H_y = j\omega \mu E_x$ ]. The other pair of transverse field components, from (3.3a), gives:

$$Z_{\text{TEM}} = \frac{-E_y}{H_x} = \sqrt{\frac{\mu}{\epsilon}} = \eta \quad (3.17b)$$

Combining the results of (3.17a) and (3.17b) gives a general expression for the transverse field as

$$\tilde{\mathbf{H}}(x, y) = \frac{1}{Z_{\text{TEM}}} \hat{\mathbf{z}} x \hat{\mathbf{e}}(x, y) \quad (3.18)$$

Note that the wave impedance is the same for a plane in a lossless medium, as derived in Chapter 1; the reader should not confuse the impedance with the characteristic impedance,  $Z_0$ , of a transmission line. The latter relates traveling voltage and current and is a function of the line geometry as well as the material filling the line, while the wave impedance relates transverse field components and is dependent only on the material constants. From (2.32), the characteristic impedance of a TEM line is  $Z_0 = V/I$ , where  $V$  and  $I$  are the amplitudes of the incident voltage and current waves.

The procedure for analyzing a TEM line can be summarized as follows:

1. Solve Laplace's equation, (3.14), for  $\phi(x, y)$ . The solution will contain several unknown constants.
2. Find these constants by applying boundary conditions for the known voltages on the conductors.
3. Compute  $\tilde{\mathbf{e}}$  and  $\tilde{\mathbf{E}}$  from (3.13) and (3.1a). Compute  $\tilde{\mathbf{H}}$  and  $\tilde{\mathbf{B}}$  from (3.18) and (3.1b).
4. Compute  $V$  from (3.15) and  $I$  from (3.16).
5. The propagation constant is given by (3.8), and the characteristic impedance is given by  $Z_0 = V/I$ .

### TE Waves

Transverse electric (TE) waves, (also referred to as H-waves) are characterized by  $E_z = 0$  and  $H_z \neq 0$ . Equations (3.5) then reduce to

$$H_x = -j\beta \frac{\partial H_z}{\partial x}, \quad H_y = j\beta \frac{\partial H_z}{\partial y}, \quad E_x = -j\omega \mu \frac{\partial H_z}{\partial y}, \quad E_y = j\omega \mu \frac{\partial H_z}{\partial x} \quad (3.19)$$

In the core  $\mu_c \gg 1$ , and the propagation constant  $\beta = \sqrt{k^2 - \kappa^2}$  is generally a function of frequency and the geometry of the line or guide.

To apply (3.19), one must first find  $H_z$  from the Helmholtz wave equation,

$$\left( \frac{\partial^2}{\partial x^2} + \frac{\partial^2}{\partial y^2} + \frac{\partial^2}{\partial z^2} + \kappa^2 \right) H_z = 0 \quad (3.20)$$

which, since  $H_z(x, y, z) = h_z(x, y) e^{-j\beta z}$ , can be reduced to a two-dimensional wave equation for  $h_z$ :  $\left( \frac{\partial^2}{\partial x^2} + \frac{\partial^2}{\partial y^2} + \kappa_c^2 \right) h_z = 0$   $(3.21)$

Since  $\kappa_c^2 = k^2 - \beta^2$ . This equation must be solved subject to the boundary conditions of the specific geometry.

The TE wave impedance can be found as:

$$Z_{\text{TE}} = \frac{E_x}{H_y} = \frac{-E_y}{H_x} = \frac{\omega M}{\beta} = \frac{k \eta}{\beta} \quad (3.22)$$

which can be seen to be frequency dependent. TE waves can be supported inside closed conductors.

### TM Waves

Transverse magnetic (TM) waves (also referred to as E-waves) are characterized by  $E_z \neq 0$  and  $H_z = 0$ . Equations (3.5) then reduce to

$$H_x = j\omega \mu \frac{\partial E_z}{\partial y}, \quad H_y = -j\omega \mu \frac{\partial E_z}{\partial x}, \quad E_x = -j\beta \frac{\partial E_z}{\partial x}, \quad E_y = -j\beta \frac{\partial E_z}{\partial y} \quad (3.23 \text{ a-d})$$

as in the TE core,  $\kappa_c \gg 1$ , and the propagation constant  $\beta = \sqrt{k^2 - \kappa_c^2}$  is a function of frequency and the geometry of the line or guide.  $E_z$  is found from the Helmholtz wave equation,

$$\left( \frac{\partial^2}{\partial x^2} + \frac{\partial^2}{\partial y^2} + \frac{\partial^2}{\partial z^2} + \kappa^2 \right) E_z = 0 \quad (3.24)$$

which since  $E_z = e_z(x, y) e^{-j\beta z}$ , can be reduced to a two dimensional wave equation for  $e_z$ :

$$\left( \frac{\partial^2}{\partial x^2} + \frac{\partial^2}{\partial y^2} + \kappa_c^2 \right) e_z = 0 \quad (3.25)$$

Since  $\kappa_c^2 = k^2 - \beta^2$ . The equation must be solved subject to the boundary conditions of the specific guide geometry.

The TM wave impedance can be found as

$$Z_{TM} = \frac{E_x}{H_y} = \frac{E_y}{H_x} = \frac{\beta}{\omega} = \frac{\beta \eta}{k} \quad (3.26)$$

which is frequency dependent. As for TE waves, TM waves can be supported inside closed conductors, as well as between two or more conductors.

The procedure for analyzing TE and TM waveguides can be summarized as follows:

1. Solve the Reduced Helmholtz Equation, (3.21) or (3.25), for  $b_{12}$  and  $e_{12}$ . The solution will contain several unknown constants and the unknown cutoff wave number,  $k_c$ .
2. Use (3.19) or (3.23) to find the transverse fields from  $b_{12}$  or  $e_{12}$ .
3. Apply the boundary conditions to the appropriate field components to find the unknown constants and  $k_c$ .
4. The propagation constant is given by (3.6) and the wave impedance by (3.22) or (3.26).

### Attenuation Due to Dielectric Loss

Attenuation in a transmission line or waveguide can be caused by either dielectric loss or conductor loss. If  $\alpha_d$  is the attenuation constant due to dielectric loss and  $\alpha_c$  is the attenuation constant due to conductor loss, then the total attenuation constant is  $\alpha = \alpha_d + \alpha_c$ .

Attenuation caused by conductor loss can be calculated using the perturbation method of Section 2.7; this loss depends on the field distribution in the guide and so must be evaluated separately for each type of transmission line or waveguide. However, if the line or guide is completely filled with a homogeneous dielectric, the attenuation due to a lossy dielectric material can be calculated from the propagation constant, and this result will apply to any guide or line with a homogeneous dielectric filling.

Thus, use the complex permittivity allows the complex propagation constant to be written as:

$$\gamma = \alpha_d + i\beta = \sqrt{k_c^2 - \omega^2 \mu_0 \epsilon_0 \epsilon_r (1 - j\alpha_d)} \quad (3.27)$$

In practice, most dielectric materials have small losses ( $\alpha_d \cdot \text{Ton} s \ll 1$ ), and so this expression can be simplified by using the first two terms of the Taylor expansion,

$$\sqrt{a^2 + x^2} \approx a + \frac{x^2}{2a}, \quad \text{for } x \ll a$$

Then 3.27 reduces to:  $\gamma = \sqrt{k_c^2 - k^2 + ik^2 \alpha_d} \approx \sqrt{k_c^2 - k^2} + \frac{ik^2 \alpha_d}{2\sqrt{k_c^2 - k^2}}$

$$\gamma = \frac{k^2 \alpha_d}{2\beta} + i\beta \quad (3.28)$$

since  $\sqrt{k_c^2 - k^2} = i\beta$ . In these results,  $k = \omega \sqrt{\mu_0 \epsilon_0}$  as the (real) wave number in the absence of loss. Equation (3.28) shows that when the loss is small the phase constant  $\beta$  is unchanged, while the attenuation constant due to dielectric loss is given by  $\alpha_d = \frac{k^2 \alpha_d}{2\beta} N_p/m$  (TE or TM waves)  $(3.29)$

This result applies to any TE or TM wave, as long as the guide is completely filled with the dielectric material. It can also be used for TEM lines, where  $k_c = 0$ , by letting  $\beta = k$ .

$$\alpha_d = \frac{k \alpha_d}{2} N_p/m \quad (\text{TEM waves}) \quad (3.30)$$

### 3.2 Parallel Plate Waveguide

The parallel plate waveguide is the simplest type of guide that can support TM and TE modes; it can also support a TEM mode since it is formed from two flat conducting plates or strips, as shown in Figure 3.2. Although it is an idealization, understanding the parallel plate guide can also be useful for modeling the propagation of higher order modes on the stripline.

In the geometry of the parallel plate waveguide of Figure 3.2, the strip width,  $W$ , is assumed to be much greater than the separation,  $d$ , so that the fringing fields at any  $x$  variation can be ignored. A material with permittivity  $\epsilon$  and permeability  $\mu$  is assumed to fill the region between the two plates. We will derive solutions for TEM, TM and TE waves.

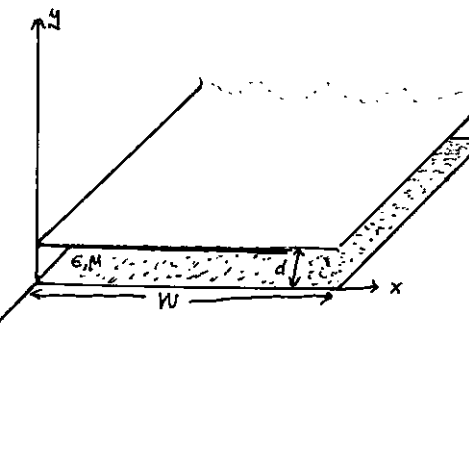


Figure 3.2 Geometry of a parallel plate waveguide.

## TEM Modes

As discussed in Section 3.1, the TEM mode solution can be obtained by solving Laplace's equation, (3.14), for the electrostatic potential  $\phi(x,y)$  between the two plates, thus

$$\nabla^2 \phi(x,y) = 0, \text{ for } 0 \leq x \leq W, 0 \leq y \leq d \quad (3.31)$$

If we assume that the bottom plate is at ground (zero) potential and the top plate at a potential of  $V_0$ , then the boundary conditions for  $\phi(x,y)$  are

$$\phi(x,0) = 0 \quad (3.32a)$$

$$\phi(x,d) = V_0 \quad (3.32b)$$

Because there is no variation in  $x$ , the general solution to (3.31) for  $\phi(x,y)$  is:

$$\phi(x,y) = A + B y$$

and the constants  $A, B$  can be evaluated from the boundary conditions of (3.32) to give the final solution as:

$$\phi(x,y) = V_0 y/d \quad (3.33)$$

The transverse electric field is, from (3.13),

$$\bar{E}(x,y) = -\nabla_y \phi(x,y) = -\frac{iV_0}{d} e^{iky} \quad (3.34)$$

so that the total electric field is:

$$E(x,y,z) = \bar{E}(x,y) e^{-jKz} = -\frac{iV_0}{d} e^{-jKz} \quad (3.35)$$

where  $K = \omega \sqrt{\mu \epsilon}$  is the propagation constant of the TEM wave, as in (3.8).

The magnetic field, from (3.18) is

$$\bar{H}(x,y,z) = \bar{h}(x,y) e^{-jKz} = \frac{1}{\eta} \hat{z} \times \bar{E}(x,y,z) = \hat{x} \frac{V_0}{\eta d} e^{-jKz} \quad (3.36)$$

where  $\eta = \sqrt{\mu \epsilon}$  is the intrinsic impedance of the medium between the parallel plates. Note that  $E_z = H_z = 0$  and the fields are similar in form to a plane wave in a homogeneous region.

The voltage of the top plate with respect to the bottom plate can be calculated from (3.15) and (3.35) as

$$V = - \int_{y=0}^d E_y dy = V_0 e^{-jKz} \quad (3.37)$$

It is instructive to compute the Poynting vector to see how power propagates in the TM<sub>01</sub> mode.

From (1.91), the time-average power passing a transverse cross-section of the parallel plate guide is:

$$P_0 = \frac{1}{2} \operatorname{Re} \int_{x=0}^W \int_{y=0}^d \bar{E} \cdot \bar{H}^* dy dx = \frac{-1}{2} \operatorname{Re} \iint_{x=0}^W \int_{y=0}^d E_y H_x^* dy dx \\ = \frac{W \operatorname{Re}(\beta) \omega \epsilon}{2K^2} |A_n|^2 \int_{y=0}^d \cos^2 \frac{n\pi y}{d} dy = \begin{cases} \frac{W \operatorname{Re}(\beta) \omega \epsilon d |A_n|^2}{4K^2} & \text{for } n \neq 0 \\ \frac{W \operatorname{Re}(\beta) \omega \epsilon d |A_n|^2}{2K^2} & \text{for } n=0 \end{cases} \quad (3.54)$$

where (3.48a,b) were used for  $E_y, H_x$ .

Thus,  $P_0$  is positive and nonzero when  $\beta$  is real.

which occurs when  $f > f_c$ . When the mode is below cutoff,  $\beta$  is imaginary, and then  $P_0 = 0$ .

TM (or TE) waveguide mode propagation has an interesting interpretation when viewed as a pair of bouncing plane waves. For example, consider the dominant TM<sub>1</sub> mode, which has a propagation constant

$$\beta_1 = \sqrt{k^2 - (\pi/d)^2} \quad (3.55)$$

and  $E_z$  field:  $E_z = A_1 \sin \frac{\pi y}{d} e^{-j\beta_1 z}$

which can be rewritten as  $E_z = \frac{A_1}{2j} [e^{j(\pi y/d - \beta_1 z)} - e^{-j(\pi y/d + \beta_1 z)}] \quad (3.56)$

This result is in the form of two plane waves traveling obliquely in the  $-y+z$  and  $+y+z$  directions, respectively, as shown in Figure 3.3. By comparison with the phase factor of (1.182), the angle  $\theta$  that each plane wave makes with the  $z$ -axis satisfies the relations:

$$k \sin \theta = \frac{\pi}{d} \quad k \cos \theta = \beta_1 \quad (3.57a, b)$$

so that  $(\pi/d)^2 + \beta_1^2 = k^2$ , as in (3.55), for  $f > f_c$ .  $\beta$  is real and less than  $k$ , so  $\theta$  is some angle between  $0^\circ$  and  $90^\circ$ , and the mode can be thought of as two plane waves alternately reflecting off the top and bottom plates.

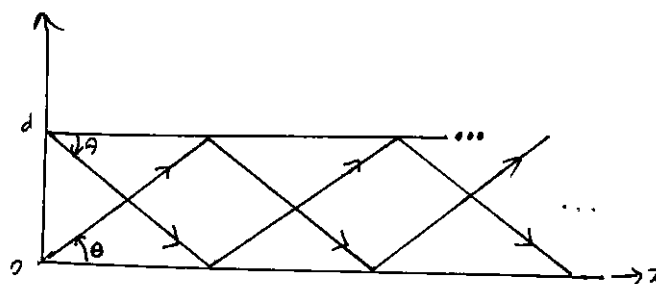


Figure 3.3 Bouncing plane wave interpretation of the TM<sub>1</sub> parallel plate waveguide mode.

The phase velocity of each plane wave along its direction of propagation ( $\theta$  direction) is  $c_{\theta}k = 1/\sqrt{\mu\epsilon}$ , which is the speed of light in the material filling the guide. However, the phase velocity of the plane waves in the  $z$  direction is  $\omega/\beta = 1/\sqrt{\mu\epsilon} \cos\theta$ , which is greater than the speed of light in the material. (This situation is analogous to ocean waves hitting a shoreline: the intersection point of the shore and an obliquely incident wave crest moves faster than the wave crest itself.) The superposition of the two plane wave fields is such that complete cancellation occurs at  $y=0$  and  $y=d$ , to satisfy the boundary condition that  $E_x=0$  at these planes. As  $\delta$  decreases to  $\theta$ ,  $\beta$  approaches zero. So that, by (3.57b),  $\theta$  approaches  $90^\circ$ . The two plane waves are then traveling up and down, with no motion in the  $+z$  direction, and no real power flow occurs in the  $z$  direction.

Attenuation due to dielectric loss can be found from (3.29). Conductor loss can be treated using the perturbation method thus,

$$\alpha_c = \frac{P_0}{2P_0} \quad (3.58)$$

where  $P_0$  is the power flow down the guide in the absence of conductor loss, as given by (3.54).  $P_0$  is the power dissipated per unit length in the two lossy conductors and can be found from (2.97) as:

$$P_0 = 2 \left( \frac{R_s}{2} \right) \int_{x=0}^W |\bar{J}_s|^2 dx = \frac{\omega^2 \epsilon^2 R_s W}{K_c^2} |A_n|^2 \quad (3.59)$$

where  $R_s$  is the surface resistivity of the conductors. Using (3.84) and (3.59) in (3.58) gives the attenuation due to conductor loss as

$$\alpha_c = \frac{2\omega R_s}{\beta d} = \frac{2\epsilon R_s}{\beta d} \text{ Np/m} \quad \text{for } n > 0 \quad (3.60)$$

As discussed previously, the TEM mode is identical to the TM<sub>0</sub> mode for the parallel plate waveguide, so the above attenuation results for the TM<sub>n</sub> mode can be used to obtain the TEM mode attenuation by letting  $n=0$ . For this case, the  $n=0$  result of (3.54) must be used in (3.58). To obtain

$$\alpha_c = \frac{R_s}{\eta d} \text{ Np/m} \quad (3.61)$$

### TE Modes

TE modes, characterized by  $E_x=0$ , can also propagate in a parallel plate waveguide. From (3.21), with  $\partial/\partial x=0$ ,  $H_z$  must satisfy the reduced wave equation.

$$\left( \frac{\partial^2}{\partial y^2} + K_c^2 \right) H_z(x,y) = 0 \quad (3.62)$$

where  $K_c = \sqrt{K^2 - \beta^2}$  is the cutoff wave number and  $H_z(x,y,z) = h_z(x,y)e^{-j\beta z}$ . The general solution to (3.62) is:

$$h_z(x,y) = A \sin k_y y + B \cos k_y y \quad (3.63)$$

The boundary conditions are that  $E_x=0$  at  $y=0, d$ ;  $E_z$  is identically zero for TE modes. From (3.19c) we have

$$E_x = \frac{-j\omega \mu}{K_c} (A \cos k_y y - B \sin k_y y) e^{-j\beta z} \quad (3.64)$$

and applying the boundary conditions shows that  $A=0$  and

$$k_y = \frac{n\pi}{d}, \quad n=1,2,3,\dots \quad (3.65)$$

as for the TM case. The final solution for  $H_z$  is then.

$$H_z(x,y) = B_n \cos \frac{n\pi y}{d} e^{-j\beta z} \quad (3.66)$$

The transverse fields can be computed from (3.19) as:

$$E_x = \frac{j\omega \mu}{K_c} B_n \sin \frac{n\pi y}{d} e^{j\beta z} \quad (3.67a)$$

$$H_y = \frac{j\beta}{K_c} B_n \sin \frac{n\pi y}{d} e^{j\beta z} \quad (3.67b)$$

$$E_y = H_x = 0 \quad (3.67c)$$

The propagation constant of the TE<sub>n</sub> mode is given as:

$$\beta = \sqrt{K^2 - \left( \frac{n\pi}{d} \right)^2}$$

which is the same as the propagation constant of the TM<sub>n</sub> mode. The cutoff frequency of the TE<sub>n</sub> mode is

$$\omega_c = \frac{n\pi}{2d\sqrt{\mu\epsilon}} \quad (3.69)$$

which is identical to that of the TM<sub>n</sub> mode. The wave impedance of the TE<sub>n</sub> mode is, from (3.22),

$$Z_{TE} = \frac{E_x}{H_y} = \frac{\omega \mu}{\beta} = \frac{k \eta}{\beta} \quad (3.70)$$

which is also identical to that of the TM<sub>n</sub> mode. The wave impedance of the TE<sub>n</sub> mode is,

which is seen to be real for propagating modes and imaginary for non-propagating modes, or cutoff modes. The phase velocity, guide wavelength, and cutoff wavelength are similar to the results obtained for the TM modes.

The power flow down the guide for a TE<sub>n</sub> mode can be calculated as:  $P_0 = \frac{1}{2} \operatorname{Re} \int_{x=0}^W \int_{y=0}^d \bar{E}_x \bar{H}_z \cdot \hat{z} dy dx = \frac{1}{2} \operatorname{Re} \int_{x=0}^W \int_{y=0}^d E_x H_z dy dx$

$$P_0 = \frac{Wkd}{4Kc^2} \frac{V}{Bn} \operatorname{Re}(\beta) \quad \text{for } n > 0 \quad (3.71)$$

which is zero if the operating frequency is below the cutoff frequency ( $\beta$  imaginary).

Note that if  $n=0$ , then  $E_x = H_z = 0$  from (3.67), and thus  $P_0 = 0$ , implying that there is no TE<sub>0</sub> mode.

Attenuation can be calculated in the same way as for the TM modes. The attenuation due to dielectric loss is given by (3.29). It is left as a problem to show that the attenuation due to conductor loss is given by:

$$\alpha_c = \frac{2Kc^2 R_s}{\omega \mu_0 d} = \frac{2Kc^2 R_s}{K \beta \eta_0 d} N_p/m \quad (3.72)$$

Figure 3.4 shows attenuation versus frequency due to conductor loss for the TEM, TM<sub>1</sub>, and TE<sub>1</sub> modes. Observe that  $\alpha_c \rightarrow \infty$  as cutoff is approached for the TM and TE modes.

Table 3.1 summarizes a number of useful results for parallel plate waveguide modes. Field lines for the TEM, TM<sub>1</sub>, and TE<sub>1</sub> modes are shown in Figure 3.5.

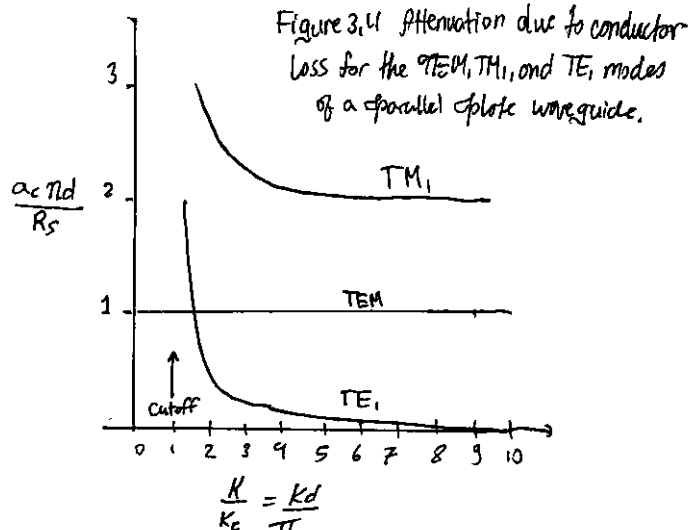


Figure 3.4 Attenuation due to conductor loss for the TEM, TM<sub>1</sub>, and TE<sub>1</sub> modes of a parallel plate waveguide.

Table 3.1 Summary of Results for Parallel plate waveguide.

Quantity	TEM mode	TM <sub>n</sub> mode	TE <sub>n</sub> mode
$K$	$\omega/\mu\epsilon$	$\omega/\mu\epsilon$	$\omega/\mu\epsilon$
$K_c$	0	$n\pi/d$	$n\pi/d$
$\beta$	$\omega/\mu\epsilon$	$\sqrt{K^2 - K_c^2}$	$\sqrt{K^2 - K_c^2}$
$\lambda_c$	$\infty$	$2\pi/k_c = 2d/n$	$2\pi/k_c = 2d/n$
$\lambda_g$	$2\pi/k$	$2\pi/\beta$	$2\pi/\beta$
$u_p$	$\omega/k = 1/\mu\epsilon$	$\omega/\beta$	$\omega/\beta$
$a_d$	$(k_m s)/2$	$(K^2 t_m s)/2\beta$	$(K^2 t_m s)/2\beta$
$a_c$	$R_s/\eta_0 d$	$2kR_s/\beta\eta_0 d$	$2k^2 R_s/(k\beta\eta_0 d)$
$E_x$	0	$iA \sin(n\pi y/d)e^{-j\beta z}$	0
$H_z$	0	0	$B \cos(2\pi y/d)e^{-j\beta z}$
$E_y$	0	0	$(i\omega\mu/k_c) B \sin(n\pi y/d)e^{-j\beta z}$
$H_x$	$(-V_0 d)/e^{-j\beta z}$	$(-i\beta/k_c) A \cos(\frac{n\pi y}{d}) e^{-j\beta z}$	0
$H_y$	$(V_0/\eta_0 d)e^{-j\beta z}$	$(i\omega\mu/k_c) A \cos(\frac{n\pi y}{d}) e^{-j\beta z}$	0
$Z$	$Z_{TEM} = \eta_0 d/\omega$	$Z_{TM} = \beta\eta_0/k$	$Z_{TE} = k\eta_0/\beta$

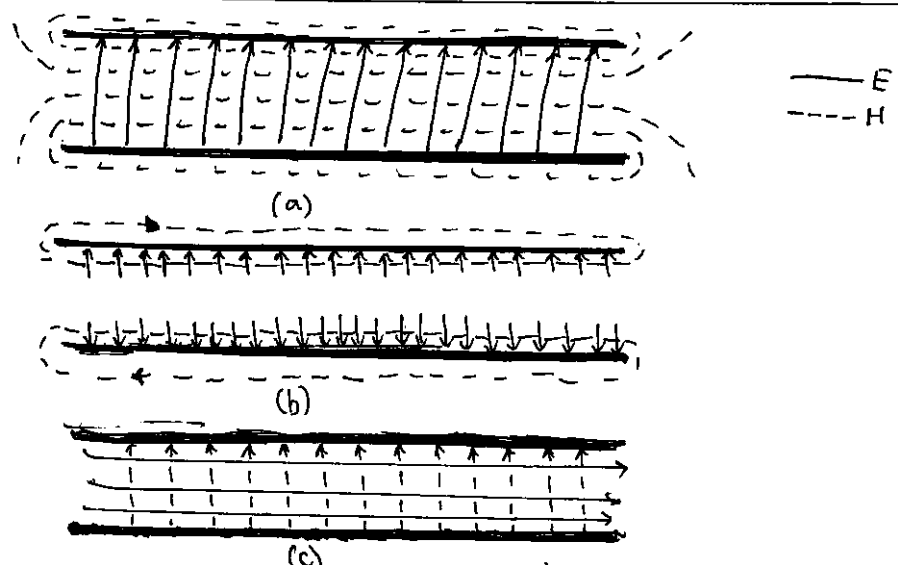


Figure 3.5 Field lines for the (a) TEM, (b) TM<sub>1</sub>, and (c) TE<sub>1</sub> modes of a parallel plate waveguide. There is no variation along the width of the waveguide.

### 3.3 Rectangular waveguide

Rectangular waveguides were one of the earliest types of transmission lines used to transport microwave signals, and they are still used for many applications. A large variety of components such as couplers, detectors, isolators, attenuators, and slotted lines are commercially available for various standard waveguide bands from 1 to 220 GHz. Figure 3.6 shows some of the standard rectangular waveguide components that are available. Because of the trend toward miniaturization and integration, most modern circuitry is fabricated using planar transmission lines using microstrips and stripline rather than waveguides. There is still, however, a need for waveguides in many places, including high power systems, millimeter wave applications, satellite systems, and precision testing applications.

#### TE Modes

The geometry of a rectangular waveguide is shown in Figure 3.7, where it is assumed that the guide is filled with a material with permittivity  $\epsilon$  and permeability  $\mu$ . It is standard convention to have the largest side of the waveguide along the  $x$ -axis, so that  $a > b$ . [Figure 3.6 photograph not included of Ka-band (WA-28) rectangular waveguide components. Clockwise from top: a variable attenuator, an E-H (magridice) junction, directional coupler, an adapter to ridge waveguide, an Eplane swept bend, an adjustable short, and a sliding matched load.]

TE waveguide modes are characterized by fields with  $E_z = 0$ , while the must satisfy the reduced wave equation of (3.21):

$$\left( \frac{\partial^2}{\partial x^2} + \frac{\partial^2}{\partial y^2} + k_c^2 \right) h_x(x,y) = 0 \quad (3.73)$$

with  $h_x(x,y,z) = h_x(x,y)e^{-j\beta z}$ ; here  $k_c = \sqrt{k^2 - \beta^2}$  is the cutoff wave number. The partial differential equation (3.73) can be solved by the separate method of separation of variables by letting

$$h_x(x,y) = X(x)Y(y) \quad (3.74)$$

and substituting into (3.73) to obtain

$$\frac{1}{X} \frac{d^2X}{dx^2} + \frac{1}{Y} \frac{d^2Y}{dy^2} + k_c^2 = 0 \quad (3.75)$$

Then, by the usual separation-of-variables argument (see Section 1.5), each of the terms in (3.75) must be equal to a constant, so we define separation constants  $k_x$  and  $k_y$  such that

$$\frac{d^2X}{dx^2} + k_x^2 X = 0 \quad , \quad \frac{d^2Y}{dy^2} + k_y^2 Y = 0 \quad (3.76 \text{ a,b})$$

and

$$k^2 + k_y^2 = k_c^2 \quad (3.77)$$

The general solution for  $h_x$  can be written as:

$$h_x(x,y) = (A \cos k_x x + B \sin k_x x)(C \cos k_y y + D \sin k_y y) \quad (3.78)$$

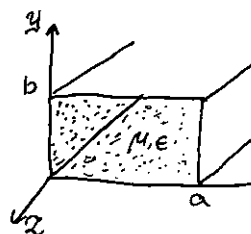


Figure 3.7 Geometry of a rectangular Waveguide

To evaluate the constants in (3.78) we must apply the boundary conditions on the electric field components tangential to the waveguide walls. That is:

$$E_x(x,y) = 0, \text{ at } y = 0, b \quad (3.79 \text{ a})$$

$$E_y(x,y) = 0, \text{ at } x = 0, a \quad (3.79 \text{ b})$$

We therefore cannot use  $h_x$  of (3.78) directly but must first use (3.19c) and (3.19d) to find  $E_x$  and  $E_y$  from  $h_x$ :

$$E_x = -\frac{j\omega \mu}{k_c^2} k_y (A \cos k_x x + B \sin k_x x)(-C \sin k_y y + D \cos k_y y)$$

$$E_y = j\omega \mu \frac{k_x}{k_c^2} k_x (A \sin k_x x + B \cos k_x x)(C \cos k_y y + D \sin k_y y)$$

Then from (3.79a) and (3.80a) we see that  $D=0$ , and  $k_y = n\pi/b$  for  $n=0,1,2,\dots$ . From (3.79b) and (3.80b) we have that  $B=0$  and  $k_x = m\pi/a$  for  $m=0,1,2,\dots$ . The final solution for  $h_x$  is then

$$H_z(x,y,z) = A_{mn} \cos(m\pi x/a) \cos(n\pi y/b) e^{-j\beta z} \quad (3.81)$$

where  $A_{mn}$  is an arbitrary amplitude constant composed of the remaining constants  $A$  and  $C$  of (3.78).

The favorite field components of the TEMs can be found using (3.19) and (3.81):

$$E_x = \frac{j\omega \mu n \pi}{k_c^2 b} A_{mn} \cos \frac{m\pi x}{a} \sin \frac{n\pi y}{b} e^{-j\beta z} \quad (3.82 \text{ a})$$

$$E_y = \frac{-j\omega \mu m \pi}{k_c^2 a} A_{mn} \sin \frac{m\pi x}{a} \cos \frac{n\pi y}{b} e^{-j\beta z} \quad (3.82 \text{ b})$$

$$H_x = \frac{jB \mu n \pi}{k_c^2 b} A_{mn} \cos \frac{m\pi x}{a} \sin \frac{n\pi y}{b} e^{-j\beta z} \quad (3.82 \text{ c})$$

$$H_y = \frac{jB \mu m \pi}{k_c^2 a} A_{mn} \cos \frac{m\pi x}{a} \sin \frac{n\pi y}{b} e^{-j\beta z} \quad (3.82 \text{ d})$$

The propagation constant is  $\beta = \sqrt{k^2 - k_c^2} = \sqrt{k^2 - \left(\frac{m\pi}{a}\right)^2 - \left(\frac{n\pi}{b}\right)^2} \quad (3.83)$

which is seen to be real corresponding to a propagating mode when

$$k > k_c = \sqrt{\left(\frac{m\pi}{a}\right)^2 + \left(\frac{n\pi}{b}\right)^2}$$

Each mode (each combination of  $m$  and  $n$ ) has a cutoff frequency  $f_{cm}$ , given by

$$f_{cm} = \frac{K_c}{2\pi\sqrt{\mu\epsilon}} = \frac{1}{2\pi\sqrt{\mu\epsilon}} \sqrt{\left(\frac{m\pi}{a}\right)^2 + \left(\frac{n\pi}{b}\right)^2} \quad (3.84)$$

The mode with the lowest cutoff frequency is called the dominant mode; because we have assumed  $a > b$ , the lowest cutoff frequency occurs for the  $TE_{10}$  ( $m=1, n=0$ ) mode!

$$f_{c10} = \frac{1}{2\pi\sqrt{\mu\epsilon}} \quad (3.85)$$

Thus the  $TE_{10}$  mode is the dominant TE mode and, as we will see, the overall dominant mode of the rectangular waveguide. Observe that the field expressions for  $\bar{E}$  and  $\bar{H}$  in (3.82) are all zero if both  $m=n=0$ ; there is no  $TE_{00}$  mode.

At the given operating frequency  $f$  only those modes having  $f > f_c$  will propagate; modes with  $f < f_c$  will lead to an imaginary  $\beta$  (or real  $\alpha$ ), meaning that all field components will decay exponentially away from the source of excitation. Such modes are referred to as cutoff modes, or evanescent modes. If more than one mode is propagating, the waveguide is said to be overmoded.

From (3.22) the wave impedance that relates the transverse electric and magnetic fields is:

$$Z_{TE} = \frac{E_x}{H_y} = \frac{-E_y}{H_x} = \frac{K_c}{\beta} \quad (3.86)$$

where  $\eta = \sqrt{\mu\epsilon}$  is the intrinsic impedance of the material filling the waveguide. Note that  $Z_{TE}$  is real when  $\beta$  is real (a propagating mode) but is imaginary when  $\beta$  is imaginary (a cutoff mode).

The guide wavelength is defined as the distance between two equal-phase planes along the waveguide and is equal to:

$$\lambda_g = \frac{2\pi}{\beta} > \frac{2\pi}{K} = \lambda \quad (3.87)$$

which is thus greater than  $\lambda$ , the wavelength of a plane wave in the medium filling the guide.

The phase velocity is  $v_p = \frac{\omega}{\beta} > \frac{\omega}{K} = \frac{1}{\sqrt{\mu\epsilon}}$  (3.88)

which is greater than  $1/\sqrt{\mu\epsilon}$ , the speed of light (plane wave) in the medium.

In the vast majority of waveguide applications the operating frequency and guide dimensions are chosen so that only the dominant  $TE_{10}$  mode will propagate. Because of the practical importance of the  $TE_{10}$  mode, we will now list the field components and derive the attenuation due to conductor loss for this case.

Specializing (3.81) and (3.82) to the  $m=1, n=0$  case gives the following results for the  $TE_{10}$  mode fields:

$$H_z = A_{10} \cos \frac{\pi x}{a} e^{-j\beta z}, \quad E_y = -\frac{j\omega\mu_0}{\pi} A_{10} \sin \frac{\pi x}{a} e^{-j\beta z}, \quad (3.89)$$

$$H_x = \frac{j\beta a}{\pi} A_{10} \sin \frac{\pi x}{a} e^{-j\beta z}, \quad E_x = E_z = H_y = 0 \quad (a, b, c, d)$$

The cutoff wave number and propagation constant for the  $TE_{10}$  mode are, respectively,

$$K_c = \frac{\pi}{a} \quad (3.90) \quad \beta = \sqrt{K_c^2 - \left(\frac{\pi}{a}\right)^2} \quad (3.91)$$

The power flow down the guide for the  $TE_{10}$  mode can be calculated as

$$\begin{aligned} P_{10} &= \frac{1}{2} \operatorname{Re} \int_{x=0}^a \int_{y=0}^b \bar{E} \times \bar{H}^* \cdot \hat{z} dy dx = \frac{1}{2} \operatorname{Re} \int_{x=0}^a \int_{y=0}^b E_y H_x^* dy dx \\ \Rightarrow P_{10} &= \frac{\omega\mu_0 a^2}{2\pi^2} \operatorname{Re}(\beta) / A_{10}^2 \int_{x=0}^a \int_{y=0}^b \sin^2 \frac{\pi x}{a} dy dx \\ \Rightarrow P_{10} &= \frac{\omega\mu_0 a^3 / A_{10}^2 b}{4\pi^2} \operatorname{Re}(\beta) \end{aligned} \quad (3.92)$$

Note that this result gives non-zero real power only when  $\beta$  is real, corresponding to a propagating mode.

Attenuation in a rectangular waveguide may occur due to the dielectric loss or conductor loss. Dielectric loss can be treated by making  $\epsilon$  complex and using the general result given in (3.29). Conductor loss is best treated using the perturbation method. The power loss per unit length due to finite wall conductivity is, from (1.181),

$$P_e = \frac{R_s}{2} \int_C |\bar{J}_s|^2 dz \quad (3.93)$$

where  $R_s$  is the surface wall resistance, and the integration contour  $C$  encloses the inside perimeter of the guide walls. There are surface currents on all four walls, but from symmetry the currents on the top and bottom wall are identical, as are the currents on the left and right side walls. So we can compute the power lost in the walls at  $x=0$  and  $y=0$  and double the sum to obtain the power loss. The surface current on the  $x=0$  (left) wall is:

$$\bar{J}_s = \bar{A} \times \bar{H}|_{x=0} = \hat{x} \times \hat{z} H_z|_{x=0} = -\hat{y} H_z|_{x=0} = -\frac{1}{2} A_{10} e^{-j\beta z} \quad (3.94a)$$

and the surface current on the  $y=0$  (bottom) wall is

$$\bar{J}_s = \hat{r} \times \bar{H}|_{y=0} = \hat{y} \times (\hat{x} H_x|_{y=0} + \hat{z} H_z|_{y=0})$$

$$\Rightarrow \bar{J}_s = -\frac{\hat{z} \beta a}{\pi} A_{10} \sin \frac{\pi x}{a} e^{-j\beta z} + \hat{x} A_{10} \cos \frac{\pi x}{a} e^{-j\beta z} \quad (3.94b)$$

Substituting (3.94) into (3.93) gives

$$\begin{aligned} P_E &= R_s \int_{y=0}^b |J_{sy}|^2 dy + R_s \int_{x=0}^a [|J_{sx}|^2 + |J_{sy}|^2] dx \\ &= R_s |A_{10}|^2 \left( b + \frac{a}{2} + \frac{\beta^2 a^3}{2\pi^2} \right) \end{aligned} \quad (3.95)$$

The attenuation due to conductor loss for the TE<sub>10</sub> mode is then

$$\begin{aligned} \alpha_c &= \frac{P_E}{2P_{10}} = \frac{2\pi^2 R_s (b + a/2 + \beta^2 a^3 / 2\pi^2)}{c \mu_0 \epsilon_0^3 b \beta} \\ \Rightarrow \alpha_c &= \frac{R_s}{a^3 b \beta k \eta} (2b\pi^2 + a^3 k^2) \text{ Np/m} \end{aligned} \quad (3.96)$$

### TM Modes

TM modes are characterized by fields with H<sub>xz</sub>=0, while E<sub>z</sub> must satisfy the reduced wave equation (3.25):

$$\left( \frac{\partial^2}{\partial x^2} + \frac{\partial^2}{\partial y^2} + k_c^2 \right) e_z(x,y) = 0 \quad (3.97)$$

with E<sub>xz</sub>(x,y,z) = e<sub>xz</sub>(x,y) e<sup>-jBz</sup> and k<sub>c</sub><sup>2</sup> = k<sup>2</sup> - β<sup>2</sup>. Equation (3.97) can be solved by the separation-of-variables procedure that was used for TE modes.

The general solution is:

$$e_z(x,y) = (A \cos k_x x + B \sin k_x x) (C \cos k_y y + D \sin k_y y) \quad (3.98)$$

The boundary conditions can be applied directly to e<sub>xz</sub>:

$$e_z(x,y) = 0, \quad \text{at } x=0, a \quad (3.99a)$$

$$e_z(x,y) = 0, \quad \text{at } y=0, b \quad (3.99b)$$

We will see that satisfaction of these conditions on e<sub>xz</sub> will lead to satisfaction of the boundary conditions for e<sub>x</sub> and e<sub>y</sub>.

Applying (3.99a) to (3.98) shows that A=0 and k<sub>x</sub>=mπ/a for m=1,2,3,...

Similarly, applying (3.99b) to (3.98) shows that C=0 and k<sub>y</sub>=nπ/b for n=1,2,3,...

The solution for E<sub>z</sub> then reduces to

$$E_z(x,y,z) = B_{mn} \sin \frac{m\pi x}{a} \sin \frac{n\pi y}{b} e^{-jBz} \quad (3.100)$$

where B<sub>mn</sub> is an arbitrary amplitude constant.

The transverse field components for the TM<sub>mn</sub> mode can be computed from (3.23) and (3.100) as:

$$E_x = \frac{-j\beta m\pi}{a k_c^2} B_{mn} \cos \frac{m\pi x}{a} \sin \frac{n\pi y}{b} e^{-jBz} \quad (3.101a)$$

$$E_y = \frac{-j\beta n\pi}{b k_c^2} B_{mn} \sin \frac{m\pi x}{a} \cos \frac{n\pi y}{b} e^{-jBz} \quad (3.101b)$$

$$H_x = \frac{j\omega m\pi}{b k_c^2} B_{mn} \sin \frac{m\pi x}{a} \frac{\cos n\pi y}{b} e^{jBz} \quad (3.101c)$$

$$H_y = \frac{-j\omega n\pi}{a k_c^2} B_{mn} \cos \frac{m\pi x}{a} \sin \frac{n\pi y}{b} e^{-jBz} \quad (3.101d)$$

As for the TE modes the propagation constant is

$$\beta = \sqrt{k^2 - k_c^2} = \sqrt{k^2 - \left(\frac{m\pi}{a}\right)^2 - \left(\frac{n\pi}{b}\right)^2} \quad (3.102)$$

and is real for propagating modes and imaginary cut-off modes. The cutoff frequencies for the TM<sub>mn</sub> modes are also the same as those of the TEM<sub>mn</sub> modes, as given in (3.84). The guide wavelength and phase velocity for TM modes are also the same as those for TE modes.

Observe that the field expressions for E and H in (3.101) are identically zero if either m or n is zero. Thus there is no TM<sub>00</sub>, TM<sub>01</sub>, or TM<sub>10</sub> mode, and the lowest order TM mode to propagate is (lowest f<sub>c</sub>) is the TM<sub>11</sub> mode, having a cutoff frequency of:  $f_{c,11} = \frac{1}{2\pi k c} \sqrt{\left(\frac{\pi}{a}\right)^2 + \left(\frac{\pi}{b}\right)^2}$  (3.103)

which is seen to be larger than f<sub>c,10</sub>, the cutoff frequency of the TE<sub>10</sub> mode.

The wave impedance relating the transverse electric and magnetic fields is, from (3.26),  $Z_{TM} = \frac{E_x}{H_y} = \frac{B\eta}{k} = \frac{B\eta}{k} \quad (3.104)$

Attenuation due to dielectric loss is computed in the same way as for TE modes with the same result. The calculation of attenuation due to conductor loss is left as a problem for the reader; Figure 3.8 shows attenuation versus frequency for some TE and TM modes in a rectangular waveguide. Table 3.2 summarises results for TE and TM wave propagation in rectangular waveguides, and figure 3.9 shows the field lines of the lowest order TE and TM modes.

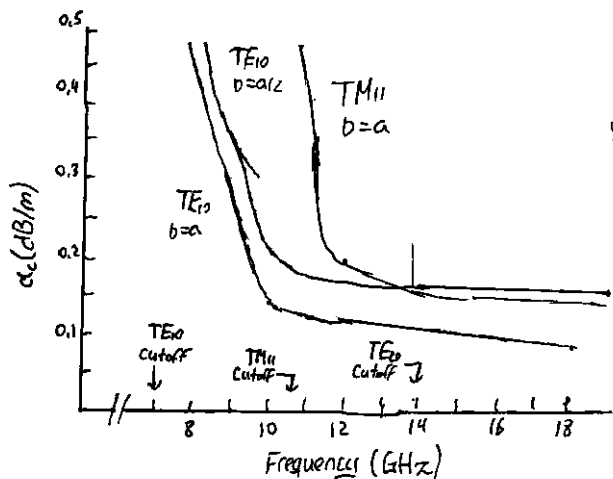


Figure 3.8 Attenuation of various modes in a Rectangular waveguide with  $a = 8.0 \text{ cm}$ .

Table 3.2 Summary of Results for Rectangular waveguide

Quantity	TEM <sub>mn</sub> Mode	TM <sub>mnn</sub> mode
$K$	$\omega/\sqrt{\mu\epsilon}$	$\omega/\sqrt{\mu\epsilon}$
$K_c$	$\sqrt{(m\pi/a)^2 + (n\pi/b)^2}$	$\sqrt{(m\pi/a)^2 + (n\pi/b)^2}$
$\beta$	$\sqrt{K^2 - K_c^2}$	$\sqrt{K^2 - K_c^2}$
$\lambda_c$	$\frac{2\pi}{K_c}$	$\frac{2\pi}{K_c}$
$\lambda_{\perp}$	$\frac{2\pi}{\beta}$	$\frac{2\pi}{\beta}$
$\nu_p$	$\frac{c}{\beta}$	$\frac{c}{\beta}$
$\alpha_d$	$\frac{K^2 \tan \delta}{2\beta}$	$\frac{K^2 \tan \delta}{2\beta}$
$E_x$	0	$B \sin \frac{m\pi x}{a} \sin \frac{n\pi y}{b} e^{-j\beta z}$
$H_z$	$A \cos \frac{m\pi x}{a} \cos \frac{n\pi y}{b} e^{-j\beta z}$	0
$E_x$	$\frac{j\omega \mu_0}{K_c^2 b} A \cos \frac{m\pi x}{a} \sin \frac{n\pi y}{b} e^{-j\beta z}$	$-\frac{j\beta m\pi}{K_c^2 a} B \cos \frac{m\pi x}{a} \sin \frac{n\pi y}{b} e^{-j\beta z}$
$E_y$	$-\frac{j\omega \mu_0}{K_c^2 a} A \sin \frac{m\pi x}{a} \cos \frac{n\pi y}{b} e^{-j\beta z}$	$\frac{j\beta n\pi}{K_c^2 b} B \sin \frac{m\pi x}{a} \cos \frac{n\pi y}{b} e^{-j\beta z}$
$H_x$	$\frac{j\beta n\pi}{K_c^2 a} A \sin \frac{m\pi x}{a} \cos \frac{n\pi y}{b} e^{-j\beta z}$	$-\frac{j\omega \mu_0}{K_c^2 b} B \sin \frac{m\pi x}{a} \cos \frac{n\pi y}{b} e^{-j\beta z}$
$H_y$	$\frac{j\beta n\pi}{K_c^2 b} A \cos \frac{m\pi x}{a} \sin \frac{n\pi y}{b} e^{-j\beta z}$	$-\frac{j\omega \mu_0}{K_c^2 a} B \cos \frac{m\pi x}{a} \sin \frac{n\pi y}{b} e^{-j\beta z}$
$Z$		$Z_{TE} = \frac{4\pi}{\beta}$
		$Z_{TM} = \frac{\beta n}{K}$

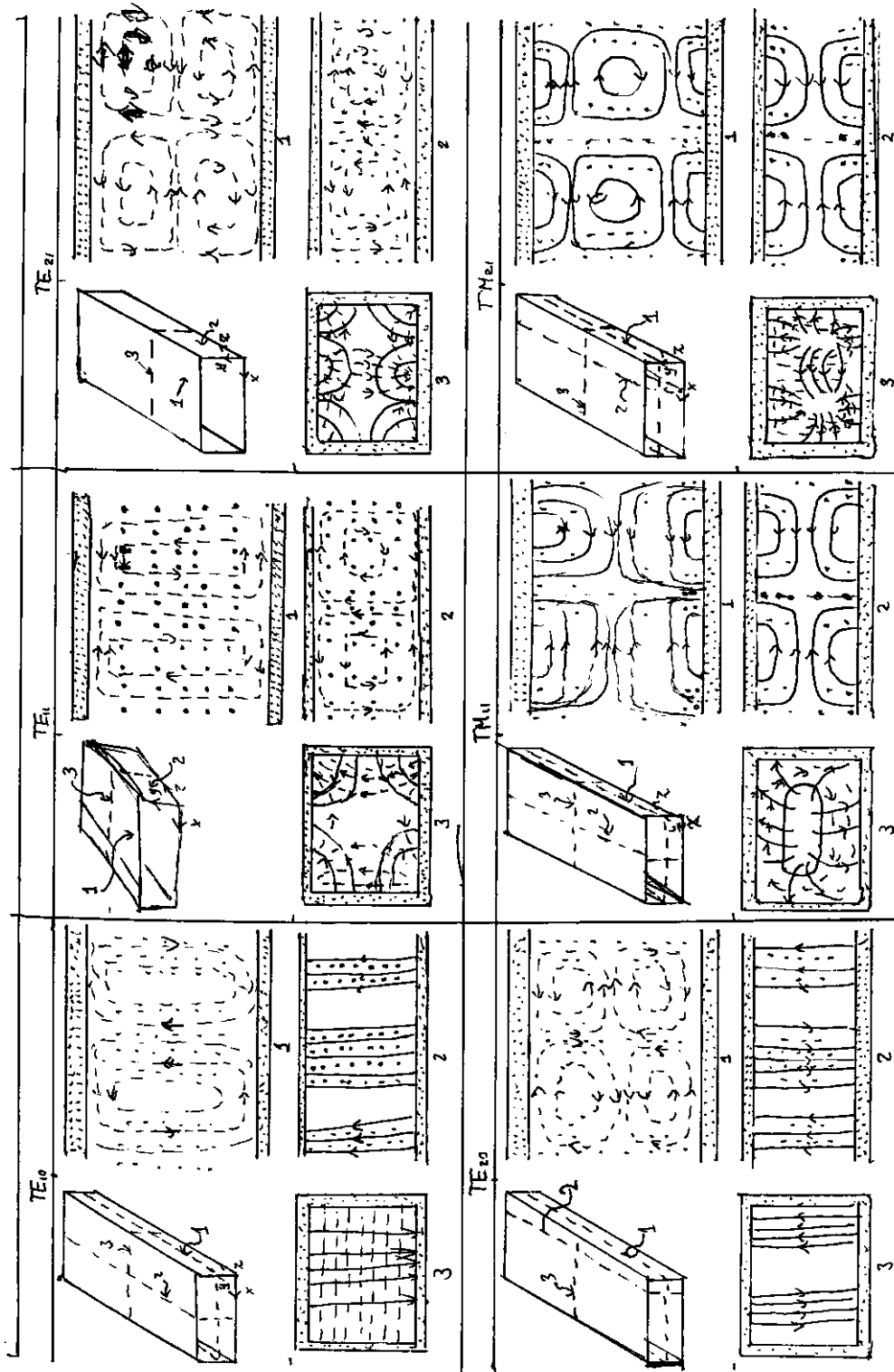


Figure 3.9 Field lines for some low order modes of a Rectangular Waveguide

**Example 3.1 Characteristics of a Rectangular Waveguide**  
 Consider a length of Teflon-filled, copper K-bond waveguide having dimensions  $a = 1.07\text{ cm}$  and  $b = 0.43\text{ cm}$ . Find the cutoff frequencies of the first five propagating modes. If the operating frequency is 15 GHz, find the attenuation due to dielectric and copper losses.

**Solution**

From Appendix G, for Teflon,  $\epsilon_r = 2.08$  and  $\tan \delta = 0.0004$ . From (3.84) the cutoff frequencies are given by

$$f_{c,mn} = \frac{c}{2\pi\sqrt{\epsilon_r}} \sqrt{\left(\frac{m\pi}{a}\right)^2 + \left(\frac{n\pi}{b}\right)^2}$$

Computing  $f_c$  for the first few values of  $m$  and  $n$  gives the following results:

mode	$m$	$n$	$f_c$ (GHz)
TE	1	0	9.72
TE	2	0	19.44
TE	0	1	24.19
TE, TM	1	1	26.07
TE, TM	2	1	31.03

Thus the TE<sub>10</sub>, TE<sub>20</sub>, TE<sub>01</sub>, TE<sub>11</sub>, and TM modes will be the first five modes to propagate.

At 15 GHz,  $k = 453.1\text{ m}^{-1}$ , and the propagation constant for the TE<sub>10</sub> mode is

$$\beta = \sqrt{\left(\frac{2\pi f \sqrt{\epsilon_r}}{a}\right)^2 - \left(\frac{\pi}{a}\right)^2} = \sqrt{k^2 - \left(\frac{\pi}{a}\right)^2} = 345.1\text{ m}^{-1}$$

From (3.29), the attenuation due to dielectric loss is

$$\alpha_d = \frac{K^2 \tan \delta}{2\beta} = 0.119 \text{ Np/m} = 1.03 \text{ dB/m}$$

The surface resistivity of the copper walls is ( $\sigma = 5.8 \cdot 10^7 \text{ S/m}$ )

$$R_s = \sqrt{\frac{\omega M_0}{2\sigma}} = 203.2 \Omega$$

and the attenuation due to conductor loss, (from 3.96) is

$$\alpha_c = \frac{R_s}{\sigma b \beta K \eta} (2b\pi^2 + a^3 k^2) = 0.050 \text{ Np/m} = 0.434 \text{ dB/m}$$

### TEM Modes of Partially Loaded Waveguide

The previous results apply to an empty waveguide as well as one filled with a homogeneous dielectric or magnetic material, but in some cases of practical interest (such as impedance matching or phase-shifting sections) a waveguide is used with a partial dielectric filling.

In this case an additional set of boundary conditions are introduced at the material interface, necessitating a new analysis. To illustrate the technique we will consider the TEM modes of a rectangular waveguide that is partially filled with a dielectric slab, as shown in Figure 3.10.

The analysis still follows the basic procedure outlined at the end of Section 3.1.

Since the geometry is uniform in the  $y$ -direction and  $n=0$ , the TEM modes have no  $y$  dependence. Then the wave equation of (3.21) for  $h_z$  can be written separately for the dielectric and air regions as:

$$\left( \frac{\partial^2}{\partial x^2} + K_d^2 \right) h_z = 0 \quad \text{for } 0 \leq x \leq t$$
(3.105a)

$$\left( \frac{\partial^2}{\partial x^2} + K_a^2 \right) h_z = 0 \quad \text{for } t \leq x \leq a$$
(3.105b)

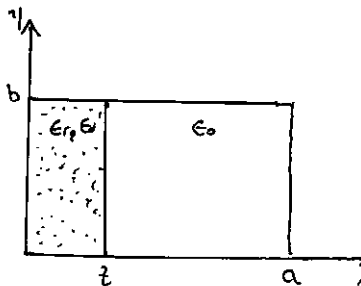


Figure 3.10 Geometry of a partially loaded rectangular waveguide.

where  $K_d$  and  $K_a$  are the cutoff wave numbers for the dielectric and air regions defined as follows:

$$\beta_d = \sqrt{\epsilon_r K_0^2 - K_d^2} \quad (3.106a), \quad \beta_a = \sqrt{K_0^2 - K_a^2} \quad (3.106b)$$

These relations incorporate the fact that the propagation constant,  $\beta$ , must be the same in both regions to ensure impedance matching (see Section 1.8) of the fields along the interface at  $x=t$ .

The solutions to (3.105) can be written as:

$$h_x = \begin{cases} A \cos kx + B \sin kx & \text{for } 0 \leq x \leq t \\ C \cos ka(a-x) + D \sin ka(a-x) & \text{for } t \leq x \leq a \end{cases} \quad (3.107)$$

where the form of the solution for  $h_x(x,a)$  was chosen to simplify the evaluation of boundary conditions at  $x=a$ .

We need  $E_y$  and  $H_z$  electric and magnetic field components to apply the boundary conditions at  $x=0$ ,  $t$ , and  $a$ .  $E_z = 0$  for TE modes, and  $H_y = 0$  since  $\nabla \cdot H = 0$ .  $E_y$  is found from (3.104) as:

$$E_y = \begin{cases} \frac{i\omega \mu_0}{k_a} (-A \sin kx + B \cos kx) & \text{for } 0 \leq x \leq t \\ \frac{i\omega \mu_0}{k_a} (C \sin ka(a-x) - D \cos ka(a-x)) & \text{for } t \leq x \leq a \end{cases} \quad (3.108)$$

To satisfy the boundary condition that  $E_y=0$  at  $x=0$  and  $x=a$  requires that  $B=D=0$ . We next enforce continuity of tangential fields ( $E_y, H_z$ ) at  $x=t$ . Equations (3.107) and (3.108) then give the following:

$$-\frac{A}{k_a} \sin kt = \frac{C}{k_a} \sin ka(a-t)$$

$$A \cos kt = C \cos ka(a-t)$$

Because this is a homogeneous set of equations, the determinant must vanish in order to have a nontrivial solution. Thus:

$$ka \tan kt + kd \tan ka(a-t) = 0 \quad (3.109)$$

Using (3.106) allows  $k_a$  and  $k_d$  to be expressed in terms of  $\beta$ , so (3.109) can be solved numerically for  $\beta$ . There is an infinite number of solutions to (3.109), corresponding to the propagation constants of the TE<sub>mo</sub> modes.

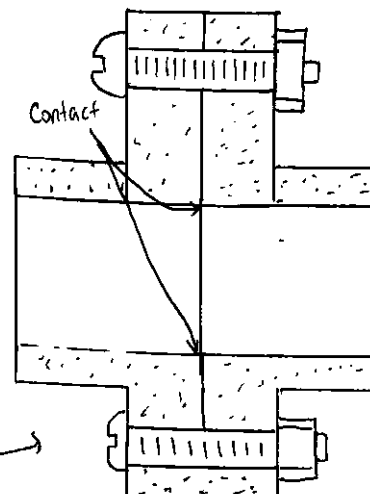
This technique can be applied to a multitude of waveguide geometries involving dielectric or magnetic material inhomogeneities, such as the surface waveguide of Section 3.6 or the ferro-loaded waveguide of Section 9.3. In some cases, however, it will be impossible to satisfy all the necessary boundary conditions with only TE or TM type modes and a hybrid combination of both types may be required.

### Point of Interest : Waveguide Flanges

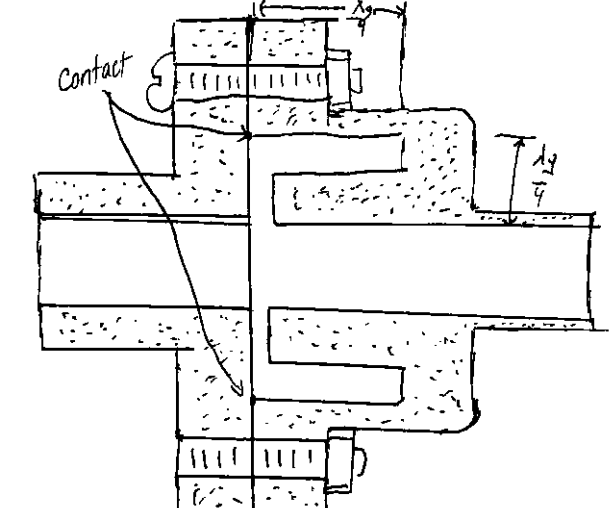
There are two commonly used waveguide flanges: the cover flange and the choke flange. As shown in the accompanying figure, two waveguides with cover-type flanges can be bolted together to form a contacting joint. To avoid reflections and resistive losses at this joint it is necessary that the contacting surfaces be clean, smooth and square because RF currents must flow across the discontinuity. In high power applications voltage breakdown may occur at an impact junction. Otherwise, the simplicity of the cover-to-cover connection makes it preferable for general use. The SWR from such a joint is typically less than 1.03.

An alternative waveguide connection uses a cover flange against a choke flange, as shown in the figure. The choke flange is machined to form an effective radial transmission line in the narrow gap between the flanges. Another  $19/16$  line is formed by a circular axial groove in the choke flange. Then the short circuit at the right-hand end of this groove is transformed into an open circuit at the contact point of the flanges. Any resistance in this contact is in series with an infinite (or very large) impedance and thus has little effect. The high impedance is transformed back into a short circuit (or very low impedance) at the edges of the waveguides to provide an effective low-resistance path for current flow across the joint. Because there is a negligible voltage drop across the ohmic contact between the flanges, voltage breakdown is avoided. Thus, the cover-to-choke connection is more useful in high power applications. The SWR for this joint is typically less than 1.05 but is more frequency dependent than that of the cover-to-cover joint.

Cover-to-cover connection



Cover-to-choke connection



### 3.4 Circular waveguide

A hollow, round metal pipe also supports TE and TM waveguide modes. Figure 3.11 shows the geometry of a circular waveguide, with inner radius  $a$ . Because cylindrical geometry is involved, it is the appropriate way to employ cylindrical coordinates.

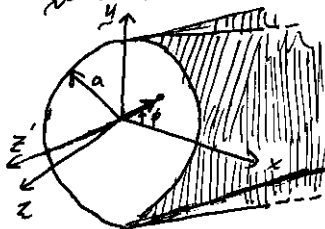


Fig 3.11 Geometry of a circular waveguide.

As in the rectangular coordinate case, the transverse fields in cylindrical coordinates can be derived from  $E_z$  or  $H_z$  field components for TE and TM modes, respectively.

Paralleling the development of Section 3.1, we can derive the cylindrical coordinates of the transverse fields from the longitudinal components

$$\text{as: } E_p = -\frac{j}{Kc^2} \left( \beta \frac{\partial E_z}{\partial p} + \frac{w_0}{P} \frac{\partial H_z}{\partial \phi} \right) \quad (3.110a)$$

$$E_\phi = -\frac{j}{Kc^2} \left( \beta \frac{\partial E_z}{\partial \phi} - \beta \frac{\partial H_z}{\partial p} \right) \quad (3.110b)$$

$$H_p = \frac{-j}{Kc^2} \left( w_0 \frac{\partial E_z}{\partial p} - \beta \frac{\partial H_z}{\partial \phi} \right) \quad (3.110c)$$

$$H_\phi = \frac{-j}{Kc^2} \left( w_0 \frac{\partial E_z}{\partial \phi} + \beta \frac{\partial H_z}{\partial p} \right) \quad (3.110d)$$

where  $Kc^2 = K^2 - \beta^2$ , and  $e^{-j\beta z}$  propagation has been assumed. For  $e^{+j\beta z}$  propagation replace  $\beta$  with  $-\beta$  in all expressions.

#### TE Modes

For TE Modes,  $E_z = 0$ , and  $H_z$  is a solution to the wave equation:

$$\nabla^2 H_z + K^2 H_z = 0$$

If  $H_z(p, \phi, z) = h_z(p, \phi) e^{-j\beta z}$ , (3.111) can be expressed in cylindrical coordinates as:

$$\left( \frac{\partial^2}{\partial p^2} + \frac{1}{p} \frac{\partial}{\partial p} + \frac{1}{p^2} \frac{\partial^2}{\partial \phi^2} + K_c^2 \right) h_z(p, \phi) = 0$$

As before, we apply the previous method of separation of variables. Thus, let

$$h_z(p, \phi) = R(p) P(\phi) \quad (3.113)$$

and substitute into (3.112) to obtain

$$\frac{1}{R} \frac{d^2 R}{dp^2} + \frac{1}{pR} \frac{dR}{dp} + \frac{1}{p^2 R} \frac{d^2 P}{d\phi^2} + K_c^2 = 0$$

or

$$\frac{P^2}{R} \frac{d^2 R}{dp^2} + \frac{P}{R} \frac{dR}{dp} + P^2 K_c^2 = -\frac{1}{p} \frac{d^2 P}{d\phi^2} \quad (3.114)$$

The left side of this equation depends only on  $p$  (not  $\phi$ ), while the right side depends only on  $\phi$ . Thus each side must be equal to a constant, which we will call  $k_\phi^2$ .

Then,  $\frac{-1}{P} \frac{d^2 P}{dp^2} = k_\phi^2 \quad \text{or} \quad \frac{d^2 P}{dp^2} + k_\phi^2 P = 0 \quad (3.115)$

In addition,  $\frac{P^2 d^2 R}{dp^2} + P \frac{dR}{dp} + (P^2 K_c^2 - k_\phi^2) R = 0 \quad (3.116)$

The general solution to (3.115) is

$$P(\phi) = A \sin k_\phi \phi + B \cos k_\phi \phi \quad (3.117)$$

Because the solution to  $h_z$  must be periodic in  $\phi$  [i.e.,  $h_z(p, \phi) = h_z(p, \phi + 2\pi n)$ ],  $k_\phi$  must be an integer,  $n$ . Thus (3.117) becomes:  $P(\phi) = A \sin n\phi + B \cos n\phi \quad (3.118)$  and (3.116) becomes:  $\frac{P^2 d^2 R}{dp^2} + P \frac{dR}{dp} + (P^2 K_c^2 - n^2) R = 0 \quad (3.119)$

which is recognized as Bessel's differential equation. The solution is:

$$R(p) = C J_n(K_c p) + D Y_n(K_c p) \quad (3.120)$$

where  $J_n(x)$  and  $Y_n(x)$  are the Bessel functions of the first and second kinds, respectively. Because  $Y_n(K_c p)$  becomes infinite at  $p=0$ , this term is physically unacceptable for a circular waveguide, so  $D=0$ . The solution for  $h_z$  can be simplified to:  $h_z(p, \phi) = (A \sin n\phi + B \cos n\phi) J_n(K_c p) \quad (3.121)$

where the constant  $B$  of (3.120) has been absorbed into the constants  $A$  and  $C$  of (3.121). We must still determine the cutoff wave number  $K_c$ , which we can do by enforcing the boundary condition that  $E_{tan}=0$  on the waveguide wall. Because  $E_z=0$ , we must have that

$$E_\phi(p, \phi) = 0 \quad \text{at } p=a \quad (3.122)$$

From (3.110b), we find that  $E_\phi$  from  $H_z$  as:

$$E_\phi(p, \phi, z) = \frac{j w_0}{Kc} (A \sin n\phi + B \cos n\phi) J_n'(K_c p) e^{-j\beta z} \quad (3.123)$$

where the notation  $J_n'(K_c p)$  refers to the derivative of  $J_n$  with respect to its argument. For  $E_\phi$  to vanish at  $p=a$ , we must have that

$$J_n'(K_c a) = 0 \quad (3.124)$$

If the roots of  $J_n'(x)$  are defined as  $p'_{nm}$ , so that  $J_n'(p'_{nm})=0$ , where  $p'_{nm}$  is the  $m^{\text{th}}$  root of  $J_n'$ , then  $K_c$  must have the value

$$K_{cm} = \frac{p'_{nm}}{a} \quad (3.125)$$

Values of  $p'_{nm}$  are given in mathematical tables; the first few listed in Table 3.3.

TABLE 3.3 of  $p'_{nm}$  for TE Modes of a Circular Waveguide

$n$	$p'_{11}$	$p'_{12}$	$p'_{13}$
0	3.832	7.016	10.174
1	1.841	5.331	8.536
2	3.254	6.706	9.970

The TE<sub>nm</sub> modes are thus defined by the cutoff wave number  $k_{c,nm} = P'_{nm}/a$ , where  $n$  refers to the number of circumferential ( $\phi$ ) variations and  $m$  refers to the number of radial ( $\rho$ ) variations. The propagation constant of the TE<sub>nm</sub> mode is

$$\beta_{nm} = \sqrt{k_c^2 - K_c^2} = \sqrt{k_c^2 - \left(\frac{P'_{nm}}{a}\right)^2} \quad (3.126)$$

with a cutoff frequency of  $f_{c,nm} = \frac{k_c}{2\pi n \mu E} = \frac{P'_{nm}}{2\pi a \mu E}$  (3.127)

The first TE mode to propagate is the mode with the smallest  $\beta_{nm}$ , which from Table 3.3 is seen to be the TE<sub>11</sub> mode. This mode is therefore the dominant circular waveguide mode and the one most frequently used. Because  $m > 1$ , there is no TE<sub>10</sub> mode, but there is a ~~TE<sub>01</sub>~~ TE<sub>01</sub> mode.

The transverse field components are, from (3.110) and (3.121)

$$E_\rho = \frac{-j\omega \mu n}{K_c^2 \rho} (A \cos n\phi - B \sin n\phi) J_n(K_c \rho) e^{-jBz} \quad (3.128A)$$

$$E_\phi = \frac{j\omega \mu}{K_c} (A \sin n\phi + B \cos n\phi) J_n'(K_c \rho) e^{-jBz} \quad (3.128B)$$

$$H_\rho = \frac{-j\beta}{K_c} (A \sin n\phi + B \cos n\phi) J_n'(K_c \rho) e^{-jBz} \quad (3.128C)$$

$$H_\phi = -\frac{j\beta n}{K_c^2 \rho} (A \cos n\phi - B \sin n\phi) J_n(K_c \rho) e^{-jBz} \quad (3.128D)$$

The waveguide impedance:  $Z_{TE} = \frac{E_\phi}{H_\phi} = -\frac{E_\phi}{H_\rho} = \frac{\eta k}{\beta}$

In the above solutions there are two remaining arbitrary amplitude constants,  $A$  &  $B$ . These constants control the amplitude of the  $\sin n\phi$  and  $\cos n\phi$  terms, which are independent. That is, because of the azimuthal symmetry of the circular waveguide, both the  $\sin n\phi$  and  $\cos n\phi$  represent valid solutions, and may both be present in a specific problem. The actual amplitude of these terms will depend on the excitation of the waveguide. From a different viewpoint, the coordinate system can be rotated about the  $z$ -axis to obtain one with either  $A=0$  or  $B=0$ .

Now consider the dominant TE<sub>11</sub> mode with an excitation such that  $B=0$ . The fields can be written as:

$$H_z = A \sin \phi J_1(K_c \rho) e^{-jBz}, \quad E_\rho = \frac{-j\omega \mu}{K_c^2 \rho} A \cos \phi J_1(K_c \rho) e^{-jBz} \quad (3.130 a, b)$$

$$E_\phi = \frac{j\omega \mu}{K_c} A \sin \phi J_1'(K_c \rho) e^{-jBz}, \quad H_\rho = \frac{-j\beta}{K_c} A \sin \phi J_1'(K_c \rho) e^{-jBz} \quad (3.130 c, d)$$

$$H_\phi = \frac{-j\beta}{K_c^2 \rho} A \cos \phi J_1(K_c \rho) e^{-jBz}, \quad E_z = 0 \quad (3.130 e, f)$$

The power slow down the guide can be computed as:

$$\begin{aligned} P_0 &= \frac{1}{2} \operatorname{Re} \int_{\rho=0}^a \int_{\phi=0}^{2\pi} \vec{E} \times \vec{H}^* \cdot \hat{z} \rho d\phi d\rho = \frac{1}{2} \operatorname{Re} \int_{\rho=0}^a \int_{\phi=0}^{2\pi} (E_\rho H_\phi^* - E_\phi H_\rho^*) \rho d\phi d\rho \\ \Rightarrow P_0 &= \frac{\omega \mu |A|^2 \operatorname{Re}(B)}{2 K_c^4} \int_{\rho=0}^a \int_{\phi=0}^{2\pi} \left[ \frac{1}{\rho^2} \cos^2 \phi J_1^2(K_c \rho) + K_c^2 \sin^2 \phi J_1'^2(K_c \rho) \right] \rho d\phi d\rho \\ \Rightarrow P_0 &= \frac{\pi \omega \mu |A|^2 \operatorname{Re}(B)}{2 K_c^4} \int_{\rho=0}^a \left[ \frac{1}{\rho} J_1^2(K_c \rho) + \rho K_c^2 J_1'^2(K_c \rho) \right] d\rho \\ \Rightarrow P_0 &= \frac{\pi \omega \mu |A|^2 \operatorname{Re}(B)}{4 K_c^4} (P_{11}'^2 - 1) J_1^2(K_c a) \end{aligned} \quad (3.131)$$

which is seen to be non-zero only when  $B$  is real, corresponding to the propagating mode. (The required integral for this result is given in appendix C.)

Attenuation due to dielectric loss is given by (3.29). The attenuation due to a lossy waveguide conductor can be found by computing the power loss per unit length ~~of~~ of guide:

$$\begin{aligned} P_L &= \frac{R_s}{2} \int_{\phi=0}^{2\pi} |\vec{J}_S|^2 a d\phi = \frac{R_s}{2} \int_{\phi=0}^{2\pi} (|H_\phi|^2 + |H_z|^2) a d\phi = \\ \dots &= \frac{|A|^2 R_s}{2} \int_{\phi=0}^{2\pi} \left( \frac{\beta^2}{K_c^4 a^2} \cos^2 \phi + \sin^2 \phi \right) J_1^2(K_c a) a d\phi \\ \Rightarrow P_L &= \frac{\pi |A|^2 R_s a}{2} \left( 1 + \frac{\beta^2}{K_c^4 a^2} \right) J_1^2(K_c a) \end{aligned} \quad (3.132)$$

The attenuation constant is then:

$$\alpha_c = \frac{P_L}{2 P_0} = \frac{R_s (K_c^4 a^2 + \beta^2)}{2 \eta k \beta a (P_{11}'^2 - 1)} \quad (3.133)$$

### TM Modes

For the TM modes of the circular waveguide, we must solve for  $E_z$  from the wave equation in cylindrical coordinates:

$$\left( \frac{\partial^2}{\partial p^2} + \frac{1}{p} \frac{\partial}{\partial p} + \frac{1}{p^2} \frac{\partial^2}{\partial \phi^2} + K_c^2 \right) E_z = 0 \quad (3.134)$$

where  $E_z(p, \phi, z) = e_z(p, \phi) e^{-jBz}$  and  $K_c^2 = K^2 - \beta^2$ . Because this equation is identical to (3.107), the general solutions are the same. Thus, from (3.121),

$$e_z(p, \phi) = (A \sin n\phi + B \cos n\phi) J_n(K_c p) \quad (3.135)$$

TABLE 3.4 Values of  $P_m$  for TM modes of a Circular waveguide

$n$	$P_{n1}$	$P_{n2}$	$P_{n3}$
0	2.495	5.529	8.657
1	3.832	7.016	10.174
2	5.135	8.417	11.620

The difference between the TE solution and the present solution is that the boundary conditions can now be applied directly to  $E_z$  of (3.135) since  $E_z(\rho, \phi) = 0$  at  $\rho = a$  (3.136)

Thus we must have:  $J_n(H_c a) = 0$  (3.137)

or  $H_c = P_{nm}/a$  (3.138)

where  $P_{nm}$  is the  $m^{\text{th}}$  root of  $J_n(x)$ , that is,  $J_n(P_{nm})=0$ . Values of  $P_{nm}$  are given in mathematical tables; the first few values listed in Table 3.4.

The propagation constant of the  $TM_{nm}$  mode is

$$\beta_{nm} = \sqrt{k_c^2 - k_z^2} = \sqrt{k^2 - (P_{nm}/a)^2} \quad (3.139)$$

and the cutoff frequency is:

$$f_{cm} = \frac{K_c}{2\pi\sqrt{\mu\varepsilon}} = \frac{P_{nm}}{2\pi a\sqrt{\mu\varepsilon}} \quad (3.140)$$

Thus, the first TM mode to propagate is the  $TM_{01}$  mode, with  $P_{01} = 2.495$ . Because this is greater than  $P_{11} = 1.841$  for the lowest order TE<sub>11</sub> mode, the TE<sub>11</sub> mode is the dominant mode for the circular waveguide. As with the TE modes,  $m \geq 1$ , so there is no TM<sub>00</sub> mode.

From (3.110), the transverse fields can be derived as:

$$E_p = \frac{-j\beta}{K_c} (A \sin n\phi + B \cos n\phi) J_n'(K_c \rho) e^{-j\beta z} \quad (3.141a)$$

$$E_\phi = \frac{-j\beta n}{K_c \rho} (A \cos n\phi - B \sin n\phi) J_n(K_c \rho) e^{-j\beta z} \quad (3.141b)$$

$$H_p = \frac{j\omega \epsilon n}{K_c \rho} (A \cos n\phi - B \sin n\phi) J_n(K_c \rho) e^{-j\beta z} \quad (3.141c)$$

$$H_\phi = \frac{-j\omega \epsilon}{K_c} (A \sin n\phi + B \cos n\phi) J_n'(K_c \rho) e^{-j\beta z} \quad (3.141d)$$

The wave impedance is:

$$Z_{mn} = \frac{E_p}{H_\phi} = \frac{E_\phi}{H_p} = \frac{\eta \beta}{k} \quad (3.142)$$

Calculation of the attenuation for TM modes is left as a problem.

Figure 3.12 shows the attenuation due to conductor loss versus frequency for various modes of a circular waveguide. Observe that the attenuation of the TE<sub>01</sub> mode decreases to a small value with increasing frequency.

This property makes the TE<sub>01</sub> mode of interest for low loss transmission over long distances. Unfortunately this mode is not the dominant mode in a circular waveguide, so in practice power can be lost from the TE<sub>01</sub> modes to lower order propagating modes.

Figure 3.13 shows the relative cutoff frequencies of the TE and TM modes,

and Table 3.5 summarizes results for wave propagation in circular waveguides.

Field lines for some of the lowest order TE and TM modes are shown in Figure 3.14.

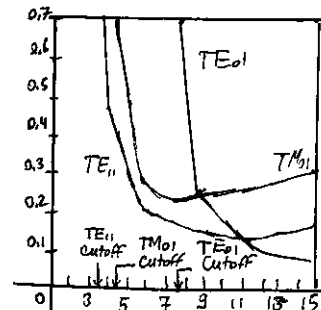


Figure 3.12 Attenuation of various modes in a circular waveguide.

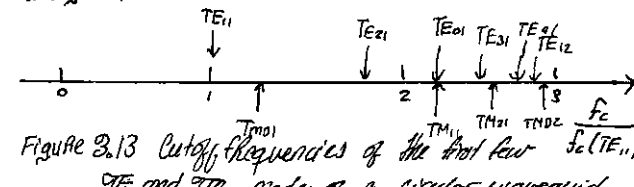


Figure 3.13 Cutoff frequencies of the first few  $\frac{f_{cm}}{f_{c,TE_{11}}}$  TE and TM modes of a circular waveguide relative to a cutoff frequency of the dominant TE<sub>11</sub> mode.

Example 3.2 characteristics of a circular waveguide

Find the cutoff frequencies of the first two propagating modes of a Teflon-filled circular waveguide with  $a = 0.35\text{cm}$ . If the interior guide is gold plated, calculate the overall loss in dB for a 30cm length operating at 14 GHz.

Solution

From Figure 3.13, the first two propagating modes of a circular waveguide are the TE<sub>11</sub> and TM<sub>01</sub> modes. The cutoff frequencies can be found using (3.127) and (3.140):

$$TE_{11}: f_c = \frac{P_{11} c}{2\pi a \sqrt{\epsilon_r}} = \frac{1.84 (3 \cdot 10^8)}{2\pi (0.0035) \sqrt{2.08}} = 12.12 \text{ GHz}$$

$$TM_{01}: f_c = \frac{P_{01} c}{2\pi a \sqrt{\epsilon_r}} = \frac{2.495 (3 \cdot 10^8)}{2\pi (0.0035) \sqrt{2.08}} = 15.92 \text{ GHz}$$

TABLE 3.5 Summary of Results for Circular Waveguide

Quantity	TE <sub>nm</sub> Mode	TM <sub>nm</sub> Mode
$\omega$	$\omega\sqrt{\mu\epsilon}$	$\omega\sqrt{\mu\epsilon}$
$H_c$	$P_{nm}/\alpha$	$P_{nm}/\alpha$
$\beta$	$\sqrt{K^2 - K_c^2}$	$\sqrt{K^2 - K_c^2}$
$\lambda_c$	$2\pi/K_c$	$2\pi/K_c$
$\lambda_g$	$2\pi/\beta$	$2\pi/\beta$
$v_p$	$\omega/\beta$	$\omega/\beta$
$\alpha_d$	$K^2 \tan \delta / 2\beta$	$K^2 \tan \delta / 2\beta$
$E_x$	0	$(A \sin n\phi + B \cos n\phi) J_n(K_c p) e^{-j\beta z}$
$H_z$	$(A \sin n\phi + B \cos n\phi) J_n'(K_c p) e^{-j\beta z}$	0
$E_y$	$\frac{-j\omega n}{K_c p} (A \cos n\phi - B \sin n\phi) J_n(K_c p) e^{-j\beta z}$	$\frac{-j\beta}{K_c} (A \sin n\phi + B \cos n\phi) J_n'(K_c p) e^{-j\beta z}$
$H_y$	$\frac{j\omega n}{K_c p} (A \sin n\phi + B \cos n\phi) J_n'(K_c p) e^{-j\beta z}$	$\frac{j\omega n}{K_c p} (A \cos n\phi - B \sin n\phi) J_n(K_c p) e^{-j\beta z}$
$H_\phi$	$\frac{-j\omega n}{K_c p} (A \cos n\phi - B \sin n\phi) J_n(K_c p) e^{-j\beta z}$	$\frac{-j\omega n}{K_c} (A \sin n\phi + B \cos n\phi) J_n'(K_c p) e^{-j\beta z}$
$Z$	$Z_{TE} = \frac{K_h}{\beta}$	$Z_{TM} = \frac{\beta R}{R}$

So the only TE<sub>11</sub> mode is propagating at 14 GHz. The wave number is :

$$k = \frac{2\pi f \sqrt{\epsilon_r}}{c} = \frac{2\pi (14 \cdot 10^9)}{3 \cdot 10^8} \sqrt{208} = 422.9 \text{ m}^{-1}$$

and the propagation constant of the TE<sub>11</sub> mode is :

$$\beta = \sqrt{K^2 - \left(\frac{P_1}{a}\right)^2} = \sqrt{(422.9)^2 - \left(\frac{1.841}{0.005}\right)^2} = 208.0 \text{ m}^{-1}$$

The attenuation due to dielectric loss is calculated from (3.29) as:

$$\alpha_d = \frac{k^2 \tan \delta}{2\beta} = \frac{(422.9)^2 (0.0024)}{2(208.0)} = 0.172 \text{ Np/m} = 1.48 \text{ dB/m}$$

The conductivity of gold is  $\sigma = 41 \cdot 10^7 \text{ S/m}$ , so the surface resistance is

$$R_s = \sqrt{\frac{\omega \mu_0}{2\sigma}} = 0.0367 \Omega$$

②

Then from (3.133) the attenuation due to conductor loss is

$$\alpha_c = \frac{R_s}{2K\eta\beta} \left( K_c^2 + \frac{K^2}{P_{11}^2 - 1} \right) = 0.0672 \text{ Np/m} = 0.583 \text{ dB/m}$$

The total attenuation is  $\alpha = \alpha_d + \alpha_c = 2.07 \text{ dB/m}$ , and the loss in the 30 cm length of guide is:

$$\text{attenuation (dB)} = \alpha (\text{dB/m}) \times L (\text{m}) = (2.07)(0.3) = 0.62 \text{ dB}$$

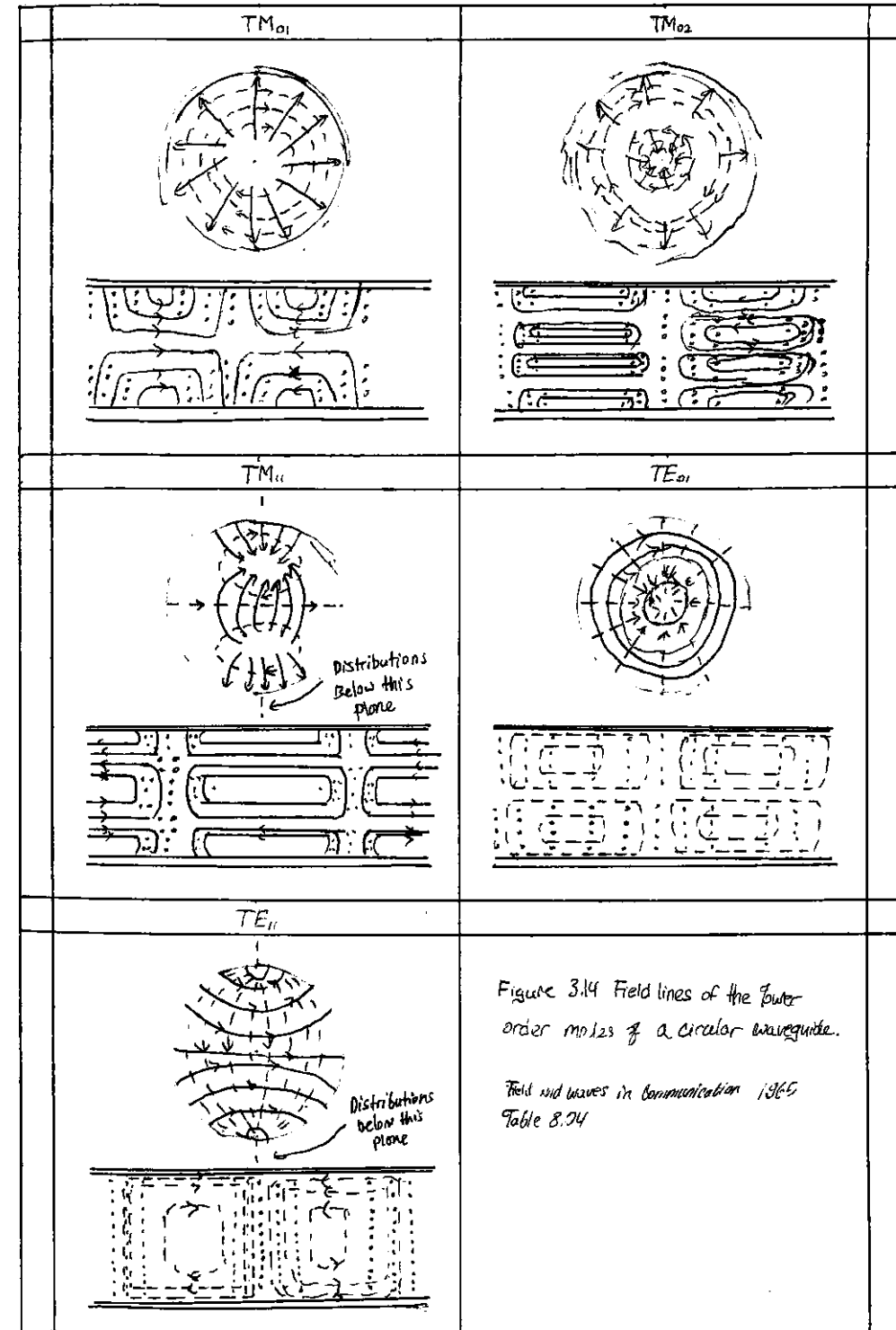


Figure 3.14 Field lines of the lower order modes of a circular waveguide.

Field and waves in communication 1365  
Table 8.34

### 3.5 COAXIAL LINE

TEM Modes

Although we have already discussed TEM mode propagation on a coaxial line in Chapter 2, we will briefly reconsider it here in the context of the general framework that is being used in this chapter.

The coaxial transmission line geometry is shown in figure 3.15, where the inner conductor is at a potential of  $V_0$  volts and the outer conductor is at 0 volts. From section 3.1 we know that the fields can be derived from a scalar potential function,  $\Phi(p, \phi)$ , which is a solution to Laplace's equation (3.14). In cylindrical coordinates Laplace's equation takes the form:

$$\frac{1}{p} \frac{\partial}{\partial p} \left( p \frac{\partial \Phi(p, \phi)}{\partial p} \right) + \frac{1}{p^2} \frac{\partial^2 \Phi(p, \phi)}{\partial \phi^2} = 0 \quad (3.143)$$

This equation must be solved for  $\Phi(p, \phi)$  subject to boundary conditions

$$\Phi(a, \phi) = V_0 \quad (3.144a)$$

$$\Phi(b, \phi) = 0 \quad (3.144b)$$

By the method of variables, let  $\Phi(p, \phi)$  be expressed in product form as:

$$\Phi(p, \phi) = R(p) P(\phi) \quad (3.145)$$

Substituting (3.145) into (3.143) and dividing by  $R P$  gives

$$\frac{1}{R} \frac{\partial}{\partial p} \left( p \frac{\partial R}{\partial p} \right) + \frac{1}{P} \frac{d^2 P}{d\phi^2} = 0 \quad (3.146)$$

By the usual separation of variables argument, the two terms in (3.146) must be equal to constants, so that:

$$\frac{1}{R} \frac{\partial}{\partial p} \left( p \frac{\partial R}{\partial p} \right) = -k_p^2 \quad (3.147)$$

$$\frac{1}{P} \frac{d^2 P}{d\phi^2} = -k_\phi^2 \quad (3.148)$$

$$k_p^2 + k_\phi^2 = 0 \quad (3.149)$$

The general solution to (3.148) is:

$$P(\phi) = A \cos n\phi + B \sin n\phi \quad (3.150)$$

where  $k_\phi = n$  must be an integer since increasing  $\phi$  by a multiple of  $2\pi$  should not change the result. Now, because the boundary conditions of (3.146) do not vary with  $\phi$ , the potential  $\Phi(p, \phi)$  should not vary with  $\phi$ , thus,  $n$  must be zero. By (3.149), this implies that  $k_p$  must also be zero, so that the equation for  $R(p)$  in (3.147) reduces to

$$\left[ \frac{1}{R} \frac{\partial}{\partial p} \left( p \frac{\partial R}{\partial p} \right) \right] = 0$$

The solution for  $R(p)$  is then

$$R(p) = C \ln p + D$$

and so

$$\Phi(p, \phi) = C \ln p + D \quad (3.151)$$

Applying boundary conditions of (3.144) gives two equations for the constants  $C$  and  $D$ :

$$\Phi(a, \phi) = V_0 = C \ln a + D \quad (3.152a)$$

$$\Phi(b, \phi) = 0 = C \ln b + D \quad (3.152b)$$

After solving for  $C$  and  $D$ , we can write the final solution for  $\Phi(p, \phi)$  as:

$$\Phi(p, \phi) = \frac{V_0 \ln b/p}{\ln b/a} \quad (3.153)$$

The  $E$  and  $H$  fields can now be found using (3.13) and (3.18), and the voltage, current, and characteristic impedance can be determined as in Chapter 2. Attenuation due to dielectric or conductor loss has already been treated in Chapter 2.

#### Higher Order Modes

The coaxial line, like the parallel plate waveguide, can also support TE and TM waveguide modes in addition to the TEM mode. In practice, these modes are usually cutoff (resonant), and so have only a reactive effect near discontinuities or sources, where they may be excited. It is important in practice, however, to be aware of the cutoff frequency of the lowest order waveguide modes to avoid propagation along these modes.

Undesirable effects can occur if two or more modes with different propagation constants are propagating at the same time. Avoiding propagation of higher order modes sets a limit on the frequency of operation for a given cable. This also affects the power handling capacity of a coaxial line or, equivalently, an upper limit on the frequency of operation for a given cable.

This also affects the power handling capacity of a coaxial line (see the point of interest on power capacity on transmission lines).

We will derive the solution for the TE modes of the coaxial line; the TE<sub>11</sub> mode is the dominant waveguide mode of the coaxial line and is of primary importance. For TE modes,  $E_z = 0$ , and  $H_z$  satisfies the wave equation of (3.112):

$$\left( \frac{\partial^2}{\partial p^2} + \frac{1}{p} \frac{\partial}{\partial p} + \frac{1}{p^2} \frac{\partial^2}{\partial \phi^2} + k_c^2 \right) H_z(p, \phi) = 0 \quad (3.154)$$

where  $H_z(p, \phi, z) = H_z(p, \phi) e^{jBz}$ , and  $k_c^2 = k_z^2 - k_\phi^2$ . The general solution to this equation, as derived in Section 3.4, is given by the product of (3.118) and (3.122):

$$H_z(p, \phi) = (A \sin n\phi + B \cos n\phi)(C \sin(k_c p) + D \cos(k_c p)) \quad (3.155)$$

In this case, as  $p \leq b$ , so we have no reason to abandon the  $Y_n$  term. The boundary conditions are:

$$E_\phi(p, \phi, z) = 0 \quad \text{for } p=a, b \quad (3.156)$$

Figure 3.15 Coaxial line

geometry.

We will derive the solution for the TE modes of the coaxial line; the TE<sub>11</sub> mode is the dominant waveguide mode of the coaxial line and is of primary importance. For TE modes,  $E_z = 0$ , and  $H_z$  satisfies the wave equation of (3.112):

$$\left( \frac{\partial^2}{\partial p^2} + \frac{1}{p} \frac{\partial}{\partial p} + \frac{1}{p^2} \frac{\partial^2}{\partial \phi^2} + k_c^2 \right) H_z(p, \phi) = 0 \quad (3.154)$$

where  $H_z(p, \phi, z) = H_z(p, \phi) e^{jBz}$ , and  $k_c^2 = k_z^2 - k_\phi^2$ . The general solution to this equation, as derived in Section 3.4, is given by the product of (3.118) and (3.122):

$$H_z(p, \phi) = (A \sin n\phi + B \cos n\phi)(C \sin(k_c p) + D \cos(k_c p)) \quad (3.155)$$

In this case, as  $p \leq b$ , so we have no reason to abandon the  $Y_n$  term. The boundary conditions are:

$$E_\phi(p, \phi, z) = 0 \quad \text{for } p=a, b \quad (3.156)$$

Using (3.110b) to find  $E_\phi$  from  $H_\phi$  gives

$$E_\phi = \frac{j\omega}{k_c} (A \sin \eta \phi + B \cos \eta \phi) [C J_n'(K_c a) + D Y_n'(K_c a)] e^{-j\beta z} \quad (3.157)$$

Applying (3.156) to (3.157) gives the two conditions equations:

$$C J_n'(K_c a) + D Y_n'(K_c a) = 0 \quad (3.158a)$$

$$C J_n'(K_c b) + D Y_n'(K_c b) = 0 \quad (3.158b)$$

Because this is a homogeneous set of equations, the only trivial ( $C=0, D \neq 0$ )

solution occurs when the determinant is zero. Thus we must have

$$J_n'(K_c a) Y_n'(K_c b) = J_n'(K_c b) Y_n'(K_c a)$$

This is the characteristic (or eigenvalue) equation for  $K_c$ . The values of  $K_c$  that satisfy (3.159) often define the  $TE_{nm}$  modes of the coaxial line.

Equation (3.159) is a transcendental equation, which must be solved numerically for  $K_c$ . Figure 3.16 shows the result of such a solution for  $n=1$  for various  $b/a$  ratios. An approximate solution that is often used in practice is:

$$K_c = \frac{2}{a+b}$$

Once  $K_c$  is known, the propagation constant or cutoff frequency can be determined. Solutions for the  $TM$  modes can be found in a similar manner; the required determinantal equation is the same as (3.159), except for the derivatives. Field lines for the  $TEM$  and  $TE_{11}$  modes of the coaxial line are shown in Figure 3.17.

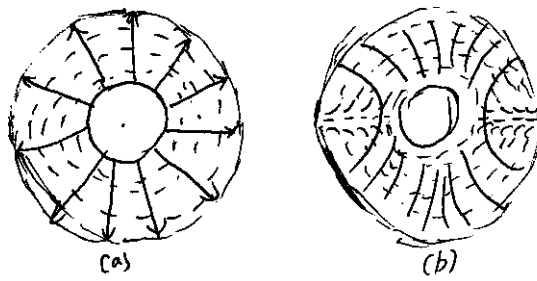


Figure 3.17 Field Lines  
for the (a) TEM and  
(b)  $TE_{11}$  modes of the  
Coaxial Line.

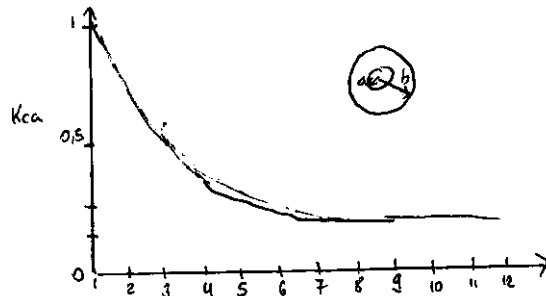


Figure 3.16 Normalized cutoff  
frequency of the dominant  
 $TE_{11}$  waveguide mode for  
a Coaxial Line.

### Example 3.3 Higher order Mode of a Coaxial Line.

Consider a RG-401U Semigrid coaxial cable, with inner and outer conductor diameters of 0.0645 in and 0.215 in, and a Teflon dielectric with  $\epsilon_r = 2.2$ . What is the highest usable frequency before the  $TE_{11}$  waveguide mode starts to propagate?

Solution

We have:

$$\frac{b}{a} = \frac{2b}{2a} = \frac{0.215}{0.0645} = 3.33$$

From Figure 3.16 this value of  $b/a$  gives  $K_c a = 0.45$  [the approximate result is  $K_c a = 2/(1+b/a) = 0.462$ ]. Thus,  $K_c = 549.4 \text{ m}^{-1}$ , and the cutoff frequency of the  $TE_{11}$  mode is:

$$f_c = \frac{c K_c}{2 \pi \sqrt{\epsilon_r}} = 17.7$$

In practice a 5% safety margin is usually recommended, so:

$$f_{max} = (1.05)(17.7 \text{ GHz}) = 18.8 \text{ GHz}$$

Most coaxial cables and connectors in common use have a  $50\Omega$  characteristic impedance, with an exception being the  $75\Omega$  cable used in television systems. The reasoning behind these choices is that an air-filled coaxial line has minimum attenuation for a characteristic impedance of about  $77\Omega$  (Problem 2.27), while maximum power capacity occurs for a characteristic impedance of about  $39\Omega$  (Problem 3.28). A  $50\Omega$  characteristic impedance thus represents a compromise between minimum attenuation and maximum power capacity. Other requirements for coaxial connectors include low SWR, higher-order-mode-free operation at a high frequency, high repeatability after a connect-disconnect cycle, and mechanical strength. Connectors are used in pairs, with a male end and a female end (or plug and jack).

Type N: This connector was developed in 1942 and is named after its inventor, P. Neill of Bell Labs. The outer diameter of the female end is about 0.625 in. The recommended upper frequency limit ranges from 11 to 18 GHz, depending on the cable size. This rugged but large connector is often found on older equipment.

TNC: This is a threaded version of the very common BNC connector. Its use is limited to frequencies below 1 GHz.

SMA: The need for smaller and lighter connectors led to the development of this connector in the 1960s. The outer diameter of the female end is about 0.25 in. It can be used up to frequencies in the range of 18-25 GHz and is probably the most commonly used connector today.

APC-7: This is a ~~less~~ precision connector (Amphenol Precision Connector) that can repeatedly achieve SWR less than 1.04 at frequencies up to 18 GHz. The connectors are genderless, with butt contact between inner and outer conductors. This connector is commonly used for measurement and instrumentation applications.

2.4mm: The need for connectors at millimeter wave frequencies led to the development of several variations of the SMA connector. One of the most common is the 2.4mm connector, which is useful to about 50 GHz. The size of this connector is similar to that of the SMA connector.

### 3.6 Surface Waves on a Grounded Dielectric Sheet.

We briefly discussed surface waves in Chapter 1 in connection with the field plane wave totally reflected from a dielectric interface, but surface waves can exist in a variety of geometries involving dielectric interfaces. Here we consider the TM and TE surface ~~waveguides~~ waves that can be excited along a grounded dielectric sheet, a dielectric rod, a corrugated conductor, and a dielectric-coated conducting rod. Surface waves are ~~excited by~~ field that decays exponentially away from the dielectric surface, with most of the fields contained in or near the dielectric. At higher frequencies the field generally becomes more tightly bound to the dielectric, making such waveguides practical. Because of the presence of the dielectric, the phase velocity of a surface wave is less than the velocity of light in a vacuum. Another reason for studying surface waves is ~~less than the velocity of light in a vacuum~~. That they may be excited on some types of planar transmission lines, such as the microstrip and slotline.

#### TM Modes

Figure 3.18 shows the geometry of a grounded dielectric slab waveguide. The dielectric sheet, of thickness  $d$  and relative permittivity  $\epsilon_r$ , is assumed to be of infinite extent in the  $y$  and  $z$  directions. We will assume propagation in the  $xZ$  propagation direction with an  $e^{-i\beta z}$  factor and no variation in the  $y$  direction ( $\partial/\partial y = 0$ ).

Because there are two distinct regions, with and without a dielectric, we must separately consider the field in these regions and then match tangential fields across the interface.  $E_z$  must satisfy the wave equation of (3.25) in each region:

$$\left(\frac{\partial^2}{\partial x^2} + \epsilon_r k_0^2 - \beta^2\right) E_{z1}(x,y) = 0 \quad \text{for } 0 \leq x \leq d \quad (3.160a)$$

$$\left(\frac{\partial^2}{\partial x^2} + k_0^2 - \beta^2\right) E_{z2}(x,y) = 0 \quad \text{for } d \leq x < \infty \quad (3.160b)$$

$$\text{where } E_z(x,y,z) = E_{z1}(x,y)e^{-i\beta z}$$

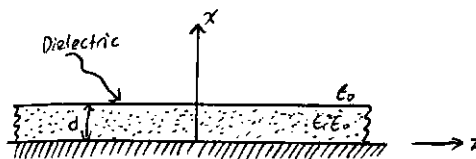


Figure 3.18 Geometry of a grounded dielectric sheet.

Some propagation constant,  $\beta$ , has been used for both regions. This must be the case to achieve phase matching of the tangential fields at the  $x=d$  interface for all values of  $z$ .

The general solutions to (3.160) are:

$$E_{z1}(x,y,z) = 0 \quad \text{at } x=0, \quad (3.163a)$$

$$E_{z2}(x,y,z) \propto e^{-\beta(x-d)} \quad \text{as } x \rightarrow \infty \quad (3.163b)$$

$$E_{z2}(x,y,z) \text{ continuous at } x=d \quad (3.163c)$$

$$H_{y2}(x,y,z) \text{ continuous at } x=d \quad (3.163d)$$

From (3.23),  $H_x = E_y = H_z = 0$ . Condition (3.163a) implies that  $B=0$  in (3.162a).

Condition (3.163b) is a result in the requirement for finite fields (and energy) infinitely far away from the source and implies that  $C=0$ . The continuity of  $E_x$  leads to:

$$A \sin(k_d d) = D e^{-\beta d} \quad (3.164a)$$

while (3.163b) is a result must be used to apply continuity to  $H_y$ , to obtain

$$\frac{\epsilon_r A}{k_c} \cos(k_d d) = \frac{D}{h} e^{-\beta d} \quad (3.164b)$$

For a non-trivial solution, the determinant of the two equations of (3.164) must vanish, leading to:  $k_c \tan k_c d = \epsilon_r h$  (3.165)

Eliminating  $\beta$  from (3.161a) and (3.163b) gives:

$$k_c^2 + \frac{h^2}{d^2} = (\epsilon_r - 1) k_0^2 \quad (3.166)$$

Equations (3.165) and (3.166) constitute a set of simultaneous transcendental equations that must be solved for the propagation constants  $k_c$  and  $h$ , given  $k_0$  and  $\epsilon_r$ . These equations are easily solved numerically, but Figure 3.19 shows a graphical representation of the solutions. Multiplying both sides of (3.166) by  $d^2$  gives:

$$(k_c d)^2 + (h d)^2 = (\epsilon_r - 1)(k_0 d)^2$$

which is the equation of a circle in the  $k_c d, h d$  plane, as shown in Figure 3.19.

The radius of the circle is  $\sqrt{\epsilon_r - 1} k_0 d$ , which is proportional to the electrical thickness of the dielectric sheet. Multiplying (3.165) by  $d$  gives

$$k_c \tan k_c d = \epsilon_r h$$

which is also plotted in Figure 3.19. The intersection of these curves implies a solution to both (3.165) and (3.166). Observe that  $k_c$  may be positive or negative; from (3.162a) this is merely a change of the sign of the constant  $A$ . As  $\sqrt{\epsilon_r - 1} k_0 d$  becomes larger, the circle may intersect more than one branch of the tangent function, implying more than one TM mode may propagate.

We define the cutoff wavenumbers for the two regions as:

$$k_{c1}^2 = \epsilon_r k_0^2 - \beta^2 \quad (3.161a)$$

$$h^2 = \beta^2 - k_0^2 \quad (3.161b)$$

where the sign on the  $h^2$  has been selected in anticipation of an exponentially decaying result for  $x>d$ . Observe that the

Solutions for negative  $h$ , however, must be excluded since we have assumed  $h$  was positive real when applying boundary condition (3.163b).

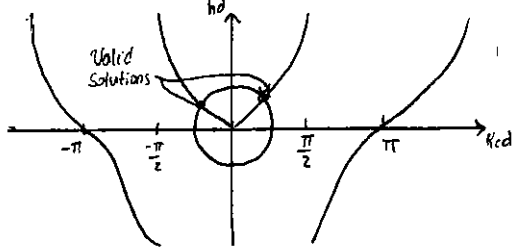


Figure 3.19 Graphical Solution of the Transcendental equation for the cutoff frequency of a TM surface wave mode of the grounded dielectric sheet.

of the circle becomes greater than  $\pi$ . The cutoff frequency of the  $TM_n$  mode can then be derived as:

$$f_c = \frac{n c}{2d\sqrt{\epsilon_r - 1}}, \quad n=0, 1, 2, \dots \quad (3.167)$$

Once  $k_z$  and  $h$  have been found for a particular surface wave mode, the field expressions can be found as:

$$E_z(x, y, z) = \begin{cases} A \sin k_z x e^{-jBz} & \text{for } 0 \leq x \leq d \\ A \sin k_z d e^{-h(x-d)} e^{-jBz} & \text{for } d \leq x < \infty \end{cases} \quad (3.168a)$$

$$E_x(x, y, z) = \begin{cases} -jB A \cos k_z x e^{-jBz} & \text{for } 0 \leq x \leq d \\ -jB A \sin k_z d e^{-h(x-d)} e^{-jBz} & \text{for } d \leq x < \infty \end{cases} \quad (3.168b)$$

$$H_y(x, y, z) = \begin{cases} -i\omega \epsilon_r A \cos k_z x e^{-jBz} & \text{for } 0 \leq x \leq d \\ -i\omega \epsilon_r A \sin k_z d e^{-h(x-d)} e^{-jBz} & \text{for } d \leq x < \infty \end{cases} \quad (3.168c)$$

$$H_z(x, y, z) = h_z(x, y) e^{-jBz} \quad \text{and } k_z^2 \text{ and } h^2 \text{ defined in (3.161a) and (3.161b)}$$

TE Modes can also be supported by the ground dielectric sheet. The  $H_z$  field satisfies the wave equations:

$$\left(\frac{\partial^2}{\partial x^2} + k_z^2\right) h_z(x, 0) = 0 \quad \text{for } 0 \leq x \leq d \quad (3.169a)$$

$$\left(\frac{\partial^2}{\partial x^2} - h^2\right) h_z(x, 0) = 0 \quad \text{for } d \leq x < \infty \quad (3.169b)$$

with  $H_z(x, y, z) = h_z(x, y) e^{-jBz}$  and  $k_z^2$  and  $h^2$  defined in (3.161a) and (3.161b). As for the TM modes, the general solutions to (3.169) are:

$$h_z(x, y) = A \sin k_z x + B \cos k_z x \quad (3.170a)$$

$$h_z(x, y) = C e^{h x} + D e^{-h x} \quad (3.170b)$$

To satisfy the radiation condition,  $C=0$ . Using (3.170a) to find  $E_y$  from  $H_z$  leads to  $A=0$  for  $E_y=0$  and  $x=0$  and to the equation:

$$-\frac{B}{k_z} \sin k_z d = \frac{j}{h} e^{-hd} \quad (3.171a)$$

for the continuity of  $E_y$  at  $x=d$ . Continuity of  $H_z$  at  $x=d$  gives

$$B \cos k_z d = D e^{-hd} \quad (3.171b)$$

Simultaneously solving (3.171a) and (3.171b) leads to the determinantal equation

$$-k_z \cot k_z d = h \quad (3.172)$$

From (3.161a) and (3.161b) we also have that

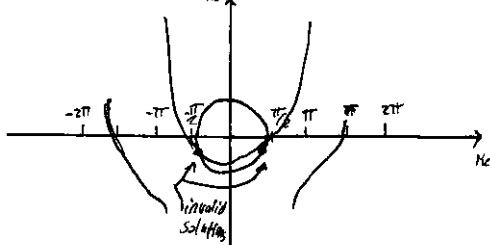
$$k_z^2 + h^2 = (\epsilon_r - 1) k_0^2 \quad (3.173)$$

Equations (3.172) and (3.173) must be solved simultaneously for the variables  $k_z$  and  $h$ . Equation (3.173) again represents circles on the  $k_zd$ ,  $hd$  plane, while (3.172) can be written as

$$-k_z d \cot k_z d = hd \quad (3.174)$$

and plotted as a family of curves in the  $k_zd$ ,  $hd$  plane, as shown in Figure 3.20. Because negative values of  $h$  must be excluded, we see from Figure 3.20 that the first TE mode does not start to propagate until the radius of the circle,  $\sqrt{\epsilon_r - 1} k_0 d$ , becomes greater than  $\pi/2$ . The cutoff frequency of the TE modes can then be found as

$$f_c = \frac{(2n-1)c}{4d\sqrt{\epsilon_r - 1}} \quad \text{for } n=1, 2, 3, \dots \quad (3.174)$$



Comparing with (3.167) shows that the order of propagation for the  $TM_n$  and  $TE_n$  modes is  $TM_0, TE_1, TM_1, TE_2, TM_2, \dots$

Figure 3.20 Graphical Solution of the Transcendental equation for the cutoff frequency of a TE surface wave mode. The figure depicts a mode below cutoff.

After finding the constants  $k_z$  and  $h$ , the field expressions can be derived as:

$$H_z(x, y, z) = \begin{cases} B \cos k_z x e^{-jBz} & \text{for } 0 \leq x \leq d \\ B \cos k_z d e^{-h(x-d)} e^{-jBz} & \text{for } d \leq x < \infty \end{cases} \quad (3.175a)$$

$$H_x(x, y, z) = \begin{cases} jB/k_z B \sin k_z x e^{-jBz} & \text{for } 0 \leq x \leq d \\ -jB/k_z B \cos k_z d e^{-h(x-d)} e^{-jBz} & \text{for } d \leq x < \infty \end{cases} \quad (3.175b)$$

$$E_y(x, y, z) = \begin{cases} -j\omega \epsilon_r B \sin k_z x e^{-jBz} & \text{for } 0 \leq x \leq d \\ j\omega \epsilon_r B \cos k_z d e^{-h(x-d)} e^{-jBz} & \text{for } d \leq x < \infty \end{cases} \quad (3.175c)$$

### Example 3.4 Surface Wave Propagation Constants

Calculate and plot the propagation constant of the first three propagation surface wave modes of a grounded dielectric sheet with  $\epsilon_r = 2.55$ , for  $d/\lambda_0 \approx 0$  to 1.2.

**Solution**

The first three propagating surface wave modes are the TM<sub>0</sub>, TE<sub>1</sub>, and TM<sub>1</sub> modes. The cutoff frequencies for these modes can be found from (3.167) and (3.174) as:

$$TM_0: f_c = 0 \Rightarrow \frac{d}{\lambda_0} = 0.$$

$$TE_1: f_c = \frac{c}{4d\sqrt{\epsilon_r - 1}} \Rightarrow \frac{d}{\lambda_0} = \frac{1}{(4\sqrt{\epsilon_r - 1})}.$$

$$TM_1: f_c = \frac{c}{2d\sqrt{\epsilon_r - 1}} \Rightarrow \frac{d}{\lambda_0} = \frac{1}{(2\sqrt{\epsilon_r - 1})}$$

The propagation constants can be found from the numerical solution of (3.165) and (3.166) for the TM modes and (3.172) and (3.173) for the TE modes.

This can be done with a relatively simple root-finding algorithm

(See the Point of Interest on Root-finding algorithms). The results are shown in Figure 3.21.

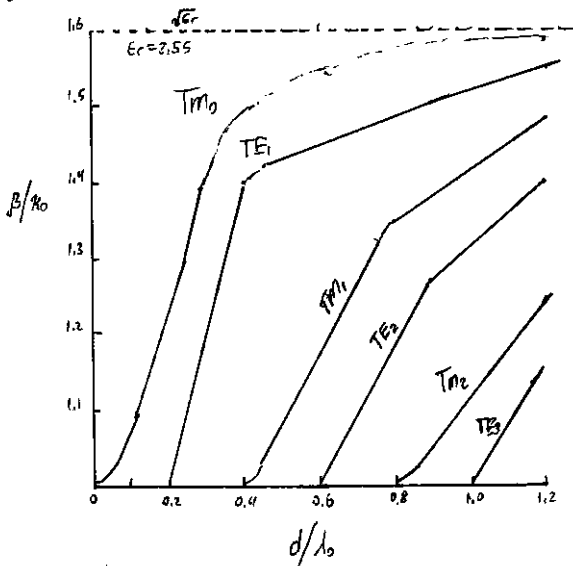


Figure 3.21 Surface wave propagation for a grounded dielectric slab with  $\epsilon_r = 2.55$ .

**Point of Interest: Root finding algorithms**

In several examples throughout this book we will need to numerically find the root of a transcendental equations. So it may be necessary to review two relatively simple but effective algorithms for doing this. Both method can be easily programmed.

In the interval-halving method the root of  $f(x)=0$  is the first bracketed values  $x_1$  and  $x_2$ . These values can often be estimated from the problem under consideration. If a single root lies between  $x_1$  and  $x_2$ , then  $f(x_1)f(x_2) < 0$ . An estimate,  $x_3$ , of the root is made by halving the interval between  $x_1$  and  $x_2$ . Thus:

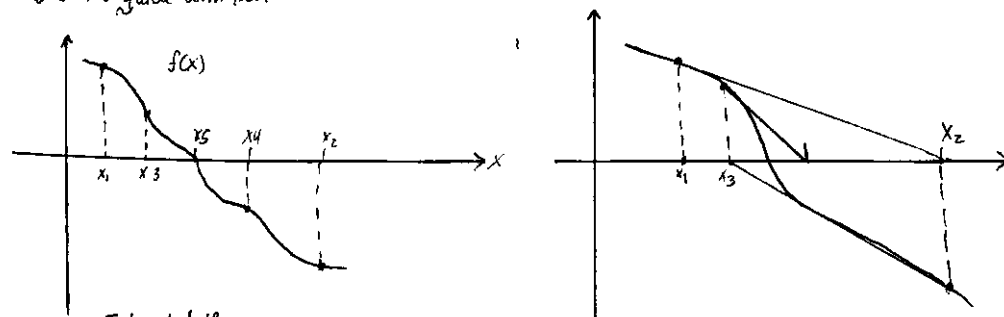
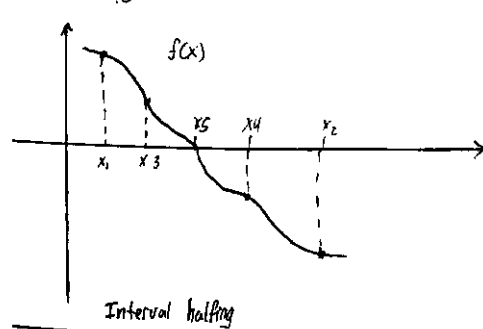
$$x_3 = \frac{x_1 + x_2}{2}$$

If  $f(x_1)f(x_3) < 0$ , then the root must lie on the interval  $x_1 < x < x_3$ ; if  $f(x_3)f(x_2) < 0$ , the root must be on the interval  $x_3 < x < x_2$ . A new estimate,  $x_4$ , can be made by halving the appropriate interval  $x_3 < x < x_2$ . A new estimate,  $x_4$ , can be made by halving the appropriate interval, and this process is repeated until the location of the root has been desired with the desired accuracy. The accompanying figure illustrates this algorithm for several iterations.

The Newton-Raphson method begins with an estimate,  $x_1$ , of the root of  $f(x) = 0$ . Then a new estimate is obtained from the formula:

$$x_2 = x_1 - \frac{f(x_1)}{f'(x_1)}$$

where  $f'(x)$  is the derivative of  $f(x)$  at  $x_1$ . This result is easily derived from a two term Taylor series expansion of  $f(x)$  near  $x=x_1$ :  $f(x) = f(x_1) + (x-x_1)f'(x_1)$ . It can also be interpreted geometrically as fitting a straight line at  $x=x_1$  with the same slope as  $f(x)$  at this point; this line then intercepts the  $x$ -axis at  $x=x_2$ , as shown in the figure. Applying the above formula gives improved estimates of the root. Convergence is generally much faster than with the interval halving method, but a disadvantage is that the derivative of  $f(x)$  is required; this can often be computed numerically. The Newton-Raphson technique can easily be applied to the case where the root is complex. (A situation that occurs, for example, when finding the propagation constant of a line or a guide with loss).



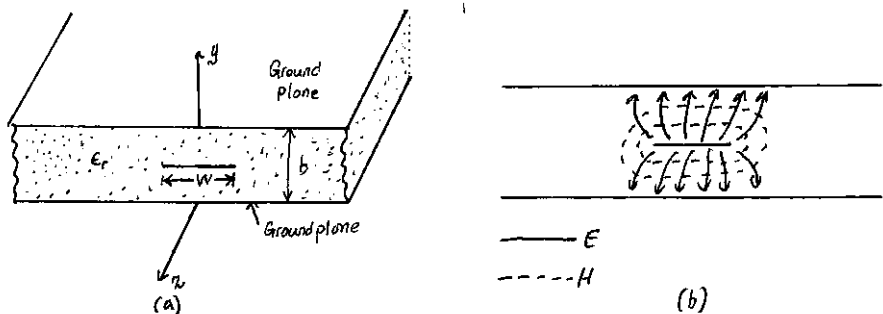


Figure 3.22 Stripline Transmission Line (a) Geometry. (b) Electric and magnetic field lines.

### 3.7 Strip Line

Stripline is a planar type of transmission line that lends itself well to microwave integrated circuits, miniaturization, and photolithographic fabrication. The geometry of the stripline is shown in Figure 3.22a. A thin conducting strip of width  $W$  is centered between two wide conducting planes of separation  $b$ , and the region between the ground planes is filled with a dielectric material. In practice stripline is usually constructed by etching the central conductor on a grounded dielectric substrate of thickness  $b/2$  and then covering with another grounded substrate. Variations of the basic geometry of Figure 3.22a include stripline with different dielectric substrate thickness (asymmetric stripline) or different dielectric constants (inhomogeneous stripline), or different dielectric constants (inhomogeneous stripline). Air dielectric is sometimes used when it is necessary to minimize loss. An example of a stripline circuit is shown in Figure 3.23.

Because stripline has two conductors and a homogeneous dielectric, it supports a TEM wave, and this is the usual mode of operation. Like parallel plate guide and coaxial line, however, stripline can also support higher order waveguide modes. These can usually be avoided in practice by restricting both the ground plane spacing and side wall width  $W$  to less than  $\lambda_d/2$ . Shorting pins between the ground planes are often used to eliminate higher order modes that can be generated when an asymmetry is introduced between the ground planes (e.g. when a surface mounted coaxial transition is used.)

Intuitively, one can think of stripline as some sort of "flattened out" coax - both have a central conductor completely enclosed by an outer conductor and are uniformly filled with a dielectric medium. A sketch for the field lines of the stripline is found in Figure 3.22b.

The geometry of stripline does not lend itself to the simple analyses that were used for previously treated transmission lines and waveguides. Because we will be concerned primarily with the TEM mode of stripline, an electrostatic analysis is sufficient to give the propagation constant and characteristic impedance.

An exact solution of Laplace's equation is possible by a conformal mapping approach [6], but the procedure and results are cumbersome. Instead we will provide closed-form solutions expressions that give good approximations to the exact results instead and then discuss an approximate numerical techniques for solving Laplace's equation for a geometry similar to a stripline.

### Formula for Propagation Constant, Characteristic Impedance, and Attenuation

From Section 3.1 we know that the phase velocity of a TEM mode is given by

$$v_p = \frac{1}{\sqrt{\mu_0 \epsilon_r}} = \frac{c}{\sqrt{\epsilon_r}}$$
 (3.176)

and thus the propagation constant of stripline is

$$\beta = \frac{c}{v_p} = \omega \sqrt{\mu_0 \epsilon_r} = \sqrt{\epsilon_r R_0}$$
 (3.177)

[Figure 3.23 Photograph of a stripline circuit assembly (cover removed), showing four quadrature hybrids, open-circuit tuning stubs, and coaxial transitions.]

In (3.176),  $c = 3 \times 10^8$  m/sec is the speed of light in free space. Using (2.13) and (2.16) allows us to write the characteristic impedance of the transmission line as

$$Z_0 = \sqrt{\frac{L}{C}} = \frac{\sqrt{LC}}{c} = \frac{1}{v_p C}$$
 (3.178)

where  $L$  and  $C$  are the inductance and capacitance per unit length of line. Thus, we can find  $Z_0$  if we know  $C$ . As mentioned previously, Laplace's equation can be solved by conformal mapping to find the capacitance per unit of stripline, but the resulting solution involves complicated special functions [6], so the practical computations simple formulas have been developed by curve fitting to the exact solution [6,7]. The resulting formula for characteristic impedance is:

$$Z_0 = \frac{30\pi}{\sqrt{\epsilon_r}} \frac{b}{W_e + 0.41b}$$
 (3.179a)

where  $W_e$  is the effective width of the center conductor given by:

$$\frac{W_e}{b} = \frac{W}{b} - \begin{cases} 0 & \text{for } W/b > 0.35 \\ (0.35 - W/b)^2 & \text{for } W/b < 0.35 \end{cases}$$
 (3.179b)

These formulas assume a strip with zero thickness and are quoted as being accurate to 1% of the exact results. It is seen from (3.179) that the characteristic impedance decreases as the strip width  $W$  increases.

When designing stripline circuits one usually needs to find the strip width, given the characteristic impedance ( $Z_0$ ) and height ( $b$ ) and relative permittivity ( $\epsilon_r$ ), which requires the inverse of the formulas in (3.179). Such formulas have been derived as :

$$\frac{W}{b} = \begin{cases} x & \text{for } \sqrt{\epsilon_r} Z_0 < 120\Omega \\ 0.85 - \sqrt{0.6-x} & \text{for } \sqrt{\epsilon_r} Z_0 > 120\Omega \end{cases} \quad (3.180a)$$

where

$$x = \frac{30\pi}{\sqrt{\epsilon_r} Z_0} - 0.441 \quad (3.180b)$$

Since stripline is a TEM line, the attenuation due to dielectric loss is of the same form as that for other TEM lines and is given in (3.30). The attenuation due to conductor loss can be found by the perturbation method or Wheeler's inductance rule. An approximate result is :

$$\alpha_c = \begin{cases} \frac{2.7 \cdot 10^{-3} R_s \epsilon_r Z_0}{30\pi(b-t)} & \text{for } \sqrt{\epsilon_r} Z_0 < 120\Omega \\ \frac{0.16 R_s}{Z_0 b} B & \text{for } \sqrt{\epsilon_r} Z_0 > 120\Omega \end{cases} \text{ Np/m} \quad (3.181)$$

with

$$A = 1 + \frac{2W}{b-t} + \frac{1}{\pi} \frac{bt}{b-t} \ln \left( \frac{2b-t}{t} \right)$$

$$B = 1 + \frac{t}{(0.5W + 0.7t)} \left( 0.5 + \frac{0.441t}{W} + \frac{1}{2\pi} \ln \frac{4\pi W}{t} \right)$$

where  $t$  is the thickness of the strip.

### Example 3.5 Stripline Design

Find the width of a  $50\Omega$  copper stripline conductor with  $t=0.32\text{ cm}$  and  $\epsilon_r=2.0$ . If the dielectric loss tangent is 0.001 and the operating frequency is  $10\text{GHz}$ , calculate the attenuation in dB/m. Assume a conductor thickness of  $t=0.01\text{mm}$ .

Solution

Because  $\sqrt{\epsilon_r} Z_0 = \sqrt{2.2}(50) = 74.2$  (100 and  $x=30\pi/\sqrt{\epsilon_r} Z_0 - 0.441 = 0.830$ , (3.180) gives the strip width as  $W=bx = (0.32)(0.830) = 0.266\text{ cm}$ .

At 10 GHz, the wave number is :

$$K = \frac{2\pi f \sqrt{\epsilon_r}}{c} = 310.6\text{ m}^{-1}$$

From (3.30) the dielectric attenuation is :

$$\alpha_d = \frac{4\pi \tan \delta}{2} = \frac{(310.6)(0.001)}{2} = 0.155 \text{ Np/m}$$

The surface resistance of Copper at 10GHz is  $R_s = 0.026\Omega$ . Then from (3.181) the conductor attenuation is :

$$\alpha_c = \frac{2.7 \cdot 10^{-3} R_s \epsilon_r Z_0 A}{30\pi(b-t)} = 0.122 \text{ Np/m}$$

Since  $A = 4.74$ , the total attenuation constant is

$$\alpha = \alpha_d + \alpha_c = 0.277 \text{ Np/m}$$

In dB,

$$\alpha(\text{dB}) = 20 \log e^\alpha = 2.41 \text{ dB/m}$$

At 10GHz, the wavelength on the stripline is

$$\lambda = \frac{c}{\sqrt{\epsilon_r} f} = 2.02\text{ cm}$$

So in terms of wavelength the attenuation is

$$\alpha(\text{dB}) = (2.41)(0.2202) = 0.049 \text{ dB/}\lambda$$

### An Approximate Electrostatic Solution

Many practical problems in microwave engineering are very complicated and do not lend themselves to straightforward analytic solutions but require some sort of numeric approach. Thus it is useful for the student to become aware of such techniques; we will introduce such methods when appropriate throughout this book, beginning with a numerical solution for the characteristic impedance of stripline.

We know that the fields of the TEM mode on stripline must satisfy Laplace's equation, (3.11), in the region between two parallel plates. The idealized stripline geometry of Figure 3.22a extends to  $\pm\infty$ , which makes the analysis more difficult. Because we suspect, Figure 3.22a extends to from the field line drawing of Figure 3.22b, that the field lines do not extend very far away from the center conductor, we can simplify the geometry by truncating the plates beyond some distance, say  $|x| > a/2$ , and placing metal walls on the sides. Thus, the geometry we will analyze is shown in Figure 3.24, where  $a \gg b$ , so that the fields around the conductor are not perturbed by the sidewalls.

We then have a closed finite region in which the potential  $\Phi(x,y)$  satisfies Laplace's equation,

$$\nabla^2 \Phi(x,y) = 0 \quad \text{for } (x| \leq a/2, 0 \leq y \leq b) \quad (3.182)$$

with the boundary conditions

$$\Phi(x,y) = 0, \text{ at } x = \pm a/2 \quad (3.183a)$$

$$\Phi(x,y) = 0, \text{ at } y = 0, b \quad (3.183b)$$

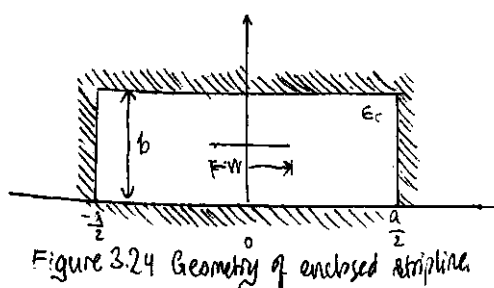


Figure 3.24 Geometry of enclosed stripline

Laplace's equation can be solved by the method of separation of variables. Because the center conductor at  $y=b/2$  will contain a surface charge density, the potential  $\Phi(x,y)$  will have a slope discontinuity there because  $D = -\epsilon_0 E_r \nabla \Phi$  is discontinuous at  $y=b/2$ . Therefore, separate solutions for  $\Phi(x,y)$  must be found for  $0 < y < b/2$  and  $b/2 < y < b$ . The general solutions for  $\Phi(x,y)$  in these two regions can be written as:

$$\Phi(x,y) = \begin{cases} \sum_{n=1}^{\infty} A_n \cos \frac{n\pi x}{a} \sinh \frac{n\pi y}{a} & \text{for } 0 < y < b/2 \\ \sum_{n=1}^{\infty} B_n \cos \frac{n\pi x}{a} \sinh \frac{n\pi (b-y)}{a} & \text{for } b/2 < y < b \end{cases} \quad (3.184)$$

Only the odd- $n$  terms are needed in (3.184) because the solution is an even function of  $x$ . The reader can verify by substitution that (3.184) satisfies Laplace's equation in the two regions and satisfies the boundary conditions of (3.183).

The potential must be continuous at  $y=b/2$ , which from the form (3.184) leads to

$$A_n = B_n \quad (3.185)$$

The remaining set of unknown coefficients,  $A_n$ , can be found by solving for the charge density on the center strip. Because  $E_y = -\partial \Phi / \partial y$ , we have

$$E_y = \begin{cases} -\sum_{n=1}^{\infty} A_n \left( \frac{n\pi}{a} \right) \cos \frac{n\pi x}{a} \cosh \frac{n\pi y}{a} & \text{for } 0 < y < \frac{b}{2} \\ \sum_{n=1}^{\infty} A_n \left( \frac{n\pi}{a} \right) \cos \frac{n\pi x}{a} \cosh \frac{n\pi (b-y)}{a} & \text{for } \frac{b}{2} < y < b \end{cases} \quad (3.186)$$

The surface charge density on the strip at  $y=b/2$  is:

$$s_s = D_y(x, y=b/2^+) - D_y(x, y=b/2^-) = \epsilon_0 E_r [E_y(x, y=b/2^+) - E_y(x, y=b/2^-)] \\ = 2\epsilon_0 \sum_{n=1}^{\infty} A_n \left( \frac{n\pi}{a} \right) \cos \frac{n\pi x}{a} \cosh \frac{n\pi b}{2a} \quad (3.187)$$

which is seen to be a Fourier series in  $x$  for the surface charge density,  $s_s$ , on the strip at  $y=b/2$ . If we know the surface charge density on the strip at  $y=b/2$ , we could easily find the unknown constants,  $A_n$ , and then the capacitance. We do not know the exact surface charge density, but we can make a good guess by approximating it as a constant over the width of the strip,

$$s_s(x) = \begin{cases} 1 & \text{for } |x| < W/2 \\ 0 & \text{for } |x| > W/2 \end{cases} \quad (3.188)$$

Equating this to (3.187) and using the orthogonality properties of the  $\cos(n\pi x/a)$  functions gives the constants  $A_n$  as:

$$A_n = \frac{2a \sin(n\pi W/2a)}{(n\pi)^2 \epsilon_0 E_r \cosh(n\pi b/2a)} \quad (3.189a)$$

The voltage of the strip conductor relative to the bottom conductor can be found by integrating the vertical electric field from  $y=0$  to  $b/2$ . Because the solution is approximate, this voltage is not constant over the width of the strip but varies with position,  $x$ . Rather than choosing the voltage at an arbitrary position, we can obtain an improved result by averaging the voltage over the width of the strip:

$$V_{avg} = \frac{1}{W} \int_{-W/2}^{W/2} \int_0^{b/2} E_y(x, y) dy dx = \sum_{n=1}^{\infty} A_n \left( \frac{2a}{n\pi W} \right) \sinh \frac{n\pi b}{2a} \quad (3.190)$$

The total charge per unit length on the center conductor is:

$$Q = \int_{-W/2}^{W/2} s_s(x) dx = W \text{ Coul/m} \quad (3.191)$$

So the capacitance per unit length of the stripline is:

$$C = \frac{Q}{V_{avg}} = \frac{W}{\sum_{n=1}^{\infty} A_n \left( \frac{2a}{n\pi W} \right) \sin \frac{n\pi W}{2a} \sinh \frac{n\pi b}{2a}} \quad F/m \quad (3.192)$$

Finally, the characteristic impedance is given by:

$$Z_0 = \sqrt{\frac{L}{C}} = \sqrt{\frac{LC}{C}} = \frac{1}{\sqrt{C}} = \frac{\sqrt{\epsilon_r}}{\sqrt{C}} \quad \text{where } C = 3e8 \cdot 10^{-15}$$

### Example 3.6 Numerical Calculation of Stripline Impedance

Evaluate the above expressions for a stripline having  $b=2.55$  and  $a=100b$  to find the characteristic impedance for  $W/b = 0.25$  to  $5.0$ . Compare with the results from (3.179).

Solution

A computer program was written to evaluate (3.192). The series was truncated after 500 terms, and the results for  $Z_0$  are as follows.

$W/b$	$Z_0, \Omega$	Numerical Eq. (3.192)	Formula Eq. (3.179)	Commercial Cad
0.25	30.3	86.6	85.3	
0.50	66.4	62.7	61.7	
1.0	43.6	41.0	40.2	
2.0	25.5	24.2	24.4	
5.0	11.1	10.8	11.9	

We see that the ~~sec~~ results are in reasonable agreement with the closed-form equation of (3.172) and the results from a commercial CAD package, particularly for wider strips where the charge density is closer to uniform. Better results could be obtained if more sophisticated estimates were used for the charge density.

### 3.8 Microstrip Line

Microstrip line is one of the most popular types of planar transmission lines primarily because it can be fabricated by photolithographic processes and is easily miniaturized and integrated with both passive and active microwave devices. The geometry of a microstrip line is shown in Figure 3.25a. A conductor of width  $W$  is printed on a thin, grounded dielectric substrate of thickness  $d$  and a relative permittivity  $\epsilon_r$ . A sketch of the field lines is shown in Figure 3.25b.

If the dielectric substrate were not present ( $\epsilon_r = 1$ ), we would have a two-wire line consisting of a flat strip conductor over a ground plane, embedded in a homogeneous medium (air). This would constitute a simple TEH transmission line with phase velocity  $v_p = c$  and propagation constant  $\beta = k_0$ .

The presence of the dielectric, particularly the fact that the dielectric does not fill the region above the strip ( $y > d$ ), complicates the behaviour and analysis of microstrip line. Unlike stripline, where all fields are contained within a homogeneous dielectric region, microstrip has some (usually most) of its field lines in the dielectric region between the strip conductor and the ground plane and some fraction in the air above the substrate. For this reason microstrip line cannot support pure TEM wave since the phase velocity of TEM fields in the dielectric region would be  $\sqrt{\epsilon_r}$ , while the phase velocity of TEM fields in the air region would be  $c$ . So a phase matching condition at the dielectric-air interface would be impossible to enforce.

In actuality, the exact fields of a microstrip constitute a hybrid TM-TE wave and require most advanced analysis techniques that we are prepared to deal with here. In most practical applications, however, the dielectric substrate is electrically very thin ( $d \ll c_0$ ), and so the fields are quasi-TEM. In other words, the fields are essentially the same as those in the static (DC) case. Thus, good approximations for the phase velocity, propagation constant, and characteristic impedance can be obtained from static, or quasi-static, solutions.

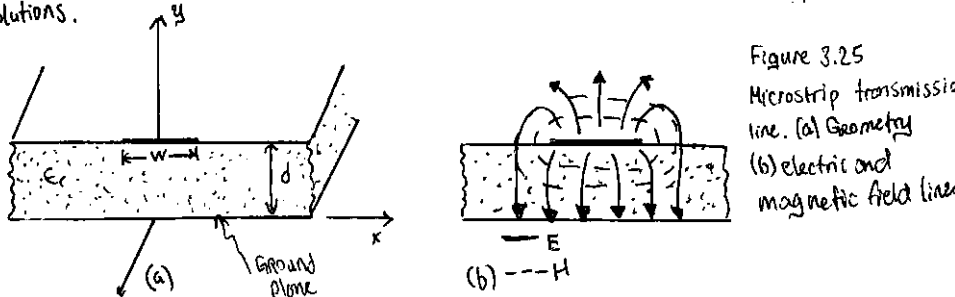


Figure 3.25  
Microstrip transmission line. (a) Geometry  
(b) electric and magnetic field lines.

Then the phase velocity and propagation constant can be expressed as:

$$v_p = \frac{c}{\sqrt{\epsilon_r}} \quad \beta = k_0 \sqrt{\epsilon_r} \quad (3.193), (3.194)$$

where  $\epsilon_r$  is the effective dielectric constant of the microstrip line. Because some of the field lines are in the dielectric region and some are in air, the effective dielectric constant satisfies the relation:

$$1 < \epsilon_{eff} < \epsilon_r$$

and depends on the substrate dielectric constant, the substrate thickness, the conductor width and the frequency.

We will present approximate design formulae for the effective dielectric constant, characteristic impedance, and attenuation of microstrip line; these results are curve-fit approximations to rigorous quasi-static solutions [8,9]. Then we will discuss additional aspects of microstrip lines, including frequency dependent effects, higher-order modes, and parasitic effects.

Formulas for effective dielectric constant, Characteristic Impedance and Attenuation

The effective dielectric constant of a microstrip line is given approximately by:

$$\epsilon_{eff} = \frac{\epsilon_r + 1}{2} + \frac{\epsilon_r - 1}{2} \frac{1}{\sqrt{1 + 12d/W}} \quad (3.195)$$

The effective dielectric constant can be interpreted as the dielectric constant of a homogeneous ~~region~~ medium that equivalently replaces the air in the dielectric regions of the microstrip line as shown in Figure 3.26. The phase velocity and propagation constant are then given by (3.193) and (3.194).

Given the dimensions of the microstrip line, the characteristic impedance can be calculated as

$$Z_0 = \begin{cases} \frac{60}{\sqrt{\epsilon_r}} \ln \left( \frac{8d}{W} + \frac{W}{4d} \right) & \text{for } W/d \leq 1 \\ \frac{120\pi}{\sqrt{\epsilon_r} [W/d + 1.393 + 0.667 \ln(W/d + 1.444)]} & \text{for } W/d \geq 1 \end{cases} \quad (3.196)$$

For a given characteristic impedance  $Z_0$  and dielectric constant  $\epsilon_r$ , the  $W/d$  ratio can be found as:

$$\frac{W}{d} = \begin{cases} \frac{8e^A}{e^{2A} - 2} & \text{for } W/d < 2 \\ \frac{2}{\pi} \left[ \beta - 1 - \ln(2\beta - 1) + \frac{\epsilon_r - 1}{2\epsilon_r} \left\{ \ln(\beta - 1) + 0.39 - \frac{0.61}{\epsilon_r} \right\} \right] & \text{for } W/d > 2 \end{cases}$$

where

$$A = \frac{Z_0}{60} \sqrt{\frac{\epsilon_r + 1}{2}} + \frac{\epsilon_r - 1}{2\epsilon_r} \left( 0.23 + \frac{0.11}{\epsilon_r} \right), \quad \beta = \frac{377\pi}{2Z_0 \sqrt{\epsilon_r}}$$

Considering a microstrip line as a quasi-TEM line, we can determine the attenuation due to dielectric loss as:

$$\alpha_d = \frac{\kappa_0 \epsilon_r (\epsilon_r - 1) \tan \delta}{2\sqrt{\epsilon_r} (\epsilon_r - 1)} \text{ Np/m} \quad (3.198)$$

where  $\tan \delta$  is the loss tangent of the dielectric. This result is derived from (3.30) by multiplying by a "filling factor,":

$$\frac{\epsilon_r (\epsilon_r - 1)}{\epsilon_r (\epsilon_r - 1)}$$

which accounts for the fact that the fields around the microstrip line are partly in air (lossless) and partly in the dielectric (lossy). The attenuation due to conductor loss is given approximately by (3.1)

$$\alpha_c = \frac{\rho_s}{Z_0 W} \text{ Np/m} \quad (3.199)$$

where  $\rho_s = \sqrt{\epsilon_0 \mu_0}/2V$  is the surface resistivity of the conductor. For most microstrip substrates, conductor loss is more significant than dielectric loss; exceptions may occur, however, with some semiconductor substrates.

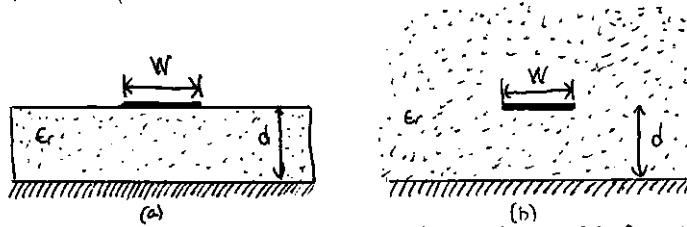


Figure 3.26 Equivalent geometry of a quasi-TEM microstrip line. (a) Original geometry. (b) equivalent geometry, where the dielectric substrate of relative permittivity  $\epsilon_r$  is replaced with the a homogeneous medium of effective relative permittivity  $\epsilon_{eff}$ .

### Example 3.7 Microstrip Line Design

Design a microstrip line on a 0.5mm alumina substrate ( $\epsilon_r=9.9$ ,  $\tan \delta = 0.001$ ) for a  $50\Omega$  characteristic impedance. Find the length of this line required to produce a phase delay of  $270^\circ$  at 10 GHz, and compute the total loss on this line assuming copper conductors. Compare the results obtained from the approximate formulas of (3.195-3.199) with those from a microwave CAD package.

#### Solution

First find  $W/d$  for  $Z_0 = 50\Omega$ , and initially guess that  $W/d < 2$ . From (3.197)

$$A = 2.142, \quad W/d = 2.9654$$

So the condition that  $W/d < 2$  is satisfied; otherwise we would use the expression for  $W/d > 2$ . Then the required line width is  $W = 0.9654d = 0.483$  mm. From (3.195) the effective dielectric constant is  $\epsilon_{eff} = 6.665$ . The line length,  $l$ , for a  $270^\circ$  phase shift is found as:

$$\phi = 270^\circ = \beta l = \sqrt{\epsilon_{eff}} k_0 l, \quad k_0 = \frac{2\pi f}{c} = 209.4 \text{ m}^{-1}, \quad l = \frac{270^\circ (\pi/180^\circ)}{\sqrt{\epsilon_{eff}} k_0} = 8.72 \text{ mm}$$

Attenuation due to dielectric loss is found from (3.198) as  $\alpha_d = 0.255 \text{ Np/m} = 0.022 \text{ dB/cm}$ . The surface resistivity for copper at 10GHz is  $0.026 \Omega$ , and the attenuation due to conductor loss is, from (3.199),  $\alpha_c = 0.0108 \text{ Np/cm} = 0.094 \text{ dB/cm}$ . The total loss on the line is then 0.101dB.

A commercial microwave CAD package gives the following results:  $W = 0.478$  mm,  $\epsilon_{eff} = 6.83$ ,  $l = 8.61$  mm,  $\alpha_d = 0.022 \text{ dB/cm}$ , and  $\alpha_c = 0.054 \text{ dB/cm}$ .

The approximate formulas give results that are within a few percent of the CAD data for line width, effective dielectric constant, line length, and dielectric attenuation. The greatest discrepancy occurs for the attenuation constant for conductor loss.

#### Frequency dependent effects and Higher Order Modes

The results for the parameters of microstrip line presented in the previous section were based on the quasi-static approximation and are strictly valid only at DC (or very low frequencies). At higher frequencies a number of effects can occur that lead to  $\phi$  variations from the quasi-static results for effective dielectric constant, characteristic impedance, and attenuation of microstrip line. In addition, new effects can arise, such as higher-order modes and parasitic resonances.

Because microstrip line is not a true TEM line, its propagation constant is not a linear function of frequency, meaning that the effective dielectric constant varies with frequency. The electromagnetic field that exists on microstrip line involves a hybrid coupling of TM and TE modes, complicated by the boundary condition imposed on air and dielectric substrate interface. In addition, the current on the strip conductor is not uniform across the width of the strip, and this distribution varies with frequency. The thickness of the strip conductor is not uniform across the width of the strip conductor also has an effect on the current distribution and hence affects the line parameters (especially the conductor loss).

The variation with frequency of the parameters of a transmission line is important for several reasons. First, if the variation is significant it becomes important to know and use the parameters at the particular frequency of interest to avoid errors in design or analysis.

Typically, for microstrip line, the frequency variation of the effective dielectric constant is more significant than the variation of characteristic impedance, both terms in terms of relative change and the relative effect on performance. A change in the effective dielectric constant may have a substantial effect on the phase delay through a long section of line, while a small change in characteristic impedance has the primary effect of introducing a small impedance mismatch. Second, a variation in line parameters with frequency means that different frequency components of a broadband signal will propagate differently. A variation in phase velocity, for example, means that different frequency components will arrive at the output of the line at different times, leading to signal dispersion and distortion of input signal.

Third, because of the complexity of modelling these effects, approximate formulas are generally used only for a limited range of frequencies and line parameters, and numerical models are usually more useful.

→ There are a number of approximate formulas, developed from numerical computer solutions and/or experimental data, that have been suggested for predicting the frequency variation of microstrip line parameters [8,9]. A popular frequency-dependent model for the effective dielectric constant has a form similar to the following formula [8]:

$$\epsilon_{\text{eff}}(f) = \epsilon_r - \frac{\epsilon_r - \epsilon_r(0)}{1 + G(f)} \quad (3.200)$$

where  $\epsilon_{\text{eff}}(f)$  represents the frequency-dependent effective dielectric constant,  $\epsilon_r$  is the relative permittivity of the substrate, and  $\epsilon_r(0)$  is the effective dielectric constant of the line at DC, as given by (3.195). The function  $G(f)$  can take various forms, but one suggested in Reference [8] is that  $G(f) = g(f_p/f)^2$ , with  $g = 0.6 + 0.009 Z_0$  and  $f_p = Z_0/8\pi d$  ( $Z_0$  is in Ohms,  $f$  is in frequency (GHz) and  $d$  is in CM). It can be seen from the form of (3.200) that  $\epsilon_{\text{eff}}(f)$  reduces to the DC value  $\epsilon_r(0)$  when  $f=0$  and increases toward  $\epsilon_r$  as frequency increases.

Approximate formulas like the above were primarily developed in the years before computer-aided design tools for RF and microwave engineering became commonly available. (See the Point of Interest on Computer aided design in Chapter 4). Such tools usually give accurate results for a wide range of line parameters and today are usually preferred over closed form approximations.

Another potential difficulty with microstrip line is that it may support several types of higher order modes, particularly at higher frequencies. Some of these are directly related to the TM and TE surface wave modes discussed in Section 3.6, while others are related to waveguide type modes in the cross-section of the line.

The TM<sub>0</sub> Surface wave mode for a grounded dielectric substrate has zero cutoff frequency, as we know from (3.167). Because some of these are directly related—the field lines of this mode are aligned with the field lines of the quasi-TEM mode of a microstrip line, it is possible for coupling to occur from the desired microstrip mode to a surface wave, leading to excess power loss and possibly undesired coupling to adjacent microstrip elements. Because the fields of the TM<sub>0</sub> surface wave are zero at DC, there is little coupling to the quasi-TEM microstrip mode until a critical frequency is reached. Studies have shown that this threshold frequency is greater than zero and less than the cutoff frequency of the TM<sub>11</sub> surface wave mode. A commonly used approximation is [8]

$$f_{T1} \approx \frac{c}{2\pi d} \sqrt{\frac{2}{\epsilon_r - 1}} \tan^{-1} \epsilon_r \quad (3.201)$$

For  $\epsilon_r$  ranging from 1 to 10, (3.201) gives a frequency that is 35% to 66% of  $f_{c1}$ , the cutoff frequency of the TM<sub>11</sub> surface wave mode.

When a microstrip circuit has transverse discontinuities (such as bends, junctions, or even step changes in width), the transverse currents on the conductors that are generated may allow coupling to TE surface wave modes. Most practical microstrip circuits involve such discontinuities, so this type of coupling is often important. The minimum threshold frequency where such coupling becomes important is given by the cutoff of the TE<sub>11</sub> surface wave, from (3.174):

$$f_{T2} \approx \frac{c}{4d\sqrt{\epsilon_r - 1}} \quad (3.202)$$

For wide microstrip lines, it is possible to excite a transverse resonance along the  $x$ -axis of the microstrip line below the strip in the dielectric region because the sides below the strip conductor appear approximately as magnetic walls. This condition occurs when the width is about  $\lambda/2$  in the dielectric, but because of field fringing the effective width of the strip is somewhat larger than the physical width. A rough approximation for the effective width is  $W+d/2$ , so the appropriate threshold frequency for transverse resonance is

$$f_{T3} \approx \frac{c}{\sqrt{\epsilon_r(2W+d)}} \quad (3.203)$$

It is rare for a microstrip line to approach this limit in practice.

Finally, a parallel plate-type-waveguide mode may propagate when the vertical spacing between the strip conductor and ground plane approaches  $\lambda/2$  in the dielectric. Thus, an approximation for the threshold frequency for this mode (valid for all microstrip lines) can be given as

$$f_{T4} \approx \frac{c}{2d\sqrt{\epsilon_r}} \quad (3.204)$$

Thinner microstrip lines will have more fringing fields that effectively lengthen the path between the strip and ground plane, thus reducing the threshold frequency as much as 50%.

The net effect of the threshold frequencies given in (3.201)-(3.204) is to impose an upper frequency limit of operation for a given microstrip geometry. This limit is a function of substrate thickness, dielectric constant, and strip width.

### Example 3.8 Frequency Dependence of Effective dielectric Constant

Use the approximate formula of (3.202) to plot the change in effective dielectric's constant over frequency for a 25Ω microstrip line on a substrate having a relative permittivity of 10.0 and a thickness of 0.65 mm. Compare the calculated phase delay at 10GHz through a 1.093 cm length of line when using  $\epsilon_{\text{eff}}(0)$  versus  $\epsilon_{\text{eff}}(10\text{GHz})$ .

Solution

The required linewidth for a 25Ω impedance is  $w=2.00\text{mm}$ . The effective dielectric constant for this line at low frequencies can be found from (3.1.95) to be  $\epsilon_{\text{eff}}(0)=7.53$ . A short computer program was used to calculate the effective dielectric constant as a function of frequency using (3.202), and the result is shown in Figure 3.27. Comparison with a commercial microwave CAD package shows that the approximate model is reasonably accurate up to about 10GHz but gives an overestimate at higher frequencies.

Using an effective dielectric constant of  $\epsilon_{\text{eff}}(0)=7.53$ , we find the phase delay through a 1.093 cm length of line to be  $\phi_0 = \sqrt{\epsilon_{\text{eff}}(0)} k_0 l = 36^\circ$ . The effective dielectric constant at 10GHz is 8.120 (CAD), with a corresponding phase delay of  $\phi_{10} = \sqrt{\epsilon_{\text{eff}}(10\text{GHz})} k_{10} l = 374^\circ$  — an error of about 14%.

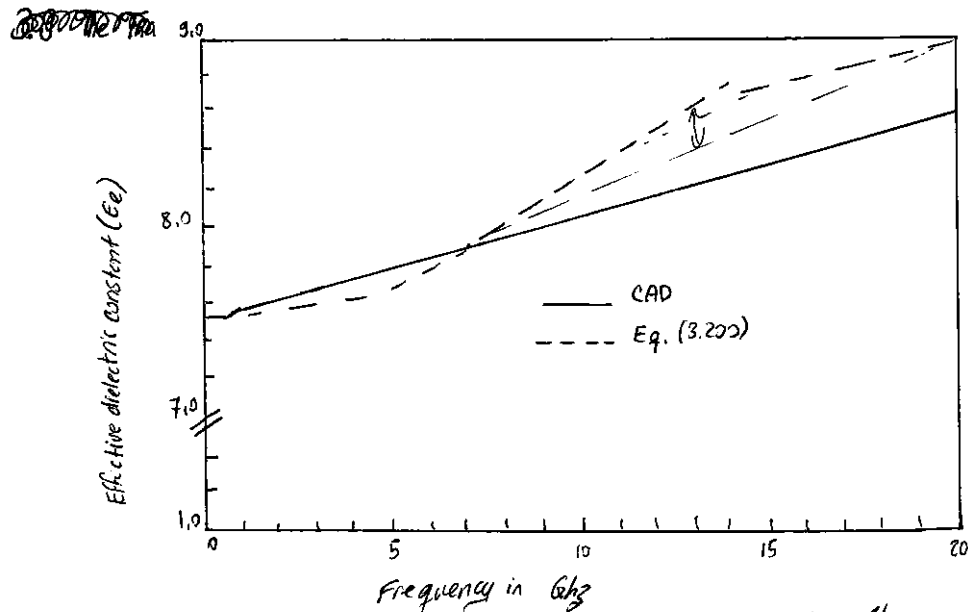


Figure 3.27 Effective Dielectric constant versus frequency for the microstrip line for Example 3.8, comparing the approximate model (3.202) with data from the computer-aided design package.

### 3.9 The Transverse Resonance Technique

According to the general solutions of Maxwell's equations for TE and TM waves given in Section 3.1, a uniform waveguide structure always has a propagation constant of the form:  $\beta = \sqrt{K^2 - K_c^2} = \sqrt{K^2 k_x^2 + k_y^2}$  (3.205)

where  $K_c = \sqrt{k_x^2 + k_y^2}$  is the cutoff wave number of the guide and, for a given mode, is a fixed function of the cross-sectional geometry of the guide. Thus if we know  $K_c$ , we can determine the propagation constant of the guide. In the previous sections we determined  $K_c$  by solving the wave equation in the guide, subject to appropriate boundary conditions. Although this technique is very powerful and general, it can be complicated for complex waveguides, especially if dielectric layers are present. In addition, the wave equation solution gives a complete field description outside the waveguide, which is often more information than we need if we are only interested in the propagation constant of the guide.

The transverse resonance technique employs a transmission line model of the transverse cross section of the waveguide and gives a much simpler and more direct solution for the cutoff frequency. This is another example where circuit and transmission line theory offers a simplified alternative to the field theory solution.

The transverse resonance procedure is based on the fact that in a waveguide cutoff, the fields form standing waves in the transverse plane of the guide, as can be inferred from the "bouncing plane wave" interpretation of waveguide modes discussed in Section 3.2. This situation can be modeled with an equivalent transmission line circuit operating at resonance. One of the following conditions of such a resonant line is the fact that, at any point on the line, the sum of the impedances seen looking to either side must be zero. That is:

$$Z_{\text{in}}^R(x) + Z_{\text{in}}^L(x) = 0 \quad \forall x \quad (3.206)$$

where  $Z_{\text{in}}^R$  and  $Z_{\text{in}}^L$  are the input impedances seen looking to the right and left, respectively, at any point  $x$  on the resonant line.

The transverse resonance technique only gives results for the cutoff frequency of the guide. If the fields or attenuation due to conductor loss are needed, the complete field theory solution will be required. The procedure will be illustrated with an example.

## TE<sub>0n</sub> Modes of a Spatially Loaded Rectangular Waveguide

The transverse resonance technique is particularly useful when the guide contains dielectric layers because the boundary conditions at the dielectric interface, which require the solution of simultaneous algebraic equations in the field theory approach, can be easily handled as functions of different transmission lines.

As an example, consider a rectangular waveguide partially filled with dielectric, as shown in Figure 3.28. To find the cutoff frequencies for the TE<sub>0n</sub> modes, the equivalent transverse resonance circuit shown in the figure can be used. The line for  $\text{cy}_{\text{d}}$  represents the dielectric-filled part of the guide and has a transverse propagation constant  $k_{\text{yd}}$  and a characteristic impedance for the TE modes given by:

$$Z_{\text{yd}} = \frac{k_n}{k_{\text{yd}}} = \frac{k_0 n_0}{k_{\text{ya}}} \quad (3.207a)$$

where  $k_0 = \omega \sqrt{\mu_0 \epsilon_0}$  and  $n_0 = \sqrt{\mu_0 / \epsilon_0}$ . For 1/4 c, the guide is air filled and has a transverse propagation constant  $k_{\text{ya}}$  and an equivalent characteristic impedance given by:

$$Z_{\text{ya}} = \frac{k_0 n_0}{k_{\text{ya}}} \quad (3.207b)$$

Applying condition (3.208) yields

$$k_{\text{ya}} \tan k_{\text{yd}} t + k_{\text{yd}} \tan k_{\text{ya}}(b-t) = 0 \quad (3.208)$$

This equation contains two unknowns,  $k_{\text{ya}}$  and  $k_{\text{yd}}$ . An additional equation is obtained from the fact that the longitudinal propagation constant,  $\beta$ , must be the same in both regions for phase matching of the tangential fields at the dielectric interface. Thus, with  $R_x = 0$ ,

$$\beta = \sqrt{E_r k_0^2 - k_{\text{yd}}^2} = \sqrt{k_0^2 - k_{\text{ya}}^2}$$

or

$$E_r k_0^2 - k_{\text{yd}}^2 = k_0^2 - k_{\text{ya}}^2$$

Equations (3.208) and (3.209) can be solved (numerically or graphically) to obtain  $k_{\text{yd}}$  and  $k_{\text{ya}}$ . There will be an infinite number of solutions, corresponding to the  $n$  dependence (number of variations in  $y$ ) of the TE<sub>0n</sub> mode.

## 3.10 Wave Velocities and Dispersion.

We have so far encountered two types of velocities related to the propagation of electro-magnetic waves:

- The speed of light in a medium ( $1/\sqrt{\mu\epsilon}$ )
- The phase velocity ( $v_p = \omega/\beta$ )

The speed of light in a medium is the velocity at which a plane wave would propagate in that medium, while the phase velocity is the speed at which a constant phase front travels.

For a TEM wave, these two quantities are identical, but for other types of guided wave propagation the phase velocity may be greater or less than this speed of light.

If the phase velocity and attenuation of a line or guide are constants that do not change with frequency, then the phase of a signal that contains more than one frequency component will not be distorted. If the phase velocity is different for different frequencies, then the individual frequencies will not maintain their original phase relationships as they propagate down the transmission line or waveguide, and signal distortion will occur. Such an effect is called dispersion since different phase velocities allow the "faster" waves to lead in phase relative to the "slower" phase waves, and the original phase relationships will gradually be dispersed as the signal propagates down the line. In such a case, there is no single phase velocity that can be attributed to the signal as a whole. However if the bandwidth of the signal is relatively small or if the dispersion is not too severe, a group velocity can be defined in a meaningful way. The velocity can be used to describe the speed at which the signal propagates.

Group Velocity / As discussed earlier, the physical interpretation of group velocity is the velocity at which a narrowband signal propagates. We will derive the relation of group velocity to the propagation constant by considering the signal  $f(t)$  in the time domain. The Fourier transform of the signal is defined as:

$$F(\omega) = \int_{-\infty}^{\infty} f(t) e^{-j\omega t} dt \quad (3.210a)$$

$$\text{and the inverse transform is: } f(t) = \frac{1}{2\pi} \int_{-\infty}^{\infty} F(\omega) e^{j\omega t} d\omega \quad (3.210b)$$

Now consider the transmission line or waveguide on which the signal  $f(t)$  is propagating as a linear system with a transfer function  $Z_i(\omega)$  that relates the output,  $F_o(\omega)$ , of the line to the input,  $F_i(\omega)$ , of the line, as shown in Figure 3.29. Thus,

$$F_o(\omega) = Z_i(\omega) F_i(\omega) \quad (3.211)$$

For a lossless matched transmission line or waveguide, the transfer function  $Z_i(\omega)$  can be expressed as

$$Z_i(\omega) = A e^{-j\beta z} = |Z_i(\omega)| e^{-j\phi} \quad (3.212)$$

where  $A$  is a constant and  $\beta$  is the propagation constant of the line or guide.

The time domain representation of the output signal,  $f_o(t)$ , can then be written as:

$$f_o(t) = \frac{1}{2\pi} \int_{-\infty}^{\infty} F_i(\omega) |Z_i(\omega)| e^{j\omega t - j\phi} d\omega \quad (3.213)$$

$$F_i(\omega) \rightarrow [Z_i(\omega)] \rightarrow F_o(\omega)$$

Figure 3.29 A transmission line or waveguide represented as a linear system with transfer function  $Z_i(\omega)$ .

If  $|Z(\omega)| = A$  is constant and the phase  $\Psi$  of  $Z(\omega)$  is a linear function of  $\omega$ , say  $\Psi = \alpha\omega$ , the output can be expressed as:

$$f_o(t) = \frac{1}{2\pi} \int_{-\infty}^{\infty} AF(\omega) e^{j\omega(t-a)} d\omega = A f(t-a) \quad (3.214)$$

which is seen to be a replica of  $f(t)$ , except for an amplitude factor  $A$  and time shift  $a$ . Thus, a transfer function of the form  $Z(\omega) = A e^{-j\omega a}$  does not distort the input signal. A lossless TEM wave has a propagation constant  $\beta = \omega/c$ , which is of this form, so a TEM line is dispersionless and does not lead to signal distortion. If the TEM line is lossy, however, the attenuation may be a function of frequency, which could lead to signal distortion.

Now consider a narrowband input signal of the form

$$s(t) = f(t) \cos \omega_0 t = \Re \{ f(t) e^{j\omega_0 t} \} \quad (3.215)$$

which represents an amplitude-modulated carrier wave of frequency  $\omega_0$ . Assume that the highest frequency component of  $f(t)$  is  $\omega_m$ , where  $\omega_m < \omega_0$ . The Fourier transform,  $S(\omega)$ , of  $s(t)$ , is:

$$S(\omega) = \int_{-\infty}^{\infty} f(t) e^{-j\omega t} e^{j\omega_0 t} dt = F(\omega - \omega_0) \quad (3.216)$$

where we have used the complex form of the input signal as expressed as (3.215). We will need to take the real part of the output inverse transform to obtain the time domain output signal. The spectra of  $F(\omega)$  and  $S(\omega)$  are depicted in Figure 3.30.

The output signal spectrum is:

$$S_o(\omega) = A F(\omega - \omega_0) e^{j\beta z} \quad (3.217)$$

and in the time domain,

$$s_o(t) = \frac{1}{2\pi} \operatorname{Re} \int_{-\infty}^{\infty} S_o(\omega) e^{j\omega t} d\omega = \frac{1}{2\pi} \operatorname{Re} \int_{\omega_0 - \omega_m}^{\omega_0 + \omega_m} A F(\omega - \omega_0) e^{j(\omega t - \beta z)} d\omega. \quad (3.218)$$

In general, the propagation constant  $\beta$  may be a complicated function of  $\omega$ . However, if  $F(\omega)$  is narrowband ( $\omega_m \ll \omega_0$ ), then  $\beta$  can often be linearized by using a Taylor series expansion about  $\omega_0$ :

$$\beta(\omega) = \beta(\omega_0) + \left. \frac{d\beta}{d\omega} \right|_{\omega=\omega_0} (\omega - \omega_0) + \frac{1}{2} \left. \frac{d^2\beta}{d\omega^2} \right|_{\omega=\omega_0} (\omega - \omega_0)^2 + \dots \quad (3.219)$$

Retaining the first two terms gives:

$$\beta(\omega) \approx \beta_0 + \beta'_0 (\omega - \omega_0) \quad (3.220)$$

where

$$\beta_0 = \beta(\omega_0), \quad \beta'_0 = \left. \frac{d\beta}{d\omega} \right|_{\omega=\omega_0}$$

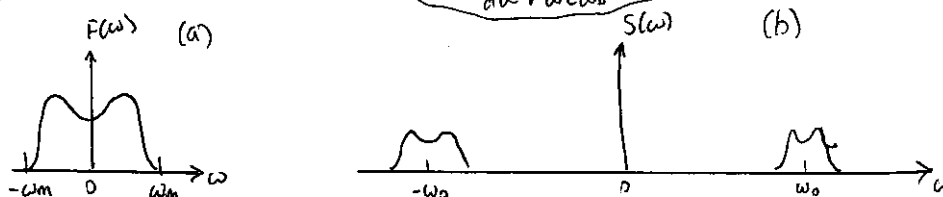


Figure 3.30 Fourier Spectra of the Signals (a)  $f(t)$  and (b)  $s(t)$

After a change of variables to  $y = \omega - \omega_0$ , the expression for  $S_o(t)$  becomes

$$S_o(t) = \frac{A}{2\pi} \operatorname{Re} \left\{ e^{j\omega_0 t - j\beta_0 z} \int_{-\omega_m}^{\omega_m} F(y) e^{j(yt - \beta'_0 z)} dy \right\}$$

$$\text{LHS} = A \operatorname{Re} \{ f(t - \beta'_0 z) e^{j\omega_0 t - j\beta_0 z} \}$$

$$\text{LHS} = A f(t - \beta'_0 z) \cos(\omega_0 t - \beta_0 z) \quad (3.221)$$

which is a time-shifted replica of the original modulation envelope,  $f(t)$ , of (3.215). The velocity of this envelope is the group velocity,  $v_g$ :

$$v_g = \frac{1}{\beta'_0} = \left( \frac{d\beta}{d\omega} \right)^{-1} \Big|_{\omega=\omega_0} \quad (3.222)$$

### Example 3.9 Waveguide wave velocities.

Calculate the group velocity for the waveguide mode propagating in an air-filled guide. Compare this velocity to the phase velocity and speed of light.

Solution

The propagation constant for a mode in an air-filled waveguide is

$$\beta = \sqrt{k_0^2 - k_c^2} = \sqrt{(\frac{\omega}{c})^2 - k_c^2}$$

Taking the derivative with respect to frequency gives

$$\frac{d\beta}{d\omega} = \frac{\frac{\omega}{c^2}}{\sqrt{(\omega/c)^2 - k_c^2}} = \frac{k_0}{c\beta}$$

So from (3.222) the group velocity is

$$v_g = \left( \frac{d\beta}{d\omega} \right)^{-1} = \frac{c\beta}{k_0}$$

The phase velocity is  $v_p = \omega/\beta = c\omega/k_0$ . Since  $\beta < k_0$ , we have that  $v_g \ll v_p$ , which indicates that the phase velocity of a waveguide mode may be greater than the speed of light, but the group velocity (the velocity of a narrow-band signal) will be less than the speed of light.

### 3.11 Summary of Transmission Lines and Waveguides

We have discussed a variety of transmission lines and waveguides in this chapter, and here we will summarize some of the basic properties of these transmission media and their relative advantages in a broader context.

We make a distinction between TEM, TE, and TM waves and soon find that transmission lines and waveguides can be categorized according to which type of waves they can support. We saw that TEM waves are non-dispersive, with no cutoff frequency, while TM and TE waves exhibit dispersion and generally have non-zero cutoff frequencies. Other electrical considerations include bandwidth, attenuation, and power-handling capacity. Mechanical factors are also very important, however, and include such considerations as physical size (volume and weight), ease of fabrication (cost), and integrability (active or passive).

Table 3.6 compares several types of transmission media with regard to these considerations; this table only gives general guidelines, as specific cases may give better or worse results than those indicated.

TABLE 3.6 Comparison of Common Transmission Lines and Waveguides

Characteristic	Coax	Waveguide	Slotline	Microstrip
Modes: Preferred, other	TEM	TE <sub>10</sub>	TEM	Quasi-TEM
TM, TE	TM, TE	TM, TE	Hybrid TM, TE	
Dispersion	None	Medium	None	Low
Bandwidth	High	Low	High	High
Loss	Medium	Low	High	High
Power Capacity	Medium	High	Low	Low
Physical Size	Large	Large	Medium	Small
Ease of fabrication	Medium	Medium	Easy	Easy
Integratability	Hard	Hard	Fair	Easy

### Other Types of Lines and guides

Although we have discussed the most common types of waveguides and transmission lines, there are many other guides and lines (and many variations) that we are not able to present in detail. A few of the more popular types are briefly mentioned here.

#### Ridge waveguide:

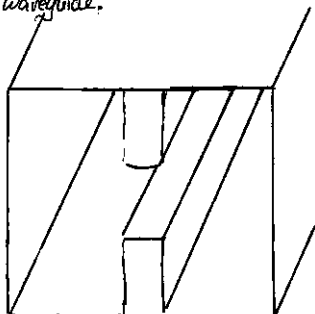


Figure 3.31 Cross-section of a Ridge waveguide. The practical bandwidth of rectangular waveguide is slightly less than an octave (a 2:1 frequency range). This is because the TE<sub>00</sub> mode begins to propagate at a frequency equal to twice the cutoff frequency of the TE<sub>10</sub> mode. The ridge waveguide shown in Figure 3.31, consists of a rectangular waveguide loaded with conducting ridges on the top and/or bottom walls. This loading tends to lower the cutoff frequency of the dominant mode, leading to increased bandwidth and better (more constant) impedance characteristics. Ridge waveguides are often used for impedance matching purposes, where the ridge may be tapered along the length of the line. The presence of the ridge, however, reduces the ground bonding capability of the waveguide.

The practical bandwidth of rectangular waveguide is slightly less than an octave (a 2:1 frequency range). This is because the TE<sub>00</sub> mode begins to propagate at a frequency equal to twice the cutoff frequency of the TE<sub>10</sub> mode. The ridge waveguide shown in Figure 3.31, consists of a rectangular waveguide loaded with conducting ridges on the top and/or bottom walls. This loading tends to lower the cutoff frequency of the dominant mode, leading to increased bandwidth and better (more constant) impedance characteristics. Ridge waveguides are often used for impedance matching purposes, where the ridge may be tapered along the length of the line. The presence of the ridge, however, reduces the ground bonding capability of the waveguide.

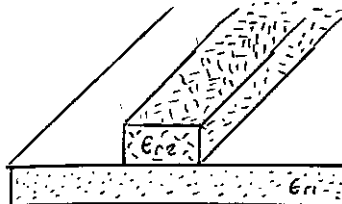


Figure 3.32 Dielectric waveguide

#### Dielectric waveguide:

As we have seen from our study of surface waves, metallic conductors are not necessary to confine and support a propagating electromagnetic field. The dielectric waveguide shown in Figure 3.32 is another example of such a guide, where  $\epsilon_{rz}$ , the dielectric constant of the ridge, is usually greater than  $\epsilon_{ri}$ , the dielectric of the substrate. The fields are thus mostly confined to the ridge and the surrounding area. This type of guide supports TM and TE modes, and is convenient for miniaturization and integration with active devices. Its small size makes it useful for millimeter wave to optical frequencies, although it can be very lossy at bends or junctions in the ridge line. Many variations of basic geometry are possible.

**Slotline:** Slotline is another one of the many possible types of planar transmission lines. The geometry of a slotline is shown in Figure 3.33. It consists of a thin slot in the ground plane on one side of a dielectric substrate. Thus, like a microstrip line, the two conductors of slotline lead to quasi-TEM type of mode. The width of the slot controls the characteristic impedance of the line.

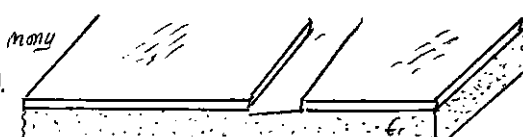
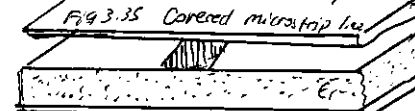


Figure 3.33 Geometry of a printed slotline.

**Coplanar waveguide:** The coplanar waveguide, shown in Figure 3.34 is similar to the slotline, and can be viewed as a slotline with a third conductor centered in the slot region. Because of the presence of the additional conductor, this type of line can support even or odd quasi-TEM modes, depending on whether the electric fields in the two slots are in the opposite or the same direction. Coplanar waveguides are particularly useful for fabricating active circuitry due to the presence of a central conductor and close proximity to the ground planes.

#### Covered microstrip:



Many variations of the basic microstrip line geometries are possible, but one of the most common is the covered microstrip, shown in Figure 3.35. The metallic cover plate is often used for electrical shielding and physical protection of the microstrip circuitry and is usually situated several substrate thickness away from the circuit. Its presence, however, can affect the operation of the circuit enough so that its effects must be taken into account during design.

## Top Point of Interest Power Capacity of Transmission Lines

The power-handling capacity of an air-filled transmission line or waveguide is usually limited by voltage breakdown, which occurs at a field strength of about  $E_d = 3.106 \text{ V/m}$  for room temperature air at sea level pressure. Thermal effects may also serve to limit the power capacity of some types of lines.

In an air-filled coaxial line the electric field varies as  $E_p = V_0 / \ln b/a$ , which has a maximum at  $r=a$  (at the inner conductor). Thus the maximum voltage before breakdown is :  $V_{max} = E_d a \ln b/a / (P_p)$ ,

and the maximum power capacity is then:

$$P_{max} = \frac{V_{max}^2}{2Z_0} = \frac{\pi a^2 E_d^2 \ln b/a}{\eta_0}$$

As might be expected, this result shows that power capacity can be increased by using a longer coaxial cable (larger  $a, b$  with fixed  $\eta_0$  for the same characteristic impedance). However, propagation of higher order modes limits the maximum operating frequency for a given cable size. Thus, there is an upper limit on the power capacity of a coaxial line for a given maximum operating frequency,  $f_{max}$ , which can be shown to be given by

$$P_{max} = \frac{0.025}{\eta_0} \left( \frac{c E_d}{f_{max}} \right)^2 = 5.8 \cdot 10^{-12} \left( \frac{E_d}{f_{max}} \right)^2$$

As an example, at 10 GHz the maximum peak power capacity of any coaxial line with no higher order modes is about 520 kW.

In an air-filled rectangular waveguide the electric fields varies as  $E_y = E_0 \sin(\frac{\pi x}{a})$ , which has a maximum value of  $E_0$  at  $x=a/2$  (the middle of the guide). Thus the maximum power capacity before breakdown is

$$P_{max} = \frac{ab E_0^2}{4Z_0} = \frac{ab E_d^2}{4Z_0}$$

which shows that power capacity increases with guide size. For most standard waveguides,  $b \approx 2a$ . To avoid propagation of the TE<sub>01</sub> mode we must have  $a < c/f_{max}$ , where  $f_{max}$  is the maximum operating frequency. Then the maximum power capacity of the guide can be shown to be:

$$P_{max} = \frac{0.11}{\eta_0} \left( \frac{c E_d}{f_{max}} \right)^2 = 2.6 \cdot 10^{-13} \left( \frac{E_d}{f_{max}} \right)^2$$

As an example, at 10 GHz the maximum peak power capacity of rectangular waveguide operating in the TE<sub>01</sub> mode is about 2300 kW, which is considerably higher than the power capacity of a coaxial cable at the same frequency.

Because arcing and voltage breakdown are high-speed transients, the voltage power limit one peak values; average power capacity is lower. In addition, it is good engineering practice to provide a safety factor of at least two. So the maximum powers that can be safely transmitted should be limited to about half of the above values. If there are reflections on the line or guide, the power capacity should be further reduced. In the worst case, a reflection coefficient magnitude of unity will double the maximum voltage on the line so the power capacity will be reduced by a factor of four.

The power capacity of a line can be increased by pressurizing the line with air or inert gas, or by using a dielectric. The dielectric strength ( $E_d$ ) of dielectric materials is greater than that of air, but the power capacity may further be limited by the heating resulting from the dielectric due to ohmic loss.

References : P.A. Rizzi, *Microwave Engineering - Passive Circuits*, Prentice-Hall, Englewood Cliffs, N.J., 1988.

- References .
- [1] C. Heaviside, *Electromagnetic Theory*, Vol 1, 1893. Reprinted by Dover, NY.
- [2] Lord Rayleigh, "On the Passage of Electric Waves Through Tubes," *Philosophical Magazine*, Vol. 43,
- [3] H.S. Parkard, "The origin of Waveguides: A Case of Multiple Rediscovery," *IEEE Transactions on Microwave Theory and Techniques*, Vol MTT-32, pp. 369, September 1984.
- [4] R. M. Barnett, "Microwave Printed Circuits - An Historical Perspective," *IEEE Transactions on microwave theory and techniques*, Vol. MTT-32, pp. 983-990, September 1984.
- [5] D.O. Grigs and H.F. Engelemon, "Microstrip - A New Transmission Technique for the Millimeter Range," *Proceedings of the IRE*, Vol. 40, pp. 1644-1650.
- [6] H. Howe, Jr., *Stripline Circuit Design*, Artech House, Dedham, Mass., 1974.
- [7] I.J. Bahl and R. Garg, "A Designers Guide to Stripline Circuits," *Micro*, January 1978, pp. 33-36.
- [8] I.J. Bahl and J.K. Trivedi, "A Designers Guide to Microstrip Line," *Micro*, May 1977, pp. 174-182.
- [9] K.C. Gupta, R. Garg, and I.J. Bahl, *Microstrip Lines and Slotline*, Artech House, Dedham, Mass., 1979.

Problems 3.1 Devise at least two variations of the basic Coaxial Transmission line geometry of Section 3.5, and discuss the advantages and disadvantages of your proposed lines in terms of size, loss, cost, higher order modes, dispersion, or other considerations. Repeat this exercise for the microstrip line geometry of Section 3.8.

3.2 Derive equations (3.5a) - (3.5d) from equations (3.3) and (3.4).

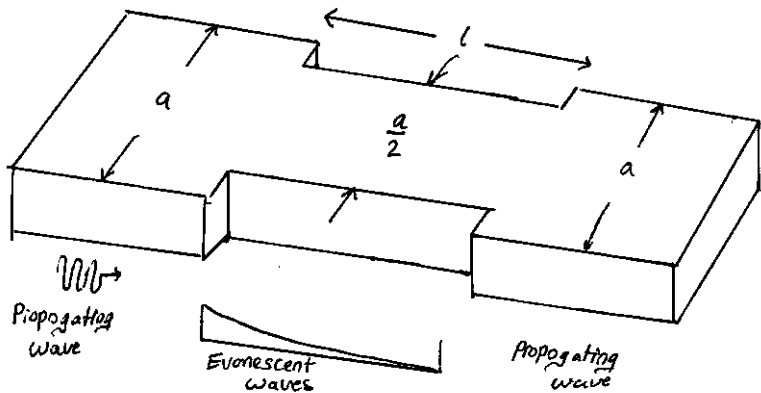
3.3 Calculate the attenuation due to conductor loss for the TE<sub>n</sub> mode of a parallel split waveguide.

3.4 Consider a section of air-filled H-band waveguide. From the dimensions given in Appendix I, determine the cutoff frequencies of the first two propagating modes. From the recommended operating range in Appendix I for the guide, determine the percentage reduction in bandwidth that this operating range represents, relative to the theoretical bandwidth for a single propagating mode.

3.5 A 10cm length of a K-band copper waveguide is filled with dielectric material with  $\epsilon_r = 2.55$  and  $\tan \delta = 0.0015$ . If the operating frequency is 12 GHz, determine the required length 15 GHz, find the total loss through the guide and the phase delay from the input to the output of the guide.

3.6 An attenuator can be made using a section of waveguide operating below cutoff, as shown in the accompanying figure. If  $a = 2.286$  cm and the operating frequency is 12 GHz, determine the required length of the below-cutoff section of waveguide to achieve an attenuation of 10 dB between the input and output guides.

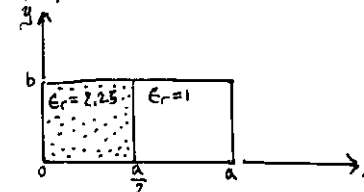
Ignore the effect of reflections at step discontinuities.



3.7 Find expressions for the electric surface current density on the walls of a rectangular waveguide for a TE<sub>10</sub> mode. Why can a narrow slot be cut along the center line of the broad wall of a rectangular waveguide without perturbing the operation of the guide? (Such a slot is often used in a slotted line for a probe to sample the standing wave field inside the guide).

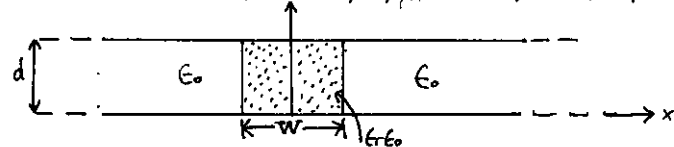
3.8 Derive the expression for the attenuation of the TM<sub>mn</sub> mode of a rectangular waveguide due to imperfectly conducting walls.

3.9 For a partially loaded rectangular waveguide shown in the accompanying figure, solve (3.109) with  $\beta=0$  to find the cutoff frequency of the TE<sub>10</sub> mode. Assume  $a=2.286$  cm,  $b=a/2$ , and  $\epsilon_r=2.25$ .



3.10 Consider the partially filled parallel plate waveguide shown in the accompanying figure. Derive the solution (fields of cutoff frequency) for the lowest order TE mode of this structure. Assume the metal plates are infinitely wide.

Can a TEM wave propagate on this structure?



3.11 Derive equations (3.110a)-(3.110d) for the transverse field components in terms of longitudinal fields, in cylindrical coordinates.

3.12 Derive the expression for the attenuation of the TM<sub>mn</sub> mode in the circular waveguide with finite conductivity.

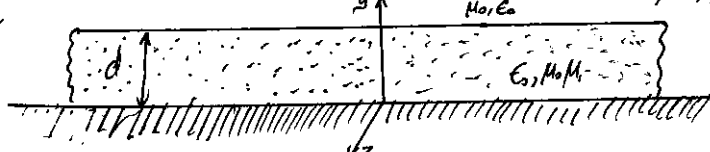
3.13 A circular copper waveguide has a radius of 0.4 cm and is filled with a dielectric material having  $\epsilon_r = 1.5$  and  $\tan \delta = 0.002$ . Identify the first four propagating modes and their cutoff frequencies. For the dominant mode, calculate the total attenuation at 20 GHz.

3.14 Derive the E and H fields of a coaxial line from the expression for the potential given in (3.153). Also find expressions for the voltage and current on the line and the characteristic impedance.

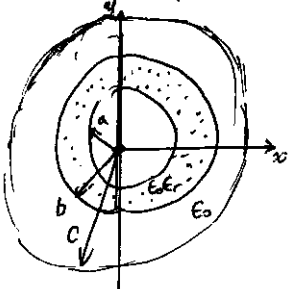
3.15 Derive the transcendental equation for the cutoff frequency of the TM modes of a coaxial waveguide. Using tables, obtain an approximate value of  $k_z a$  for the TM<sub>11</sub> mode if  $b/a = 2$ .

3.16 Derive an expression for the attenuation of a TE surface wave on a grounded dielectric substrate when the ground plane has finite conductivity.

3.17 Consider the grounded magnetic substrate shown in the accompanying figure. Derive a solution for the TM surface waves that can propagate on this structure.



3.18 Consider the partially filled coaxial line shown in the accompanying figure. Can a TEM wave propagate on this line? Derive the solution for the TM<sub>0m</sub> (no azimuthal variation) modes of this geometry.



3.19 A copper stripline transmission line is to be designed for a  $10\Omega$  characteristic impedance. The ground plane separation is 1.02 mm and the dielectric constant 2.20, with  $\tan \delta = 0.001$ . At 5 GHz, find the guide wavelength on the line and the total attenuation.

3.20 A copper microstrip transmission line is to be designed for a  $10\Omega$  characteristic impedance. The substrate is 0.51 mm thick, with  $\epsilon_r = 2.20$  and  $\tan \delta = 0.001$ . At 5 GHz, find the guide wavelength on the line and the total attenuation. Compare these results with those for the similar stripline case of the preceding problem.

3.21. A  $100\Omega$  microstrip line is printed on a substrate of thickness 0.0762 cm with a dielectric constant of 2.2. Ignoring losses and fringing field, find the shortest length of this line that appears at its input as a capacitor of 5 pF at 2.5 GHz. Repeat for an inductance of 5 nH. Using a microwave CAD package with a physical model for a microstrip line, compute the actual input impedance seen when losses are included (assume copper conductors and  $\tan \delta = 0.001$ ).

3.22 A microwave antenna feed network operating at 5 GHz requires a  $5\Omega$  printed transmission line that is 16λ long. Possible choices are (1) copper microstrip with  $d = 0.16$  cm,  $\epsilon_r = 2.20$ , and  $\tan \delta = 0.001$ , or (2) copper stripline, with  $b = 0.32$  cm,  $\epsilon_r = 2.20$ ,  $t = 0.01$  mm, and  $\tan \delta = 0.001$ . Which line should be used if attenuation is to be minimized.

3.23 Consider the TE modes of an arbitrary uniform waveguiding structure in which the transverse fields are related to  $H_3$  as in 3.19). If  $H_3$  is of the form  $H_3(x,y,z) = h_3(x,y)e^{-jBz}$ , where  $h_3(x,y)$  is a real function, compute the Poynting vector and show that Real power-flow flows only in the z direction. Assume  $B$  is real, corresponding to the propagating mode.

3.24 A piece of rectangular waveguide is filled with air for  $z < 0$  and dielectric filled for  $z > 0$ . Assume that both regions can support only the dominant TE<sub>10</sub> mode and that a TE<sub>10</sub> mode is incident on the interface from  $z < 0$ . Using a field analysis, write general expressions for the transverse field components of the incident, reflected, and transmitted waves in the two regions and enforce the boundary conditions at the dielectric interface to find the reflection and transmission coefficients. Compare these results to those obtained with an impedance approach, using ZFE for each region.

3.25 Use the transverse resonance technique to derive a transcendental equation for the propagation constant of the TM modes of a rectangular waveguide that is filled with air for  $0 < z < a$  and dielectric filled for  $z > a$ .

3.26 Apply the transverse resonance technique to find the propagation constants for the TE surface waves that can be supported by the structure of problem 3.17.

3.27 An X-band waveguide filled with hexolite is operating at 9.06 GHz. Calculate the speed of light in this material and the phase and group velocities in the waveguide.

3.28 As discussed in the point of interest on the power-handling capacity of transmission lines, the maximum power capacity of a coaxial line is limited by voltage breakdown and is given by

$$P_{\text{max}} = \frac{\pi a^2 E_d^2}{\eta_0} \ln \frac{b}{a}$$

where  $E_d$  is the field strength at breakdown. Find the value of  $b/a$  that maximizes the maximum power capacity and show that the corresponding characteristic impedance is  $80\Omega$ .

3.29 A microstrip circuit is fabricated on an aluminum substrate having a dielectric constant of 9.9, a thickness of 2.0 mm, and a  $50\Omega$  linewidth of 1.93 mm. Find the threshold frequencies of the four higher order modes discussed in Section 3.8, and recommend the maximum operating frequency for this microstrip circuit.

## Chapter Four) Microwave Network Analysis.

Circuits operating at low frequencies, for which the circuit dimensions are small relative to the wavelength, can be treated as an interconnection of lumped passive or active components with unique voltages and currents defined at any point in the circuit. In this situation the circuit dimensions are small enough such that there is negligible phase delay from one point in the circuit to another. In addition, the fields can be considered as TEM fields supported by two or more conductors.

This leads to a quasi-static type of solution to Maxwell's equations and to the well known Kirchhoff voltage and current laws and impedance concepts in circuit theory [2]. As the reader is aware, there is a powerful and useful set of techniques for analyzing low-frequency circuits.

In general, these techniques cannot be directly applied to microwave circuits, but it is the purpose of the present chapter to show how basic circuit and network concepts can be extended to handle many microwave analysis and design problems of practical interest.

→ The main reason for doing this is that it is usually much easier to apply the simple and intuitive ideas of circuit analysis to a microwave problem than it is to solve Maxwell's equations for the same problem. In a way, field analysis gives us much more information about the particular problem under consideration than we actually need. That is, because the solution to Maxwell's equations for a given problem is complete, it gives the electric and magnetic fields at all points in space. However, usually we are only interested in voltage and current at a set of terminals, the power flow through the device, or some other type of "terminal" property, as opposed to the minute field descriptions at all points of space. Another reason for using circuit or network analysis is that it is then very easy to modify the original problem, or combine several elements together to find a response, without having to reanalyze in detail the behavior of each element in combination with its neighbors. A field analysis using Maxwell's equations for such problems would be hopelessly difficult. There are situations, however, in which such circuit analysis techniques are an oversimplification which may lead to erroneous results. In cases such as these one must resort to field analysis approaches, using Maxwell's equations. Fortunately, there are a number of commercially available computer-aided design packages that can model RF and microwave problems using both field theory analysis and network analysis.

It is part of the education of a microwave engineer to be able to determine when network analysis concepts apply and when they should be cast aside in favor of more rigorous analysis.

→ The basic procedure for microwave network analysis is as follows. We first treat a set of basic, canonical problems rigorously, using field analysis and Maxwell's equations (as we have done in chapters 2+3) for a variety of transmission line and waveguide problems. When so doing, we try to obtain quantities that can directly be related to circuit and transmission line parameters. For example, when we treated various transmission lines and waveguides in chapter 3 we derive the propagation constant and characteristic impedance of the line. This allowed the transmission line or waveguide to be treated as an idealized distributed component characterized by its length, propagation constant, and characteristic impedance of the line. This allowed the transmission guide or waveguide to be treated as an ideally distributed component characterized by its length, propagation constant, and characteristic impedance. At this point, we can interconnect various components and use network and/or transmission line theory to analyze the behavior of the entire system of components, including effects such as multiple reflections, loss, impedance transformations, and transitions from one transmission medium to another. (e.g. coax to microstrip). As we will see, a transmission transition between different transmission lines, or a discontinuity on a transmission line, generally cannot be treated as a simple junction between two transmission lines, but typically includes some type of equivalent circuit to account for the reactances associated with the transition or discontinuity.

→ Microwave network theory was originally developed in the service of Radar systems and component development at the MIT Radiation Lab in the 1940s. This work was continued at the Polytechnic Institute of Brooklyn and other locations by researchers such as E. Weber, N. Marcuvitz, A.A. Oliner, L.B. Felsen, A. Hessel, and many others [2].

## 4.1 Impedance And Equivalent Voltage And Currents

### Equivalent Voltages and Currents

At microwave frequencies the measurement of voltage and currents is difficult (or impossible), unless a clearly defined terminal pair is available.

Such a terminal pair may be present in the case of TEM-type lines (such as coaxial cable, microstrip line, or stripline), but does not strictly exist for non-TEM lines (such as rectangular, circular, or surface waveguides).

Figure 4.1 Shows the electric and magnetic field lines for an arbitrary two-conductor TEM transmission line. As in chapter 3, the voltage,  $V$ , of the + conductor relative to the - conductor can be found as :

$$V = \int_{-b}^b \vec{E} \cdot d\vec{l} \quad (4.1)$$

where the integration path begins on the + conductor and ends on the (-) conductor. It is important to realize that, because of the electrostatic nature of the transverse fields between the two conductors, the voltage defined in (4.1) is unique and does not depend on the shape of the integration path. The total current flowing on the + conductor can be determined from the application of Ampere's law as:  $I = \oint_C \vec{H} \cdot d\vec{l}$

where the integration contour is any closed path enclosing the + conductor (but not the - conductor). A characteristic impedance  $Z_0$  can then be defined for traveling waves as:

$$Z_0 = \frac{V}{I} \quad (4.3)$$

At this point, after having defined and determined a voltage, current, and characteristic impedance (and assuming we know the propagation constant for the line), we can proceed to apply the circuit theory for transmission lines developed in chapter 2 to characterize this line as a circuit element.

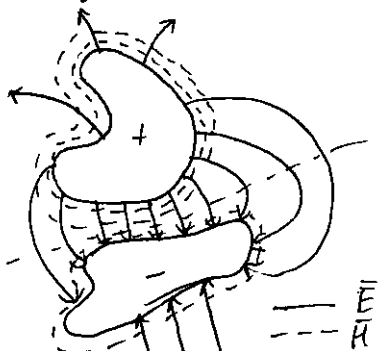


Figure 4.1 Electric and magnetic field lines for an arbitrary two-conductor TEM line.

The situation is more difficult for waveguides. To see why, we will look at the case of a rectangular waveguide as shown in figure 4.2.

For the dominant TE<sub>10</sub> mode, the transverse fields can be written as, from Table 3.2:

$$\{ E_y(x,y,z) = \frac{j\omega a}{\pi} A \sin \frac{\pi x}{a} e^{-jBz} = A e_y(x,y) e^{-jBz} \quad (4.4a) \}$$

$$\{ H_x(x,y,z) = \frac{jB a}{\pi} A \sin \frac{\pi x}{a} e^{-jBz} e^{jBz} = A h_x(x,y) e^{-jBz} \quad (4.4b) \}$$

Figure 4.2 Electric field lines for the TE<sub>10</sub> mode of the rectangular waveguide.

Applying (4.1) to the electric field of (4.4a) gives:  $V = \frac{-j\omega a}{\pi} A \sin \frac{\pi x}{a} e^{-jBz} \int_y dy$

Thus it is seen that the voltage depends on the position,  $x$ , as well as the length of the integration contour along the  $y$  direction. For example, integrating from  $y=0$  to  $b$  for  $x=a/2$  gives a voltage that is quite different from that obtained from  $y=0$  to  $b$  for  $x=0$ . What then is the correct voltage? The answer is that there is no "correct" voltage in a sense of being unique and pertinent for all applications. A similar problem arises with current and impedance. We will now show we can define equivalent voltages, currents, and impedances that can be useful for non-TEM lines.

There are many ways to define equivalent voltage, current, and impedance for waveguides since these quantities are not unique for non-TEM lines, but the following considerations usually lead to the most useful results [1,3,4].

- Voltage and Current are defined only for a particular waveguide mode, and are defined so that the voltage is proportional to the transverse electric field and the current is proportional to the transverse magnetic field.
- In order to be useful in manners similar to voltages and currents of circuit theory, the equivalent voltage and current should be defined so that their product gives the power flow of the waveguide mode.
- The ratio of the current and voltage to the current for a single traveling wave should be equal to the characteristic impedance of the line. That impedance may be chosen arbitrarily, but is usually selected as equal to the wave impedance of the line, or else normalized to unity.

For an arbitrary waveguide made both positively and negatively traveling waves the transverse fields can be written as:

$$\bar{E}_t(x,y,z) = \bar{e}(x,y)(A^+ e^{-jBz} + A^- e^{jBz}) = \frac{\bar{e}(x,y)}{C_1} (V e^{jBz} + V' e^{-jBz}) \quad (4.6a)$$

$$\bar{H}_t(x,y,z) = \bar{h}(x,y)(A^+ e^{-jBz} - A^- e^{jBz}) = \frac{\bar{h}(x,y)}{C_2} (I^+ e^{-jBz} - I^- e^{jBz}) \quad (4.6b)$$

where  $\bar{e}$  and  $\bar{h}$  are the transverse field variations of the mode, and  $A^+$ ,  $A^-$  are the field amplitudes of the traveling waves. Because  $\bar{E}_t$  and  $\bar{H}_t$  are related by the wave impedance,  $Z_{\text{w}}$ , according to (3.22) or (3.26), we have also that:  $\bar{h}(x,y) = \hat{Z} \times \bar{e}(x,y) / Z_{\text{w}}$   $(4.7)$

Equation (4.6) also defines equivalent voltage and current waves as:

$$V(z) = V^+ e^{jBz} + V^- e^{-jBz} \quad (4.8a)$$

$$I(z) = I^+ e^{-jBz} - I^- e^{jBz} \quad (4.8b)$$

with  $V^+ / I^+ = V^- / I^- = \hat{Z}$ . This definition embodies the idea of making the equivalent voltage and current proportional to the transverse electric and magnetic fields, respectively. The proportionality constants for this relationship are  $C_1 = V^+ / A^+ = V^- / A^-$  and  $C_2 = I^+ / A^+ = I^- / A^-$ , and can be determined from the remaining two conditions for power and impedance.

The complex power flow for the incident wave is given by:

$$P^+ = \frac{1}{2} |A^+|^2 \int_S \bar{e} \times \bar{h}^* \cdot \hat{z} \, ds = \frac{V^+ I^+}{2(C_1 C_2)} \int_S \bar{e} \times \bar{h}^* \cdot \hat{z} \, ds \quad (4.9)$$

Because we want this power to be equal to  $(1/2) V^+ I^*$ , we have that

$$C_1 C_2^* = \int_S \bar{e} \times \bar{h}^* \cdot \hat{z} \, ds \quad (4.10)$$

where the surface integration is over the cross section of the waveguide.

$$\text{The characteristic impedance is: } Z_0 = \frac{V^+}{I^+} = \frac{V^-}{I^-} = \frac{C_1}{C_2} \quad (4.11)$$

Since  $V^+ = C_1 A^+$  and  $I^+ = C_2 A^+$ , from (4.6a) and (4.6b). If it is desired to have  $Z_0 = Z_{\text{w}}$ , the wave impedance ( $Z_{\text{TE}}$  or  $Z_{\text{TM}}$ ) of the mode, then:

$$\frac{C_1}{C_2} = Z_{\text{w}} \quad (Z_{\text{TE}} \text{ or } Z_{\text{TM}}) \quad (4.12a)$$

Alternatively, it may be desirable to normalize the characteristic impedance to unity ( $Z_0 = 1$ ), in which case we have:

$$\frac{C_1}{C_2} = 1 \quad (4.12b)$$

For a given waveguide mode, (4.10) and (4.12) can be solved for the constants  $C_1$  and  $C_2$ , and equivalently the voltages and currents defined. Higher order modes can be treated in the same way, so that a general field in the waveguide can be expressed in the following form:

$$\bar{E}_t(x,y,z) = \sum_{n=1}^N \left( \frac{V_n^+}{C_{1n}} e^{-jB_n z} + \frac{V_n^-}{C_{2n}} e^{jB_n z} \right) \bar{e}_n(x,y) \quad (4.13a)$$

$$\bar{H}_t(x,y,z) = \sum_{n=1}^N \left( \frac{I_n^+}{C_{1n}} e^{-jB_n z} - \frac{I_n^-}{C_{2n}} e^{jB_n z} \right) \bar{h}_n(x,y) \quad (4.13b)$$

where  $V_n^\pm$  and  $I_n^\pm$  are the equivalent voltages and currents for the  $n^{\text{th}}$  mode, and  $C_{1n}$  and  $C_{2n}$  are the proportionality constants for each mode.

Example 4.1 Equivalent Voltage and Current For a Rectangular Waveguide  
Find the equivalent voltages and currents for a  $TE_{10}$  mode in a rectangular waveguide.

Solution

The transverse field components and power flow of the  $TE_{10}$  rectangular waveguide mode and the equivalent transmission line model of this mode can be written as follows:

Waveguide Fields

$$E_y = (A^+ e^{-jBz} + A^- e^{jBz}) \sin \frac{\pi x}{a}$$

$$H_x = \frac{-1}{Z_{\text{TE}}} (A^+ e^{-jBz} - A^- e^{jBz}) \sin \frac{\pi x}{a}$$

$$P^+ = \frac{-1}{2} \int_S E_y H_x^* dx dy = \frac{ab}{4Z_{\text{TE}}} |A^+|^2 \quad P^+ = \frac{1}{2} V^+ I^+*$$

We now find the constants  $C_1 = V^+ / A^+ = V^- / A^-$  and  $C_2 = I^+ / A^+ = I^- / A^-$  that relate the equivalent voltages  $V^\pm$  and currents  $I^\pm$  to the field amplitudes  $A^\pm$ .

Equating incident power gives:

$$\frac{ab |A^+|^2}{4Z_{\text{TE}}} = \frac{1}{2} V^+ I^+* = \frac{1}{2} |A^+|^2 C_1 C_2^*$$

If we choose  $Z_0 = Z_{\text{TE}}$ , then we will also have that

$$\frac{C_1}{I^+} = \frac{C_1}{C_2} = Z_{\text{TE}}$$

Solving for  $C_1, C_2$  gives:

$$C_1 = \sqrt{ab/2}$$

$$C_2 = \frac{\sqrt{ab/2}}{Z_{\text{TE}}}$$

which completes the transmission line equivalence for the  $TE_{10}$  mode. ■

## The Concept of Impedance

We have used the idea of impedance in several different ways. So it may be useful at this point to summarise this important concept. The term impedance was first used by Oliver Heaviside in the nineteenth century to describe the complex ratio  $V/I$  in AC circuits consisting of resistors, inductors, and capacitors; the impedance concept quickly became indispensable in the analysis of AC circuitry. It was then applied to transmission lines, in terms of lumped element equivalent circuits and the distributed series impedance and shunt admittance of the line. In the 1930s, S.A. Schelkunoff recognized that the impedance concept could be extended to electromagnetic fields in a systematic way, and noted that the impedance should be regarded as a characteristic of the type of field, as well as the medium [2]. In addition, in relation to the analogy between transmission lines and plane wave properties propagation, impedance may even be dependent on direction. The concept of Impedance, then, forms an important link between field theory and transmission line or circuit theory.

We summarize the various types of impedance we have used so far, and their notation:

- $\eta = \sqrt{\mu/\epsilon}$  = intrinsic impedance of the medium. This impedance is dependent only on the material parameters of the medium, and is equal to the wave impedance for plane waves.
- $Z_w = E_t/H_t = V_w/I_w$  = wave impedance. This impedance is characteristic of the specific type of wave, TEM, TM, TE waves each have different wave impedances ( $Z_{TEM}$ ,  $Z_{TM}$ ,  $Z_{TE}$ ), which may depend on the type of line or guide, the material, and the operating frequency.
- $Z_c = V^+/I^+$  = characteristic impedance. Characteristic impedance is the ratio of voltage to current for a wave traveling on a transmission line. Because voltage and current are uniquely defined for TEM waves, the characteristic impedance of a TE or TM wave is unique. TE and TM waves, however, do not have a uniquely defined voltage and current, so the characteristic impedance of such waves may be defined in different ways.

## Example 4.2 Application of Waveguide Impedance.

Consider a rectangular waveguide with  $a=2.286\text{ cm}$  and  $b=1.105\text{ cm}$  (X-band guide), air filled for  $\epsilon_r < 1$  and Pexolite filled ( $\epsilon_r=2.54$ ) for  $z > 0$ , as shown in Figure 4.3. If the operating frequency is  $10\text{ GHz}$ , use an equivalent transmission line model to compute the reflection coefficient of a  $TE_{10}$  wave incident on the interface from  $z < 0$ . Solution

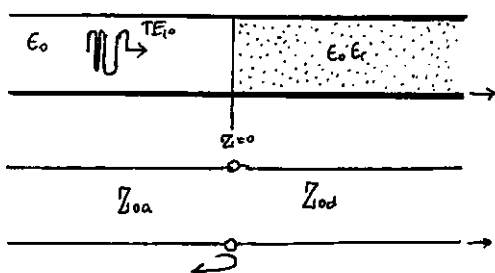
The waveguide propagation constants in the air ( $Z_{c1}$ ) and the dielectric ( $Z_{c2}$ ) regions are:

$$\beta_a = \sqrt{k_0^2 - \left(\frac{\pi}{a}\right)^2} = 158.0\text{ m}^{-1}$$

$$\beta_d = \sqrt{\epsilon_r k_0^2 - \left(\frac{\pi}{a}\right)^2} = 304.1\text{ m}^{-1}$$

where  $k_0 = 209.4\text{ m}^{-1}$

The reader may verify that the  $TE_{10}$  mode is the only propagating mode in either waveguide region. We can set up an equivalent transmission line for the  $TE_{10}$  mode in each waveguide, and treat the problem as the reflection of an incident voltage wave at the junction of the two transmission lines.



By example 4.1 and Table 3.2, the equivalent characteristic impedance of the two lines are:

$$Z_0 = \frac{k_0 \eta_0}{\beta_a} = \frac{(209.4)(377)}{158.0} = 500\Omega$$

$$Z_{0d} = \frac{k_0 \eta_0}{\beta_d} = \frac{(209.4)(377)}{304.1} = 259.6\Omega$$

The reflection coefficient seen by looking into the dielectric filled region is then:

$$\Gamma = \frac{Z_{0d} - Z_{0a}}{Z_{0d} + Z_{0a}} = -0.316$$

With this result, expressions for the incident, reflected, and transmitted waves can be written in terms of fields, or in terms of equivalent voltages and currents. ■

→ We now consider the arbitrary one port network shown in Figure 4.4 and derive a general relation between its impedance properties and electromagnetic energy stored in, and the power dissipated by, the network.

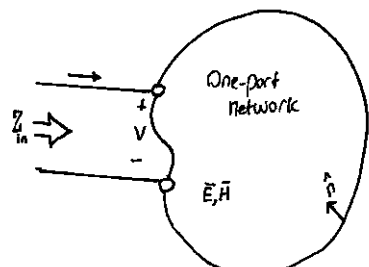


Figure 4.4 An arbitrary one port network.

The complex power delivered to this network is given by (1.91):

$$P = \frac{1}{2} \oint \bar{E} \times \bar{H}^* \cdot d\bar{s} = P_e + 2j\omega(W_m - W_e) \quad (4.14)$$

where  $P_e$  is real and represents the average power dissipated by the network, and  $W_m$  and  $W_e$  represent the stored magnetic and electric energy, respectively. Note that the unit normal vector in Figure 4.4 is pointing into the volume.

If we define real transverse amplitudes  $\bar{E}$  and  $\bar{h}$  over the terminal plane of the network such that:  $\bar{E}_t(x,y,z) = V(z)\bar{E}(x,y)e^{-jBz}$   $(4.15a)$

$$\bar{h}_t(x,y,z) = I(z)\bar{h}(x,y)e^{-jBz} \quad (4.15b)$$

with a normalization such that:

$$\int_S \bar{E} \times \bar{h} \cdot dS = 1$$

then we can express (4.14) in terms of the terminal voltage and current:

$$P = \frac{1}{2} \int_S VI^* \bar{E} \bar{h} \cdot dS = \frac{1}{2} VI^* \quad (4.16)$$

Then the input impedance is:

$$Z_{in} = R + jX = \frac{V}{I} = \frac{VI^*}{\frac{1}{2}|I|^2} = \frac{P}{\frac{1}{2}|I|^2} = \frac{P_e + 2j\omega(W_m - W_e)}{\frac{1}{2}|I|^2} \quad (4.17)$$

thus we see that the real part,  $R$ , of the input impedance is related to dissipated power, while the imaginary part,  $X$ , is related to the net energy stored in the network. If the network is lossless, then  $P_e=0$  and  $R=0$ . Then  $Z_{in}$  is purely imaginary, with a reactance

$$X = \frac{4\omega(W_m - W_e)}{|I|^2} \quad (4.18)$$

which is positive for an inductive load ( $W_m > W_e$ ), and negative for a capacitive load ( $W_m < W_e$ ).

Even and Odd Properties of  $Z(w)$  and  $\Gamma(w)$

Consider the driving point impedance,  $\{Z(w)\}$ , at the input port of an electrical network. The voltage and current at this port are related as  $V(w) = Z(w)I(w)$ . For an arbitrary frequency dependence, we can find the time domain voltage by taking the inverse Fourier Transform of  $V(w)$ :

$$v(t) = \frac{1}{2\pi} \int_{-\infty}^{\infty} V(w)e^{jwt} dw \quad (4.19)$$

Because  $v(t)$  must be real, we have that  $v(t) = V^*(t)$ , or

$$\int_{-\infty}^{\infty} V(w)e^{jwt} dw = \int_{-\infty}^{\infty} V^*(w)e^{-jwt} dw = \int_{-\infty}^{\infty} V^*(-w)e^{jwt} dw$$

where the last term was obtained by a change of variable  $w$  to  $-w$ . This shows that  $V(w)$  must satisfy the relation

$$V(-w) = V^*(w) \quad (4.20)$$

which means that  $Re\{V(w)\}$  is even in  $w$ , while  $Im\{V(w)\}$  is odd in  $w$ . Similar results hold for  $I(w)$ , and for  $Z(w)$ . Since

$$V^*(-w) = Z^*(-w)I^*(-w) = Z^*(-w)I(w) = V(w) = Z(w)I(w)$$

thus, if  $Z(w) = R(w) + jX(w)$ , then  $R(w)$  is even in  $w$  and  $X(w)$  is odd in  $w$ . These results can also be inferred from (4.17).

Now consider the reflection coefficient at the input port:

$$\Gamma(w) = \frac{Z(w) - Z_0}{Z(w) + Z_0} = \frac{R(w) - Z_0 + jX(w)}{R(w) + Z_0 + jX(w)} \quad (4.21)$$

Then

$$\Gamma(-w) = \frac{R(w) - Z_0 - jX(w)}{R(w) + Z_0 - jX(w)} = \Gamma^*(w) \quad (4.22)$$

which shows that the real and imaginary parts of  $\Gamma(w)$  are even and odd, respectively, in  $w$ . Finally, the magnitude of the reflection coefficient is

$$|\Gamma(w)|^2 = \Gamma(w)\Gamma^*(w) = |\Gamma(w)|\Gamma(-w) = |\Gamma(-w)|^2 \quad (4.23)$$

which shows that the real and imaginary  $|\Gamma(w)|^2$  and  $|\Gamma(w)|$  are even functions of  $w$ . This result implies that only even series of the form:  $a + bw^2 + cw^4 \dots$  can be used to represent  $|\Gamma(w)|$  or  $|\Gamma(w)|^2$ .

## 4.2 Impedance and Admittance Matrices.

In the previous section we have seen how equivalent voltages and currents can be defined for TEM and non-TEM waves. Once such voltages and currents have been defined for various points on the microwave network, we can use the impedance and/or admittance matrices of circuit to relate these terminal or port quantities to each other, and thus to essentially arrive at a matrix description of the network. This type of representation lends itself to the development of equivalent circuits of arbitrary networks, which will be quite useful when we discuss the passive design of passive components such as couplers and filters. The term port was introduced by H.H. Wheeler in the 1950s to replace the less descriptive and more cumbersome phrase "two-terminal pair" (2,3).)

We begin by considering an arbitrary  $N$ -port microwave network, as depicted in Figure 4.5. The ports in Figure 4.5 may be any type of transmission line or transmission line equivalent of a single propagating waveguide mode. If one of the physical ports of the network is a waveguide supporting more than one propagating mode, additional electrical ports can be added to account for these modes.

At a specific point on the  $n$ th port, a terminal plane,  $t_n$ , is defined along with equivalent voltages and currents for the incident ( $V_{n+}, I_{n+}$ ) and reflected ( $V_{n-}, I_{n-}$ ) waves. The terminal planes are important in providing a phase reference for the voltage and current phasors. Now at the  $n$ th terminal plane, the total voltage and current are given by:

$$V_n = V_{n+} + V_{n-} \quad (4.24a)$$

$$I_n = I_{n+} - I_{n-} \quad (4.24b)$$

As seen from (4.8) when  $Z = 0$ :

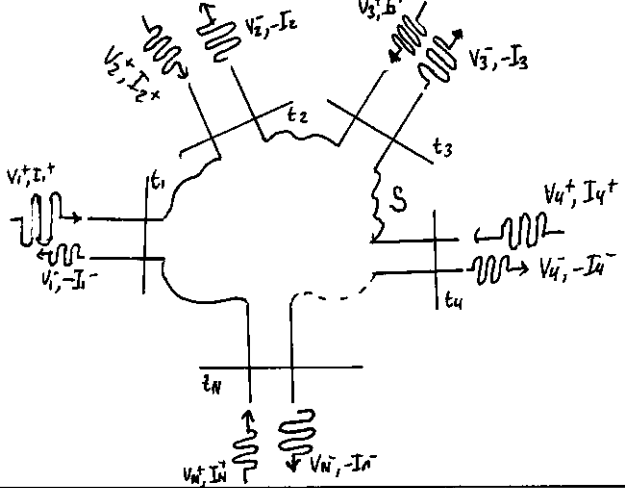


Figure 4.5. An arbitrary  $N$ -port microwave Network.

The impedance matrix  $[Z]$  of the microwave network then relates these voltages and currents:

$$\begin{bmatrix} V_1 \\ V_2 \\ \vdots \\ V_N \end{bmatrix} = \begin{bmatrix} Z_{11} & Z_{12} & \cdots & Z_{1N} \\ Z_{21} & Z_{22} & \cdots & Z_{2N} \\ \vdots & \vdots & \ddots & \vdots \\ Z_{N1} & \cdots & \cdots & Z_{NN} \end{bmatrix} \begin{bmatrix} I_1 \\ I_2 \\ \vdots \\ I_N \end{bmatrix} \quad \text{or in matrix form as } [V] = [Z][I] \quad (4.25)$$

Similarly, we can define an admittance matrix  $[Y]$  as:

$$\begin{bmatrix} I_1 \\ I_2 \\ \vdots \\ I_N \end{bmatrix} = \begin{bmatrix} Y_{11} & Y_{12} & \cdots & Y_{1N} \\ Y_{21} & Y_{22} & \cdots & Y_{2N} \\ \vdots & \vdots & \ddots & \vdots \\ Y_{N1} & \cdots & \cdots & Y_{NN} \end{bmatrix} \begin{bmatrix} V_1 \\ V_2 \\ \vdots \\ V_N \end{bmatrix} \quad \text{or in a matrix form as } [I] = [Y][V] \quad (4.26)$$

of course, the  $[Z]$  and  $[Y]$  matrices are inverses of each other:

$$[Y] = [Z]^{-1} \quad (4.27)$$

Note that both the  $[Z]$  and  $[Y]$  matrices relate the total port voltages and currents.

From (4.25), we see that  $Z_{ij}$  can be found as:

$$Z_{ij} = \frac{V_i}{I_j} \Big|_{\substack{I_k=0 \text{ for } k \neq i}} \quad (4.28)$$

In words, (4.28) states that  $Z_{ij}$  can be found by driving port  $j$  with current  $I_j$ , opencircuiting all other ports ( $I_k=0$  for  $k \neq j$ ), and measuring the open-circuit voltage at port  $i$ . Thus,  $Z_{ii}$  is the input impedance seen looking into port  $i$  when all other ports are open-circuited, and  $Z_{ij}$  is the transfer impedance between ports  $i$  and  $j$  when all other ports are open-circuited.

Similarly, from (4.26),  $Y_{ij}$  can be found as:

$$Y_{ij} = \frac{I_i}{V_j} \Big|_{\substack{V_k=0 \text{ for } k \neq j}} \quad (4.29)$$

which states that  $Y_{ij}$  can be determined by driving port  $j$  with the voltage  $V_j$ , short-circuiting all other ports ( $V_k=0$  for  $k \neq j$ ), and measuring the short-circuit current at port  $i$ .

In general, each  $Z_{ij}$  or  $Y_{ij}$  element may be complex. For an arbitrary  $N$ -port network, the impedance and admittance matrices are  $N \times N$  in size, so there are  $2N^2$  independent quantities or degrees of freedom. In practice, however, many networks are either reciprocal or lossless, or both. If the network is reciprocal (not containing any active devices or nonreciprocal media, such as ferrites or plasmas), we will show that the impedance and admittance matrices are symmetric, so that  $Z_{ij} = Z_{ji}$ , and  $Y_{ij} = Y_{ji}$ . If the network is lossless, we can show that all  $Z_{ij}$  or  $Y_{ij}$  elements are purely imaginary. Either of these special cases serves to reduce the number of independent quantities or degrees of freedom that an  $N$ -port network may have. We now derive the above characteristics for reciprocal and lossless networks.

### Reciprocal Networks

Consider the arbitrary network of Figure 4.5 to be reciprocal (no active devices, ferrites or plasmas), with short circuits placed at all terminal planes except those of ports 1 and 2. Let  $E_a, H_a$  and  $E_b, H_b$  be the fields anywhere in the network due to two independent sources,  $a$  and  $b$ , located somewhere in the network. Then the Reciprocity Theorem of (1.156) states that:

$$\oint \overline{E_a} \times \overline{H_b} \cdot d\bar{s} = \oint \overline{E_b} \times \overline{H_a} \cdot d\bar{s} \quad (4.30)$$

where  $S$  is a closed surface along the boundaries of the network and through the terminal plane ports. If the boundary walls of the network and transmission lines are metal, the  $\overline{E}_{\text{tan}} = 0$  on these walls (assuming perfect conductors).

If the network or the transmission lines are open structures, like microstrip line or slotline, the boundaries of the network can be taken arbitrarily far from the lines so that  $\bar{E}_{\text{ext}}$  is negligible. Then the only nonzero contribution to the integrals of (4.30) come from the cross-sectional areas of ports 1 and 2.

From Section 4.1, the fields due to sources a and b can be evaluated at the terminal planes  $\bar{z}_1$  and  $\bar{z}_2$  as:

$$\bar{E}_a = V_{ia} \bar{e}_1, \quad I_{1a} = I_{2a} h_1 \quad (4.31a)$$

$$\bar{E}_b = V_{ib} \bar{e}_1, \quad I_{1b} = I_{2b} h_1 \quad (4.31b)$$

$$\bar{E}_{2a} = V_{ia} \bar{e}_2, \quad I_{2a} = I_{1a} h_2 \quad (4.31c)$$

$$\bar{E}_{2b} = V_{ib} \bar{e}_2, \quad I_{2b} = I_{1b} h_2 \quad (4.31d)$$

where  $\bar{e}_1, \bar{h}_1$  and  $\bar{e}_2, \bar{h}_2$  are the transverse modal fields of port 1 or 2, respectively, and the  $V$ s and  $I$ s are the equivalent total voltages and currents. (For instance,  $\bar{E}_{1b}$  is the transverse electric field at the terminal plane  $\bar{z}_1$  of port 1 due to source b.) Substituting the fields of (4.31) into (4.30) gives

$$(V_{ia} I_{1b} - V_{ib} I_{1a}) \int_{S_1} \bar{e}_1 \times \bar{h}_1 \cdot d\bar{s} + (V_{ia} I_{2b} - V_{ib} I_{2a}) \int_{S_2} \bar{e}_2 \times \bar{h}_2 \cdot d\bar{s} = 0 \quad (4.32)$$

where  $S_1$  and  $S_2$  are the cross-sectional areas at the cross-sectional areas at the terminal planes of ports 1 and 2.

As in Section 4.1, the equivalent voltages and currents have been defined so that the power through a given port can be expressed as  $VI^*/2$ ; then, comparing (4.31) to (4.6) implies that  $C = C_2 = 1$  for each port; so that:

$$\int_{S_1} \bar{e}_1 \times \bar{h}_1 \cdot d\bar{s} = \int_{S_2} \bar{e}_2 \times \bar{h}_2 \cdot d\bar{s} = 1 \quad (4.33)$$

This reduces (4.32) to:

$$V_{ia} I_{1b} - V_{ib} I_{1a} + V_{ia} I_{2b} - V_{ib} I_{2a} = 0 \quad (4.34)$$

Now use the  $2 \times 2$  admittance matrix of the (effectively) two-port network to eliminate the  $I$ s:

$$I_1 = Y_{11} V_1 + Y_{12} V_2$$

$$I_2 = Y_{21} V_1 + Y_{22} V_2$$

Substitution into (4.34) gives:  $(V_{ia} V_{2b} - V_{ib} V_{2a}) / (Y_{12} - Y_{21}) = 0$   $(4.35)$

Because the sources of a and b are independent, the voltage  $V_{ia}, V_{ib}, V_{2a}$ , and  $V_{2b}$  can take on arbitrary values. So in order for (4.35) to be satisfied for any choice of sources, we must have  $Y_{12} = Y_{21}$ , and since the choice of which ports are labeled as 1 and 2 is arbitrary, we have the general result that:

$$Y_{ij} = Y_{ji} \quad (4.36)$$

Then if  $[Y]$  is a symmetric matrix, its inverse,  $[Z]$  is also symmetric.

### Lossless Networks

Now consider a reciprocal lossless N-port junction; we will show that the elements of the impedance and admittance matrices must be purely imaginary. If the network is lossless, then the net real power delivered to the network must be zero. Thus,  $\text{Re}\{P_{\text{avg}}\} = 0$ , where,

$$\begin{aligned} P_{\text{avg}} &= \frac{1}{2} [V]^t [I]^* = \frac{1}{2} ([Z][I])^t [I]^* = \frac{1}{2} [I]^t [Z]^* [I]^* \\ &= \frac{1}{2} (I_1 Z_{11} I_1^* + I_1 Z_{12} I_2^* + I_2 Z_{21} I_1^* + I_2 Z_{22} I_2^*) \\ &= \frac{1}{2} \sum_{n=1}^N \sum_{m=1}^N \text{Im} Z_{mn} I_m^* \end{aligned} \quad (4.37)$$

We have used the result from the matrix algebra that  $([A][B]^t) = [B]^t [A]^t$ . Because the  $I$ s are independent, we must have the real part of each self term ( $I_m Z_{mn} I_m^*$ ) equal to zero. Since we could set all port currents equal to zero except for the  $n^{\text{th}}$  current, so:  $\text{Re}\{I_n Z_{nn} I_n^*\} = |I_n|^2 \text{Re}\{Z_{nn}\} = 0$   
or  $\text{Re}\{Z_{nn}\} = 0$   $(4.38)$

Now let all port currents be zero except for  $I_m$  and  $I_n$ .

Then (4.37) reduces to:  $\text{Re}\{(I_n I_m^* + I_m I_n^*) Z_{mn}\} = 0$

$$\text{Since } Z_{mn} = Z_{nm}.$$

However,  $(I_n I_m^* + I_m I_n^*)$  is purely a real quantity. That is, in general, non-zero. Thus we must have  $\text{Re}\{Z_{mn}\} = 0$   $(4.39)$ . Then (4.38) and (4.39) imply that  $\text{Re}\{Z_{mn}\} = 0$  for any  $m, n$ . The reader can verify that this also leads to an imaginary  $[Y]$  matrix.

### Example 4.3 Evaluation of Impedance Parameters.

Find the  $Z$  parameters of the two-port T-network shown in Fig 4.6.

#### Solution

From (4.28),  $Z_{11}$  can be found as the input impedance of port 1 when port 2 is open circuited:

$$Z_{11} = \frac{V_1}{I_1} \Big|_{I_2=0} = Z_A + Z_C + \frac{V_1}{I_1} \quad \text{Port 1} \quad \text{Port 2} \quad V_1 \quad V_2 \leftarrow$$

The transfer impedance  $Z_{12}$  can be found by measuring the open circuit voltage at port 1 when a current  $I_2$  is applied at port 2. By voltage division,

$$Z_{12} = \frac{V_1}{I_2} \Big|_{I_1=0} = \frac{V_2}{I_2} \frac{Z_C}{Z_B + Z_C} = Z_C$$

The reader can easily verify  $Z_{12} = Z_{21}$ , indicating a reciprocal circuit.

Finally,  $Z_{22}$  is found as:

$$Z_{22} = \frac{V_2}{I_2} \Big|_{I_1=0} = Z_B + Z_C$$

### Example 4.4 Evaluation of Scattering Parameters

Find the scattering parameters of the 8 dB attenuator circuit shown in Figure 4.8.

Solution

From (4.41),  $S_{11}$  can be found as the reflection coefficient seen at port 1 when port 2 is terminated in a matched load ( $Z_{D2} = 50\Omega$ ):

$$S_{11} = \frac{V_1^-}{V_1^+} \Big|_{V_2^+=0} = \Gamma^{(1)} \Big|_{V_2^+=0} = \frac{Z_{in}^{(1)} - Z_0}{Z_{in}^{(1)} + Z_0} \Big|_{Z_0 \text{ on port 2}}$$

$$\text{but } Z_{in}^{(1)} = 8.56 + [141.8(8.56+50)]/(141.8+8.56+50) = 52.2 \Omega \text{ so } S_{11} = 0.$$

Because of the symmetry of the circuit,  $S_{22} = 0$ .

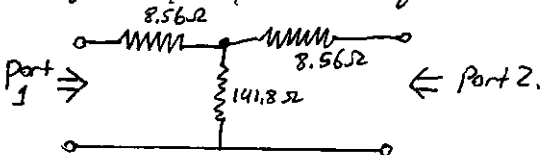


Figure 4.8. A matched 3dB attenuator with a  $50\Omega$  characteristic impedance (example 4.4)

We can find  $S_{21}$  by applying an incident wave at port 1,  $V_1^+$ , and measuring the outcome wave at port 2,  $V_2^-$ . This is equivalent to the transmission coefficient from port 1 to port 2:  $S_{21} = \frac{V_2^-}{V_1^+} \Big|_{V_2^+=0}$

From the fact that  $S_{11} = S_{22} = 0$ , we know that  $V_1^- = 0$  when port 2 is terminated in  $Z_0 = 50\Omega$ , and that  $V_2^+ = 0$ . In this case we have that  $V_1^+ = V_1$  and  $V_2^- = V_2$  as the voltage across the  $50\Omega$  load resistor at port 2:  $V_2^- = V_2 = V_1 \left( \frac{41.44}{41.44 + 8.56} \right) / \frac{50}{50 + 8.56} = 0.707 V$ .

where  $41.44 = 141.8(58.56)/(141.8 + 58.56)$  is the resistance of the parallel combination of the  $50\Omega$  load and the  $8.56\Omega$  resistor with the  $141.8\Omega$  resistor. Thus,  $S_{21} = S_{12} = 0.707$ .

If the input power is  $|V_1^+|^2/2Z_0$ , then the output power is  $|V_2^-|^2/2Z_0 = |S_{21}|V_1^+|^2/2Z_0 = |V_1^+|^2/4Z_0$ , which is one-half (-3dB) of the input power.

writing Statistics:

192 AS pages / 178 Text pages

⇒ Compression Ratio: 1.079

≈ 1:1 Ratio with 8% variation

50 days to complete

filling this notebook. (SF 192AS)

$$\frac{192 \text{ pages}}{50 \text{ days}} = \frac{3.84 \text{ pages}}{\text{day}} \approx 4 \text{ pages/day/booklet}$$

in avg

with about 10 pages written per day.

$$\frac{178 \text{ pages}}{10 \text{ pages/day}} = 17.8 \text{ days.}$$

$$\frac{17.8 \text{ days}}{50 \text{ days}} = 0.356$$

giving us Ratios  
Occupancy Rates:

$$\frac{7 \text{ days}}{1 \text{ week}} \cdot 0.356 = \frac{2.492 \text{ days}}{1 \text{ week}} \text{ writing this book, excluding other writing projects.}$$

$$\frac{30 \text{ days}}{1 \text{ month}} \cdot 0.356 = \frac{10.68 \text{ days}}{1 \text{ month}} \frac{60 \text{ days}}{2 \text{ months}} = \frac{21.36 \text{ days}}{2 \text{ months.}}$$

Total completion ETA

$$178/721 = 0.2468\%$$

ETA: 150 days — ETA: 54.3 days  
(ideal)